Distribution Agreement

In presenting this thesis or dissertation as a partial fulfillment of the requirements for an advanced degree from Emory University, I hereby grant to Emory University and its agents the non-exclusive license to archive, make accessible, and display my thesis or dissertation in whole or in part in all forms of media, now or hereafter known, including display on the world wide web. I understand that I may select some access restrictions as part of the online submission of this thesis or dissertation. I retain all ownership rights to the copyright of the thesis or dissertation. I also retain the right to use in future works (such as articles or books) all or part of this thesis or dissertation.

Signature:

_____ _____

Erica Shannon Torres Date

Investigating the roles of H2A.Z in transcription and nucleosomal organization through its relationships with other chromatin proteins.

By
Erica Shannon Torres
Doctor of Philosophy

Graduate Division of Biological and Biomedical Science
Genetics and Molecular Biology

_____
Roger B. Deal, Ph.D.
Advisor

_____
Victor G. Corces, Ph.D.
Committee Member

_____
Meleah A. Hickman, Ph.D.
Committee Member

_____
William G. Kelly, Ph.D.
Committee Member

_____
Ken H. Moberg, Ph.D.
Committee Member

Accepted:

_____
Lisa A. Tedesco, Ph.D.
Dean of the James T. Laney School of Graduate Studies

_____
Date

Investigating the roles of H2A.Z in transcriptional regulation and nucleosomal organization through its relationships with other chromatin proteins.

By

Erica Shannon Torres
B.S. Florida State University, 2011

Advisor: Roger B. Deal, Ph.D.

An abstract of
A dissertation submitted to the Faculty of the
James T. Laney School of Graduate Studies of Emory University
in partial fulfillment of the requirements for the degree of
Doctor of Philosophy
in Genetics and Molecular Biology
2018

Abstract

Investigating the roles of H2A.Z in transcription and nucleosomal organization through its relationships with other chromatin proteins.

By Erica Shannon Torres

The well-organized chromatin structure of DNA packaged into nucleosomes can determine how genetic information encoded by DNA is used in different conditions. Factors contributing to DNA accessibility include the activity of chromatin remodeling complexes and exchanging histones for variant histones within nucleosomes. The histone variant H2A.Z acts to promote or repress transcription by either stabilizing or destabilizing nucleosome structure, but the underlying mechanisms are unclear. Therefore, much work is needed to understand the context that makes H2A.Z incorporation into chromatin necessary for transcriptional regulation.

Previous work in *Arabidopsis thaliana* showed that the repressive function of the BRM ATPase of the SWI2/SNF2 complex makes the transcriptional activating function of H2A.Z necessary for transcription of the developmental switch gene *Flowering Locus C (FLC)*. Thus, I performed chromatin and transcriptional profiling in Arabidopsis plants to evaluate the genetic interaction between BRM and H2A.Z at target genes. I found 8 classes of genes involved in transcriptional regulation and responses to stimuli that establish that H2A.Z and BRM directly regulate transcription of genes either redundantly or with opposing roles. Profiling genomic nucleosomal changes resulting from loss of BRM and/or H2A.Z showed that H2A.Z is associated with varying nucleosome dynamics, and BRM tends to destabilize or reposition nucleosomes flanking nucleosome-depleted regions.

To identify additional factors opposing H2A.Z-mediated transcription at the *FLC* locus, I conducted a forward genetic suppressor screen. I identified mutants depleted of H2A.Z-containing nucleosomes that still showed *FLC* transcription. By mapping suppressor mutations from the screen, I identified 9 candidate H2A.Z antagonists. Further work to distinguish whether the candidate mutations identified can suppress H2A.Z-nucleosome depletion phenotypes has potential to expand our understanding of what repressive factors make H2A.Z necessary for transcription.

In summary, I comprehensively profiled how H2A.Z and BRM interact to contribute to transcriptional regulation and nucleosomal organization and identified additional factors that may necessitate the role of H2A.Z for transcriptional regulation. These findings expand our view of how H2A.Z interacts with other factors in a complex chromatin context to regulate genomic processes, which have biological implications for development and how organisms respond to their environment.

Investigating the roles of H2A.Z in transcriptional regulation and nucleosomal organization through its relationships with other chromatin proteins.

By

Erica Shannon Torres
B.S. Florida State University, 2011

Advisor: Roger B. Deal, Ph.D.

A dissertation submitted to the Faculty of the
James T. Laney School of Graduate Studies of Emory University
in partial fulfillment of the requirements for the degree of
Doctor of Philosophy
in Genetics and Molecular Biology
2018

Acknowledgements

I would like to thank my advisor Roger Deal for providing critical guidance as well as the independence to grow as a scientist during my graduate training. I would also like to thank the members of my committee Victor Corces, Meleah Hickman, Bill Kelly, and Ken Moberg, as well as former member Xiaodong Cheng for their time, critical feedback, and advice throughout the progression of my dissertation work. Funds from Emory University and awarded to me from the Ruth L. Kirschstein Predoctoral Individual National Research Service Award through the National Institute of General Medicine of the National Institutes of Health under award number (F31GM113631-01A1) were greatly appreciated and were essential for this work. I am grateful to have had the opportunity to perform this work as a student in the Genetics and Molecular biology program within the Laney Graduate School at Emory University. Such a training environment provided enriching collegial exchange with other scientists, financial support, and career development opportunities over and above my scientific training. My lab mates, past and present, have also cultivated an atmosphere of drive, learning, and comradery and will truly be missed. I would also like to thank the Biology Department for their administrative and financial support, and especially Jan Hawes for doing everything in her power to keep our resources in working order.

I am grateful for the endless love, overflowing joy, and continuous grace that Jesus Christ offered daily to provide the strength to serve people and honor God by completing this work. From driving 300 miles to covering housework while I wrote, I deeply appreciate all the ways that Alex Torres has sacrificed for me and been my companion through this journey. On top of the joy she brings, my daughter Isabella has given me greater purpose and my time more value. My family, especially Darlene, Eric, and Dusty Mills, have loved and supported me in my pursuits: believing in me, anchoring me to what is important, and preparing me to do hard things. My church and especially my coffee girls have challenged me, supported me, and made life in Atlanta vibrant. These and many other relationships with people such as Alev Ozdemir, Lindsey Bolin, and Marissa Davis have been crucial to my health, resilience, and well being while completing this work.

Table of Contents

CHAPTER 1: INTRODUCTION

Chromatin as the mediator of responsive genes

Building a functional living organism requires the flow of information from genes that are encoded by DNA, transcribed into RNA molecules, and then translated into operative proteins to carry out metabolism and other processes (Wu 2014). We know that individual steps in this progression can feedback to influence previous phases, and countless additional regulatory steps occur throughout this highly regulated procedure. (Wu 2014). In addition to maintaining development and homeostatic processes, having the ability to adapt processes from transcription to translation to respond to external stressors is crucial for survival. While many organisms can resort to fight-or-flight methods of defense response, plants are sessile organisms, so they must modify themselves to better suit their living conditions (Rymen and Sugimoto 2012). Consequently, various environmental stimuli trigger changes in the plant's transcriptome, proteome, and metabolic arsenal produced by various proteins (Urano et al., 2010; Wu 2014). Transcriptional changes in particular take advantage of unique gene sets suited to equip plants for specific conditions (Urano et al., 2010; Barah et al., 2016). Once a stimulus is perceived, it initiates a signaling cascade that can trigger a transcriptional response by these genes that can then be translated into a physiological response (Urano et al., 2010; Wu 2014). Governing the expression of these environmentally responsive genes is a highly organized chromatin structure consisting of DNA associating with proteins and RNA (Mondal et al., 2010; Zhu et al., 2013). Therefore, eliciting a transcriptional response to stimuli depends on whether DNA encoding the appropriate genes are in an accessible chromatin conformation (Zhu et al., 2013).

Chromatin structure and regulation

Nucleosomes: DNA + histones

The primary unit of chromatin is made up of ~147 base pairs (bp) of DNA wrapped 1.65 times around an octamer of histones to form nucleosomes (Luger et al., 2000). Two histone H2A-H2B dimers and a tetramer of two copies each of histones H3 and H4 associate with DNA to create the nucleosome core particle (Burton et al., 1978; Luger et al., 2000). Electrostatic interactions drive the association between the negatively charged DNA phosphate backbone and the positively charged histone residues (Burton et al., 1978; Luger et al., 1997). Therefore, the thermodynamic interaction between DNA and the histone octamer exists in an equilibrium between loosely and more tightly associating conformations (Li et al., 2005b; Jimenez-Useche and Yuan 2012). Since the DNA must bend to wrap around the histone octamer, some nucleotide sequences combine to form a more flexible DNA molecule that is better suited for nucleosome positioning (Fig. 1.1A, Widom 2001; Zhang et al., 2015; Todolli et al., 2017). Thus, an array of nucleosomes can form along a DNA molecule, which can be compared to "beads on a string."

These intrinsic properties of nucleosomes establish a certain level of stability that can be further altered by external factors (Zhou et al., 2016). In addition to histone-DNA interactions, internucleosomal interactions and further trans-acting factors drive higher order chromatin organization within the nucleus (Todolli et al., 2017; Vergara and Gutierrez 2017). The structure of chromatin can be modified by many different factors, including post-translational modifications to histones, incorporation of histone variants into nucleosomes, changes contributed by chromatin remodeling complexes, contributions by long non-coding RNA, and modifications to the DNA itself (Berger 2007; March-Diaz and Reyes 2009; Mondal et al., 2010; Hargreaves and Crabtree 2011; Engreitz et al., 2016; Seymour and Becker 2017). Regulating chromatin structure provides a way to modulate how the underlying DNA can be used and has implications for replication, repair, and transcription of the DNA (Nagai et al., 2017; Lai and Pugh 2017).

During transcription or replication of DNA, RNA or DNA polymerases move along individual, unzipped DNA strands as a part of larger complexes (Fig. 1.1B, Lai and Pugh 2017). These processes that need access to the DNA sequence must perturb the association between DNA

and histones. Consequently, the histone-DNA interactions create an energetic barrier that must be overcome for the polymerases to pass through (Weber et al., 2014). The level of hindrance however can dependent on the presence of histone modifications, the composition of nucleosomes, or the activity of chromatin remodelers (Weber et al 20014; Lai and Pugh 2017). Histones are not just obstructions to polymerases, but one study suggests that packaging DNA around nucleosomes can help facilitate transcription. This was demonstrated by *in vitro* work at one yeast locus showing that RNA polymerase is more efficient at transcribing genes organized into a chromatin structure than along naked DNA (Nagai et al., 2017).

Histone post-translational modifications influence chromatin structure

DNA wraps around the core octamer of histones, but the C-terminal and N-terminal tails of the histones remain unstructured and extend outside of the nucleosome core particle (Luger et al., 1997). These histone tails as well as the core regions can be post-translationally modified to impart additional properties to the nucleosome (Fig. 1.1C, Berger 2007; Tessarz and Kouzarides 2014; Zhao and Garcia 2015). Some modifications, such as lysine acetylation, can directly neutralize histone amino acid charges and disrupt intra- and internucleosomal interactions (Dion et al., 2005; Shogren-Knaak et al., 2006; Zhang et al., 2017b), while other modifications serve as signals that can be read by proteins equipped with complementary domains dedicated to recognizing specific amino acid modifications (Dhar et al., 2017). Although many post-translational modifications to histones have been identified, several have well documented functions corresponding with chromatin function relating to transcriptional repression (H3K27me3, H3K9me3, H2AK119u1, etc.) or transcriptional activity (H3K4me3, H3K36me, H4K16ac, H3K27ac, etc.) (Berger 2007; Zhao and Garcia 2015; Davie et al., 2016; Becker et al., 2016; Endoh et al., 2012). For example, the lysine 27 on histone H3 is tri-methylated (H3K27me3) by Polycomb repressive complex 2 (PRC2) to contribute to gene repression (Lafos et al., 2011; Derkacheva and Hennig 2013) and demethylated by the histone demethylase REF6 for reactivation (Li et al., 2016). Acetylation and deacetylation of the lysine 27

residue on H3 (H3K27ac) contribute to promote transcriptional activity and transcriptional repression, respectively, both through the chemical properties of acetylation and by blocking the tri-methylation of H3K27 (Berger 2007). The presence of these histone modifications recruit or antagonize additional factors such as transcriptional regulators, chromatin remodelers, and splicing factors that can further influence chromatin organization and gene activity (Berger 2007; Dhar et al., 2017).

Histone variants confer unique properties to nucleosomes

Core, or canonical, histones are expressed during the S-phase of the cell cycle when histones are needed in mass to accommodate the newly synthesized DNA (March-Diaz and Reyes 2009). Histone variants or replacement histones are expressed in cells independently of replication and are targeted to specific locations in the genome that correspond with their unique roles in chromatin (Fig. 1.1D, March-Diaz and Reyes 2009). Histone variants have been identified for each histone except H4, with the most diverse family of histone variants coming from H2A variants (March-Diaz and Reyes 2009). Histone H2A variant H2A.X is involved in numerous mitotic and meiotic processes, stem cell biology, and aging (Turinetto and Giachino 2015). Although its contributions to the process of DNA damage repair are not clearly defined, it is best known for its role in marking double stranded breaks (Turinetto and Giachino 2015). Still other histone variants are confined to heterochromatic regions such as the histone H3 variant Cenp-A and orthologs that are required for centromere function and mitosis (Blower and Karpen 2001). The histone H2A variant H2A.Z is one variant in particular that is involved in a variety of processes in both euchromatin and heterochromatin, including regulating transcription of environmentally responsive genes (Coleman-Derr and Zilberman 2012; Bönisch and Hake 2012). Each of these variant histones influence chromatin organization to contribute to many different processes by offering different compositions and unique sets of post-translational modifications (Fig. 1.1D, Bönisch and Hake 2012).

Specific enzymes specialize in chromatin remodeling

Chromatin remodeling complexes are macromolecular machines containing a DNA-dependent catalytic subunit that can use the energy of ATP-hydrolysis to disrupt DNA-histone interactions (Hargreaves and Crabtree 2011). This hydrolysis empowers the remodelers to reposition nucleosomes along the DNA strand, evict histone dimers or whole octamers, or exchange canonical histones for histone variants within the nucleosome (Hargreaves and Crabtree 2011; Narlikar et al., 2013; Clapier et al., 2017). Chromatin remodeling complexes can be broken down into four subfamilies based on the conserved domains of their primary ATPases, including SWI2/SNF2, ISWI, CHD, and SWR1/INO80 families (Hargreaves and Crabtree 2011). The SWR1/INO80 subfamily is primarily involved in inserting or removing the histone variant H2A.Z into or out of chromatin (Mizuguchi et al., 2004; Papamichos-Chronakis et al., 2011). INO80 can also position nucleosomes around nucleosome-depleted regions (NDR) (Krietenstein et al., 2016). ISWI chromatin remodelers are important for positioning nucleosomes and creating repeated nucleosome position phasing relative to chromatin landmarks like transcription start sites (TSSs) (Krietenstein et al., 2016). CHD family chromatin remodelers contain ATPases together with chromodomains that are targeted to methylated histones. Remodelers in the CHD family are generally associated with nucleosome assembly and subsequent remodeling to establish proper positioning and spacing after replication (Liu et al., 2015; Torigoe et al., 2013; Hargreaves and Crabtree 2011). The SWI2/SNF2 family of chromatin remodelers can bind to nucleosomes and use the energy of ATP hydrolysis to disrupt nucleosome structure and translocate nucleosomes *in vitro* (Zofall et al., 2006). However, the mechanisms of how SWI2/SNF2 complexes contribute to transcriptional regulation of individual genes is more ambiguous *in vivo (*Hargreaves and Crabtree 2011). Two families of chromatin remodelers that have proven important to regulate transcription of environmentally responsive genes and that are studied in this dissertation research are the SWI2/SNF2 and the SWR1 complexes (Ma et al., 2011).

SWR1 and H2A.Z

SWR1 chromatin remodeling complex incorporates H2A.Z into chromatin

The SWR1 chromatin-remodeling complex is the primary complex responsible for incorporating H2A.Z into nucleosomes (Lu et al., 2009). SWR1 uses the energy from ATP-hydrolysis to remove histone H2A/H2B dimers containing canonical H2A from nucleosomes and replaces them with histone H2A.Z/H2B dimers (Mizuguchi et al., 2004). The SWR1 complex has been characterized extensively in yeast and homologous complexes have also been identified in other eukaryotes (Lu et al., 2009; Hargreaves and Crabtree 2011). The yeast SWR1 complex consists of the primary ATPase SWR1 and 14 other subunits (Lu et al., 2009). In Arabidopsis, the SWR1 complex had not been purified until recently (Sijacic, et al., in preparation). However, work in Arabidopsis has shown that orthologs of yeast SWR1 complex subunits interact to form a complex that has been functionally characterized as important for H2A.Z incorporation into chromatin (Choi et al., 2007; March-Diaz et al., 2007; Deal et al., 2007; Lu et al., 2009; Bieluszewski et al., 2015). The Arabidopsis SWR1 subunits studied so far include the ATPase PIE1 and subunits ARP6, SWC6/SEF, SWC2, Rvb1/2, and H2A.Z (Choi et al., 2007; Deal et al., 2007; Lu et al., 2009; Bieluszewski et al., 2015; March-Diaz et al., 2008).

Some of the SWR1 subunits are shared between the SWR1 complex, the INO80 complex that removes H2A.Z from chromatin, and the NuA4 complex which can acetylate histones including H2A.Z (Bieluszewski et al., 2015; Jarillo and Pineiro 2015; Lu et al., 2009). The ARP6 subunit is unique to the SWR1 complex however and is essential for proper H2A.Z incorporation (Deal et al., 2007; Lu et al., 2009; Hargreaves and Crabtree 2011). Because of its selective role in SWR1 function to incorporate H2A.Z into chromatin, *arp6* mutants have even been used as a proxy to study H2A.Z depletion in the place of H2A.Z mutants (Sura et al., 2017).

H2A.Z regulates chromatin organization and transcription

Incorporation of H2A.Z into nucleosomes is essential for life in many eukaryotes (Liu et al., 1996; Clarkson et al., 1999; Faast et al., 2001; Whittle et al., 2008). However, H2A.Z mutants in yeast and plants are still viable, making them especially tractable organisms to study H2A.Z function

(Jackson and Gorovsky 2000; Coleman-Derr and Zilberman 2012). The pleiotropic phenotypes described for mutants depleted of H2A.Z-containing nucleosomes show that H2A.Z is still crucial for many processes in plants, including development, responses to stimuli, and maintaining genomic integrity (Jarillo and Pineiro 2015; Coleman-Derr and Zilberman 2012). H2A.Z regulates responses to endogenous signals such as salicylic acid, ethylene response, and auxin (Hu et al., 2011; Lee and Seo 2017; March-Diaz et al., 2008). Transcriptional regulation by H2A.Z affects environmentally responsive processes such as immune response, response to temperature changes, and phosphate starvation response (March-Diaz et al., 2008; Zilberman et al., 2008; Kumar and Wigge 2010; Smith et al., 2010). H2A.Z is also important to regulate transcription of genes that are subject to more stable epigenetic regulation such as the developmental switch gene *Flowering Locus C* (*FLC*) (Deal et al., 2007; Choi et al., 2007; March-Diaz et al., 2007; Lazaro et al., 2008). Moreover, the role of H2A.Z in chromatin contributes to genomic processes such as meiosis, DNA damage repair, and homologous recombination (Rosa et al., 2013).

Multiple genes can encode H2A.Z proteins, each with their own potential sub-functionalization. Arabidopsis has three different H2A.Z proteins: HTA8/H2A.Z.8, HTA9/H2A.Z.9, and HTA11/H2A.Z.11 (Deal et al., 2007). They function largely redundantly, since depletion of any one form of H2A.Z shows no obvious phenotype, but depletion of two or more results in defects in development and immune response (Choi et al., 2007; March-Diaz et al., 2008; Coleman-Derr and Zilberman 2012). Having multiple forms of H2A.Z is not unique to plants and has been documented in many other organisms including humans (Eirin-Lopez et al., 2009).

The unique properties of H2A.Z make it an important factor for chromatin-associated processes (Jarillo and Pineiro 2015). Although 60% of the amino acid sequence is conserved between H2A and H2A.Z, H2A.Z has different residues in the docking domain where it interacts with the H3-H4 tetramer, the L1 loop where it interacts with the other H2A-H2B dimer, and at an acidic patch where H2A or H2A.Z interact with other nucleosomes or other chromatin associating proteins (Suto et al., 2000). Within chromosomes, histone H2A.Z usually localizes to the 5' ends of genes near the

transcription start sites (TSSs), however it can also localize to the 3' ends or across gene bodies of genes where it opposes transcription (Deal et al., 2007; Coleman-Derr and Zilberman 2012; Sura et al., 2017). H2A.Z also plays a role to regulate transcription from distal enhancer regions (Gevry et al., 2009; Dalvai et al., 2012; Dai et al., 2017). Histone acetylation, nucleosome free regions, and specific nucleotide sequences have all proven important for H2A.Z targeting to chromatin, but it is excluded from chromatin where DNA is methylated (Raisner et al., 2005; Coleman-Derr and Zilberman 2012; Ranjan et al., 2013). In addition to functioning at transcriptionally active regions of the genome, H2A.Z localizes to heterochromatin and opposes the spreading of heterochromatin (Meneghini et al., 2003; Swaminathan et al., 2005).

When H2A.Z is incorporated into chromatin it can act to either promote or repress transcription (Marques et al., 2010). The mechanisms of how H2A.Z contributes to transcriptional regulation have been the focus of many studies, and yet we still do not fully understand how and when H2A.Z assumes transcriptionally repressive or promoting roles. Correlative work suggests that acetylation of H2A.Z and its role at either enhancers or the 5' end of genes is associated with transcriptional activation, while ubiquitination of H2A.Z and its localization across gene bodies correlate with transcriptional repression (Marques et al., 2010; Dalvai et al 2012 Dalvai et al., 2012; Valdes-Mora et al., 2012; Valdes-Mora et al., 2017; Surface et al., 2016; Ku et al., 2012; Coleman-Derr and Zilberman 2012). The positional correlations of H2A.Z were shown in plants, however H2A.Z acetylation and ubiquitination have not been identified in plants thus far (Coleman-Derr and Zilberman 2012). An *in vitro* study demonstrated that H2A.Z-containing nucleosomes are sufficient to mediate +1 nucleosome stability which influences transcriptional initiation and can affect the rate of transcriptional elongation through chromatin (Weber et al., 2014; Rudnizky et al., 2016). However, conflicting reports about how H2A.Z contributes to chromatin organization *in vitro* and *in vivo* provide evidence that H2A.Z can stabilize or destabilize nucleosomes as well as promote or inhibit nucleosome mobility in different contexts and experimental conditions (Bönisch and Hake 2012; Hu et al., 2012; Park et al., 2004; Rudnizky et al., 2016; Li et al., 2005a; Gevry et al., 2009). Overall, it

seems that the DNA sequence, histone modifications, and nucleosome composition context in which H2A.Z is found contributes to how H2A.Z modulates nucleosome stability and positioning (Bönisch and Hake 2012).

H2A.Z not only contributes specific properties to nucleosomes, but also interacts with a unique set of factors distinct from H2A to influence transcription and chromatin organization, resulting in context specific functions (Zhang et al., 2017c; Bönisch and Hake 2012). For example, H2A.Z can recruit chromatin-associated proteins that impact chromatin organization (Surface et al., 2016). One of the ways that H2A.Z does this is by facilitating access for transcription factor binding at regulatory regions, thus influencing transcriptional initiation by mediating transcription factor activity (Hu et al., 2012). In yeast, H2A.Z and SWR1 subunits are associated with targeting loci to the nuclear periphery for transcriptional regulation (Yoshida et al., 2010; Light et al 2010 Light et al., 2010). In Arabidopsis, the SWR1 complex interacts with proteins important for anchoring chromatin to the nuclear matrix during transcriptional regulation, suggesting that H2A.Z contributes to nuclear localization in Arabidopsis by interacting with other nuclear factors (Lee and Seo 2017). H2A.Z can also interact with the Heterochromatin Protein 1 (HP1) to facilitate chromatin compaction (Fan et al., 2004). Each new study uncovering how H2A.Z interacts with other chromatin associating factors helps us get a more comprehensive picture of how H2A.Z regulates chromatin organization and transcription. Furthermore, factors antagonizing the function of H2A.Z can help us understand what pressures make its function necessary in chromatin.

SWI2/SNF2 and BRM

SWI2/SNF2 chromatin remodeling

Another chromatin remodeling complex, SWI2/SNF2, also plays a key role in regulating environmentally responsive genes and has been found to create a context that makes H2A.Z incorporation necessary for transcriptional activation in Arabidopsis (Farrona et al., 2011; Sarnowska et al., 2016). The SWI2/SNF2 complex was first isolated in yeast where it has been extensively

characterized and is conserved among yeast, humans, plants, and other organisms (Sarnowska et al., 2016). The subunits in Arabidopsis that associate to form the SWI2/SNF2 complex generally consist of an ATPase (SPLAYED, BRAHMA, MINU1, or MINU2), two SWI3(A-D) subunits, a BAF60/SWP73(A/B) homolog, two actin-related proteins (ARP4 &7), and one SNF5 subunit (BUSHY), with additional accessory proteins that can associate as well (Han et al., 2015; Li et al., 2016; Brzezinka et al., 2016; Vercruyssen et al., 2014). The SWI2/SNF2 complex thus remodels chromatin as well as mediates how other factors interact with chromatin (Sarnowska et al., 2016).

BRM acts as one of the primary ATPases of the SWI2/SNF2 complex that contributes both to transcriptional repression and activation of many genes, depending on context (Bezhani et al., 2007; Archacki et al., 2016). These genes are involved in numerous developmental functions such as cell proliferation and development, maintaining the root stem cell niche (Yang et al., 2015), leaf maturation (Efroni et al., 2013), vegetative growth and flowering time (Farrona et al., 2011, Li et al., 2015a), proper inflorescence architecture (Zhao et al., 2015), and chlorophyll biogenesis (Zhang et al., 2017a). BRM also regulates hormonal responses and responses to environmental stimuli such as GA signaling (Archacki et al., 2013), cytokinin response (Efroni et al., 2013), absciscic acid response (Han et al., 2012), drought response, and heat stress memory (Brzezinka et al., 2016).

In mammals, exchanging SWI2/SNF2 subunits provides alternate functions and is crucial for proper neural differentiation (Lessard et al., 2007). In Arabidopsis, interchanging subunits of the SWI2/SNF2 complex confer unique functions to modulate leaf development, flower development, fertility, and flower timing (Vercruyssen et al., 2014, Sacharowski et al., 2015, Buszewicz et al., 2016). For example, SWI3C preferentially associates with the ATPase BRM over other ATPase paralogs, and SWI3D and SWI3C do not purify together even though two such SWI3 subunits usually assemble into the SWI2/SNF2 complex (Vercruyssen et al., 2014). SWP73A and SWP73B have distinct functions in developmental processes. SWP73A has more specific functions relating to flowering timing, and SWP73B functions more generally in developmental processes (Sacharowski et al., 2015). Likewise, the ATPases BRM and SYD have redundant as well as unique roles in

developmental processes (Bezhani et al., 2007). The specific role of BRM in chromatin regulation is still unclear and most mechanistic insights on SWI2/SNF2 function have been provided by *in vitro* experiments. SWI2/SNF2 is targeted to chromatin by acetylated histone tails and the ATPase function of SWI2/SNF2 disrupts nucleosome-DNA interactions to contribute to changes in chromatin organization such as repositioning and changes in nucleosome occupancy (Chatterjee et al., 2011; Narlikar et al., 2013; Tolstorukov et al., 2013; Clapier et al., 2017).

In Arabidopsis, BRM has been linked to a variety of nucleosomes changes. For example, some locus-by-locus studies suggest that BRM acts to reposition, destabilize, or stabilize nucleosomes (Han et al., 2012; Wu et al., 2015; Brzezinka et al., 2016). Moreover, other SWI2/SNF2 subunits found in complex with BRM modulate nucleosome positioning and stability (Jegu et al., 2014; Sacharowski et al., 2015). SWI/SNF can also contribute to disrupting gene loops in Arabidopsis during gene repression (Jegu et al., 2014) and mammalian homologs of BRM regulate large chromatin loops (Kim et al., 2009). However, *in vivo* it is difficult to determine whether these observations are directly due to the remodeling action of BRM and the SWI2/SNF2 complex or whether they are due to factors that interact with the SWI2/SNF2 complex (Kwok et al., 2015).

BRM can associate with other factors outside of the SWI2/SNF2 complex to influence nucleosome organization. Transcription factors can recruit BRM and the SWI2/SNF2 complex and reciprocally, the SWI2/SNF2 complex is important for transcription factor binding at some loci (Wu et al., 2012, Vercruyssen et al., 2014, Efroni et al., 2013, Zhao et al., 2015, Zhang et al., 2016). The transcriptionally activating function of BRM can antagonize the repressive activity of the Polycomb Repressive Complex (Yang et al., 2015; Li et al., 2016). BRM also interacts with other histone modifiers and co-localizes with the ISWI complex that influence chromatin organization (Li et al., 2016; Brzezinka et al., 2016). The transcriptionally repressive role of BRM has also been found to antagonize the function of H2A.Z in chromatin for at least one locus in Arabidopsis, but the extent of this genetic relationship has not been investigated (Farrona et al., 2011). Therefore, BRM interacting with additional factors may have an effect on chromatin organization that is not associated with the

catalytic functions of BRM but are rather induced indirectly based on how BRM interacts with other factors.

SWR1 and SWI2/SNF functions overlap in the genome

Overlaps between the SWR1 and the SWI2/SNF2 complex

Several different lines of evidence suggest that the SWR1 and SWI2/SNF2 complexes may interact at some level to modulate chromatin structure and contribute to transcriptional regulation. The SWR1 complex and SWI2/SNF2 subunits are known to function in the same or related processes involving development and responses to stimuli (Ma et al., 2011; Archacki et al., 2016; March-Diaz et al., 2008; Coleman-Derr and Zilberman 2012). More directly, Farrona et al. (2011) showed that BRM and H2A.Z antagonistically regulate transcription of the *FLC* gene. In yeast, cooperative functions between H2A.Z and the SWI2/SNF2 complex have been proposed, since some genes require both for proper transcriptional activation based on a synthetic genetic interaction between H2A.Z and the SWI2/SNF2 complex (Santisteban et al., 2000). Furthermore, in mammals, SWI2/SNF2 subunits physically interact with H2A.Z, although the implications of this interaction have not been explored (Li et al., 2012; Zhang et al., 2017c). Although BRM and H2A.Z have overlapping functions in Arabidopsis for some general biological processes and antagonistic functions to regulate at least one locus, the extent of their genetic interaction has not been evaluated.

Scope of the dissertation

Studying how two chromatin-associating factors interact *in vivo*, we can understand specific facets of their individual functions as they relate to chromatin organization. We are particularly interested in exploring how H2A.Z incorporation by the SWR1 complex interacts with other chromatin associating factors to contribute to transcriptional regulation of genes important for responding to environmental stimuli. Since BRM and H2A.Z both appear to have context specific functions and have demonstrated antagonistic roles in transcription, we exploited this genetic

relationship to begin parsing out how BRM and H2A.Z contribute to nucleosome organization and transcriptional regulation (Fig. 1.2A).

Since the antagonistic relationship between BRM and H2A.Z was described in Arabidopsis and Arabidopsis is a well-established, multicellular model organism used for studying chromatin function, we chose to evaluate how H2A.Z function interacts with other chromatin proteins in the small flowering plant *Arabidopsis thaliana* (Farrona et al. 2011; Saez-Vasquez and Gadal 2010). Being easily cultivated, transformed, and having extensive functional genomic tools, Arabidopsis lends itself to molecular and genetic analyses (Lamesch et al., 2012). In addition to containing orthologs for the majority of human genes, the Arabidopsis genome is small (~145 MB), diploid, sequenced, and extensively annotated, making genome wide analyses practical (Arabidopsis Genome 2000; Jones et al., 2008; Lamesch et al., 2012).

In Chapter 2, I discuss my work that evaluates the genetic intersections of H2A.Z and the SWI2/SNF2 chromatin-remodeling complex, and their contributions to nucleosome organization. I did this by first evaluating the roles of H2A.Z and BRM in regulating transcript levels of targeted genes and then by measuring nucleosome stability and positioning at the genes they transcriptionally regulate (Fig. 1.2A). I was able to identify 8 different antagonistic and coordinate genetic relationships between H2A.Z and BRM in how they contribute to transcription. This included sets of genes that were not differentially expressed unless both factors were missing. This work did not find a consistent type of nucleosomal change associated with depletion of H2A.Z-containing nucleosomes. However, I provide evidence that BRM contributes to nucleosome stabilization where it binds and contributes to destabilization or repositioning of nucleosomes flanking nucleosome-depleted regions. These observations support the idea that BRM and H2A.Z do not interact in a simple antagonistic relationship, but each play a part in a much more complex network of factors that contribute to a myriad of different types of chromatin regulation.

As described before, BRM sets up a chromatin environment that makes incorporation of H2A.Z by the SWR1 complex necessary for transcriptional activation of the *FLC* gene (Farrona et al.,

2011). It is likely that there are other factors that make the transcriptional activating function of H2A.Z necessary at a locus such as *FLC* that is highly regulated at the chromatin level (He 2012). Therefore, I performed a forward genetic suppressor screen to identify additional factors that create a chromatin context that requires H2A.Z-containing nucleosomes for transcriptional activation of the *FLC* gene (Fig. 1.2B). One mutant line was identified from our screen that suppressed the requirement for H2A.Z incorporation into chromatin to get high levels of *FLC* transcription. After mutations that segregated with this phenotype were mapped, candidate causal genes were identified from the suppressor screen as potentially relieving the need for H2A.Z for *FLC* transcriptional activation. However, the causal gene remains to be validated. This work is discussed in Chapter 3.

Both of these experimental systems made important strides toward understanding the larger context in which H2A.Z functions *in vivo*. In addition to providing data sets that will be valuable for future studies of nucleosome dynamics in Arabidopsis, my findings help to generalize some locus specific observations for how BRM impacts nucleosome organization across the genome. By identifying co-targeted genes as well as transcription factor binding sites that coincide with both H2A.Z and BRM, I was able to generate new hypotheses about ways that H2A.Z and BRM may interact to regulate chromatin at light regulated genes. Future directions and greater implications of this work are discussed further in Chapter 4.

Chapter 1 Figures

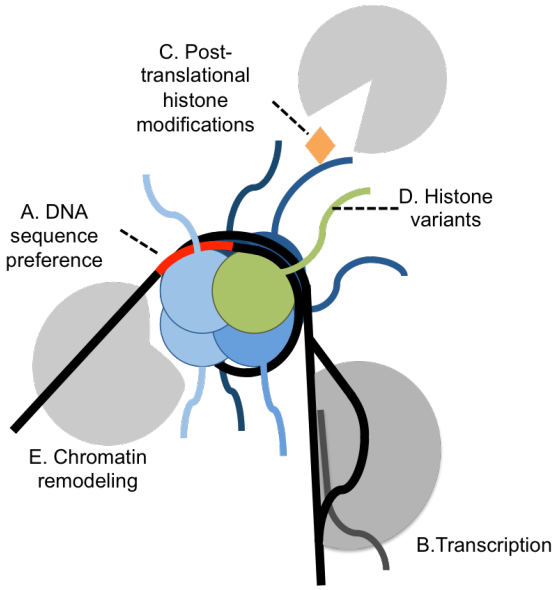

Figure 1.1. Many factors influence nucleosome position and stability. (**A**) Nucleosomes show preferences for certain nucleotide sequences. (**B**) The act of transcription or replication along a DNA strand by nucleic acid polymerases applies pressure to the interactions between DNA and nucleosomes. (**C**) Histones are post-translationally modified (shown as a gold diamond) by enzymes considered "writers," removed by "eraser" enzymes, and interpreted by "reader" proteins to regulate nucleosomal organization and DNA access. (**D**) Variants of the canonical histones confer unique properties to individual nucleosomes. (**E**) The catalytic activity of chromatin remodeling complexes associate with nucleosomes to modify nucleosome position, composition, and stability.

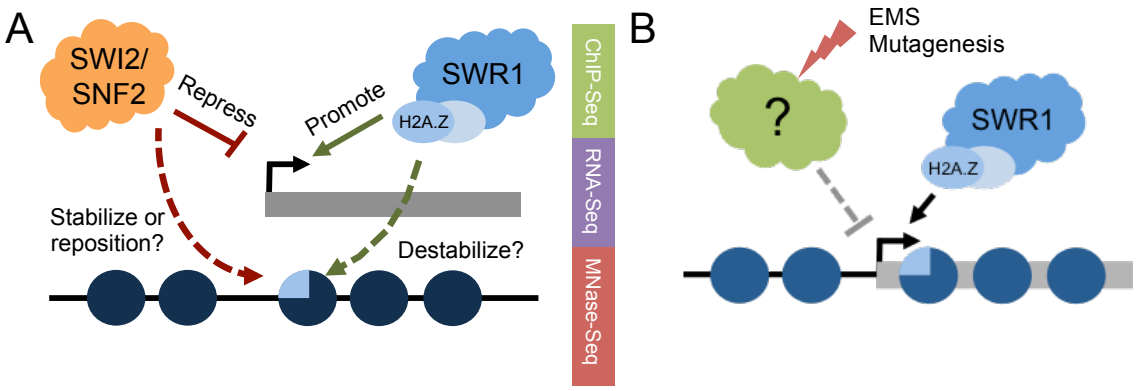

Figure 1.2. Experimental models. (**A**) Since the transcriptionally repressive function of the SWI2/SNF2 complex (orange) can make H2A.Z incorporation by the SWR1 complex (light blue) necessary for transcriptional activation, we wanted to test the extent of this antagonism across the genome. We used a three-fold genomics approach on mutants for components of each chromatin remodeling complex compared to wildtype plants (relevant experiments are listed to the right of each factor tested). We evaluated localization of a SWI2/SNF2 subunit and H2A.Z with chromatin immunoprecipitation followed by sequencing of isolated DNA (ChIP-seq, green), changes in steady state transcript levels with RNA-sequencing (RNA-seq, purple), and measured changes in nucleosome occupancy and positioning by sequencing nucleosomal DNA after digestion of chromatin with Micrococcal nuclease (MNase-seq, red). With the MNase-seq experiment combined with the ChIP-seq experiment, we tested whether BRM stabilized or repositioned nucleosomes that H2A.Z was responsible for destabilizing (shown as red and green dashed lines). (**B**) We performed EMS-mutagenesis (signified by red lightning) to conduct a forward genetic suppressor screen and identify additional antagonists (green) of the transcriptional promoting role of H2A.Z incorporation into chromatin by the SWR1 complex (light blue).

Literature Cited

Archacki R, Yatusevich R, Buszewicz D, Krzyczmonik K, Patryn J, Iwanicka-Nowicka R, Biecek P, Wilczynski B, Koblowska M, Jerzmanowski A, Swiezewski S (2016) Arabidopsis SWI/SNF chromatin remodeling complex binds both promoters and terminators to regulate gene expression. Nucleic Acids Res

Barah P, B NM, Jayavelu ND, Sowdhamini R, Shameer K, Bones AM (2016) Transcriptional regulatory networks in Arabidopsis thaliana during single and combined stresses. Nucleic Acids Res 44: 3147-64

Becker JS, Nicetto D, Zaret KS (2016) H3K9me3-Dependent Heterochromatin: Barrier to Cell Fate Changes. Trends Genet 32: 29-41

Berger SL (2007) The complex language of chromatin regulation during transcription. Nature 447: 407-12

Bieluszewski T, Galganski L, Sura W, Bieluszewska A, Abram M, Ludwikow A, Ziolkowski PA, Sadowski J (2015) AtEAF1 is a potential platform protein for Arabidopsis NuA4 acetyltransferase complex. BMC Plant Biol 15: 75

Bönisch C, Hake SB (2012) Histone H2A variants in nucleosomes and chromatin: more or less stable? Nucleic Acids Research 40: 10719-10741

Brzezinka K, Altmann S, Czesnick H, Nicolas P, Gorka M, Benke E, Kabelitz T, Jahne F, Graf A, Kappel C, Baurle I (2016) Arabidopsis FORGETTER1 mediates stress-induced chromatin memory through nucleosome remodeling. Elife 5:

Burton DR, Butler MJ, Hyde JE, Phillips D, Skidmore CJ, Walker IO (1978) The interaction of core histones with DNA: equilibrium binding studies. Nucleic Acids Res 5: 3643-63

Choi K, Park C, Lee J, Oh M, Noh B, Lee I (2007) Arabidopsis homologs of components of the SWR1 complex regulate flowering and plant development. Development 134: 1931-41

Clapier CR, Iwasa J, Cairns BR, Peterson CL (2017) Mechanisms of action and regulation of ATP-dependent chromatin-remodelling complexes. Nat Rev Mol Cell Biol 18: 407-422

Clarkson MJ, Wells JR, Gibson F, Saint R, Tremethick DJ (1999) Regions of variant histone His2AvD required for Drosophila development. Nature 399: 694-7

Coleman-Derr D, Zilberman D (2012) Deposition of histone variant H2A.Z within gene bodies regulates responsive genes. PLoS Genet 8: e1002988

Davie JR, Xu W, Delcuve GP (2016) Histone H3K4 trimethylation: dynamic interplay with pre-mRNA splicing. Biochem Cell Biol 94: 1-11

Deal R, Topp CN, McKinney EC, Meagher RB (2007) Repression of Flowering in Arabidopsis Requires Activation of FLOWERING LOCUS C Expression by the Histone Variant H2A.Z. The Plant Cell Online 19: 74-83

Derkacheva M, Hennig L (2013) Variations on a theme: Polycomb group proteins in plants. J Exp Bot

Dhar S, Gursoy-Yuzugullu O, Parasuram R, Price BD (2017) The tale of a tail: histone H4 acetylation and the repair of DNA breaks. Philos Trans R Soc Lond B Biol Sci 372:

Dion MF, Altschuler SJ, Wu LF, Rando OJ (2005) Genomic characterization reveals a simple histone H4 acetylation code. Proc Natl Acad Sci U S A 102: 5501-6

Efroni I, Han SK, Kim HJ, Wu MF, Steiner E, Birnbaum KD, Hong JC, Eshed Y, Wagner D (2013) Regulation of leaf maturation by chromatin-mediated modulation of cytokinin responses. Dev Cell 24: 438-45

Endoh M, Endo TA, Endoh T, Isono K, Sharif J, Ohara O, Toyoda T, Ito T, Eskeland R, Bickmore WA, Vidal M, Bernstein BE, Koseki H (2012) Histone H2A mono-ubiquitination is a crucial step to mediate PRC1-dependent repression of developmental genes to maintain ES cell identity. PLoS Genet 8: e1002774

Faast R, Thonglairoam V, Schulz TC, Beall J, Wells JR, Taylor H, Matthaei K, Rathjen PD, Tremethick DJ, Lyons I (2001) Histone variant H2A.Z is required for early mammalian development. Curr Biol 11: 1183-7

Farrona S, Hurtado L, March-Diaz R, Schmitz RJ, Florencio FJ, Turck F, Amasino RM, Reyes JC (2011) Brahma is required for proper expression of the floral repressor FLC in Arabidopsis. PLoS One 6: e17997

Gevry N, Hardy S, Jacques PE, Laflamme L, Svotelis A, Robert F, Gaudreau L (2009) Histone H2A.Z is essential for estrogen receptor signaling. Genes Dev 23: 1522-33

Hargreaves DC, Crabtree GR (2011) ATP-dependent chromatin remodeling: genetics, genomics and mechanisms. Cell Res 21: 396-420

He Y (2012) Chromatin regulation of flowering. Trends Plant Sci 17: 556-62

Hu G, Cui K, Northrup D, Liu C, Wang C, Tang Q, Ge K, Levens D, Crane-Robinson C, Zhao K (2012) H2A.Z Facilitates Access of Active and Repressive Complexes to Chromatin in Embryonic Stem Cell Self-Renewal and Differentiation. Cell Stem Cell

Jackson JD, Gorovsky MA (2000) Histone H2A.Z has a conserved function that is distinct from that of the major H2A sequence variants. Nucleic Acids Res 28: 3811-6

Jarillo JA, Pineiro M (2015) H2A.Z mediates different aspects of chromatin function and modulates flowering responses in Arabidopsis. Plant J 83: 96-109

Jimenez-Useche I, Yuan C (2012) The effect of DNA CpG methylation on the dynamic conformation of a nucleosome. Biophys J 103: 2502-12

Kim SI, Bresnick EH, Bultman SJ (2009) BRG1 directly regulates nucleosome structure and chromatin looping of the alpha globin locus to activate transcription. Nucleic Acids Res 37: 6019-27

Krietenstein N, Wal M, Watanabe S, Park B, Peterson CL, Pugh BF, Korber P (2016) Genomic Nucleosome Organization Reconstituted with Pure Proteins. Cell 167: 709-721 e12

Ku M, Jaffe JD, Koche RP, Rheinbay E, Endoh M, Koseki H, Carr SA, Bernstein BE (2012) H2A.Z landscapes and dual modifications in pluripotent and multipotent stem cells underlie complex genome regulatory functions. Genome Biol 13: R85

Kumar SV, Wigge PA (2010) H2A.Z-containing nucleosomes mediate the thermosensory response in Arabidopsis. Cell 140: 136-47

Lafos M, Kroll P, Hohenstatt ML, Thorpe FL, Clarenz O, Schubert D (2011) Dynamic regulation of H3K27 trimethylation during Arabidopsis differentiation. PLoS Genet 7: e1002040

Lai WKM, Pugh BF (2017) Understanding nucleosome dynamics and their links to gene expression and DNA replication. Nat Rev Mol Cell Biol 18: 548-562

Lee K, Seo PJ (2017) Coordination of matrix attachment and ATP-dependent chromatin remodeling regulate auxin biosynthesis and Arabidopsis hypocotyl elongation. PLoS One 12: e0181804

Lessard J, Wu JI, Ranish JA, Wan M, Winslow MM, Staahl BT, Wu H, Aebersold R, Graef IA, Crabtree GR (2007) An essential switch in subunit composition of a chromatin remodeling complex during neural development. Neuron 55: 201-15

Li B, Pattenden SG, Lee D, Gutiérrez J, Chen J, Seidel C, Gerton J, Workman JL (2005a) Preferential occupancy of histone variant H2AZ at inactive promoters influences local histone modifications and chromatin remodeling. Proceedings of the National Academy of Sciences of the United States of America 102: 18385-18390

Li C, Gu L, Gao L, Chen C, Wei CQ, Qiu Q, Chien CW, Wang S, Jiang L, Ai LF, Chen CY, Yang S, Nguyen V, Qi Y, Snyder MP, Burlingame AL, Kohalmi SE, Huang S, Cao X, Wang ZY, Wu K, Chen X, Cui Y (2016) Concerted genomic targeting of H3K27 demethylase REF6 and chromatin-remodeling ATPase BRM in Arabidopsis. Nat Genet 48: 687-93

Li G, Levitus M, Bustamante C, Widom J (2005b) Rapid spontaneous accessibility of nucleosomal DNA. Nat Struct Mol Biol 12: 46-53

Li Z, Gadue P, Chen K, Jiao Y, Tuteja G, Schug J, Li W, Kaestner KH (2012) Foxa2 and H2A.Z mediate nucleosome depletion during embryonic stem cell differentiation. Cell 151: 1608-16

Liu X, Li B, GorovskyMa (1996) Essential and nonessential histone H2A variants in Tetrahymena thermophila. Mol Cell Biol 16: 4305-11

Lu PY, Levesque N, Kobor MS (2009) NuA4 and SWR1-C: two chromatin-modifying complexes with overlapping functions and components. Biochem Cell Biol 87: 799-815

Luger K, Mader AW, Richmond RK, Sargent DF, Richmond TJ (1997) Crystal structure of the nucleosome core particle at 2.8 A resolution. Nature 389: 251-60

Luger K, Mader A, Sargent DF, Richmond TJ (2000) The atomic structure of the nucleosome core particle. J Biomol Struct Dyn 17 Suppl 1: 185-8

Ma KW, Flores C, Ma W (2011) Chromatin configuration as a battlefield in plant-bacteria interactions. Plant Physiol 157: 535-43

March-Diaz R, Garcia-Dominguez M, Florencio FJ, Reyes JC (2007) SEF, a new protein required for flowering repression in Arabidopsis, interacts with PIE1 and ARP6. Plant Physiol 143: 893-901

March-Diaz R, Garcia-Dominguez M, Lozano-Juste J, Leon J, Florencio FJ, Reyes JC (2008) Histone H2A.Z and homologues of components of the SWR1 complex are required to control immunity in Arabidopsis. Plant J 53: 475-87

March-Diaz R, Reyes JC (2009) The beauty of being a variant: H2A.Z and the SWR1 complex in plants. Mol Plant 2: 565-77

Marques M, Laflamme L, Gervais AL, Gaudreau L (2010) Reconciling the positive and negative roles of histone H2A.Z in gene transcription. Epigenetics 5: 267-72

Meneghini MD, Wu M, Madhani HD (2003) Conserved histone variant H2A.Z protects euchromatin from the ectopic spread of silent heterochromatin. Cell 112: 725-36

Mizuguchi G, Shen X, Landry J, Wu WH, Sen S, Wu C (2004) ATP-driven exchange of histone H2AZ variant catalyzed by SWR1 chromatin remodeling complex. Science 303: 343-8

Nagai S, Davis RE, Mattei PJ, Eagen KP, Kornberg RD (2017) Chromatin potentiates transcription. Proc Natl Acad Sci U S A 114: 1536-1541

Narlikar GJ, Sundaramoorthy R, Owen-Hughes T (2013) Mechanisms and functions of ATP-dependent chromatin-remodeling enzymes. Cell 154: 490-503

Papamichos-Chronakis M, Watanabe S, Rando OJ, Peterson CL (2011) Global regulation of H2A.Z localization by the INO80 chromatin-remodeling enzyme is essential for genome integrity. Cell 144: 200-13

Raisner RM, Hartley PD, Meneghini MD, Bao MZ, Liu CL, Schreiber SL, Rando OJ, Madhani HD (2005) Histone variant H2A. Z marks the 5′ ends of both active and inactive genes in euchromatin. Cell 123: 233

Rosa M, Von Harder M, Cigliano RA, Schlogelhofer P, Scheid OM (2013) The Arabidopsis SWR1 Chromatin-Remodeling Complex Is Important for DNA Repair, Somatic Recombination, and Meiosis. Plant Cell

Rudnizky S, Bavly A, Malik O, Pnueli L, Melamed P, Kaplan A (2016) H2A.Z controls the stability and mobility of nucleosomes to regulate expression of the LH genes. Nat Commun 7: 12958

Rymen B, Sugimoto K (2012) Tuning growth to the environmental demands. Curr Opin Plant Biol 15: 683-90

Sacharowski SP, Gratkowska DM, Sarnowska EA, Kondrak P, Jancewicz I, Porri A, Bucior E, Rolicka AT, Franzen R, Kowalczyk J, Pawlikowska K, Huettel B, Torti S, Schmelzer E, Coupland G, Jerzmanowski A, Koncz C, Sarnowski TJ (2015) SWP73 Subunits of Arabidopsis SWI/SNF Chromatin Remodeling Complexes Play Distinct Roles in Leaf and Flower Development. Plant Cell 27: 1889-906

Santisteban MS, Kalashnikova T, Smith MM (2000) Histone H2A.Z regulats transcription and is partially redundant with nucleosome remodeling complexes. Cell 103: 411-22

Sarnowska E, Gratkowska DM, Sacharowski SP, Cwiek P, Tohge T, Fernie AR, Siedlecki JA, Koncz C, Sarnowski TJ (2016) The Role of SWI/SNF Chromatin Remodeling Complexes in Hormone Crosstalk. Trends Plant Sci 21: 594-608

Schmid M, Davison TS, Henz SR, Pape UJ, Demar M, Vingron M, Scholkopf B, Weigel D, Lohmann JU (2005) A gene expression map of Arabidopsis thaliana development. Nat Genet 37: 501-6

Shogren-Knaak M, Ishii H, Sun JM, Pazin MJ, Davie JR, Peterson CL (2006) Histone H4-K16 acetylation controls chromatin structure and protein interactions. Science 311: 844-7

Simonet NG, Reyes M, Nardocci G, Molina A, Alvarez M (2013) Epigenetic regulation of the ribosomal cistron seasonally modulates enrichment of H2A.Z and H2A.Zub in response to different environmental inputs in carp (Cyprinus carpio). Epigenetics Chromatin 6: 22

Smith AP, Jain A, Deal RB, Nagarajan VK, Poling MD, Raghothama KG, Meagher RB (2010) Histone H2A.Z regulates the expression of several classes of phosphate starvation response genes but not as a transcriptional activator. Plant Physiol 152: 217-25

Sura W, Kabza M, Karlowski WM, Bieluszewski T, Kus-Slowinska M, Paweloszek L, Sadowski J, Ziolkowski PA (2017) Dual role of the histone variant H2A.Z in transcriptional regulation of stress-response genes. Plant Cell

Suto RK, Clarkson MJ, Tremethick DJ, Luger K (2000) Crystal structure of a nucleosome core particle containing the variant histone H2A.Z. Nature Structural Biology 7: 1121

Tessarz P, Kouzarides T (2014) Histone core modifications regulating nucleosome structure and dynamics. Nat Rev Mol Cell Biol 15: 703-8

Todolli S, Perez PJ, Clauvelin N, Olson WK (2017) Contributions of Sequence to the Higher-Order Structures of DNA. Biophys J 112: 416-426

Urano K, Kurihara Y, Seki M, Shinozaki K (2010) 'Omics' analyses of regulatory networks in plant abiotic stress responses. Curr Opin Plant Biol 13: 132-8

Weber CM, Ramachandran S, Henikoff S (2014) Nucleosomes are context-specific, H2A.Z-modulated barriers to RNA polymerase. Mol Cell 53: 819-30

Whittle CM, McClinic KN, Ercan S, Zhang X, Green RD, Kelly WG, Lieb JD (2008) The genomic distribution and function of histone variant HTZ-1 during C. elegans embryogenesis. PLoS Genet 4: e1000187

Wu MF, Yamaguchi N, Xiao J, Bargmann B, Estelle M, Sang Y, Wagner D (2015) Auxin-regulated chromatin switch directs acquisition of flower primordium founder fate. Elife 4: e09269

Yang S, Li C, Zhao L, Gao S, Lu J, Zhao M, Chen CY, Liu X, Luo M, Cui Y, Yang C, Wu K (2015) The Arabidopsis SWI2/SNF2 Chromatin Remodeling ATPase BRAHMA Targets Directly to PINs and Is Required for Root Stem Cell Niche Maintenance. Plant Cell 27: 1670-80

Yi H, Sardesai N, Fujinuma T, Chan CW, Veena, Gelvin SB (2006) Constitutive expression exposes functional redundancy between the Arabidopsis histone H2A gene HTA1 and other H2A gene family members. Plant Cell 18: 1575-89

Zhang T, Zhang W, Jiang J (2015) Genome-Wide Nucleosome Occupancy and Positioning and Their Impact on Gene Expression and Evolution in Plants. Plant Physiol 168: 1406-16

Zhang Y, Ku WL, Liu S, Cui K, Jin W, Tang Q, Lu W, Ni B, Zhao K (2017) Genome-wide identification of histone H2A and histone variant H2A.Z-interacting proteins by bPPI-seq. Cell Res 27: 1258-1274

Zhao Y, Garcia BA (2015) Comprehensive Catalog of Currently Documented Histone Modifications. Cold Spring Harb Perspect Biol 7: a025064

Zhu Y, Dong A, Shen WH (2013) Histone variants and chromatin assembly in plant abiotic stress responses. Biochim Biophys Acta 1819: 343-8

Zilberman D, Coleman-Derr D, Ballinger T, Henikoff S (2008) Histone H2A.Z and DNA methylation are mutually antagonistic chromatin marks. Nature 456: 125-9

CHAPTER 2: THE HISTONE VARIANT H2A.Z AND CHROMATIN REMODELER BRAHMA ACT COORDINATELY AND ANTAGONISTICALLY TO REGULATE TRANSCRIPTION AND NUCLEOSOME DYNAMICS.

E. Shannon Torres and Roger B. Deal

This work is under review for publication in *Plant Physiology*.

Abstract

Plants adapt to changes in their environment by regulating transcription and chromatin organization. The histone H2A variant H2A.Z and the SWI2/SNF2 ATPase BRAHMA have overlapping roles in positively and negatively regulating environmentally responsive genes in *Arabidopsis*, but the extent of this overlap was uncharacterized. Both have been associated with various changes in nucleosome positioning and stability in different contexts, but their specific roles in transcriptional regulation and chromatin organization need further characterization. We show that H2A.Z and BRM act both cooperatively and antagonistically to contribute directly to transcriptional repression and activation of genes involved in development and response to environmental stimuli. We identified 8 classes of genes that show distinct relationships between H2A.Z and BRM and their roles in transcription. We found that H2A.Z contributes to a range of different nucleosome properties, while BRM stabilizes nucleosomes where it binds and destabilizes and/or repositions flanking nucleosomes. H2A.Z and BRM contribute to +1 nucleosome destabilization, especially where they coordinately regulate transcription. We also found that at genes regulated by both BRM and H2A.Z, both factors overlap with the binding sites of light-regulated transcription factors PIF4, PIF5, and FRS9, and that some of the FRS9 binding sites are dependent on H2A.Z and BRM for accessibility. Collectively, we comprehensively characterized the antagonistic and cooperative contributions of H2A.Z and BRM to transcriptional regulation, and illuminated their interrelated roles in chromatin

organization. The variability observed in their individual functions implies that both BRM and H2A.Z have more context-specific roles within diverse chromatin environments than previously assumed.

Introduction

As sessile organisms, plants have evolved a plethora of physiological responses to deal with adverse environmental conditions. External signals are often transmitted to the nucleus, triggering a transcriptional response network that facilitates a multidimensional response to the external stimuli (Rymen and Sugimoto 2012; Barah et al., 2016, Urano et al., 2010) In eukaryotes, DNA associates with histones and other nuclear proteins to form a highly condensed chromatin structure. The arrangement of these proteins can either facilitate or obstruct transcription factor (TF) binding to target regulatory sequences, and therefore impact the ability of transcriptional machinery to modulate these transcriptional responses (Weber et al., 2014; Lai and Pugh 2017).

At its most basic level, chromatin is made up of DNA wrapped around an octamer of histones to form nucleosomes (Luger et al., 1997). Chromatin-binding proteins such as histone post-translational modifying enzymes and chromatin remodelers interact with nucleosomes and influence their positioning, stability, and and ability to interact with other proteins, thus regulating DNA accessibility (Vergara and Gutierrez 2017). Chromatin remodeling complexes (CRCs) use the energy of ATP to disrupt the interaction between DNA and histones in order to evict nucleosomes, eject histone dimers, slide nucleosomes, or exchange canonical histones for variant forms (Narlikar et al., 2013; Clapier et al., 2017). Chromatin remodeling is a key part of regulating genome stability, DNA replication, DNA damage repair, and transcription, which in turn affects development, homeostasis, and how an organism responds to changes in the environment (Probst and Mittelsten Scheid 2015; Vergara and Gutierrez 2017).

The combined effects of many chromatin-regulating proteins at a locus create opposing and redundant forces that maintain proper transcription level and integrate a myriad of endogenous and exogenous signals (Vergara and Gutierrez 2017). One way to define the individual contributions of

chromatin regulating factors *in vivo* is to evaluate how such proteins coordinately or antagonistically contribute to chromatin organization and transcription. Studies in *Arabidopsis thaliana* evaluating the histone H2A variant H2A.Z, which is deposited by the SWR1 CRC, and the SWI2/SNF2 CRC separately have revealed that they both modulate chromatin organization and transcription to regulate developmental processes and responses to the environment (Wu et al., 2015; Lee and Seo 2017). More directly, Farrona et al. (2011) proposed that the SWI2/SNF2 ATPase BRAHMA (BRM) and the incorporation of H2A.Z into chromatin by the SWR1 CRC have antagonistic roles to modulate *Flowering Locus C* (*FLC)* transcription levels and the developmental timing of flowering. In yeast, mutations in H2A.Z increase dependence on the SWI2/SNF2 complex for transcriptional activation of several genes, implying that the histone variant and chromatin remodeler have cooperative functions (Santisteban et al., 2000). Furthermore, in mammals, SWI2/SNF2 subunits interact with H2A.Z, although the implications of this interaction have not been explored (Li et al., 2012; Zhang et al., 2017c). While the SWR1 CRC and the SWI2/SNF2 complex have parallel roles in development and environmental responses in plants, there is a dearth of studies that focus on the direct intersection of these two complexes in chromatin and transcriptional regulation. Since an antagonistic relationship was already established between H2A.Z and BRM at the *Arabidopsis FLC* gene, we decided to characterize the extent to which these two factors interact in chromatin organization and transcriptional regulation.

In this study, we demonstrate that H2A.Z and BRM interact to impact nucleosome organization and regulate transcription across the *Arabidopsis* genome. We assessed the overall and direct transcriptional contributions of H2A.Z and BRM by performing transcriptional profiling in combination with BRM and H2A.Z localization information in wild type, single, and double mutants. Using mutants lacking BRM, mutants for the ARP6 subunit of the SWR1 CRC that are defective in H2A.Z incorporation into chromatin, or double mutants depleted for both, we identified 8 different classes of co-targeted genes where transcription is coordinately or antagonistically regulated by H2A.Z and BRM, including genes that are up- or down- regulated only in double mutants. The genes

regulated by both H2A.Z and BRM contribute to a number of biological processes, including development and responses to various stimuli. By experimentally verifying that these genes are direct targets of H2A.Z or BRM, the regulatory relationships we identified allude to cooperative and antagonistic functions between BRM and H2A.Z in chromatin regulation and transcription.

We further explored how BRM and H2A.Z contribute to nucleosome organization to facilitate these transcriptional changes by measuring nucleosome occupancy and positioning. We found that BRM is involved in nucleosome stabilization at nucleosome-depleted regions (NDR), both distal and proximal to the transcription start sites (TSS), and contributes to destabilization and/or repositioning of flanking nucleosomes. On the other hand, H2A.Z-containing nucleosomes show highly variable changes in nucleosome properties upon H2A.Z depletion. At loci where both H2A.Z and BRM are found together in the genome, BRM usually destabilizes nucleosomes, especially the +1 nucleosome, while H2A.Z can also destabilize +1 nucleosomes at some loci. In addition, we identified binding sites of light-responsive TFs PIF4, PIF5, and FRS9 that are enriched at BRM and H2A.Z co-targeted genes, and show that nucleosome occupancy is dependent on BRM and H2A.Z at some FRS9 binding sites. These findings point to a role for both H2A.Z and BRM in regulating nucleosome positioning and stability in coordinately and antagonistically regulated genes involved in light response and other responses to stimuli. Collectively, our findings indicate that the relationship between BRM and H2A.Z is more complex than solely antagonizing or complementing the chromatin organizing function of the other, and our datasets will be useful for future studies to explore the contexts in which BRM and H2A.Z contribute to chromatin organization or transcriptional regulation.

Results

Analysis of transcriptional changes in arp6 *and* brm *mutants*

Both H2A.Z and BRM contribute to transcriptional repression and transcriptional activation, but it is unknown how the presence of one might affect the role of the other in transcriptional regulation. (Marques et al., 2010; Archacki et al., 2016). To identify the genes in *Arabidopsis* that are

transcriptionally regulated by BRM and H2A.Z, we performed RNA sequencing (RNA-seq) experiments. We used plants with the *brm-1* allele, since it was previously characterized as a BRM null mutant (Hurtado et al., 2006). To study plants with H2A.Z-depleted nucleosomes, we used null mutants for the ARP6 component of the SWR1 chromatin remodeling complex (CRC) which is responsible for incorporating H2A.Z into nucleosomes (Deal et al., 2007). In *Arabidopsis*, three genes encode the pool of H2A.Z proteins and there are no completely null triple H2A.Z mutants available, which complicates genetic work (Coleman-Derr and Zilberman 2012). Other studies have verified that ARP6 is required for proper H2A.Z incorporation into nucleosomes and *arp6* mutants phenocopy H2A.Z mutants, making *arp6* mutants a logical proxy for H2A.Z mutants in our genetic study (Sura et al., 2017; March-Diaz et al., 2008; Berriri et al., 2016). Therefore, we identified the genes that are differentially expressed (DE) in *brm-1* mutants, *arp6-1* mutants, and *arp6-1;brm-1* double mutants compared to wild type (WT) plants. We focused our analyses on genes that had >1.5x fold change and a false discovery rate of <0.2. We chose this less stringent cutoff so as to avoid excluding true positives while describing general processes regulated by ARP6. We later use additional criteria to identify specific genes for downstream analyses. RNA was isolated from above soil, green tissue from developmentally staged plants with 4-5 leaves. We collected tissue based on developmental stage instead of age of the plant because *brm* and *arp6;brm* double mutants present delayed developmental progression (Boyes et al., 2001;Hurtado et al., 2006). After performing RNA-seq, we identified 2,109 genes that were DE in *arp6* (1,036 genes up-regulated and 1,073 genes down-regulated), 4,250 genes DE in *brm* (2,317 genes up and 1,933 genes down), and 3,203 genes DE in *arp6;brm* mutants (1,517 genes up and 1,686 genes down) (Fig. 2.1A). To determine the general processes influenced by ARP6 and BRM, we identified overrepresented gene ontology (GO) terms associated with all DE genes in each mutant compared to WT.

In *Arabidopsis*, BRM regulates many developmental processes and responses to environmental stimuli, and integrates signals to allocate resources between stress response and growth (Farrona et al., 2011; Han et al., 2012; Wu et al., 2012; ; Efroni et al., 2013; Archacki et al., 2013; Li

et al., 2015a; Yang et al., 2015; Zhao et al., 2015; Archacki et al., 2016; Brzezinka et al., 2016; Zhang et al., 2016). H2A.Z also facilitates the transcriptional activation and repression of environmentally responsive genes (Coleman-Derr and Zilberman 2012; Berriri et al., 2016; Sura et al., 2017). In our data, we find a similar enrichment for DE genes in *arp6* and *brm* mutants related to responses to environmentally regulated genes, development, and transcriptional regulation (Fig. 2.2A-C). GO terms specifically overrepresented in the DE genes in *arp6* mutants include rRNA processing/modification, response to gibberellin stimulus, and defense response to virus (Fig. 2.2A). GO terms specific to the DE genes in *brm* mutants include peptide transport, pollen-pistil interaction, cold acclimation, systemic acquired resistance, and translation, and some unique responses to hormones and abiotic stimuli (Fig. 2.2C).

GO terms that were significantly overrepresented among DE gene sets from both *brm* and *arp6* mutants include responses to stimuli, regulation of transcription, and regulation of metabolic processes (Fig. 2.2B). Stimuli highlighted by the analysis include external biotic stimuli such as response to bacterium or fungus, innate immune response, and defense response; endogenous stimuli such as hormone stimuli (jasmonic acid or salicylic acid); and abiotic stimuli such as cold, wounding, salt, osmotic stress, or oxidative stress, many of which have been reported previously (Coleman-Derr and Zilberman 2012; Berriri et al., 2016; Li et al., 2016; Archacki et al., 2016). Although many terms are shared between the lists of differentially expressed genes in *arp6* and *brm* mutants, it is worth noting that the actual genes that are associated with a shared term are not always the same. This suggests that ARP6 and BRM contribute to similar general processes, albeit in some cases by affecting different genes.

Assessing H2A.Z and BRM localization

Although many genes are DE in *arp6* and *brm* mutants, these are not necessarily direct targets of H2A.Z or BRM. Since ‘regulation of transcription’ is a GO term enriched in DE gene sets from each mutant, the gene products that are mis-expressed in the mutants may go on to cause

secondary changes in transcription. To identify the genes directly targeted by H2A.Z and BRM, we analyzed our RNA-seq data in combination with data from BRM and H2A.Z chromatin immunoprecipitation experiments followed by sequencing (ChIP-seq). To assess BRM localization, we used previously published BRM-GFP ChIP-seq peaks generated from 14 day-old seedlings grown on plates (Li et al., 2016). Archacki et al. (2016) compared these ChIP-seq sites to their BRM ChIP-chip sites generated from 3 week-old plants grown on soil. The authors saw that even in different growth conditions and a different developmental stage, which consequently included different tissues, BRM was stably associated with similar sites with significant overlap between the two data sets (Archacki et al., 2016). Since our WT plants are at the same developmental stage as the published BRM ChIP-seq data we selected, we are confident that they sufficiently represent BRM localization for our experiments.

To assess H2A.Z localization relative to DE genes, we performed ChIP-seq for H2A.Z on green tissue from developmentally staged plants with 4-5 leaves from *arp6* mutants*, brm* mutants, and WT plants. Once sequence reads were mapped to the genome, Homer software (Heinz et al., 2010) was used to determine significant peaks in ChIP-seq read signal indicative of H2A.Z localization within each genotype. Since we are using *arp6* mutants as a proxy for H2A.Z mutants, we plotted H2A.Z ChIP-seq read signal from *arp6* mutants at H2A.Z peaks and confirmed that nucleosomes that normally contain H2A.Z are depleted of it in *arp6* mutants (Fig. 2.3A). To focus our analysis on sites where H2A.Z localization is dependent on ARP6, we removed the few H2A.Z peaks called in WT that overlapped with peaks called in *arp6* mutants (n=801). This left us with 11,877 ARP6-dependent H2A.Z peaks to assess how H2A.Z localization relates to transcriptional changes observed in the *arp6* mutants.

Identifying differentially expressed H2A.Z and BRM target genes

To determine which of the transcriptional changes detected in our RNA-seq data are directly associated with H2A.Z and BRM localization, we identified DE target genes for either factor by

integrating transcriptome data with H2A.Z and BRM ChIP-seq data. If an H2A.Z or BRM ChIP-seq peak fell within a gene body or if the closest TSS to a binding site was a DE gene, the gene was considered a target of that factor. Only 471 (45%) of up- and 449 (42%) of down-regulated *arp6* DE genes are directly associated with an ARP6-dependent H2A.Z peak (Fig. 1B,C). In *brm* mutants, 1,552 (67%) of up- and 786 (41%) of down-regulated genes are direct targets of BRM (Fig. 2.1B,C). In *arp6;brm* double mutants, the changes in gene expression were considered direct effects of the mutations if they were targets for H2A.Z, BRM, or both. Therefore, 1,082 (71.3%) were up- and 1,058 (62.8%) were down-regulated targets of either factor in the *arp6;brm* mutants (Fig. 2.1B,C). Therefore, we defined H2A.Z and BRM DE target genes 1) by RNA-seq data showing that the genes are DE in the *arp6*, *brm,* or *arp6;brm* mutants respectively, as well as 2) using ChIP-seq data to confirm that H2A.Z or BRM are normally found at these genes in WT plants. From this point on in the study, we focused our analysis on the DE BRM and ARP6-dependent H2A.Z target genes as genes whose transcription is directly regulated by H2A.Z/ARP6 and BRM. Collectively, the defined DE target genes support the notion that both BRM and H2A.Z contribute to gene repression and activation in different contexts (Marques et al., 2010; Archacki et al., 2016).

H2A.Z and BRM directly regulate transcription of developmental and environmental response genes

To better understand what types of genes are directly targeted by H2A.Z and BRM, we performed a GO analysis on DE genes in each mutant that are direct targets of both factors. We identified many interconnected terms for genes targeted by both H2A.Z and BRM that relate to development/growth and responses to environmental stimuli (esp. fungal response, osmotic stress, cold, and light) and hormones (auxin, ethylene, jasmonic acid, salicylic acid) (Fig 2.2F,G). Demonstrating the interconnected nature of these terms, we know that the plant transcriptional network for responding to cold shares components with both defense and light stimuli responses (Catala et al., 2011; Barah et al., 2016). Also, the hormone response and metabolic process terms

identified also relate to various aspects of defense response (Alazem and Lin 2015; Hiruma et al., 2010; Alazem and Lin 2015).

The DE genes that are direct targets of either H2A.Z in *arp6* mutants or BRM in *brm* mutants are individually enriched for similar GO terms as the list of GO terms that describe the total list of DE genes in either mutant. Of note, response to giberellin and red light were processes enriched in the DE target genes from either *arp6* or *brm* mutants individually, even though they were not processes that were overrepresented in the list of genes that are targets of both H2A.Z and BRM (Fig. 2.2D,E). Also, GO terms relating to aging and sensence were enriched in the list of BRM targets uniquely DE in *brm* mutants, but were not identified in the total list of DE genes and have not been reported before in BRM studies (Fig. 2.2E). Further work to understand whether any of these transcriptional changes produce phenotypes that are present in the *arp6;brm* double mutants, but not the single mutants will show whether BRM and H2A.Z have addititve, redundant, or antagonistic roles in these processes.

H2A.Z and BRM coordinately and antagonistically regulate gene transcription

Since Farrona et al. (2011) suggested that H2A.Z and BRM antagonistically regulate transcription of the *FLC* gene in *Arabidopsis*, we wanted to test whether this antagonistic relationship extends to other genes across the genome. We also tested the hypothesis that H2A.Z and BRM could work together to regulate gene transcription as suggested by their roles in yeast (Santisteban et al., 2000). After verifying which differentially expressed genes are direct targets of H2A.Z and BRM using ChIP-seq data, we identified 8 gene classes that are either coordinately or antagonistically regulated by H2A.Z and BRM based on whether their transcript levels changed in one or more mutants (Fig. 2.1D). To describe these gene classes, we will refer to genotypes and transcriptional changes with the following abbreviations: A=*arp6-1*, B=*brm-1*, D=*arp6-1;brm-1* double mutant, "+" = genes up-regulated in the specified mutant, "-" = genes down-regulated in the specified mutant, "=" = genes not DE in the specified mutant, n = number of genes in the class. We first identified genes that are coordinately regulated by H2A.Z/ARP6 and BRM. This category includes target genes that

are up-regulated in both *arp6-1* and *brm-1* mutants compared to WT plants (Class 1: A+, B+, n=70), targets down-regulated in both *arp6* and *brm* mutants relative to WT (Class 2: A-, B-, n=51), and target genes with no change in transcript level in the individual mutants, but that are up- (Class 3: A=,B=,D+, n=159) or down-regulated (Class 4: A=, B=, D-, n=88) in the *arp6;brm* double mutants relative to WT (Fig. 2.1D,E). Classes 1 and 2 indicate that both H2A.Z and BRM are independently required for the proper regulation of these genes (Fig 2.1E). Classes 3 and 4 are DE target genes in the double mutants but not the single mutants, which are particularly interesting because these are genes where BRM and H2A.Z are presumed to work redundantly (Fig. 2.1E).

We also identified different classes of target genes where H2A.Z and BRM act antagonistically. This category of genes includes those either up- or down-regulated in a single mutant but that are neither DE in the other mutant nor the double mutant (Class 5: A+, B=, D=, n=91; Class 6: A-, B=, D=, n=99; Class 7: A=, B+, D=, n=324; Class 8: A=, B-, D=, n=305) (Fig. 2.1D,E). Since the loss of the second factor suppresses the change in transcript levels observed in the single mutant, H2A.Z and BRM seem to have opposing functions at these genes that become evident in the single mutants (Fig. 2.1E). Using class 5 as an example, these are H2A.Z and BRM target genes that have increased transcript levels in the *arp6* mutants when H2A.Z is depleted from nucleosomes (Fig. 2.1D). These same genes however are no longer significantly differentially expressed relative to WT when BRM is also depleted in the double mutants (Fig. 2.1D). Therefore, it seems that H2A.Z does not merely play a repressive role at these genes but does so by opposing the positive regulatory contribution of BRM at genes in class 5 (Fig. 2.1E). Alternatively, at genes in class 6, H2A.Z opposes the repressive role of BRM (Fig. 2.1E). Reciprocally, BRM also opposes the positive and negative contributions of H2A.Z to transcriptional regulation in classes 7 and 8, respectively. The mechanisms behind how H2A.Z and BRM positively and negatively regulate transcription at these genes, and how one opposes the function of the other still remain to be determined.

To determine the processes that may be influenced by each genetic interaction between H2A.Z and BRM, we evaluated GO terms for biological processes significantly enriched in our 8

coordinately or antagonistically regulated gene sets. Genes in Class 4 (A=,B=,D-) do not have any significantly enriched GO terms, but the other classes were enriched for developmental and responsive processes. Response to light stimulus is enriched in three gene classes (Class 6: A-, B=, D=; Class 7: A=,B+, D=; Class 8: A=,B-, D=), response to karrakin is enriched in 5 classes (Class 3: A=, B=, D+; Class 5: A+ ,B=, D=; Class 6: A-, B=, D=; Class 7: A=, B+, D=; Class 8: A=, B-, D=), and plant-pathogen interaction and defense response to fungus are enriched for three gene sets that include genes that are up-regulated in one or both genotypes (Class 1: A+, B+; Class 5: A+, B=, D=; Class 7: A=, B+, D=). Additionally, sequence-specific DNA binding transcription factor activity was enriched for 5 out of the 8 gene sets, emphasizing the roles of BRM and H2A.Z again in modulating other processes indirectly by controlling the expression of transcriptional regulators. The GO terms collectively enriched for genes in the 8 classes of H2A.Z and BRM co-targets DE in at least one mutant are similar to those target genes DE in both mutants (Fig. 2.2F,G).

H2A.Z localization is not dependent on BRM

One explanation for how BRM and H2A.Z/ARP6 could coordinately regulate gene expression (i.e. Figure 2.1E, Classes 1-4) is that BRM may regulate H2A.Z levels in chromatin. To assess whether BRM is important for H2A.Z occupancy, we analyzed H2A.Z levels at regions significantly enriched for H2A.Z in either WT plants or *brm* mutants. Some sites with significant H2A.Z localization in WT plants were not identified as significant in *brm* mutants based on peak calling parameters, and reciprocally, some sites of enrichment were identified in *brm* mutants but not in WT plants (Fig. 2.3A). To see if sites unique to one genotype represent sites of H2A.Z depletion or gain in *brm* mutants, we plotted the H2A.Z ChIP-seq read signal from WT and *brm* plants across these regions of H2A.Z enrichment unique to either genotype. We observed comparable levels of H2A.Z enrichment in both genotypes even though the read signal did not meet the peak calling threshold for both genotypes (Fig. 2.3B). Since we only observed marginal differences between in

H2A.Z levels in *brm* mutants and WT plants, this suggests that H2A.Z levels in chromatin are not generally dependent on BRM.

BRM contributes to nucleosome stability and positioning at nucleosome-depleted regions.

The chromatin remodeling roles of BRM as a SWI2/SNF2 ATPase and H2A.Z incorporation into nucleosomes by the SWR1 CRC both can affect nucleosome stability and positioning at individual loci (Han 2012; Wu et al 2012; Brzezinka et al., 2016; Rudnizky et al., 2016). Identifying sites where both H2A.Z and BRM influence chromatin organization allows us to determine whether the presence of one could antagonize or enhance the chromatin modulating function of the other. To assess the genome wide contributions of H2A.Z and BRM to nucleosome organization, we performed Micrococcal Nuclease (MNase) digestion followed by sequencing (MNase-seq) on green tissue from 4-5 leaf developmentally-staged *arp6, brm,* and *arp6;brm* and WT plants. The endonuclease activity of MNase specifically digests nucleosome-free DNA and leaves behind nucleosome-protected DNA, which provides a measure of where and how often a nucleosome is associated with a locus in our material (Allan et al., 2012). Thus, MNase-seq experiments allow us to evaluate how H2A.Z and BRM influence nucleosome occupancy and positioning (Allan et al., 2012; Zhang et al., 2015). Using H2A.Z and BRM ChIP-seq data, we evaluated nucleosomal changes that occur in our mutants at sites enriched for either H2A.Z, BRM, or both in order to focus our analysis and describe ways H2A.Z and BRM influence nucleosome stability and positioning.

To survey to what extent BRM contributes to nucleosome occupancy and positioning across the genome, we evaluated nucleosome dynamics in *brm* mutants compared to WT plants using MNase-seq data. By plotting nucleosome levels across sites where BRM localizes, we found that BRM is enriched at nucleosome-depleted regions (NDRs) and is often flanked on either side by well-positioned nucleosomes (Fig. 2.4A). Some of these well-positioned flanking nucleosomes become more stable in the absence of BRM in the *brm* mutant, suggesting that BRM contributes to nucleosome destabilization at the regions bordering where it binds. These results support previous

findings that have shown another SWI2/SNF2 subunit also localizes to NDRs (Jegu et al., 2017). They also expand on the observation that BRM localizes between two well-positioned nucleosomes in a site-specific study since we show that finding two well-positioned nucleosomes flanking BRM sites is a genomic trend (Wu et al., 2015).

The well-positioned nucleosomes on either side of the BRM peaks could play a role in transcriptional regulation and be impacted specifically where we see transcriptional changes in *brm* mutants. To test whether these well-positioned nucleosomes are impacted by changes in transcription, we plotted the nucleosome signals from WT and *brm* mutants around BRM ChIP-seq peaks that were located either upstream of TSSs or spanning the TSSs of genes that are either up- or down-regulated in *brm* mutants relative to WT plants (Fig. 2.4B-D). When BRM localizes to the TSS of a gene that is either up- or down-regulated, one well-positioned nucleosome was found up-stream of the TSS, but to the downstream side of the BRM ChIP-seq peak DNA was more accessible to MNase digestion (Fig. 2.4B,D). One explanation for this is that BRM localization actually extends past the defined BRM peaks. However, by plotting BRM ChIP-seq signal at defined BRM ChIP peaks, we find that the more open chromatin conformation extends past BRM enriched sites in the direction of transcription (Fig. 2.5A). Another explanation is that other factors may override the contribution BRM makes to nucleosome positioning downstream of BRM peaks, so that there is a more dispersed nucleosome signal relative to BRM binding when genes are transcribed. Based on the nucleosome average plot profiles, there were no significant changes in nucleosome occupancy at BRM peaks at either up- or down-regulated genes in *brm* mutants compared to WT, although there was some increase in nucleosome occupancy directly downstream of where BRM localized (Fig. 2.4B). When BRM is found upstream of the TSS, it is still flanked by well-positioned nucleosomes on both sides (Fig 2.4B). K-means clustering did not indicate that there were any subsets of upstream BRM peaks that might show the same degree of directionality that was observed for peaks that associate with TSSs (Fig. 2.5B). Together, the nucleosome patterns at BRM peaks support the notion that BRM binds both to the NDR adjacent to the TSS and also to upstream sites with open chromatin structure, such as

regulatory regions within promoters or enhancers. We do not observe notable changes in nucleosome occupancy across all sites where BRM localizes when we compare between WT and *brm* mutant nucleosomes (Fig. 3A). Therefore, in a general sense it seems that BRM is not required to produce these NDRs but may perform other functions once targeted there.

Since locus specific studies have described roles for BRM and other SWI2/SNF2 subunits in nucleosome positioning and destabilization, we decided to quantify how often BRM is associated with different types of nucleosome dynamics (Han et al 2012; Wu et al., 2015; Brzezinka et al., 2016; Sacharowski et al., 2015). Using DANPOS2 software, nucleosomes were defined as dynamic if they had significant changes in nucleosome positioning (different position of nucleosome read summits), occupancy (different height of nucleosome read summits), fuzziness (difference in the standard deviation of nucleosome read positions), or any combination of the three in mutants relative to nucleosomes in WT tissue (Chen et al., 2013). We found that 25% of BRM peaks have significant nucleosome changes in *brm* mutants (based on an FDR cutoff of <0.05) (Fig. 2.6B). The chromatin landscape flanking BRM binding sites appears to have different nucleosome occupancy levels in *brm* mutants than those within BRM bindings sites, based on the previous nucleosome read plots (Fig 32.4A). Therefore, we evaluated whether the types of nucleosome changes at the bordering regions of BRM ChIP-seq peaks are enriched for different types of changes than what is observed for nucleosomes found where BRM directly associates within peak centers (illustrated in Fig. 2.6A). For this purpose, we defined BRM peak borders as a ± 200 bp range around the start or end of a BRM ChIP-seq peak to describe how BRM contributes to nucleosome dynamics at the well-positioned nucleosomes that flank BRM sites (Fig. 2.6A). We further separated peaks into size quartiles so that the largest and smallest peaks would not skew observations at intermediate sized peaks. This also allows for a more relative comparison between changes observed within the standard 400 bp sized border regions we defined and the BRM ChIP-seq peak centers, which have variable sizes (from 300 bp to 4kb).

To identify how often nucleosome occupancy, positioning, or fuzziness depends on BRM, we quantified the proportion of different types of nucleosome changes that are observed among all nucleosomes considered dynamic between WT plants and *brm* mutants. Evaluating the *brm* mutant genome as a whole, 35% of the nucleosomes that change in *brm* mutants experience a decrease in occupancy. However, specifically evaluating changes that take place where BRM localizes directly (peak centers, and particularly the smaller ones in Q1 & Q2), 55% of the dynamic nucleosomes show decreases in occupancy (Fig. 2.6C). Similarly, 15% of the nucleosomes that change across the genome experience an increase in fuzziness in *brm* mutants, while 25-30% of the nucleosomes in smaller BRM peak centers experience an increase in fuzziness (Fig. 2.6D). This enrichment for decreased nucleosome occupancy in combination with enrichment for increased nucleosome fuzziness at BRM peaks in *brm* mutants suggests that BRM contributes to the stability of any nucleosomes that are found where BRM binds (Fig. 2.6A).

Next, we measured the types of nucleosomal changes that occur in *brm* mutants in the regions flanking BRM peaks in comparison to the types of changes directly where BRM binds. The proportion of dynamic nucleosomes that have increases in fuzziness and decreases in occupancy at BRM peak borders is comparable to the levels seen across the genome (Fig. 2.6C,D). However, the nucleosomes at BRM peak borders at lower quartiles show a greater proportion of nucleosome position changes (30-33%) relative to the proportion observed across the genome (25%) or at BRM peak centers (approx. 25%) (Fig. 2.6E). Of the nucleosomes that change at BRM peak borders in *brm* mutants, a greater proportion experience increases in occupancy than decreases in occupancy or changes in positioning or fuzziness (Fig. 2.6C-F). Therefore, our MNase-seq data in combination with BRM ChIP-seq data demonstrate that BRM localizes to NDRs and contributes more to nucleosome stability where it directly associates with chromatin, while contributing more to destabilization or the positioning of flanking nucleosomes (Fig. 2.6A).

H2A.Z has a variable influence on the surrounding nucleosome landscape

When H2A.Z is incorporated into nucleosomes, it can change both intra-nucleosomal interactions as well as the interactions between nucleosomes and other nuclear proteins (Bonisch and Hake 2012). Consequently, H2A.Z-containing nucleosomes have been associated with a range of nucleosome dynamics including changes in nucleosome stability and positioning (Bonisch and Hake 2012; Rudnizky et al., 2016). Before assessing whether specific types of nucleosomal changes are enriched at sites where H2A.Z is found in relation to BRM function, we used MNase-seq experiments to evaluate whether H2A.Z-containing nucleosomes are enriched for specific types of nucleosomal changes in *arp6* mutants compared to WT plants.

When we evaluated nucleosome occupancy in the *arp6* mutants, we noticed there were large gaps in nucleosome read signal (Fig. 2.7). We then compared our *arp6* MNase-seq nucleosome signals to *arp6* genomic DNA and found that the gaps in nucleosome read signal correspond to large genomic deletions in the *arp6* mutants (Fig. 2.7). These deletions would skew our MNase-seq results, making them appear as a loss of a nucleosome in the mutant compared to WT when instead there was a loss of genomic DNA in this mutant line. We therefore mapped the mutations using CNVnator software which reported 1,545 deletions (>200 bp) compared to the TAIR10 reference genome (Abyzov et al., 2011). Although some of these deletions are strain differences since they were also missing in our WT plants compared to the reference genome, the total deleted portion collectively covers 5.88 megabases of DNA, which is a large portion of the ~145 megabase Arabidopsis genome (Bevan and Walsh 2005). To ensure that we are analyzing nucleosome dynamics at regions of the genome that are present in *arp6* and *arp6;brm* mutants, we removed nucleosomes from our analysis if they were called as dynamic by DANPOS2 but also overlapped with deleted regions. We also required a minimum of 1 read per 10 bp area visualized as a cutoff when analyzing nucleosome plot profiles to exclude missing regions from our analyses.

By using MNase-seq data in combination with our H2A.Z ChIP-seq data, we evaluated whether specific types of nucleosomal changes (changes in positioning, occupancy, or fuzziness) were enriched at nucleosomes that normally contain H2A.Z, but that are depleted of H2A.Z in *arp6*

mutants. Only a fraction of nucleosomes that normally contain H2A.Z in WT plants (14.6%, Fig. 2.8A) had significant changes when comparing nucleosomes in *arp6* plants using the DANPOS2 software. A similar, yet slightly higher proportion of the H2A.Z sites associated with up- or down-regulated genes in the *arp6* mutants contained significant nucleosome changes of at least one type, considering that 17.5% of H2A.Z peaks at genes down-regulated and 18.3% of H2A.Z peaks at gene up-regulated have significant nucleosome changes (Fig. 2.8A). After accounting for the deleted regions, we quantified the proportion of nucleosomes that changed in *arp6* mutants that had changes in occupancy, fuzziness, or positioning, using the same definitions we used to analyze nucleosomal changes in *brm* mutants. Using H2A.Z ChIP-seq peaks to focus our analysis, we found that the collection of nucleosomes that normally contain H2A.Z in WT but lose H2A.Z in *arp6* mutants experience both increases and decreases in fuzziness, increases and decreases in occupancy, and changes in positioning (these categories are not mutually exclusive) (Fig. 2.8B and Fig. 2.9A-C). We further evaluated whether H2A.Z-containing nucleosomes are enriched for any particular type of nucleosomal change in comparison to the levels that are observed across the genome. Even though H2A.Z has comparable levels of nucleosomes that experience increases and decreases in fuzziness upon H2A.Z depletion in *arp6* mutants (Fig. 2.8B), the proportion of nucleosomes that become less fuzzy in *arp6* mutants at H2A.Z peaks (27.4%) is greater than what is observed across the genome (19.9%) (Fig 2.9C). This emphasizes the role that H2A.Z plays in nucleosome destabilization in the genome. There were no other enrichments of one type of nucleosomal changes where H2A.Z localizes compared to changes observed in the *arp6* genome as a whole. We also specifically evaluated the types of nucleosomal changes that are enriched at subsets of H2A.Z-containing nucleosomes where H2A.Z either contributes to transcriptional repression or activation. We observed enrichment for nucleosome position changes and a shift toward nucleosome destabilization (a depletion of less fuzziness and more with increased fuzziness) at genes that are up-regulated in the *arp6* mutants (Fig. 2.9A,C). This trend suggests that the role of H2A.Z in transcriptional repression has a greater correlation with nucleosome stabilization (decreasing fuzziness and inhibiting position

shifts) than with nucleosome destabilization. However, this correlation is consistent with the types of changes we would expect to correspond with an increase in transcription and may not be directly due to H2A.Z function.

When assessing the types of changes that coincide with H2A.Z depletion from nucleosomes that normally would contain it, it is important to compare them to changes observed at other places in the genome. Only 9.38% of total dynamic nucleosomes called between *arp6* mutants and WT are found where H2A.Z localizes (total dynamic nucleosomes=21,967, those at H2A.Z peaks=2,061). This means that other nucleosome changes are taking place in the genome due to secondary effects of H2A.Z depletion and SWR1 defects rather than the direct loss of H2A.Z alone. The preference for nucleosome occupancy changes in *arp6* dynamic nucleosomes may be attributable to changes in transcription, changes in chromatin organization/localization within the nucleus, or the direct effects of depleting chromatin of H2AZ alone. However, some secondary changes could also be due to some unaccounted deletions in the *arp6* genome.

BRM contributes to nucleosome destabilization when it is in proximity to H2A.Z.

Since both BRM and H2A.Z contribute to nucleosome stability and positioning individually, we wanted to evaluate whether they work coordinately or antagonistically on nucleosomes where they overlap. We defined 2,963 regions of overlap between BRM ChIP-seq peaks and H2A.Z ChIP-seq peaks (significant by Fisher's exact test, p-value < 2.2e-16) (Fig. 2.10A). By plotting the ChIP-seq read signal for BRM and H2A.Z at these regions of overlap and dividing them into 4 K-means clusters, we determined that these are primarily regions of peripheral overlap instead of sites with strong co-localization (Fig. 2.10B). We then identified 88 regions of H2A.Z-BRM overlap that also contained significant nucleosome changes in both respective mutants compared to WT nucleosomes. These regions allow a more direct comparison between the roles that BRM and H2A.Z play in nucleosome dynamics. At these regions of shared overlap, H2A.Z and BRM both contribute to significant changes in nucleosome positioning at 42% (37/88) of nucleosomes, however only 21%

(19/88) of these nucleosomes are changed in both genotypes. H2A.Z contributes evenly to increases and decreases in the degree of nucleosome occupancy changes (Fig 2.10C) and fuzziness changes (Fig 2.10D) in regions of BRM/H2A.Z overlap. These observations demonstrate that H2A.Z has a range of contributions to nucleosome stability at these sites, consistent with what is observed at H2A.Z sites alone (Fig. 2.8B).

Alternatively, *brm* mutants have a greater proportion of nucleosomes with an increase in occupancy and decrease in fuzziness compared to WT at regions of H2A.Z/BRM overlap. These data indicate that BRM plays a greater role in nucleosome destabilization at sites where it overlaps with H2A.Z (Fig. 2.10C, D). This is consistent with the fact that there are more increases in nucleosome occupancy at BRM peak borders than at the centers (Fig. 2.4A and Fig. 2.6F) and that H2A.Z and BRM have more peripheral overlaps (Fig 2.10B). Collectively, these observations indicate that H2A.Z and BRM do not solely antagonize the function of the other in chromatin, but can also cause similar changes in nucleosome organization.

BRM contributes to nucleosome destabilization of +1 nucleosomes at genes coordinately regulated with H2A.Z.

To asses the roles of H2A.Z and BRM in nucleosome stability as they relate to transcriptional regulation, we plotted the average profiles of nucleosome read signals from WT, *arp6*, *brm*, and *arp6;brm* plants surrounding the transcription start sites (TSS) of DE genes (Fig. 2.11 and Fig. 2.12). We focused our analysis on TSSs from the 8 antagonistically or coordinately regulated DE H2A.Z/BRM target gene classes we identified earlier in the study based on their transcriptional changes in the mutants (Fig. 2.1C). While there are some nucleosome occupancy changes detected within gene bodies in mutants, we primarily focused our analysis on changes observed for the +1 nucleosome because it acts as a first physical barrier for transcriptional regulation (Weber et al., 2014).

At these DE gene classes, *brm, arp6* and *arp6;brm* mutants showed an increase in +1 nucleosome occupancy, with the most dramatic changes seen in the coordinately regulated gene Classes 1 and 2 (Fig. 7A and Fig. S6). The *brm* and *arp6;brm* mutants also show +1 nucleosome occupancy increases at gene Classes 3 and 4 (Fig. 2.11A and Fig. 2.12). It is interesting to note that the role of BRM in +1 nucleosome stabilization is unaffected by the direction of transcriptional change (Fig. 2.11A and Fig. 2.12). In *arp6* mutants, +1 nucleosome occupancy is mostly unchanged at genes DE in *arp6* or *arp6;brm* mutants (Classes 3-6) but show slight increases in nucleosome stability where H2A.Z opposes the regulatory functions of BRM at DE genes in *brm* mutants (Classes 7 and 8; Fig. 2.11A,D and Fig. 2.12). Although the loss of BRM results in +1 nucleosome occupancy increases at genes, especially in Class 3 and 4, significant changes in transcription do not happen in these gene classes until there is a loss of both H2A.Z and BRM in the *arp6;brm* mutants (Fig. 2.11A and Fig. 2.12). This means that at these gene classes (3 and 4), the increase in nucleosome stability in the BRM mutants is not sufficient to cause significant changes in transcription until the loss of H2A.Z.

BRM is enriched at the NDR just upstream of the +1 nucleosome at our 8 gene classes (Fig. 2.11B), so it may be influencing +1 nucleosome stability by interacting with the +1 nucleosome either peripherally or through recruiting other chromatin modifying factors to interact with the +1 nucleosome. Having more stable +1 nucleosomes at BRM targets in *brm* mutants is consistent with our observations that BRM contributes to nucleosome destabilization at the borders/flanking regions where it localizes and particularly when it co-localizes with H2A.Z (Fig 2.6D,F and Fig 2.10C,D). Further work to determine whether BRM destabilizes the +1 nucleosomes or whether it recruits or blocks other factors which indirectly contribute to +1 nucleosome stabilization will help us better understand the role of BRM in transcriptional regulation.

BRM and H2A.Z may interact with TFs to facilitate transcriptional regulation

We originally wanted to expand on the work of Farrona et al (2011) to test the extent of the antagonistic relationship between BRM and ARP6/H2A.Z beyond what was observed at the *FLC* gene. Our work presenting variable nucleosome changes where the two factors overlap as well as at DE co-targeted genes (Fig. 2.10 and 2.11) suggest that the BRM-H2A.Z relationship is more complex than a simple antagonism. H2A.Z and/or BRM may have more consistent roles in chromatin regulation as they relate to the functions of specific transcription factors (TFs). For example, both H2A.Z and the SWI2/SNF2 complex have been implicated in regulating chromatin accessibility for TFs (John et al., 2008; Sacharowski et al., 2015; Jegu et al., 2017). H2A.Z eviction from +1 nucleosomes is regulated by the HSFA1a TFs to regulate heat response genes (Cortijo et al., 2017) and conversely BRM can be recruited to chromatin by TFs (Wu 2012; Efroni et al., 2013; Vercruyssen et al., 2014; Zhao et al., 2015; Buszewicz et al., 2016; Zhang et al., 2016). These previously defined relationships between H2A.Z, BRM, and TFs prompted us to evaluate how H2A.Z and BRM contribute to nucleosome organization surrounding TF binding sites where they co-localize.

To identify TFs that may be associated with specific regulatory relationships between H2A.Z and BRM, we identified significantly enriched sequence motifs found in accessible chromatin regions associated with the 8 DE gene classes we identified (Fig 2.1D,E). Accessible chromatin sites were defined in a previous study using an ATAC-seq data set from leaf mesophyll cells, which is the predominant cell-type in our tissue (Sijacic et al., 2017). The motifs enriched at accessible regions across 7 of our DE gene classes are statistically similar to the target motifs for 78 different TFs (none were enriched for gene class 1) (Table 2.1). Of the factors identified, 15 have previously been reported to associate with the SWI2/SNF2 complex in Arabidopsis (Table 2.1; Efroni et al., 2013, Jegu et al., 2017; Zhang et al., 2017a).

Several of the TFs identified are involved in responses to light (SOC1, FRS9, HY5, MYC2, CIB2, BZR1, BIM1/2/3, and PIF1/3/4/5/7). These factors are intriguing because they are consistent with the multiple GO terms relating to responses to light stimuli that are enriched in our 8 classes of

DE H2A.Z-BRM target genes (Fig. 2.2). Both H2A.Z and BRM also independently regulate genes in response to various light stimuli.

One family of light responsive TFs that was predicted to associate with both coordinately-regulated and antagonistically-regulated gene classes is the basic helix-loop-helix, PHYTOCHROME-INTERACTING FACTOR (PIF) family of transcription factors (PIF1, 3, 4, 5, and 7) (Table 2.1). These TFs act as both positive and negative regulators of transcription, similar to H2A.Z and BRM (De Lucas and Prat 2014; Lee and Choi 2017). PIFs also integrate light response and hormone signals in plants to regulate growth and development in response to changes in light stimuli similar to the types of genes that are DE targets of H2A.Z and BRM (Fig 2.2) (De Lucas and Prat 2014; Lee and Choi 2017). Relationships between PIF TFs and either H2A.Z or the SWI2/SNF2 complex have been described before, making the PIF TFs interesting candidates for follow-up analyses (Efroni et al., 2013; Wigge 2013; Galvao et al., 2015; Jegu et al., 2017; Zhang et al., 2017a).

Before testing whether BRM or H2A.Z affect chromatin organization at PIF TF binding sites, we assessed the degree of overlap between BRM, H2A.Z and previously reported binding sites for PIF4 and PIF5 (Pedmale et al., 2016). We found that PIF4 and PIF5 peaks overlap with a combination of H2A.Z and BRM together, H2A.Z only, BRM only, or neither, with a slight preference toward overlapping with BRM rather than H2A.Z (Fig. 2.13A, Fig. 2.14A). To evaluate H2A.Z and BRM localization relative to PIF4 sites that overlap with H2A.Z and BRM, we plotted H2A.Z and BRM ChIP-seq signals (normalized to input) from WT plants relative to WT nucleosome patterns across the PIF4 ChIP-seq peaks (Fig 2.13B). Using K-means clustering to separate the nucleosome profiles around PIF4 sites into four different subsets, we found that BRM is enriched at the center of PIF4 peaks and H2A.Z is enriched at one or both sides of the PIF4 peaks (Fig. 2.13B). This suggests that BRM preferentially interacts with PIF4 binding sites and H2A.Z has a more peripheral interaction, consistent with BRM binding to NDR and H2A.Z localizing within flanking nucleosomes.

To evaluate whether chromatin organization surrounding PIF4 binding sites is dependent on H2A.Z or BRM, we plotted the nucleosome read signal from WT plants, *arp6* mutants, *brm* mutants, and *arp6;brm* double mutants across size-scaled PIF4 binding sites (Fig. 2.13C). We specifically plotted nucleosome read signals across PIF4 peaks that overlap with BRM ChIP-seq peaks (without H2A.Z), H2A.Z ChIP-seq peaks (without BRM), both, or neither (Fig. 2.13C-F). By K-means clustering the nucleosome profiles around PIF4 sites into four different clusters, we measured nucleosome changes at binding sites that are flanked by less accessible chromatin on one or both sides as well as sites that are found in more accessible chromatin (Fig. 2.13C-F). However, there are no clear differences in nucleosome occupancy around PIF4 sites when comparing the mutant nucleosomes to those in WT (Fig. 2.13C-F). This implies that BRM and H2A.Z do not necessarily impede or facilitate accessibility to PIF4 binding sites.

We did observe differences in the chromatin architecture inherent to the PIF4 binding sites that are associated with either BRM or H2A.Z. The clustered profiles demonstrate that more distinct nucleosome peaks flank PIF4 binding sites found in combination with H2A.Z sites (Fig. 2.13C, E, G). This suggests that well-phased nucleosomes surround PIF4 binding sites where H2A.Z is found. PIF4 binding sites found with BRM tend to be more accessible regions, consistent with BRM localizing to NDRs (Fig. 2.13C, D). We also compared WT nucleosome patterns at all PIF4 sites divided into whether they overlap with BRM alone, H2A.Z alone, both, or neither. It appears that BRM and H2A.Z localization additively correlate with more open chromatin conformations at PIF4 sites (Fig. 2.13G). This observation suggests that both function at more open PIF4 binding sites rather than maintaining a closed chromatin conformation. We also evaluated how the accessibility of PIF5 binding sites is affected in *arp6*, *brm* and *arp6;brm* mutants and discovered similar results as what we observed for PIF4 sites (Fig. 2.14). This is consistent with the fact that PIF4 and PIF5 have overlapping functions at many shared sites (De Lucas and Prat 2014). Thus, our results indicate that BRM localizes to PIF4 and PIF5 sites that are accessible, H2A.Z correlates with PIF4 and PIF5 sites within well-phased nucleosomes, and accessibility to PIF4 and PIF5 sites are not dependent on BRM

and H2A.Z. Since there are no changes in the accessibility of these PIF binding sites in *brm* mutants, BRM may be recruited to these sites after PIF4 or PIF5 binds and another factor makes the region available.

Nucleosome organization at FRS9 sites is dependent on BRM and H2A.Z

FAR1-Related Sequence 9 (FRS9), a member of the FRS far-red light responsive TF family was also predicted to interact with 6 of our classes of DE H2A.Z-BRM target genes based on our motif discovery analysis (Lin et al. 2004). Little is known about FRS9 function, but it is expressed in young rosette tissue and regulates the inhibition of hypocotyl elongation by red light (Lin et al. 2004). Also, other FRS9 paralogs bind PIF4 target genes to repress their transcription (Ritter et al., 2017). Using publically available FRS9 binding sites from DAP-seq experiments (O'malley et al., 2016), we tested whether nucleosome organization at FRS9 binding sites is dependent on H2A.Z or BRM. For this analysis, we plotted MNase-seq nucleosome signals from *arp6*, *brm*, *arp6*;*brm* and WT plants across sized-scaled FRS9 binding sites. Similar to how PIF4 and PIF5 were analyzed, we divided FRS9 binding sites into those sites that overlapping H2A.Z ChIP-seq peaks (without BRM), overlapping BRM ChIP-seq peaks (without H2A.Z), overlapping both, or neither (Fig. 2.15). In contrast to how BRM and H2A.Z showed more peripheral interactions at PIF4 binding sites, BRM and H2A.Z have a great degree of overlap at the FRS9 binding sites that overlap with both BRM and H2A.Z (Fig. 2.15B). This may indicate a more coordinated function between BRM and H2A.Z in nucleosome organization at these sites.

Since relationships between nucleosomes and TF binding sites do not follow a simple presence-absence pattern, we evaluated how 4 K-means clustered nucleosome patterns associated with FRS9 binding sites are affected in *arp6*, *brm*, or *arp6;brm* double mutants compared to those in WT plants. At FRS9 sites overlapping with both BRM and H2A.Z peaks, there was an increase in nucleosome occupancy in the *brm* and *arp6;brm* mutants with a notable subset of nucleosomes that also have increased occupancy in *arp6* mutants (Fig. 2.15 C-F). These occupancy changes

demonstrate that both factors can contribute to nucleosome destabilization at FRS9 binding sites (Fig 2.15C).

These changes in occupancy were not detected at FRS9 sites that have neither H2A.Z nor BRM present (Fig. 2.15F), demonstrating that changes in nucleosome stability observed in the mutants can be attributed to losing H2A.Z and BRM. To better understand the individual contributions of BRM and H2A.Z, we plotted the average nucleosome signal in the *arp6, brm* and *arp6;brm* mutants and WT plants at FRS9 sites that overlapped with BRM and not H2A.Z and, conversely, those that overlap H2A.Z and not BRM. In the *brm* and *arp6;brm* mutants, FRS9 sites overlapping with BRM but not H2A.Z had increased occupancy for bordering nucleosomes, but a decrease in occupancy within the more accessible regions of FRS9 binding sites (Fig. 2.15D, clusters 2 and 3). Since we see an increase and decrease in nucleosome occupancy so close together, BRM may be responsible for moving nucleosomes from the bordering regions into the FRS9 binding sites to maintain more specific control of FRS9 or other TFs binding there. Both the peaks that are associated with H2A.Z but not BRM and those that have H2A.Z and BRM display more nucleosome phasing than what is observed in the peaks that do not have H2A.Z, similar to the nucleosome patterns we observed surrounding PIF4 binding sites (Fig. 2.13B, and Fig. 2.15C,E). Since this phasing is not disrupted in the *arp6* mutants, but rather we observed an increase in the occupancy of the already well-positioned nucleosomes, H2A.Z may be needed at FSR9 sites to modulate chromatin accessibility in response to these already well-positioned nucleosomes (Fig. 2.15C).

Clustering FRS9 binding sites into four categories with K-means clustering allowed us to see the distribution of well-positioned nucleosomes at either side of the FRS9 binding sites (Fig. 2.15C). The nucleosome position that experiences the most dynamic changes at FRS9 sites in the mutant lines corresponds with nucleosomes that would normally contain H2A.Z (Fig 2.15B,C). H2A.Z appears to contribute to nucleosome occupancy, since we see increased nucleosome occupancy in *arp6* and *arp6;brm* mutants at FRS9 sites with H2A.Z but not BRM (Fig 2.15E). Although H2A.Z was not sufficient to destabilize nucleosomes in a way that resulted in nucleosome occupancy changes in the

arp6 mutants where H2A.Z overlaps with BRM, its presence could still correlate with and contribute to the role of BRM destabilizing nucleosomes. However, we see that nucleosomes at many of the borders of FRS9 peaks still accumulate in the *brm* mutants even at FRS9 binding sites where BRM localizes without H2A.Z (Fig. 2.15D). Thus, it seems that H2A.Z is not necessary for BRM to destabilize nucleosomes at FRS9 binding sites.

Discussion

H2A.Z and BRM have similar and redundant roles as well as antagonistic roles in regulating transcription

Originally, we set out to test the hypothesis that BRM antagonizes the activating function of H2A.Z by stabilizing or repositioning nucleosomes which was first proposed in response to their antagonistic relationship regulating *FLC* transcription (Farrona et al., 2011). Through the work reported here, we learned that the relationship between BRM and H2A.Z in transcriptional regulation is not a simple antagonism, but includes several different relationships. We identified gene sets where BRM antagonizes the repressive function and the activating function of H2A.Z (Classes 7 and 8), and reciprocally, where H2A.Z antagonizes the activating and repressive functions of BRM (Classes 5 and 6). We also identified genes that depend on either ARP6 or BRM to modulate transcript level (Classes 1 and 2) and genes where the additive function of both factors contributes to transcriptional repression or activation (Classes 3 and 4).

H2A.Z levels in chromatin are independent of BRM

One hypothesis that would explain how BRM and H2A.Z coordinately or antagonistically regulate transcription is that one factor may regulate the ability of the other factor to associate with the loci that they both target. Others have observed H2A.Z protein levels increase in nuclear fractions in RNAi knock down plants for the BAF60 SWI2/SNF2 subunit, however they measured nuclear H2A.Z levels not necessarily H2A.Z levels in chromatin (Jegu et al., 2014). Since *brm* mutants do not

have a consistent increase or decrease in H2A.Z-containing nucleosome levels in our ChIP-seq experiments (Fig. 2.3A), our results indicate that BRM does not affect H2A.Z levels in chromatin. An alternative hypothesis would be that H2A.Z and BRM interact to regulate transcription by H2A.Z recruiting BRM, because H2A.Z plays a role in recruiting the SWI2/SNF2 complex to at least one locus in human cells (Gevry et al., 2009). However, this seems unlikely since BRM and H2A.Z have a relatively small (yet significant) overlap in the genome (Fig 2.10A).

BRM and H2A.Z destabilize +1 nucleosomes

At DE BRM-H2A.Z co-targeted genes, BRM localizes just upstream of the TSS and H2A.Z is enriched at the +1 nucleosome (Fig. 2.11B). When H2A.Z and BRM coordinately regulate gene transcription, they both contribute to +1 nucleosome destabilization (Fig. 2.11A, Classes 1 and 2). At other DE gene classes, BRM usually destabilizes +1 nucleosomes, while H2A.Z must contribute in other ways to transcriptional regulation. BRM and H2A.Z have been associated with +1 nucleosome stability in combination with other factors as well. Mutants for the FORGETTER1 TF that interacts with BRM perturb +1 nucleosome occupancy of genes involved in heat stress memory (Brzezinka et al., 2016). Our data showing an increase in +1 nucleosome occupancy in *brm* mutants supports a role for BRM in contributing to how FORGETTER1 destabilizes +1 nucleosomes after heat exposure. At the +1 nucleosomes of some heat responsive genes, H2A.Z eviction contributes to nucleosome destabilization, emphasizing a role for H2A.Z in +1 nucleosome stability (Cortijo et al., 2017). We found however that when H2A.Z is found proximal to BRM, H2A.Z tends to destabilize +1 nucleosomes of DE genes (Fig. 2.11A,D).

While the +1 nucleosome presents a barrier to transcription (Weber et al., 2014), the direction of transcriptional changes observed in BRM mutants is not inherently coupled to the change in nucleosome stability caused by BRM. For example, in classes 3 and 4 of co-regulated genes, +1 nucleosome occupancy increases in BRM mutants at genes transcriptionally regulated by BRM and H2A.Z, but there are no significant transcription changes until the genome is depleted of H2A.Z-

containing nucleosomes in *arp6;brm* double mutants (Fig. 2.11A). Changes in transcriptional regulation can also correspond with changes in the accessibility of the DNA that is associated with the +1 nucleosome without changing the nucleosome occupancy (Huebert et al., 2012). Additionally, changes in occupancy can be uncoupled from transcription changes (Mueller et al., 2017). This means that although +1 nucleosomes appear to have an increase in nucleosome occupancy in BRM mutants, and H2A.Z does not show a consistent change in nucleosome occupancy at these gene classes, the actual DNA that associates with them may have different degrees of accessibility depending on other factors such as histone modifications or interactions with other chromatin interacting proteins. In addition to contributing to transcriptional initiation, H2A.Z can help facilitate transcriptional elongation in Arabidopsis (Rudnizky et al., 2016; Weber et al 2014). The overall destabilization role of both factors in co-regulated genes may also allude to both H2A.Z and BRM contributing to transcriptional elongation rather than strictly transcriptional initiation at co-targeted genes.

BRM destabilizes nucleosomes flanking NDRs

The specific role of BRM in chromatin regulation to date has been evaluated locus by locus, so we are the first to assay how BRM contributes to global nucleosome organization in *Arabidopsis* (Wu et al., 2015; Han 2015; Brzezinka et al., 2016). We demonstrate that BRM localizes to NDRs across the genome and is flanked by well-positioned nucleosomes whose stability often depends on BRM. These results expand on previous locus specific studies by both finding that well-positioned nucleosomes surrounding BRM binding sites is a general genomic trend and that the stability of many of these flanking nucleosomes depends on BRM (Sacharowski et al., 2015; Wu et al., 2015). Since the BAF60 subunit of the SWI2/SNF2 complex has been observed localizing to open chromatin, we provide further evidence that the SWI2/SNF2 complex binds to NDRs by finding that the BRM SWI2/SNF2 ATPase binds to NDRs (Jegu et al., 2017). The fact that we see an increase in +1 nucleosome occupancy in the absence of BRM and H2A.Z at genes where both are needed for proper transcriptional regulation (especially Classes 1 and 2) is consistent with studies that show that both

factors disrupt interactions between DNA and nucleosomes (Schnitzler et al., 2001; Rudnizky et al., 2016). It is interesting to note that although BRM localizes to NDRs, it appears that other factors established the open confirmation of these regions and BRM may further modulate how other factors interact with the regions as we observed at PIF4 and PIF5 binding sites (Fig. 2.13 and Fig. 2.14)

Other chromatin factors may contribute to the roles of BRM and H2A.Z in chromatin organization and transcriptional regulation

Some of the changes that we observed may not be due to the specific catalytic functions of BRM or inherent properties of H2A.Z incorporation into chromatin by the SWR1 complex but rather be contributed by other chromatin regulating factors that interact with them. The SWI2/SNF2 complex is known to interact with a histone acetyl transferase (HD2C), a H3K27me3 histone demethylase (REF6), and potentially the ISWI CRC (Brzezinka et al., 2016; Buszewicz et al., 2016; Li et al., 2016). BRM also antagonizes the function of the Polycomb Repressive Complex 2, so some of the nucleosomal changes we observe may not be due to a direct contribution by BRM but a result of nucleosomal changes that come with Polycomb repressive complex associated silencing activity (Li et al., 2015a). Additionally, interchanging subunits of the SWI2/SNF2 complex can confer unique functions to modulate specific developmental processes (Vercruyssen et al., 2014; Sacharowski et al., 2015). This could mean that some of the variability in BRM's role in chromatin regulation could correspond with which SWI2/SNF2 subunits co-localize with it. BRM and the paralogous SWI2/SNF2 ATPase SPLAYED have both unique and redundant roles in *Arabidopsis*, so some contributions from BRM that are redundant with SPLAYED will be obscured from our analyses (Bezhani et al., 2007).

In other organisms, post-translational modifications to H2A.Z, such as ubiquitination and acetylation, have been shown to correlate with the role of H2A.Z in transcriptional repression and activation, respectively (Marques et al., 2010; Dalvai et al., 2012; Valdes-Mora et al., 2012). Assuming that similar post-translational modifications to H2A.Z exist in *Arabidopsis*, they likely

contribute to some of the variability in nucleosome positioning and stability that we describe for H2A.Z. However, more work is still needed to create a clear and comprehensive description of how histone-modifying enzymes interact with H2A.Z and SWR1 to affect chromatin organization and regulate transcription.

Although many of the SWR1 complex subunits are shared with other CRCs, ARP6 is unique to the SWR1 complex and is essential for proper H2A.Z incorporation (Deal et al., 2007; Lu et al., 2009; Hargreaves and Crabtree 2011). This highlights the fact that the primary function reported for ARP6 in *Arabidopsis* is to incorporate H2A.Z into chromatin as part of the SWR1 complex (Deal et al., 2007; Sura et al., 2017). Thus, we used *arp6* mutants as a proxy for H2A.Z mutants in this study. ARP6 does however have functions independent of H2A.Z in yeast to localize some chromatin regions to the nuclear periphery, and some SWR1 complex subunits in *Arabidopsis* appear to have non-overlapping roles in regulating defense response (Yoshida et al., 2010; Berriri et al., 2016). Therefore, we specifically focused our analyses on regions of the genome that normally contain H2A.Z and were depleted of H2A.Z-containing nucleosomes in *arp6* mutants, thus excluding any effects from ARP6 functions that may be independent of H2A.Z and, conversely, effects from H2A.Z that may be ARP6-independent. However, it is still possible that some of our observations describe ARP6 function in addition to H2A.Z function, since we cannot parse the individual contributions of ARP6 and H2A.Z in our study.

BRM and H2A.Z interact with binding sites for light responsive TFs

Based on our GO analyses, H2A.Z and BRM regulate transcriptional networks of genes that are involved in defense, temperature and light responses as well as growth (Fig. 2.2). This supports the idea that both H2A.Z and BRM contribute to the balancing act plants go through to choose between normal growth and responses to stimuli. More specifically, overlapping DE target genes suggest that H2A.Z and BRM are important to integrate signals and regulate transcription in response to light stimuli. Since we show that BRM and H2A.Z co-localize with FRS9, PIF4, and PIF5 binding

sites (Fig. 2.13, Fig. 2.14 and Fig. 2.15), our findings indicate that interacting with light responsive TFs is one way that H2A.Z and BRM respond to light stimuli.

We are the first to suggest a relationship between FRS9 with either BRM or H2A.Z, but relationships between different PIF TFs and either H2A.Z or the SWI2/SNF2 complex have been reported previously. Yeast two-hybrid experiments demonstrate that BRM itself actually interacts with PIF1 and to some extent with PIF3 and PIF4 (Zhang et al. 2016), and mass spectrometry experiments show that the SWI2/SNF2 complex associates with PIF1 and 3 as well (Efroni et al., 2013). PIF1 is at least partly responsible for recruiting BRM to particular loci, however whether PIF4 and PIF5 TFs interact with BRM or H2A.Z *in vivo* was previously unknown (Zhang et al., 2017a; Efroni et al., 2013). In addition to the SWI2/SNF2 complex, H2A.Z and PIF proteins have a moderate genetic overlap in regulating flowering timing and growth in response to temperature changes, but the details of this relationship are not well understood (Wigge 2013; Galvao et al., 2015). By finding PIF TF binding sites enriched at genes co-regulated by and H2A.Z and BRM, we expand on these previously described relationships and provide resources to further explore their interactions.

Our finding of PIF TF binding at DE BRM-targeted genes provides further support for these interactions between the SWI2/SNF2 complex and PIF TFs (Table 2.1, Fig. 2.13-2.14). We also discovered that chromatin accessibility at PIF4 and PIF5 TF binding sites is not dependent on BRM nor H2A.Z (Fig. 2.13-2.14). Although BRM is not necessary for nucleosome organization surrounding the PIF TF binding sites, BRM may act to antagonize the function of PIF4/5 at sites where they both bind. Setting the precedent for this, the BAF60 subunit of SWI2/SNF2 competes with PIF4 for binding sites to oppose its role in hypocotyl elongation (Jegu et al., 2017).

Although *in vitro* work shows that the SWI2/SNF2 complex from other organisms repositions nucleosomes toward bound TFs to evict them (Li et al., 2015b), we did not see changes in nucleosome occupancy or positioning at PIF TF binding sites in *brm* mutants to suggest that this is the case for these TF binding sites. Alternatively, FRS9 sites can be occupied by nucleosomes and both H2A.Z and BRM regulate nucleosome occupancy at FRS9 binding sites (Fig 2.15B). Expanding

what we know about FRS9 binding sites, we demonstrate that they overlap with BRM and H2A.Z in the genome and are found at target genes distributed across the 8 classes of DE co-targets of H2A.Z and BRM.

In other organisms, the SWI2/SNF2 CRC and H2A.Z both contribute to enhancer function to regulate transcription by regulating where TFs bind (Euskirchen et al., 2011; Brunelle et al., 2015; Alver et al., 2017). Recent work also suggests that H2A.Z may function at enhancers in *Arabidopsis* (Dai et al., 2017). However as of yet, only a small number of enhancers have been identified and characterized in plants (Zhu et al., 2015). The fact that BRM localizes to NDR more distal to TSSs and that H2A.Z and BRM are associated with TF binding sites and transcriptional regulation may indicate a role for BRM and H2A.Z in enhancer regulation in plants as well.

Large deletions in *SWR1 mutants may account for an over estimation of nucleosome occupancy decreases*

To our knowledge no one has ever reported that there are a considerable number of large genomic deletions in SWR1 mutants in *Arabidopsis*. Our discovery of these deletions is in line with the roles of the SWR1 complex and H2A.Z in maintaining genome stability and previous reports that specifically show that *arp6* mutants have a greater crossover density, are more susceptible to DNA damage, and have meiotic defects (Choi et al., 2013; Rosa et al., 2013). Contrary to our observations of nucleosome occupancy, other groups have reported a general decrease in nucleosome occupancy in *arp6* mutants, which could be due to changes in the genome rather than changes to chromatin organization (Dai et al., 2017). In our analysis of nucleosome occupancy, we controlled for the loss of genomic regions in *arp6* mutants so that we did not erroneously report a deleted region as a decrease in nucleosome occupancy. Future studies that measure chromatin accessibility in SWR1 mutants should take care to account for similar genomic differences.

3-D nuclear organization in Arabidopsis may involve H2A.Z and BRM

While BRM and H2A.Z localize to a large portion of genes in the genome, only a fraction of

these target genes is differentially expressed in the mutants, which is consistent with observations from previous studies of BRM (Li et al., 2016). In addition to how they directly impact the remodeling of individual nucleosomes, the roles of BRM and H2A.Z in transcriptional regulation may contribute to or be a consequence of larger nuclear organization of chromatin. Transcription can be oversimplified if viewed as an isolated linear process of initiation, elongation, and termination proceeding down a DNA molecule. In reality, transcription is one of many processes that take place in a highly regulated chromatin environment that is organized in an intricate 3-dimensional space within the nucleus (Vergara and Gutierrez 2017; Barneche and Baroux 2017). Both H2A.Z and the SWI2/SNF2 complex have been implicated in regulating larger scale nuclear organization in other organisms, contributing to chromatin looping and chromosome localization within the nucleus (Yoshida et al., 2010; Light et al., 2010; Maruyama et al., 2012; Kitamura et al., 2015; Imbalzano et al., 2013). The fact that H2A.Z and the SWR1 complex associate with nuclear scaffold/matrix attachment regions in Arabidopsis suggests that similar functions for both are yet to be described in plants (Lee and Seo 2017). Likewise, the SWI2/SNF2 complex has been implicated in chromatin looping in *Arabidopsis* and other organisms, as well as *in vitro* (Jegu et al., 2014, Kim et al., 2009, Bazett-Jones et al., 1999). Therefore, changes in higher order structure may be affected by depleting the plants of BRM and H2A.Z-containing nucleosomes, which could explain some of the variable changes in nucleosome stability we observed in *brm* and *arp6* mutants and why some H2A.Z and BRM associated nucleosomes do not dramatically change. Additionally, plants respond to changes in light signals with chromatin de-condensation and nuclear reorganization, so a deeper mechanistic understanding of BRM and/or H2A.Z may elucidate how chromatin changes occur on a larger scale in response to changes in light or other stimuli (Van Zanten et al., 2010; Bourbousse et al., 2015).

Concluding statements

Within the nucleus, combinatorial effects from a range of factors regulate chromatin organization in different contexts. This can make it difficult to understand the extent to which any one

factor contributes to chromatin organization as a whole. *In vitro* studies work to simplify the system to understand individual chromatin-influencing components, but they are far removed from the constant flux of regulatory pressures that a locus experiences *in vivo*. In our study, we attempted to parse the chromatin regulatory contributions of H2A.Z and BRM *in vivo* and chose to simplify our approach by identifying and then specifically evaluating direct target loci of H2A.Z and BRM where they antagonistically or coordinately regulate transcription through multiple regulatory relationships (Fig 2.1E). We found that not only do H2A.Z and BRM work at co-targeted genes to positively and negatively regulate genes, but some of their roles are functionally redundant (Fig. 2.1E). In addition, we identified genes where H2A.Z and BRM act either negatively or positively to affect transcript level in ways that are opposed by the other factor (Fig. 2.1E). We discovered that BRM contributes more to stabilizing nucleosomal changes where it directly binds to chromatin with more destabilizing effects on flanking nucleosomes. However, H2A.Z-containing nucleosomes have no clear enrichment for a specific type of nucleosome dynamic when it is found on its own or in association with BRM. At co-targeted DE genes, BRM and H2A.Z contribute to nucleosome stability to varying degrees, but they appear to both regulate +1 nucleosome occupancy where either is required for transcriptional regulation (Fig. 2.11A). Some of the variability in H2A.Z and BRM function may be explained by their interactions with specific TFs, such as the three TFs we identified (Fig. 2.13-2.15). While these datasets help us better survey how both H2A.Z and BRM contribute to transcription and nucleosome organization, more cell-type and locus-specific studies are needed to understand their full contribution to chromatin.

These genetic dissections indicate that the relationship between BRM and H2A.Z is more complicated than one property of each factor contributing to or antagonizing a single function of the other. Therefore, the influence of additional factors must make the roles of H2A.Z and BRM necessary to regulate transcription levels in different contexts. Further *in vivo* genetic and molecular studies will help us identify which factors define the context dependent functions of BRM and H2A.Z, while *in vitro* studies would help simplify the experimental system and define the direct

interactions between H2A.Z and BRM as well as additional identified factors. This highlights the challenge we face in chromatin research to create simple enough systems to understand the true complexity of how individual chromatin associating factors function on a sophisticated chromatin template within the nucleus (Probst and Mittelsten Scheid 2015).

Materials and Methods

Plant material

We used previously characterized *Arabidopsis* T-DNA insertion lines *arp6-1* (GARLIC_599_G03; Deal et al., 2005) and *brm-1* (SALK_030046, Hurtado et al., 2006) and genotyped the strains using primers described previously (Deal et al., 2005; Hurtado et al., 2006). The *arp6-1;brm-1* mutant was generated from genetic crosses of *arp6-1* homozygous and *brm-1* heterozygous lines. Plants were sown on soil, stratified at 4 °C for two days, and then moved to grow at 20 °C in long day light conditions (16 hr light/8 hr dark). Above ground plant tissue for all genomic experiments was collected at 10 hrs after dawn from 4-5 leaf developmentally staged plants (Boyes et al., 2001) from the following genetic backgrounds: WT (collected 12-13 days post stratification (dps)); *arp6-1* (12-14 dps); *brm-1* (13-16 dps); and *arp6;brm* (16-24 dps, delayed collection due to delayed germination). One cotyledon was removed from each plant to use for genotyping with the Phire^{TM} Plant Direct PCR Kit (Thermo Scientific).

RNA-seq material

Three plants each for three biological replicates of 4-5 leaf developmentally staged above soil seedling material were collected and pooled for WT, *arp6*, *brm*, and *arp6;brm* plants. RNA was isolated using the Spectrum Plant Total RNA Kit (Sigma) and incubated at 37 °C for 30 min with DNase to remove DNA using the Turbo DNA-free kit (Ambion). The integrity of the RNA was confirmed on a 2% agarose gel in 1x TAE visualized with GELRED nucleic acid stain (Sigma), and

the samples were quantified with a spectrophotometer. Libraries were prepared from 100 ng of RNA from each sample using the Ovation RNA-seq for Model Organisms kit (NuGEN), which is a strand specific library preparation kit that depletes the transcripts of rRNA. Libraries were quantified with qPCR (NEB), pooled, and sequenced with the Illumina NextSeq500 to generate paired-end 36-nt sequence reads.

RNA-seq data analysis

Sequencing reads were mapped to the TAIR10 *Arabidopsis thaliana* reference genome using Tophat2 (using the second strand option and default parameters), generating an average of 75.5M mapped reads per library. The accepted hits file was name-sorted (option –n) rather than position sorted and indexed using SAMtools (Trapnell et al., 2012; Li et al., 2009). Read counts were quantified for each exon using the htseq-counts program, with name order and strict intersection options (Anders et al., 2015). Differential expression was calculated using edgeR software (Robinson et al., 2010; Mccarthy et al., 2012). Differentially expressed genes were determined with a false discovery rate (FDR) cutoff of <0.2 and a $\log_2$ fold change of ± 0.6 (~1.5 x fold change). GO terms were generated using AgriGO for the total set of genes that were DE in the mutants relative to WT plants. GeneCodis was used to analyze GO terms for DE direct target genes of H2A.Z and BRM (Carmona-Saez et al., 2007; Nogales-Cadenas et al., 2009; Tabas-Madrid et al., 2012; Tian et al., 2017). These two separate programs were used for GO analyses based on how generally (AgriGO) or specifically (GeneCodis) they summarized the overlap between gene lists.

ChIP-seq material

For ChIP-seq experiments, we collected at least 0.5 g of tissue from two biological replicates each of WT, *arp6-1*, and *brm-1* plants. (WT, 12-13 dps; *arp6*, 12-14 dps; *brm*, 13-16 dps; *arp6;brm* 16-24 dps). Above ground developmentally staged 4-5 leaf plant tissue was collected at 10 hrs after dawn, cross-linked as described previously (Gendrel et al., 2005), frozen, and ground in liquid

nitrogen. Nuclei were isolated as previously described (Gendrel et al., 2005). Chromatin was sonicated using a Bioruptor® (Diagenode) (40 min on high (45 sec on/ 15 sec off)). Each sample was diluted in 1.1 mL of ChIP dilution buffer (described in Gendrel et al., 2005) and 50 µl was saved as the input sample. Then H2A.Z-containing chromatin was immunoprecipitated from the 1.1 mL of chromatin solution using 2 µg of H2A.Z antibody purified to specifically recognize unmodified H2A.Z peptides (Deal et al., 2007). The chromatin solution was incubated with the H2A.Z antibody for 2 hr then for 1 more hour in combination with 60 µl of Dynabeads™ Protein-A magnetic beads (Invitrogen). DNA collected from the immunoprecipitation and from the inputs was purified using 1.8x volume of SPRI beads (Beckman Coulter) then quantified with Quant-IT™ Picogreen® dsDNA Assay Kit (Invitrogen). Sequencing libraries were prepared from 1 ng of DNA per sample with the Accel-NGS® 2S Plus DNA Library kit (Swift Biosciences) and sequenced on an Illumina NextSeq500 using 76 nt single-end reads.

ChIP-seq data analysis

ChIP-seq reads were mapped to the TAIR10 *A. thaliana* reference genome with Bowtie2, using default parameters (Langmead and Salzberg 2012). An average of 13.9 M reads were converted to binary files, sorted, indexed and quality filtered (with the –q 2 option) using SAMtools software (Li et al., 2009). H2A.Z peaks were called with Homer findpeaks software, using options "style histone" and "–region" (Heinz et al., 2010). H2A.Z peaks from two biological replicates were intersected to find the regions that were called in both replicates for each genotype using Bedtools software (Quinlan 2014). H2A.Z peaks in WT that overlapped with H2A.Z peaks called in *arp6* mutants with less than a 2-fold difference in enrichment between the two genotypes were removed from the analysis to ensure that the datasets analyzed represent ARP6-dependent H2A.Z peaks. These were the H2A.Z peaks we used throughout the study. We integrated BRM-GFP ChIP-seq peaks into our analysis from a previously published data set (Li et al., 2016). Also, we used previously published ChIP-seq data for PIF4 (AT2G43010) (SRX1005830) and PIF5 (AT3G59060) (SRX1495297)

(Pedmale et al., 2016) and DAP-seq peaks for FRS9 (O'malley et al., 2016). H2A.Z and BRM ChIP-seq peaks were annotated based on the genes that they overlapped (-u ODS option) or were assigned to the nearest TSS (-u TSS option) using PeakAnnotator software (Salmon-Divon et al., 2010). Before preparing bigwig files, we first used the SAMtools view command (with option –s) to scale data sets so that all samples had same number of reads. We also combined the two biological replicates with SAMtools merge. Using the deepTools software suite, we then prepared bigwig files using default parameters for the bamCoverage program, then we subtracted the input signal from the ChIP signals by 10 bp bins with the bamCompare command for each genotype (Li et al., 2009; Li 2011; Ramirez et al., 2014). Heatmaps and average profile plots were generated from these bigwigs using deepTools computeMatrix, plotHeatmap, and plotProfile programs (Ramirez et al., 2014).

MNase-seq material

Tissue from two biological replicates of 100 mg of pooled above ground 4-5 leaf stage plants was collected from WT*, arp6-1*, *brm-1*, *and arp6-1;brm-1* plants grown on soil in long day light conditions (16 hr light/ 8 hr dark). Nuclei were isolated as described previously (Gendrel et al., 2005). After purification, nuclei were resuspended in 500 µl of TM2 solution (10 mM Tris (pH 7.5), 2 mM $MgCl_2$, and 1X Roche Complete protease inhibitor tablet). We spun nuclei down at 3,000 x g for 10 min then removed the supernatant and re-suspended the pellet in 500 µl of MNase reaction buffer (16 mM Tris-Cl (pH 8.0), 50 mM NaCl, 2.5 mM $CaCl_2$, 1 mM EDTA, Protease inhibitor tablet). Samples consisting of 500 µl of nuclei were incubated with 7.5 U MNase for 7.5 min at 37 °C, and then the reaction was stopped by adding EDTA to a final concentration of 10 mM. Nuclei were lysed by adding SDS (to 1% of the final sample volume). The solution was mixed and spun down at 1,300 x g for 3 min to remove insoluble debris. After moving the supernatant to a new tube, samples were treated with RNase A (1 mg/mL, Ambion) and then with Proteinase K (Invitrogen) to remove RNA and proteins, respectively. DNA fragments were purified with MinElute PCR purification kit (Qiagen). To purify nucleosome associated DNA fragments that were <400 bp, we used a 0.6x bead-

to-sample ratio of SPRI beads prepared as described previously (Faircloth and Glenn 2014). Sequencing libraries were prepared with the ThruPLEX® DNA-Seq Kit (Rubicon Genomics), using 25 ng of MNase-digested DNA as the input. Purified, indexed libraries were pooled and sequenced on an Illumina NextSeq500 generating 76 bp paired-end reads.

MNase-seq data analysis

Sequence reads were mapped to the TAIR10 *Arabidopsis thaliana* reference genome using Bowtie2 (using default parameters except for -p 6) and were then further sorted and indexed using SAMtools (Li et al., 2009; Langmead and Salzberg 2012). We filtered reads using the SAMtools view command, with the –q 2 option to filter for quality and option –f 0x02 to filter for properly paired reads. Libraries were subsampled using the SAMtools –s parameter to normalize all samples to the same number of reads (30.46 M reads). We analyzed the mapped reads from each biological replicate for each of the four genotypes to generate nucleosome peak files and nucleosome occupancy wiggle files using the DANPOS2 dpos program (Chen et al., 2013). Values in the *.allPeaks.xls file output from the dpos program were used to determine dynamic nucleosomes. These dynamic nucleosomes are defined as those with a FDR <0.05 for the difference between the occupancy value at the summit position of a point of difference in control and treatment samples (point_diff_FDR <0.05) and then individual types of dynamic nucleosome changes were described with the following additional criteria. Fuzziness scores were defined as the standard deviation of read positions in each peak. Significant nucleosome fuzziness changes were defined as those with a FDR of <0.05 for the difference between WT and mutant fuzziness scores (fuzziness_diff_FDR <0.05). Significant occupancy changes were defined as those with a FDR of <0.05 of the difference between the occupancy value at the peak summit position in the WT and the mutant (smt_diff_FDR <0.05). Position shifts were defined as a 20-95 bp difference in peak summit position between WT and mutant nucleosomes (treat2control_dis 20-95 bp). To measure nucleosome occupancy across the genome, we converted the DANPOS generated wiggle files to bigwig files using the wigToBigWig

software (UCSC). Heatmaps were generated from these bigwig files using deepTools software: computeMatrix, plotHeatmap, and plotProfile programs (Ramirez et al., 2014).

Identifying deletions in arp6 *mutants*

We isolated genomic DNA from mature rosette leaf material (~5 mg per plant) from 50 pooled *arp6* mutants using a standard phenol:chloroform extraction followed by ethanol precipitation. We used 1 μg of sonicated DNA to prepare a sequencing library (NEXTflex Rapid DNA-seq (option 2), Bioo Scientific), and then sequenced on an Illumina HiSeq2000, generating 125 bp paired-end reads. Sequenced reads were mapped using BWA mem software, indexed and quality sorted (-s option) using SAMtools, and randomly subsetted using a python script, leaving 61.5 M mapped reads (Li and Durbin 2009; Li et al., 2009; Li 2011). Deletions were called in the *arp6* mutant using CNVnator (v0.3.3) software using bin sizes of 100 bp (Abyzov et al., 2011).

Motif Enrichement Analysis

ATAC-seq transposase hypersensitivity sites (THSs) from mesophyll cells were identified and annotated previously (Sijacic et al., 2017). We used python scripts to pull out the annotated mesophyll THSs that were associated with genes from our 8 differentially expressed BRM and H2A.Z target gene classes (defined in Fig.1D). We scaled all THSs to be 150 bp in width and then used the Regulatory Sequence Analysis Tool for plants (RSAT plants) to obtain the corresponding DNA sequences and mask any repeated sequences (Medina-Rivera et al., 2015). Motifs that were enriched in our lists of THSs were discovered using DREME and MEME programs from the MEME-ChIP suite then paired with TFs predicted to bind to the motifs using the Tomtom program (Bailey et al., 2009) THS sequences were compared to both the CIS-BP and DAP-seq TF binding databases for these analyses (Weirauch et al., 2014; O'malley et al., 2016). Motifs and their associated TF were considered significant they had an E-value of < 0.05.

Accession Numbers

All high throughput sequencing data described in this paper has been deposited to the NCBI GEO database under record number XXX. The BRM ChIP-seq data used in our analysis is available under GEO number SRX1184288. The PIF4 and PIF ChIP-seq data used in our analyses are available under GEO numbers SRX1005830 (PIF4) and SRX1495297 (PIF5).

Acknowledgements

This research was supported by funds from Emory University and funds awarded to E. Shannon Torres from the Ruth L Kirschstein Predoctoral Individual National Research Service Award through the National Institute of General Medicine of the National Institutes of Health under award number (F31GM113631-01A1). The content is solely the responsibility of the authors and does not necessarily represent the official views of the National Institutes of Health. I would like to thank Kelsey Maher, Paja Sijacic, Marko Bajic for critical comments on this manuscript. Marko Bajic, Katie Duval, and Alex Torres helped collect and crosslink material for ChIP-seq experiments. Ben Rambo-Martin, Shawn Foley, David Nicholson, and Bob Haines all contributed computational assistance during the data analysis.

Figure 2.1

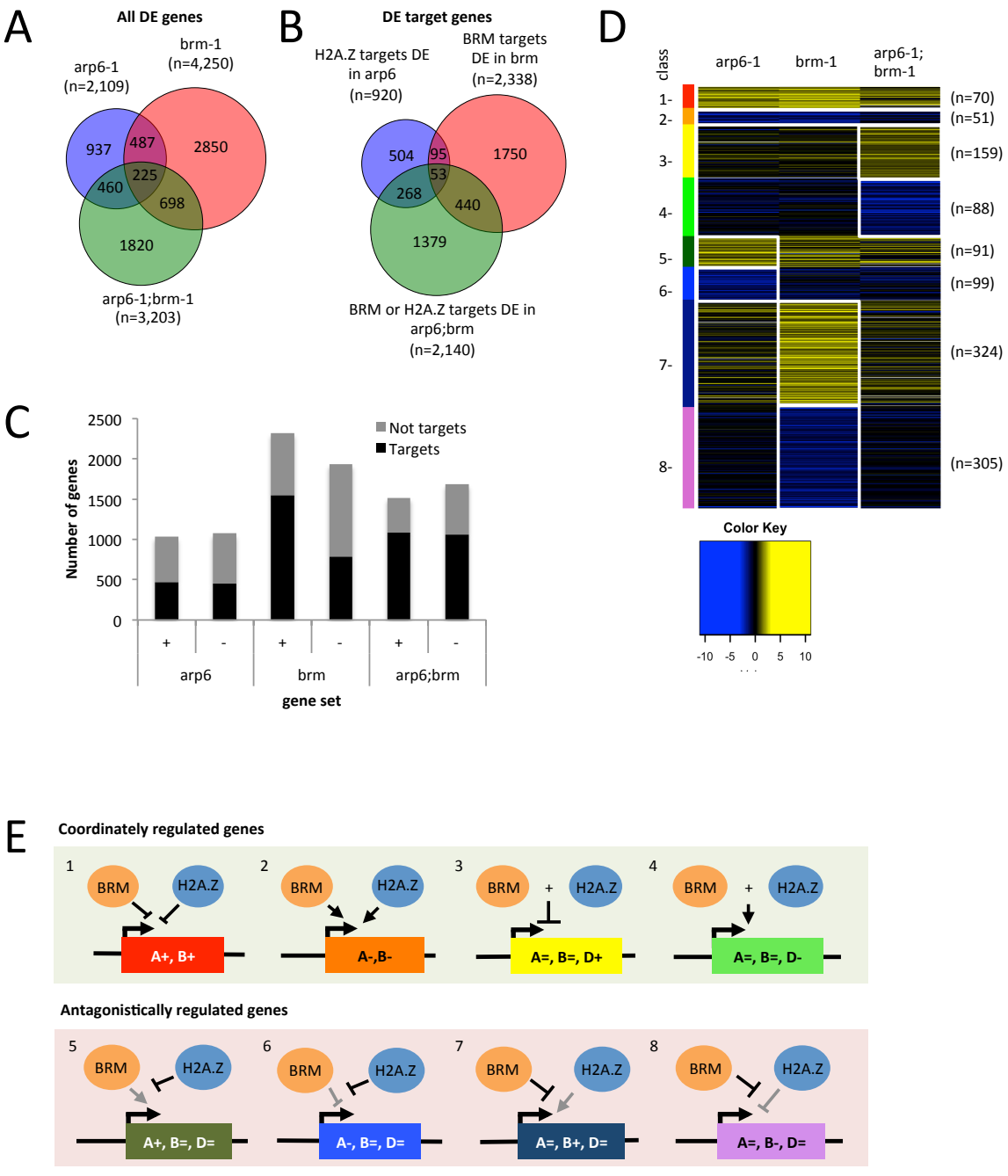
A
All DE genes
arp6-1 (n=2,109)
brm-1 (n=4,250)
arp6-1;brm-1 (n=3,203)
937
487
2850
460
225
698
1820
B
DE target genes
H2A.Z targets DE in arp6 (n=920)
BRM targets DE in brm (n=2,338)
BRM or H2A.Z targets DE in arp6;brm (n=2,140)
504
95
1750
53
268
440
1379
C
Number of genes
2500
2000
1500
1000
500
0
Not targets
Targets
+
-
arp6
brm
arp6;brm
gene set
D
class
arp6-1
brm-1
arp6-1; brm-1
1-
2-
3-
4-
5-
6-
7-
8-
(n=70)
(n=51)
(n=159)
(n=88)
(n=91)
(n=99)
(n=324)
(n=305)
Color Key
-10
-5
0
5
10
E
Coordinately regulated genes
1
BRM
H2A.Z
A+, B+
2
BRM
H2A.Z
A-,B-
3
BRM
+
H2A.Z
A=, B=, D+
4
BRM
+
H2A.Z
A=, B=, D-
Antagonistically regulated genes
5
BRM
H2A.Z
A+, B=, D=
6
BRM
H2A.Z
A-, B=, D=
7
BRM
H2A.Z
A=, B+, D=
8
BRM
H2A.Z
A=, B-, D=

Figure 2.1. H2A.Z and BRM regulate transcription through various cooperative and antagonistic relationships. (**A**) Venn diagram shows the number of differentially expressed (DE) genes in each genotype and their significant overlap (hypergeometric test, p-value >0.001) with the genes DE in other mutants relative to WT. (**B**) Venn diagram shows the number of H2A.Z target genes DE in *arp6-1*, BRM target genes DE in *brm-1* mutants, and H2A.Z or BRM target genes DE in *arp6-1;brm-1* mutants relative to WT as well as their degree of overlap (hypergeometric test, p>0.001) . (**C**) Histogram showing the number of direct DE target genes (black) and DE genes that are not targets (grey) that are up-regulated (+) or down-regulated (-) in *arp6*, *brm*, or *arp6;brm* mutants compared to WT. (**D**) Heatmap showing the average $\log_2$ fold change of genes in 8 classes of genes regulated antagonistically and coordinately by BRM and H2A.Z. Genes up-regulated are indicated in yellow and genes that are down-regulated are indicated in blue with a gradient black representing no change in transcription. The 8 different classes are indicated by various colors to the left and are divided into gene classes based on their pattern of transcription change in the different genotypes. Coordinately regulated genes include those that are up- (1-red) or down-regulated (2-orange) in both *arp6* and *brm* mutants relative to WT, genes that are up- (3-yellow) or down-regulated (4-light green) in the *arp6;brm* double mutant, but not the single mutants. Antagonistically regulated genes are divided into those genes that are up- (5-dark green) or down-regulated (6-light blue) in the *arp6* mutants but not *brm* or *arp6;brm* double mutants relative to WT, or genes that are up- (7-dark blue) or down-regulated (8-pink) in the *brm* mutants but not *arp6* or *arp6;brm* double mutants relative to WT. White boxes around gene sets highlight the significantly DE genes used to define the corresponding gene class, and the number of genes in each class (n) is shown to the right of the heatmap. (**E**) Diagram depicting the 8 genetic relationships between BRM and H2A.Z at coordinately regulated gene sets (top, green box) and antagonistically regulated gene sets (bottom, red box). The number to the top left of each diagram and the color of the targeted gene in the diagram correspond to the gene class defined in the heatmap (D). Inside the targeted gene is the transcription level relative to WT as increasing (+), decreasing (-), or not changing (=) in *arp6* (A), *brm* (B), or

arp6;brm (D) mutants. Arrows represent a positive contribution to transcriptional regulation; lines with blunt ends represent a negative contribution to transcriptional regulation. Plus signs (+) between BRM and H2A.Z indicate a combined contribution to regulate transcription. Grey lines indicate the contribution of the opposing factor in the absence of the other factor.

Figure 2.2

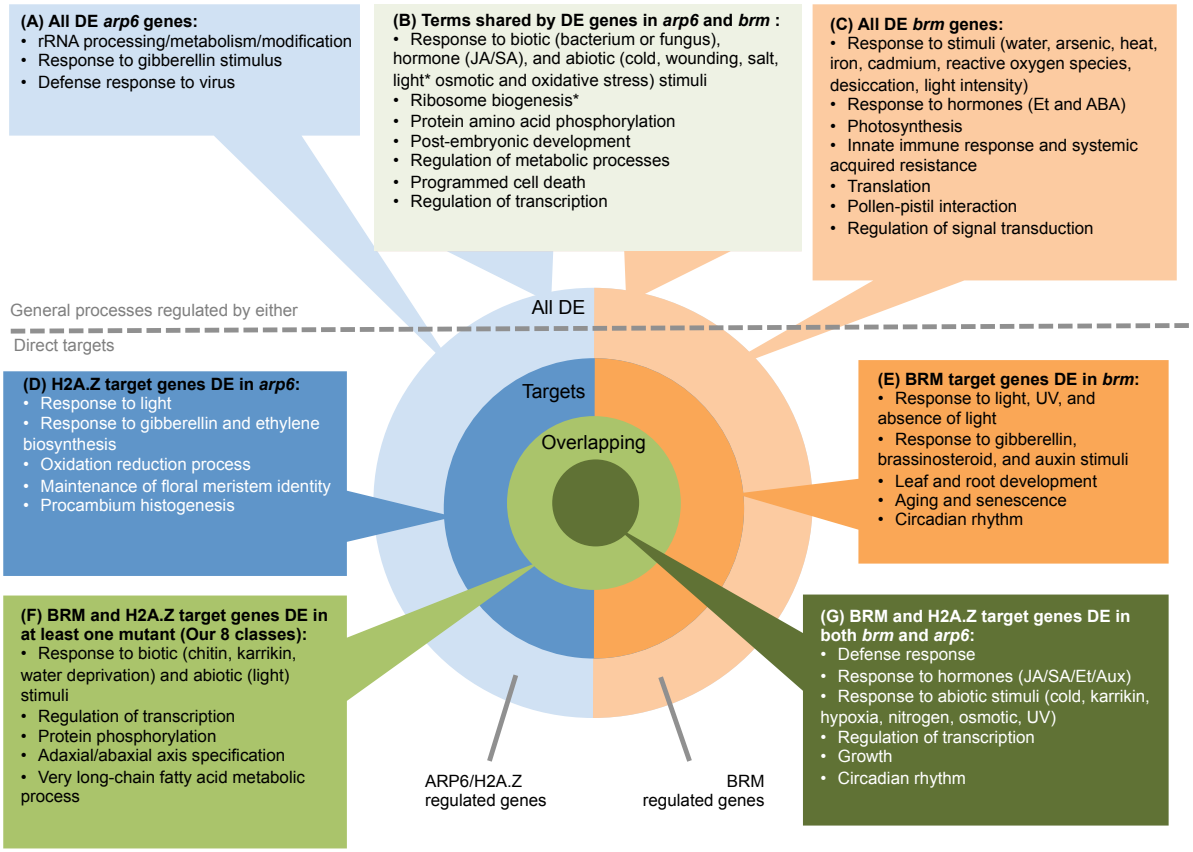

Figure 2.2. Gene Ontology (GO) analysis summary of BRM and ARP6/H2A.Z regulated genes. The circle displays the types of genes surveyed for GO analysis: all genes DE in *arp6* (**A**, light blue), all genes differentially expressed (DE) in *brm* (**C**, light orange), and the genes that are DE that are also targets of H2A.Z (**D**, dark blue) or BRM (**E**, dark orange), followed by genes that are DE targets of both H2A.Z and BRM and DE in at least one mutant (**F**, bright green), or both *arp6* and *brm* (**G**, dark green). Boxes surrounding the circle diagram list the terms associated with each category. Hormones are abbreviated as JA – jasmonic acid, ABA – abscisic acid, Aux- auxin, and Et – ethylene. The light green box (**B**) summarizes processes that are enriched in genes DE in both *arp6* and *brm* mutants and GO terms marked with an asterisk (*) represent terms that were enriched for the total set of DE genes in one mutant but that were enriched in the set of up- or down-regulated in the other mutant instead of the list of total DE genes. The grey dotted line separates the GO term

summary boxes for general processes regulated by each factor from processes with genes that are direct targets of H2A.Z or BRM.

Figure 2.3

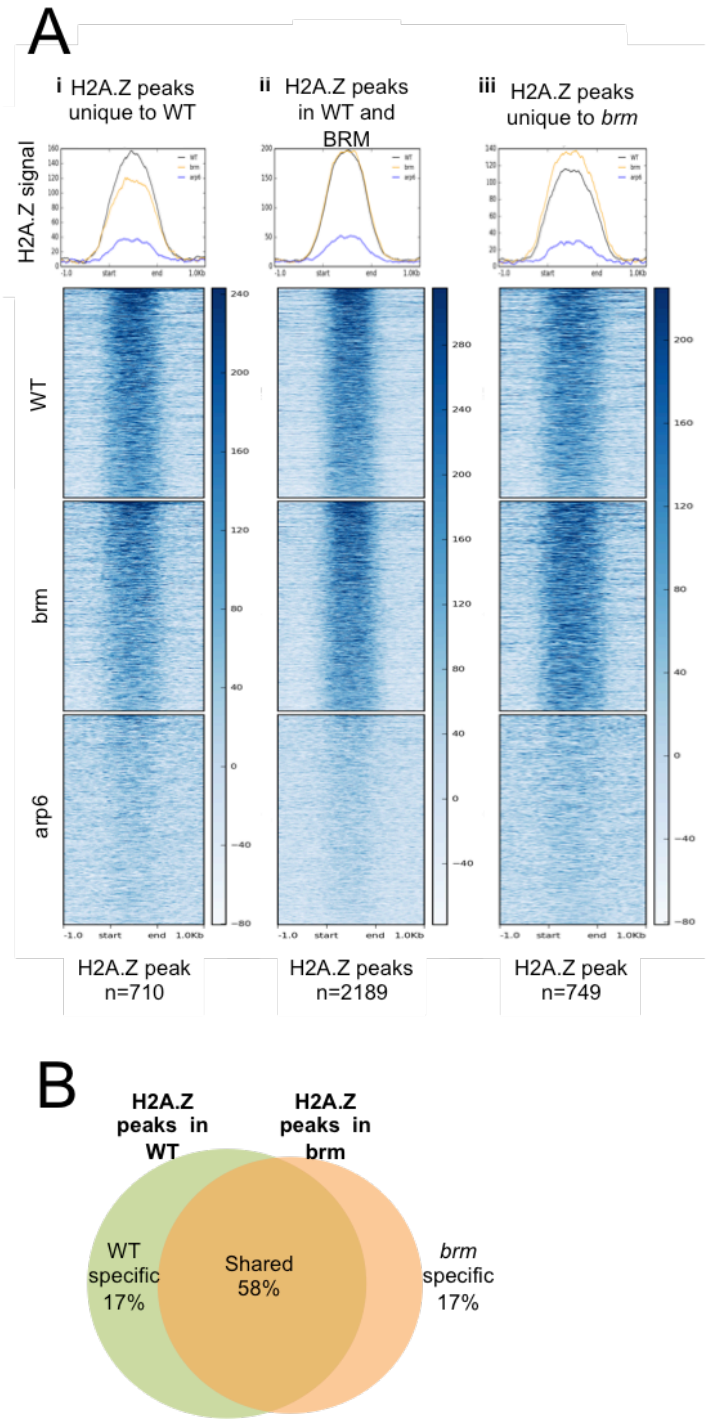

Figure 2.3. H2A.Z levels in chromatin are independent of BRM and dependent on ARP6. (**A**) Heat maps showing the H2A.Z IP signal from wild type plants (top box), *brm-1* mutants (middle

box), and *arp6-1* (bottom box). Signal is shown for ±500 bp up- and down-stream of size-scaled H2A.Z peaks that overlap with BRM peaks and that were called in i) WT alone ii) both WT and *brm*, or iii) *brm* alone. The average signal of each genotype is summarized as a profile plot at the top of the corresponding heat map, showing H2A.Z IP signals from WT (dark blue), *brm* (light blue), and *arp6* (yellow) plants. To generate the IP signals for heat maps to represent each genotype, two biological H2A.Z ChIP-seq replicates were combined and input read signals were subtracted. (**B**) Venn diagram shows the distribution of H2A.Z peaks called in WT plants (green) and *brm* mutants (orange).

Figure 2.4

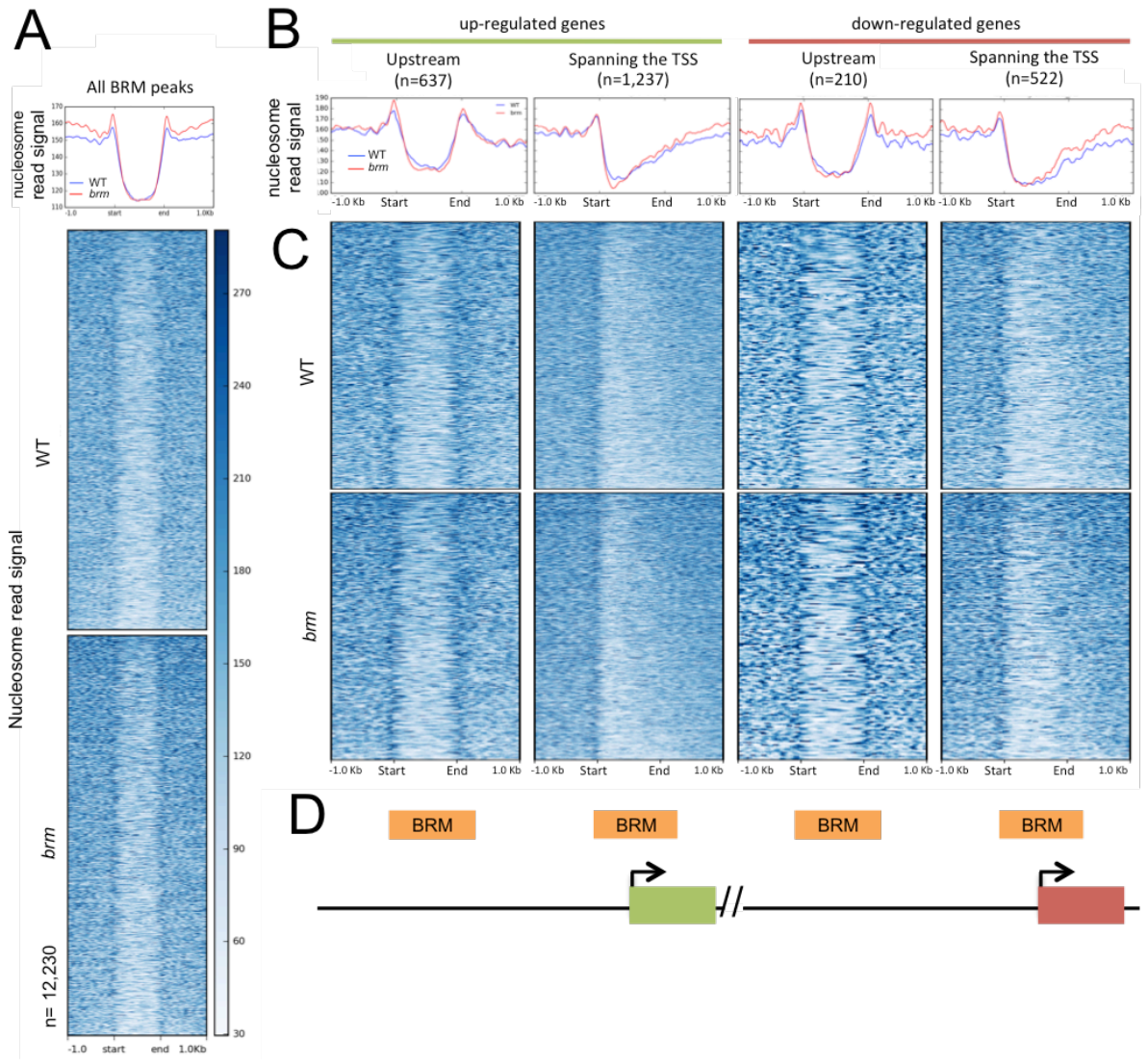

Figure 2.4. BRM is flanked by two well-positioned nucleosomes that are disrupted by transcription. (**A**) Profile plot and heatmap showing nucleosome read signals ± 1kb around all BRM peaks size-scaled to be 1 kb wide. Nucleosome reads are from an MNase-seq experiment in WT (blue line, top box of heatmap) and *brm* mutants (red line, bottom box of heatmap). (**B**) Average profile plots show nucleosome read signals from WT (blue) and *brm* (red) plants at select BRM ChIP-seq peaks associated with DE genes. Signals are plotted ± 1kb around the start and ends of peaks scaled to be 1 kb in width. BRM peaks were divided into those (i) up-stream of or (ii) spanning the transcription start site (TSS) of genes up-regulated in *brm* mutants or BRM peaks that are (iii) up-

stream of or (iv) span the TSS of a gene down-regulated *in brm* mutants. The diagram below the plots illustrates the general position of BRM peaks (orange box) used for the plots relative to the start of genes that are DE in *brm* mutants. (**C**) Heatmaps corresponding corresponding to the same sites as B, showing nucleosome read signals ± 1kb around all BRM peaks size-scaled to be 1 kb wide. Nucleosome reads are from an MNase-seq experiment in WT plants (top) and *brm* mutants (bottom). (**D**) Schematic showing the general relationship between the BRM peaks (orange) plotted in B and C and their associated target genes that are up- (green) or down-regulated (red) in *brm* mutants.

Figure 2.5

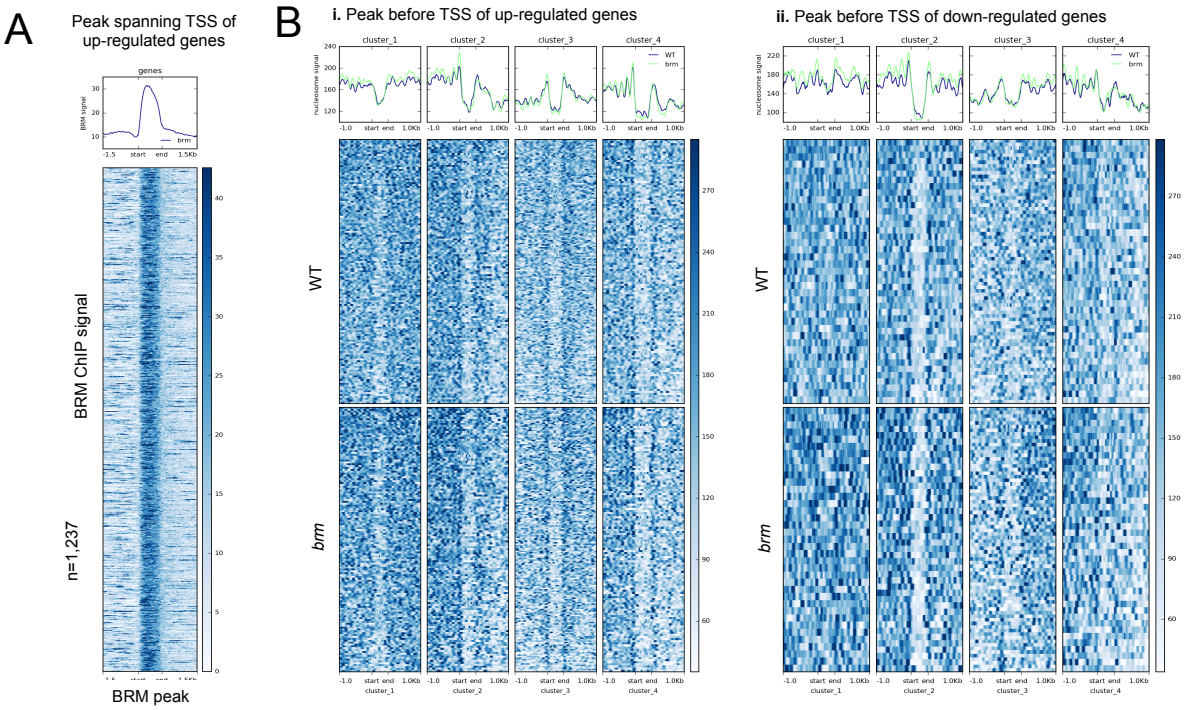

Figure 2.5 Nucleosome patterns surrounding BRM at DE BRM target genes show distinct occupancy patterns. (**A**) Plot profile and heatmap showing BRM-GFP ChIP-seq read signals surrounding BRM peaks that are upstream of genes that are up-regulated in *brm* mutants (the same sites shown in 2.4B,C). Plot shows reads ± 1kb around the BRM peaks size-scaled to be 1 kb wide. (**B**) K-means clustered heatmaps and average profile plots showing nucleosome read signals from WT plants (blue, top) and *brm* mutants (green, bottom) around size-scaled BRM peaks found upstream of the TSSs of (i) up- and (ii) down-regulated genes in *brm* mutants.

Figure 2.6

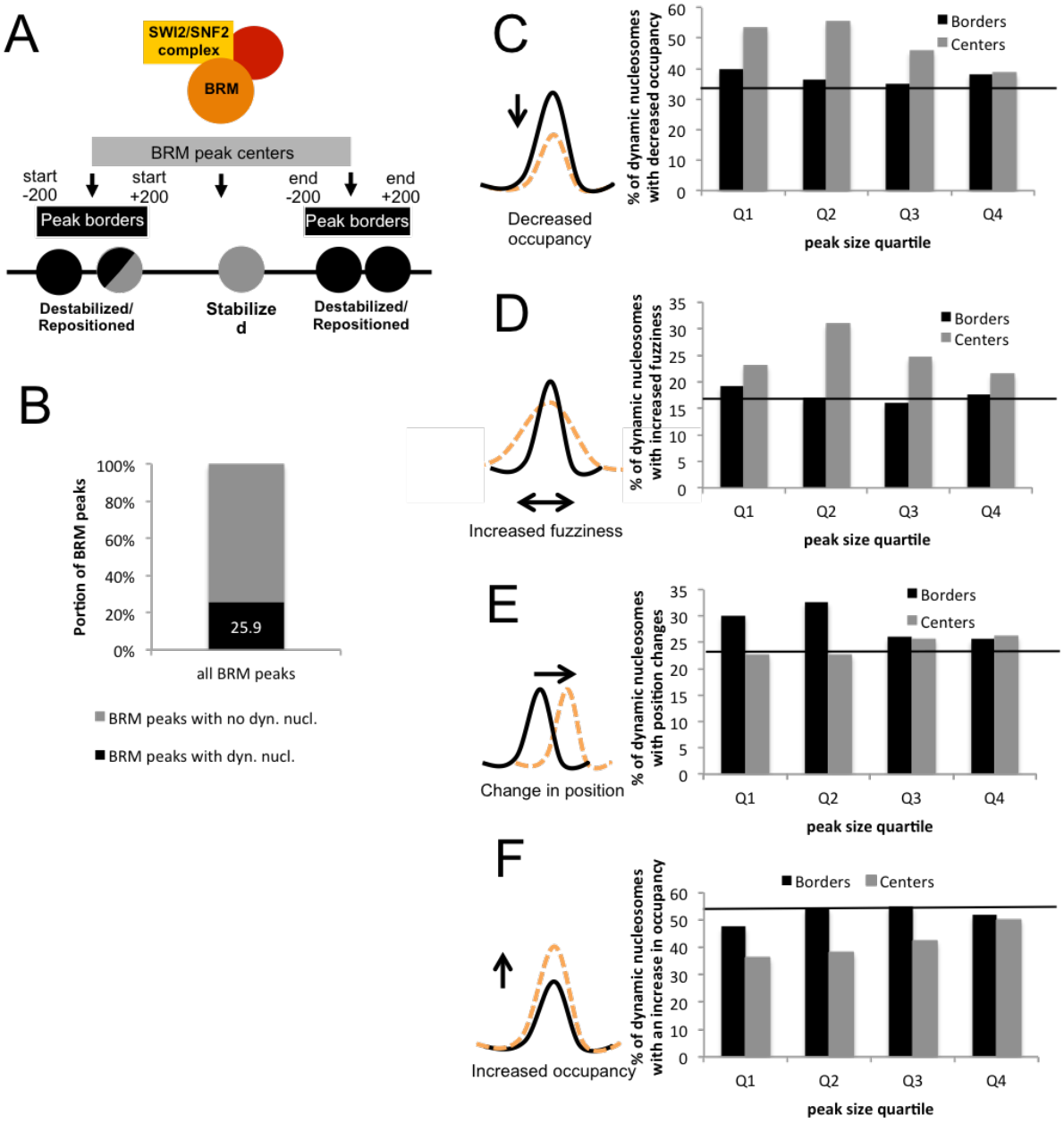

Figure 2.6. BRM contributes to nucleosome stability and positioning differentially at nucleosome-depleted regions and flanking areas. (**A**) Depiction of BRM in the *Arabidopsis* SWI2/SNF2 complex associating with chromatin and stabilizing nucleosomes within peaks and repositioning nucleosomes at peak borders. Nucleosomes within the center are colored grey and nucleosomes within border regions are colored black. Two-toned nucleosomes represent how the data

are not mutually exclusive but can contain nucleosomes that fall in both border and center categories. (**B**) Histogram showing the portion of BRM peaks that contains dynamic nucleosomes (dyn. nucl.) in the *brm* mutants (black) compared to the portion of peaks that do not have any nucleosomes with significant dynamic changes in the mutant (grey). (**C-F**) Histograms summarizing the proportion of dynamic nucleosomes found at the borders (black) or centers (gray) of BRM peaks that show a decrease in occupancy (**C**), change in position (**D**), an increase in fuzziness (**E**), or an increase in occupancy (**F**) in *brm* mutants. Peak centers included nucleosomes fully contained within the defined peaks and borders include those that overlap with a peak start or end. The proportion of dynamic nucleosomes across the genome with the indicated type of change in *brm* mutants is shown as a black line for comparison. BRM peaks were separated into size quartiles for analysis: Q1: 300-415 bp, Q2: 415-546 bp, Q3: 546-776 bp, Q4: 776 bp-4kb. Diagrams to the left of the histograms represent the nucleosome changes described in *brm* mutants (orange dashed line) compared to WT nucleosomes (black line).

Figure 2.7

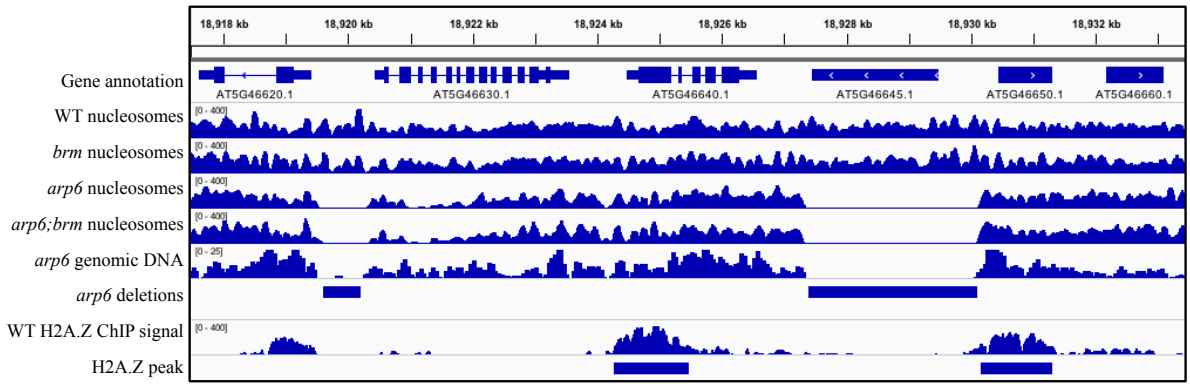

Figure 2.7. The *arp6* mutant genome contains large genomic deletions. Integrated Genome Viewer (IGV) screen shot demonstrating two large genomic deletions present in *arp6* mutants. Tracks from top to bottom show gene annotations, WT MNase-seq nucleosome signal, *brm* mutant nucleosome signal, *arp6* mutant nucleosome signal, *arp6;brm* mutant nucleosome signal, *arp6* input DNA sample from H2A.Z ChIP-seq experiment, CNVnator called deletions in *arp6* mutants, WT H2A.Z ChIP-seq signal normalized to input, H2A.Z peaks demarcating significant H2A.Z enrichment.

Figure 2.8

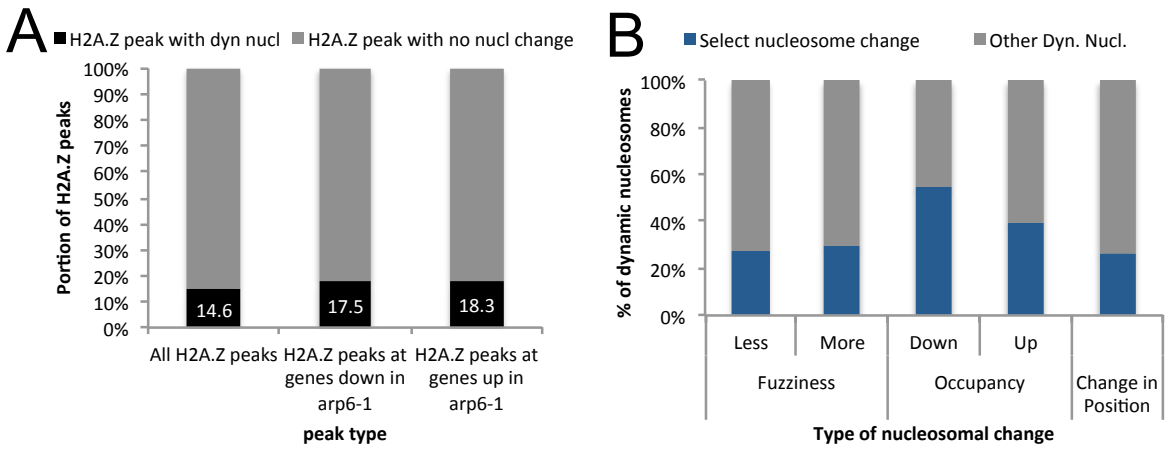

Figure 2.8. H2A.Z contributes to a range of nucleosome changes. (**A**) Histogram showing the proportion of nucleosomes at H2A.Z peaks that overlap with nucleosomes that show significant dynamic changes in arp6 mutants (black) compared to peaks that do not overlap significant nucleosomal changes in the mutant (grey). Three different categories of H2A.Z peaks are described including all H2A.Z peaks, H2A.Z peaks at genes that are down-regulated in *arp6* mutants, and H2A.Z peaks associated with genes that are up-regulated in *arp6* mutants.

(**B**) Histogram summarizing the percentage of each type of DANPOS2-called dynamic nucleosomes (blue) compared to all other dynamic nucleosomes (grey) called within H2A.Z peaks when comparing *arp6* nucleosomes to WT nucleosomes.

Figure 2.9

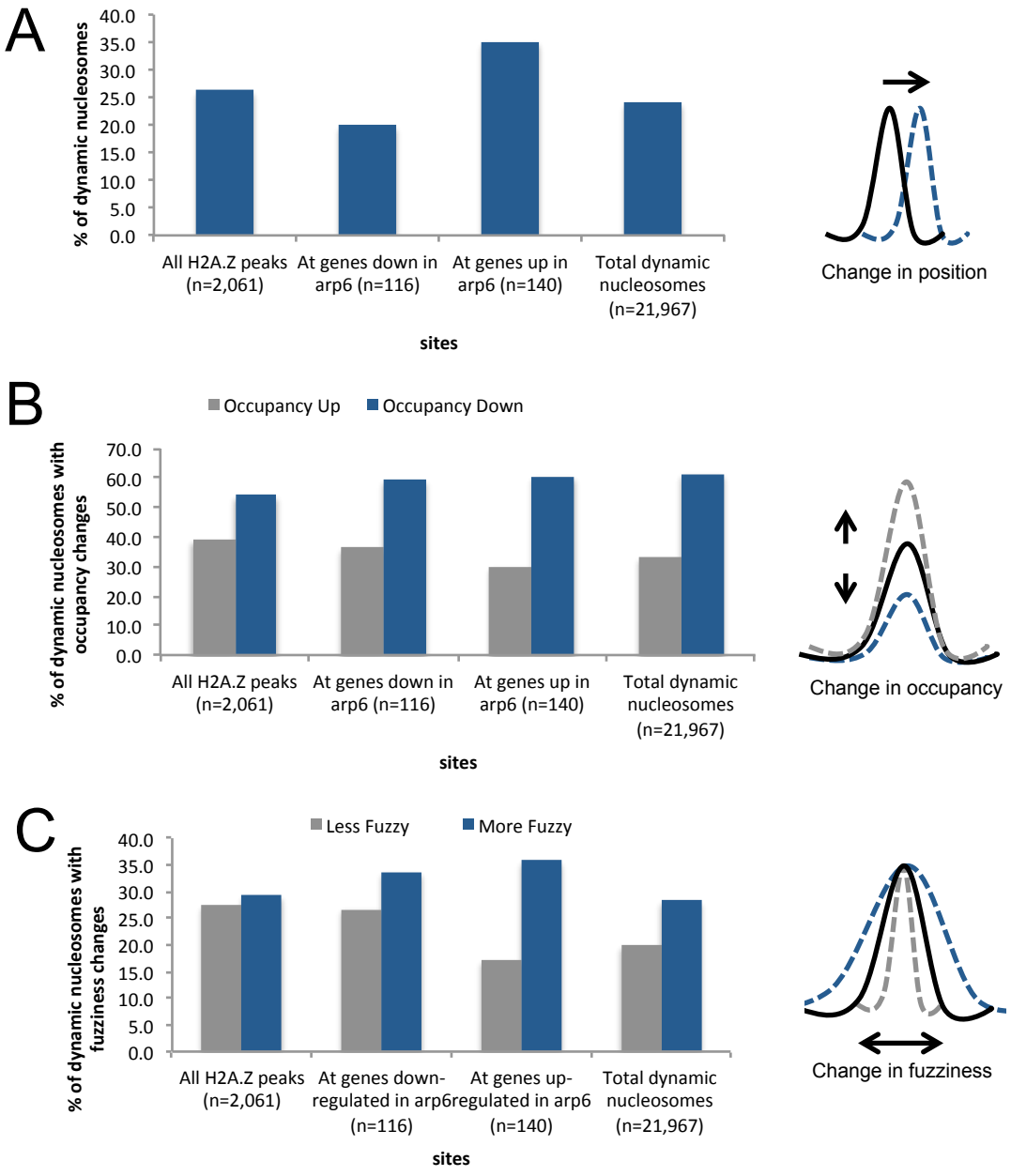
A
% of dynamic nucleosomes
40.0
35.0
30.0
25.0
20.0
15.0
10.0
5.0
0.0
All H2A.Z peaks (n=2,061)
At genes down in arp6 (n=116)
At genes up in arp6 (n=140)
Total dynamic nucleosomes (n=21,967)
sites
Change in position
B
Occupancy Up
Occupancy Down
% of dynamic nucleosomes with occupancy changes
70.0
60.0
50.0
40.0
30.0
20.0
10.0
0.0
All H2A.Z peaks (n=2,061)
At genes down in arp6 (n=116)
At genes up in arp6 (n=140)
Total dynamic nucleosomes (n=21,967)
sites
Change in occupancy
C
Less Fuzzy
More Fuzzy
% of dynamic nucleosomes with fuzziness changes
40.0
35.0
30.0
25.0
20.0
15.0
10.0
5.0
0.0
All H2A.Z peaks (n=2,061)
At genes down-regulated in arp6 (n=116)
At genes up-regulated in arp6 (n=140)
Total dynamic nucleosomes (n=21,967)
sites
Change in fuzziness

Figure 2.9. Quantifying H2A.Z contributions to nucleosome occupancy, positioning, and fuzziness changes in *arp6* mutants. Histograms showing the percent of total dynamic nucleosomes with (**A**) changes in nucleosome positioning, (**B**) occupancy, and (**C**) fuzziness at H2A.Z peaks. Regions analyzed correspond to all H2A.Z peaks (n=2,061), H2A.Z peaks that associate with genes that are down- (n=116) or up-regulated in *arp6* (n=140), or total dynamic nucleosomes (n=21,967) in the *arp6* genome. Diagrams to the right of the histogram indicate the type of change being described when comparing WT nucleosomes (black line) to nucleosomes in *arp6* mutants (dashed lines, colors correspond to the histogram legend).

Figure 2.10

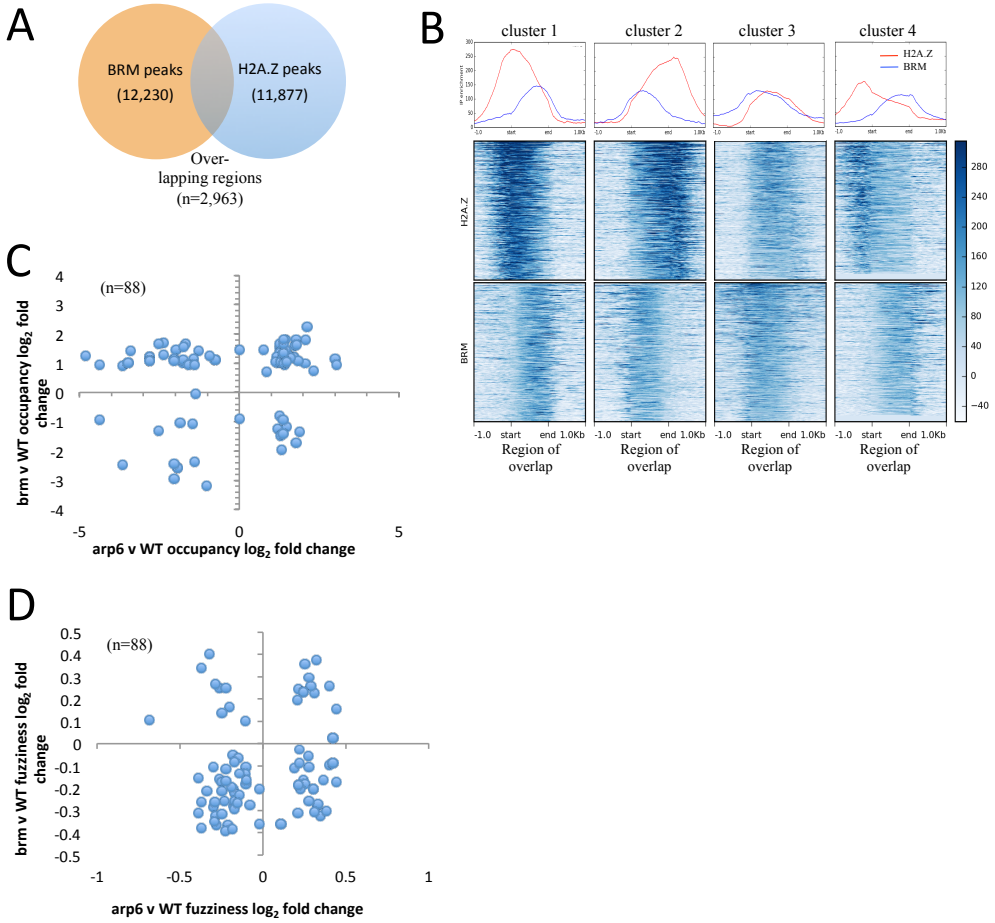

Figure 2.10. BRM destabilizes nucleosomes where BRM and H2A.Z overlap. (**A**) Venn diagram shows the number of BRM peaks, H2A.Z peaks, and regions of overlap between the two. (**B**) Average profile plots and heatmaps show four K-means clustered H2A.Z and BRM ChIP-seq read signal patterns (normalized to input) at regions of overlap between BRM and H2A.Z peaks. Regions of overlap with dynamic nucleosomes identified in each mutant relative to wild type nucleosomes (n=88) were further evaluated. Scatter plots display the $\log_2$ fold change in nucleosome occupancy (**C**) and fuzziness (**D**) in regions of H2A.Z/BRM overlap that contain dynamic nucleosomes in both *brm* mutants (y-axis) and *arp6* mutants (x-axis) compared to WT.

Figure 2.11

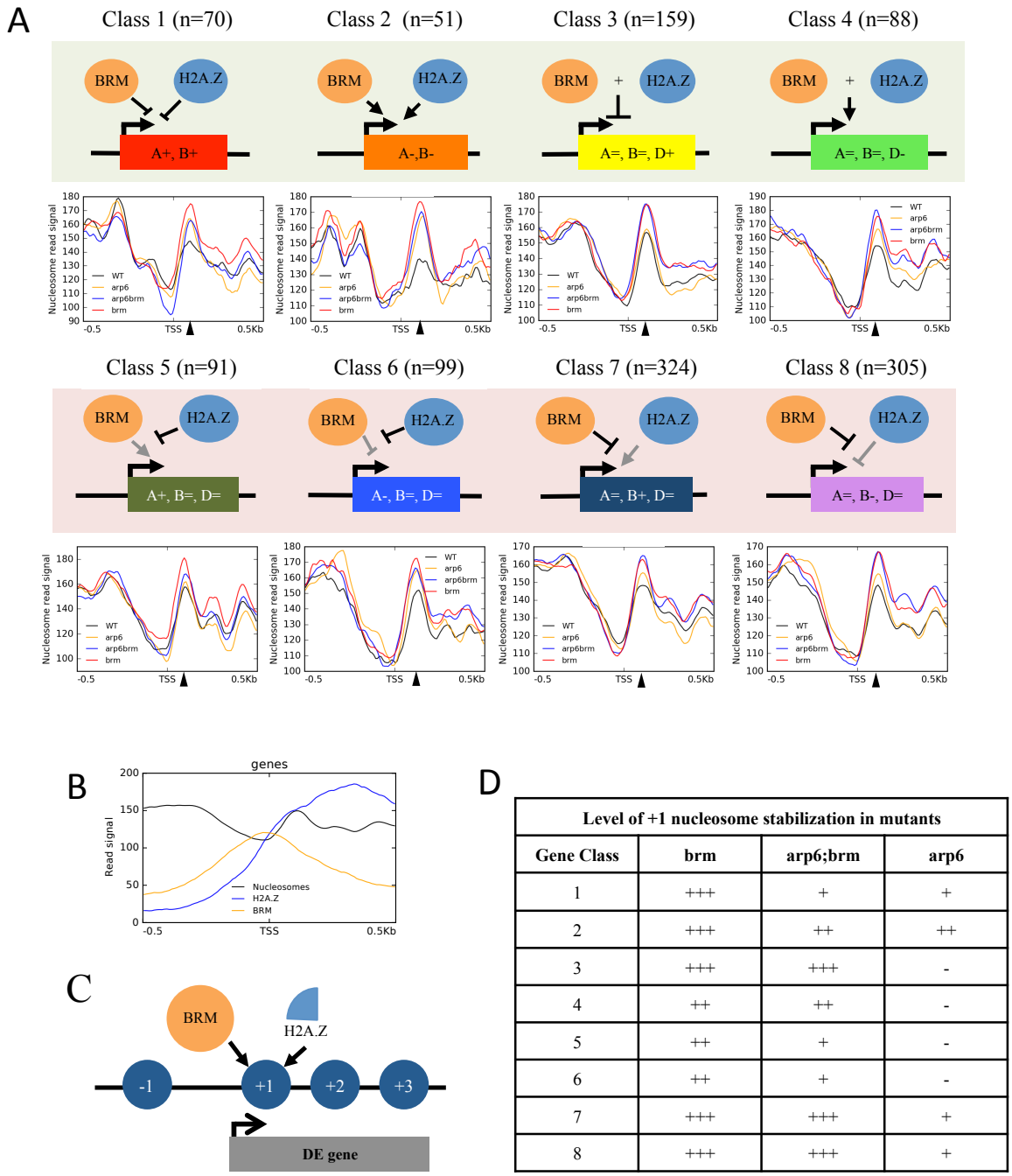

Level of +1 nucleosome stabilization in mutants			
Gene Class	**brm**	**arp6;brm**	**arp6**
1	+++	+	+
2	+++	++	++
3	+++	+++	-
4	++	++	-
5	++	+	-
6	++	+	-
7	+++	+++	+
8	+++	+++	+

Figure 2.11. BRM and H2A.Z destabilize the +1 nucleosome at DE targets. (**A**) Profile plots showing the average nucleosome read signal from WT plants (black), *arp6* (orange), *arp6;brm* (blue), and *brm* mutants (red) ±500 bp around the TSSs of the 8 classes of DE H2A.Z and BRM target genes.

Black triangles on the x-axis indicate the position of the +1 nucleosome. The diagrams above the plots describe the genetic relationships between BRM and H2A.Z/ARP6 for each gene class and are the same as those described in Fig. 1. (**B**) Profile plot showing the read signal for WT nucleosomes (black), H2A.Z ChIP-seq (blue), and BRM ChIP-seq (orange), averaged across ±500 bp up- and downstream of the TSSs of the DE BRM and H2A.Z target genes. (**C**) Diagram representing how we used ChIP-seq, MNase-seq, and RNA-seq data sets in the previous figures, to evaluated the relationship between BRM localization in WT (orange), H2A.Z localization in WT (light blue) and nucleosomes (blue circles) around the TSSs of DE BRM and H2A.Z target genes. (**D**) Table summarizes the extent to which the +1 nucleosomes become stabilized in *brm, arp6;brm* and *arp6* mutants at the 8 DE BRM-H2A.Z target gene classes defined in Fig 1. The level of nucleosome stabilization in the mutant was defined based on the overlaps between different measures of variance at the +1 nucleosome read signals plotted in Fig. 2.12. The degree to which the +1 nucleosome was stabilized in the mutants compared to WT is defined as no change (- = mean of one falls within the 95% confidence interval of the other); a small change (+ = the mean of one sample does not overlap with the 95% confidence interval of the other); a medium change (++ = the standard error of one sample does not overlap with the 95% confidence interval of the other); or a large change in nucleosome occupancy (+++ = there is no overlap between 95% confidence intervals for the two samples).

Figure 2.12

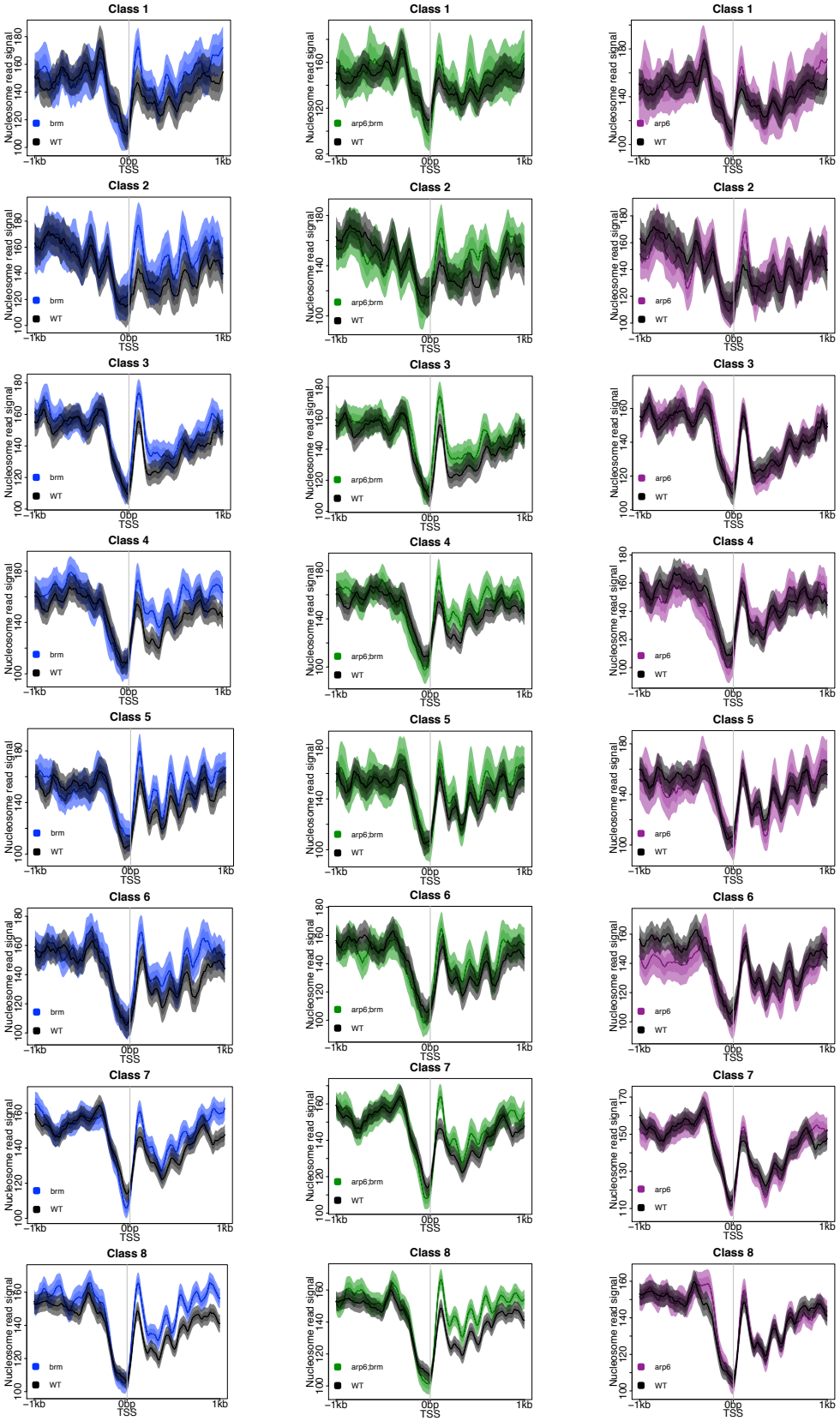
Class 1
Class 2
Class 3
Class 4
Class 5
Class 6
Class 7
Class 8
Nucleosome read signal
brm
arp6;brm
arp6
WT
−1kb
0bp
TSS
1kb

Figure 2.12. Nucleosome patterns at coordinately and antagonistically H2A.Z and BRM regulated gene sets. Individual comparisons of nucleosome patterns at the coordinately and antagonistically regulated gene classes between WT and *brm*, *arp6;brm,* and *arp6* mutants in Fig 2.11. The average profile plots display nucleosome read signals generated from MNase-seq experiments plotted ±1 kb around the TSSs of our 8 DE gene classes identified in Fig. 2.1. Profiles show nucleosome read signals from *brm* (blue, left), *arp6;brm* (green, center), and *arp6* mutants (pink, right) compared to WT plants (black). The mean of the read signals are shown as a dashed line and the standard error and 95% confidence intervals are shaded (darker and lighter respectively) with the corresponding color.

Figure 2.13

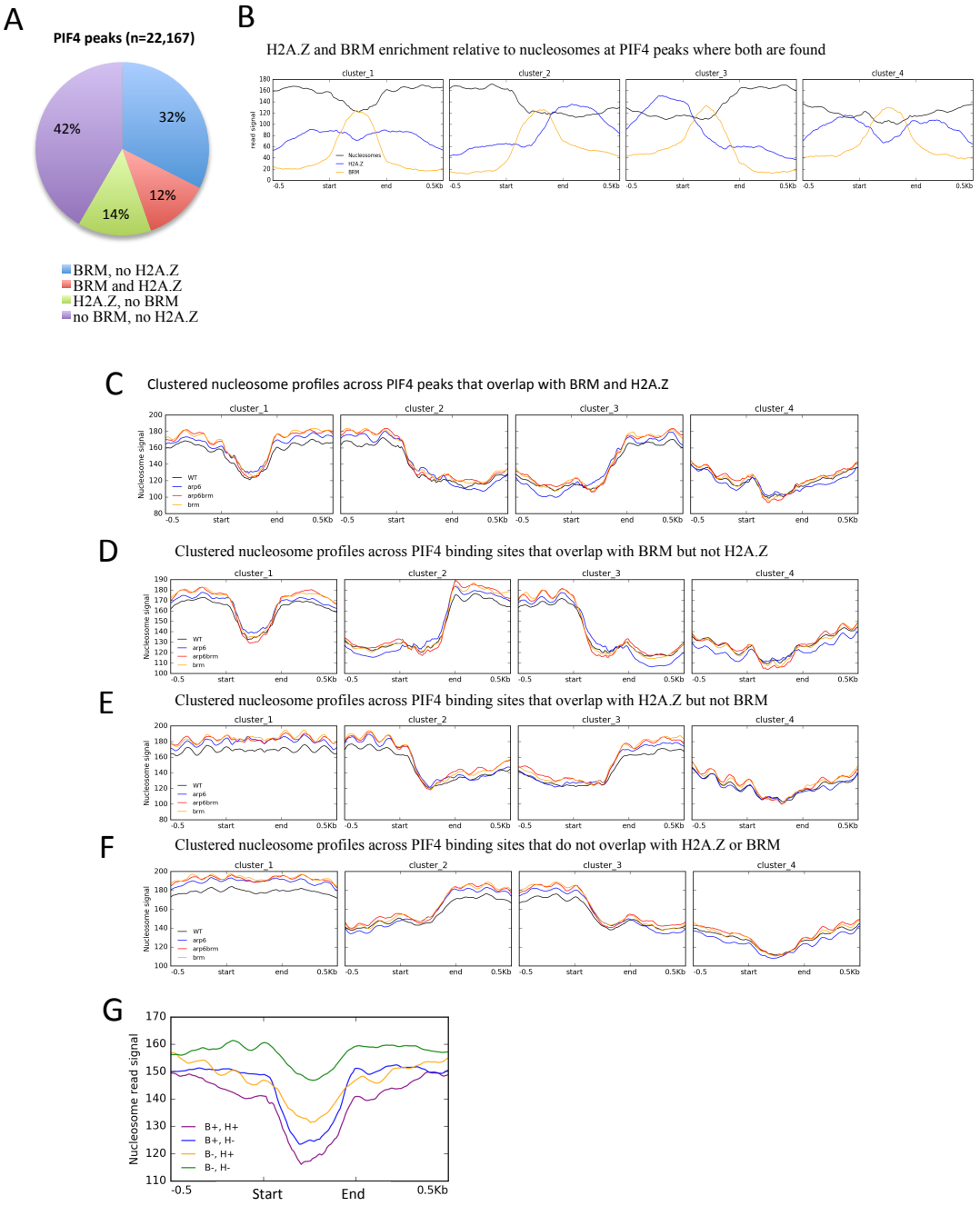

Figure 2.13 BRM and H2A.Z overlap with PIF4 peaks but do not affect the surrounding chromatin environment. (**A**) Pie chart showing the proportion of PIF4 peaks that overlap with H2A.Z alone (blue), BRM and H2A.Z (red), BRM alone (green), or neither (purple). (**B**) Average profile plots showing the BRM (orange) and H2A.Z (blue) ChIP-seq read signals plotted along with

WT nucleosome patterns (black) at size-scaled PIF4 binding sites. Nucleosome patterns are subdivided into 4 K-means clusters. (**C-F**) Average K-means clustered profile plots showing nucleosome reads from MNase-seq experiments surrounding size-scaled PIF4 ChIP-seq binding sites that overlap with BRM and H2A.Z (**C**), overlap with BRM and not H2A.Z (**D**), overlap with H2A.Z and not BRM (**E**), and do not overlap with either (**F**). Plots show nucleosome profiles from WT (black), *arp6* (blue), *arp6;brm* (red), and *brm* plants (orange). (**G**) Average profile plot showing the WT nucleosome patterns at PIF4 sites that have both BRM and H2A.Z (B+, H+; purple), BRM and not H2A.Z (B+, H-; blue), H2A.Z and not BRM (B-, H+; orange), or no BRM nor H2A.Z (B-, H-; green).

Figure 2.14

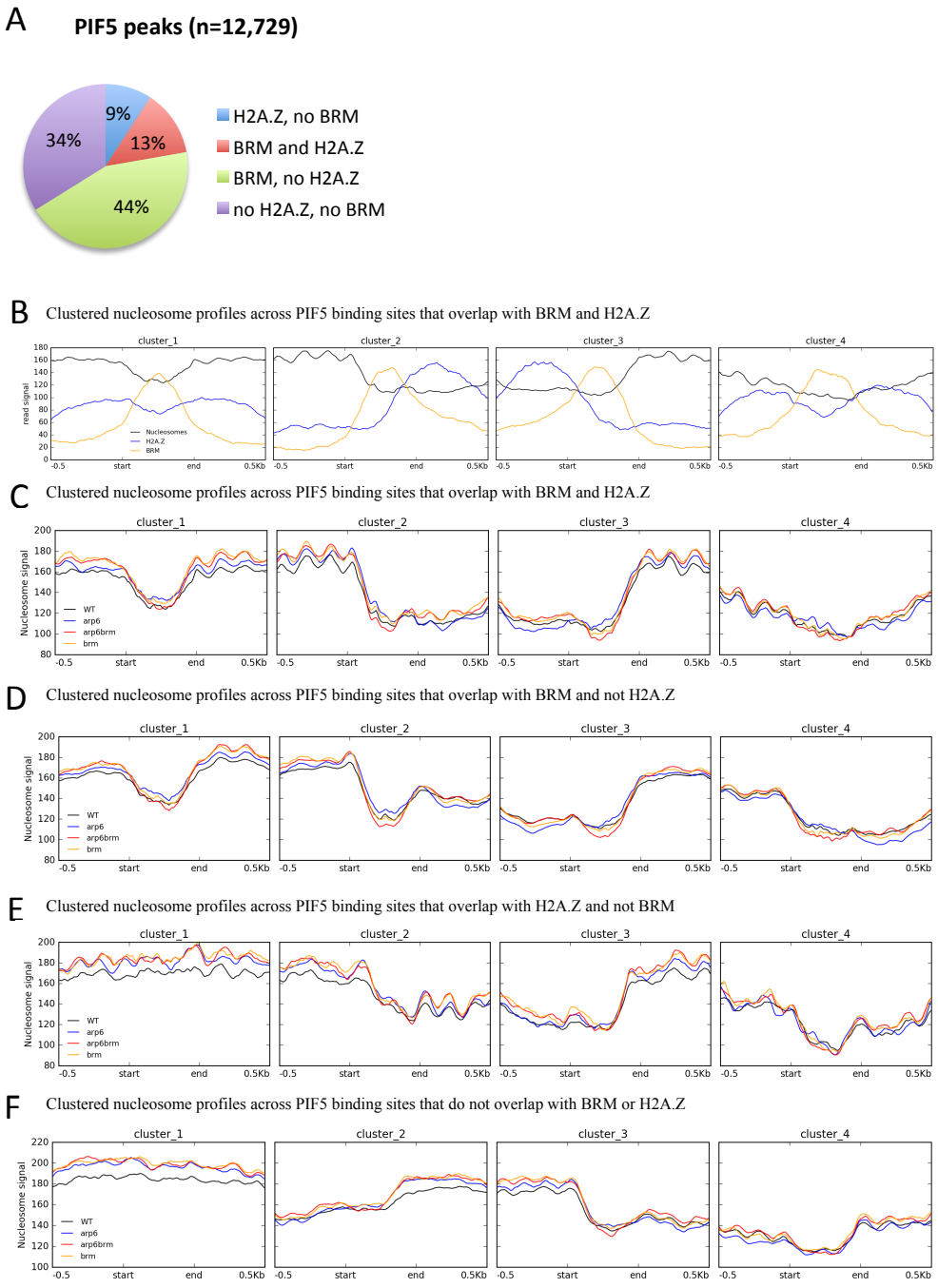

Figure 2.14 BRM and H2A.Z overlap with PIF5 peaks but do not affect the surrounding chromatin environment. (**A**) Pie chart showing the proportion of PIF5 peaks that overlap with H2A.Z alone (blue), BRM and H2A.Z (red), BRM alone (green), or neither (purple). (**B**) Average

profile plots showing the BRM (orange) and H2A.Z (blue) ChIP-seq read signals plotted along with WT nucleosome patterns (black) at size-scaled PIF5 binding sites. Nucleosome patterns are subdivided into 4 K-means clusters. (**C-F**) Average K-means clustered profile plots showing nucleosome reads from MNase-seq experiments surrounding size-scaled PIF5 ChIP-seq binding sites that overlap with BRM and H2A.Z (**C**), overlap with BRM and not H2A.Z (**D**), overlap with H2A.Z and not BRM (**E**), and do not overlap with either (**F**). Plots show nucleosome profiles from WT (black), *arp6* (blue), *arp6;brm* (red), and *brm* plants (orange).

Figure 2.15

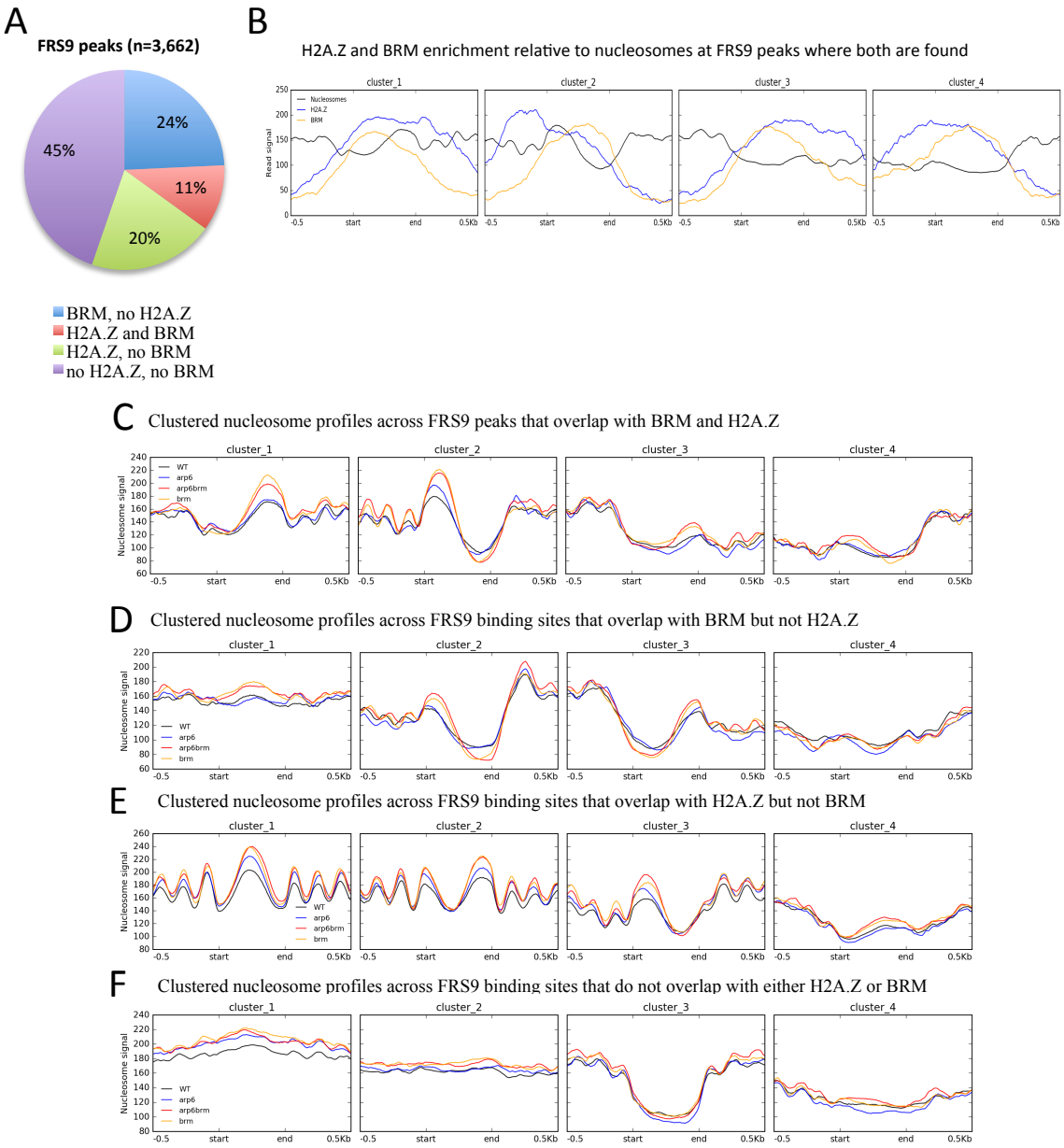

Figure 2.15. BRM and H2A.Z can contribute to nucleosome stability at FRS9 binding sites. (**A**) Pie chart showing the proportion of FRS9 peaks that overlap with H2A.Z alone (blue), BRM and H2A.Z (red), BRM alone (green), or neither (purple). (**B**) Average profile plots showing the BRM (orange) and H2A.Z (blue) ChIP-seq read signals plotted along with WT nucleosome patterns (black) at size-scaled FRS9 binding sites. Nucleosome patterns are subdivided into 4 K-means clusters. (**C-F**)

Average K-means clustered profile plots showing nucleosome reads from MNase-seq experiments surrounding size-scaled FRS9 ChIP-seq binding sites that overlap with BRM and H2A.Z (**C**), overlap with BRM and not H2A.Z (**D**), overlap with H2A.Z and not BRM (**E**), and do not overlap with either (**F**). Plots show nucleosome profiles from WT (black), *arp6* (blue), *arp6;brm* (red), and *brm* plants (orange).

Table 2.1. Summary of MEME-TOMTOM output showing transcription factors (TFs) that potentially associate with our 8 classes of DE genes

* = TF that can associate with AtSWI2/SNF2 subunits based on previous publications (Efroni et al., 2013; Zhang et al., 2016), **x**= TF binding sites are enriced at this gene class

Mutant genotypes and direction of transcriptional changes of the 8 DE gene classes in these mutants are described with the following abbreviations: A=*arp6-1*, B=*brm-1*, D=*arp6-1*;*brm-1*, "+" =up-regulated in mutant, "-" =down-regulated in mutant, "=" = not DE in the mutant

Gene Class		Class 1	Class 2	Class 3	Class 4	Class 5	Class 6	Class 7	Class 8
Gene regulation description		A+, B+	A-, B-	A=, B=, D+	A=, B=, D-	A-, B=, D=	A-, B=, D=	A=, B+, D=	A=, B-, D=
Number of genes in class		70	51	159	88	91	99	324	305
Number of THS associated with genes in class		211	162	424	221	244	331	964	760
Number of different types of TFs identified		0	11	49	28	18	5	34	32
List of TFs	Number of gene classes where TF binding sites are enriched								
ABF1*	4			x	x	x		x	
ABF2/ATAREB1	4			x	x			x	x
ABF3*	3			x		x		x	
ABI5	4			x	x	x		x	x
Adof1	1			x					
AREB3	3				x			x	x
AT1G47655	2					x		x	
AT1G69570	2		x	x		x			
AT3G46070	1							x	
AT5G02460	1			x					
ATAREB1	3			x	x			x	x
AtbZIP63	2				x				x
AtIDD11	1			x					
BAM8	1			x					
BEE2	1			x					
BEH2	1			x					
BEH3	1			x					
BEH4	1			x					
BES1	2			x				x	
bHLH104	4			x	x	x			x
bHLH13/JAM2	3			x				x	
bHLH18	4			x	x	x		x	
bHLH31/BPE/ZCW32	2			x					x
bHLH34	2			x	x				
bHLH43	1								x
bHLH69	1			x					
bHLH74	2			x				x	
bHLH77/ace3, en87	1			x					
BIM1*	1			x					
BIM2	1			x					
BIM3	1			x					
BPC1	7		x	x	x	x	x	x	x
BPC5	7		x	x	x	x	x	x	x
BPC6	6		x	x	x		x	x	x
bZIP16	3				x			x	x
bZIP28	1								x
bZIP3*	1								x
bHLH31	1							x	
bZIP42*	1								x
bZIP43	1								x
bZIP44	1								x
bZIP48	1								x
bZIP53	1								x
bZIP68	5			x	x	x		x	x
BZR1	5			x	x	x		x	x
CDF3	1		x						
CIB2	2			x				x	
AT1G69570	1			x		x			
DYT1	1			x					
FRS9	6		x	x	x		x	x	x
GBF1	4				x	x		x	x
GBF2	4				x	x		x	x
GBF3*	3				x			x	x
GBF5*	1								x
GBF6/bZIP11	1								x
GT3a*	1			x					
HBI1	1			x					
HCA2/DOF5.6	1			x					

Table 2.1 (continued)

HY5	5			x	x	x		x	x
ILR3	2			x	x				
MYC2*	1			x					
MYC4	1			x					
PIF4/SRL2	5			x	x	x		x	x
PIF5/PIL6	2			x	x				
PIF7	4			x	x			x	x
PIL5/PIF1*	1			x					
POC1/PIF3*	4			x	x	x			x
PTF1*	1		x						
SOC1	4			x	x	x		x	
SPT (PIF family)	2			x				x	
TF3A	1							x	
TCP1*	1		x						
TCP16*	2						x	x	
TCP21	1		x						
TCP22*	1		x						
TCP3*	1		x						
UNE10	4			x	x			x	x
WRKY45	1							x	
WRKY7	1							x	

Literature Cited

Abyzov A, Urban AE, Snyder M, Gerstein M (2011) CNVnator: an approach to discover, genotype, and characterize typical and atypical CNVs from family and population genome sequencing. Genome Res 21: 974-84

Afgan E, Baker D, van den Beek M, Blankenberg D, Bouvier D, Cech M, Chilton J, Clements D, Coraor N, Eberhard C, Gruning B, Guerler A, Hillman-Jackson J, Von Kuster G, Rasche E, Soranzo N, Turaga N, Taylor J, Nekrutenko A, Goecks J (2016) The Galaxy platform for accessible, reproducible and collaborative biomedical analyses: 2016 update. Nucleic Acids Res 44: W3-W10

Alazem M, Lin NS (2015) Roles of plant hormones in the regulation of host-virus interactions. Mol Plant Pathol 16: 529-40

Allan J, Fraser RM, Owen-Hughes T, Keszenman-Pereyra D (2012) Micrococcal nuclease does not substantially bias nucleosome mapping. J Mol Biol 417: 152-64

Allen RS, Nakasugi K, Doran RL, Millar AA, Waterhouse PM (2013) Facile mutant identification via a single parental backcross method and application of whole genome sequencing based mapping pipelines. Front Plant Sci 4: 362

Anders S, Pyl PT, Huber W (2015) HTSeq--a Python framework to work with high-throughput sequencing data. Bioinformatics 31: 166-9

Arabidopsis Genome I (2000) Analysis of the genome sequence of the flowering plant Arabidopsis thaliana. Nature 408: 796-815

Archacki R, Buszewicz D, Sarnowski TJ, Sarnowska E, Rolicka AT, Tohge T, Fernie AR, Jikumaru Y, Kotlinski M, Iwanicka-Nowicka R, Kalisiak K, Patryn J, Halibart-Puzio J, Kamiya Y, Davis SJ, Koblowska MK, Jerzmanowski A (2013) BRAHMA ATPase of the SWI/SNF Chromatin Remodeling Complex Acts as a Positive Regulator of Gibberellin-Mediated Responses in Arabidopsis. PLoS One 8: e58588

Archacki R, Yatusevich R, Buszewicz D, Krzyczmonik K, Patryn J, Iwanicka-Nowicka R, Biecek P, Wilczynski B, Koblowska M, Jerzmanowski A, Swiezewski S (2016) Arabidopsis SWI/SNF chromatin remodeling complex binds both promoters and terminators to regulate gene expression. Nucleic Acids Res

Austin RS, Vidaurre D, Stamatiou G, Breit R, Provart NJ, Bonetta D, Zhang J, Fung P, Gong Y, Wang PW, McCourt P, Guttman DS (2011) Next-generation mapping of Arabidopsis genes. Plant J 67: 715-25

Austin RS, Chatfield SP, Desveaux D, Guttman DS (2014) Next-generation mapping of genetic mutations using bulk population sequencing. Methods Mol Biol 1062: 301-15

Bailey TL, Boden M, Buske FA, Frith M, Grant CE, Clementi L, Ren J, Li WW, Noble WS (2009) MEME SUITE: tools for motif discovery and searching. Nucleic Acids Res 37: W202-8

Ballare CL (1999) Keeping up with the neighbours: phytochrome sensing and other signalling mechanisms. Trends Plant Sci 4: 97-102

Barah P, B NM, Jayavelu ND, Sowdhamini R, Shameer K, Bones AM (2016) Transcriptional regulatory networks in Arabidopsis thaliana during single and combined stresses. Nucleic Acids Res 44: 3147-64

Barneche F, Baroux C (2017) Unreeling the chromatin thread: a genomic perspective on organization around the periphery of the Arabidopsis nucleus. Genome Biol 18: 97

Bazett-Jones DP, Cote J, Landel CC, Peterson CL, Workman JL (1999) The SWI/SNF complex creates loop domains in DNA and polynucleosome arrays and can disrupt DNA-histone contacts within these domains. Mol Cell Biol 19: 1470-8

Becker JS, Nicetto D, Zaret KS (2016) H3K9me3-Dependent Heterochromatin: Barrier to Cell Fate Changes. Trends Genet 32: 29-41

Berger SL (2007) The complex language of chromatin regulation during transcription. Nature 447: 407-12

Berriri S, Gangappa SN, Kumar SV (2016) SWR1 Chromatin-Remodeling Complex Subunits and H2A.Z Have Non-overlapping Functions in Immunity and Gene Regulation in Arabidopsis. Mol Plant 9: 1051-65

Bevan M, Walsh S (2005) The Arabidopsis genome: a foundation for plant research. Genome Res 15: 1632-42

Bezhani S, Winter C, Hershman S, Wagner JD, Kennedy JF, Kwon CS, Pfluger J, Su Y, Wagner D (2007) Unique, shared, and redundant roles for the Arabidopsis SWI/SNF chromatin remodeling ATPases BRAHMA and SPLAYED. Plant Cell 19: 403-16

Bi X, Cheng YJ, Hu B, Ma X, Wu R, Wang JW, Liu C (2017) Nonrandom domain organization of the Arabidopsis genome at the nuclear periphery. Genome Res 27: 1162-1173

Bieluszewski T, Galganski L, Sura W, Bieluszewska A, Abram M, Ludwikow A, Ziolkowski PA, Sadowski J (2015) AtEAF1 is a potential platform protein for Arabidopsis NuA4 acetyltransferase complex. BMC Plant Biol 15: 75

Blower MD, Karpen GH (2001) The role of Drosophila CID in kinetochore formation, cell-cycle progression and heterochromatin interactions. Nat Cell Biol 3: 730-9

Bonisch C, Hake SB (2012) Histone H2A variants in nucleosomes and chromatin: more or less stable? Nucleic Acids Res 40: 10719-41

Bönisch C, Hake SB (2012) Histone H2A variants in nucleosomes and chromatin: more or less stable? Nucleic Acids Research 40: 10719-10741

Bourbousse C, Mestiri I, Zabulon G, Bourge M, Formiggini F, Koini MA, Brown SC, Fransz P, Bowler C, Barneche F (2015) Light signaling controls nuclear architecture reorganization during seedling establishment. Proc Natl Acad Sci U S A 112: E2836-44

Boyes DC, Zayed AM, Ascenzi R, McCaskill AJ, Hoffman NE, Davis KR, Gorlach J (2001) Growth stage-based phenotypic analysis of Arabidopsis: a model for high throughput functional genomics in plants. Plant Cell 13: 1499-510

Brzezinka K, Altmann S, Czesnick H, Nicolas P, Gorka M, Benke E, Kabelitz T, Jahne F, Graf A, Kappel C, Baurle I (2016) Arabidopsis FORGETTER1 mediates stress-induced chromatin memory through nucleosome remodeling. Elife 5:

Burton DR, Butler MJ, Hyde JE, Phillips D, Skidmore CJ, Walker IO (1978) The interaction of core histones with DNA: equilibrium binding studies. Nucleic Acids Res 5: 3643-63

Buszewicz D, Archacki R, Palusinski A, Kotlinski M, Fogtman A, Iwanicka-Nowicka R, Sosnowska K, Kucinski J, Pupel P, Oledzki J, Dadlez M, Misicka A, Jerzmanowski A, Koblowska MK (2016) HD2C histone deacetylase and a SWI/SNF chromatin remodeling complex interact and both are involved in mediating the heat stress response in Arabidopsis. Plant Cell Environ

Carmona-Saez P, Chagoyen M, Tirado F, Carazo JM, Pascual-Montano A (2007) GENECODIS: a web-based tool for finding significant concurrent annotations in gene lists. Genome Biol 8: R3

Carter B, Bishop B, Ho KK, Li H, Overway E, Dugard C, Huang R, Jia W, Zhang H, Carpita N, Pascuzzi P, Deal R, Ogas J (2017) The Chromatin Remodelers PKL and PIE1 Act in an Epigenetic Pathway that Determines H3K27me3 Homeostasis in Arabidopsis. In revision at Plant Cell.

Catala R, Medina J, Salinas J (2011) Integration of low temperature and light signaling during cold acclimation response in Arabidopsis. Proc Natl Acad Sci U S A 108: 16475-80

Chatterjee N, Sinha D, Lemma-Dechassa M, Tan S, Shogren-Knaak MA, Bartholomew B (2011) Histone H3 tail acetylation modulates ATP-dependent remodeling through multiple mechanisms. Nucleic Acids Res 39: 8378-91

Chen K, Xi Y, Pan X, Li Z, Kaestner K, Tyler J, Dent S, He X, Li W (2013) DANPOS: dynamic analysis of nucleosome position and occupancy by sequencing. Genome Res 23: 341-51

Choi K, Park C, Lee J, Oh M, Noh B, Lee I (2007) Arabidopsis homologs of components of the SWR1 complex regulate flowering and plant development. Development 134: 1931-41

Choi K, Zhao X, Kelly KA, Venn O, Higgins JD, Yelina NE, Hardcastle TJ, Ziolkowski PA, Copenhaver GP, Franklin FC, McVean G, Henderson IR (2013) Arabidopsis meiotic crossover hot spots overlap with H2A.Z nucleosomes at gene promoters. Nat Genet 45: 1327-36

Clapier CR, Iwasa J, Cairns BR, Peterson CL (2017) Mechanisms of action and regulation of ATP-dependent chromatin-remodelling complexes. Nat Rev Mol Cell Biol 18: 407-422

Clarkson MJ, Wells JR, Gibson F, Saint R, Tremethick DJ (1999) Regions of variant histone His2AvD required for Drosophila development. Nature 399: 694-7

Clough SJ, Bent AF (1998) Floral dip: a simplified method for Agrobacterium-mediated transformation of Arabidopsis thaliana. Plant J 16: 735-43

Cole B, Kay SA, Chory J (2011) Automated analysis of hypocotyl growth dynamics during shade avoidance in Arabidopsis. Plant J 65: 991-1000

Coleman-Derr D, Zilberman D (2012) Deposition of histone variant H2A.Z within gene bodies regulates responsive genes. PLoS Genet 8: e1002988

Cortijo S, Charoensawan V, Brestovitsky A, Buning R, Ravarani C, Rhodes D, van Noort J, Jaeger KE, Wigge PA (2017) Transcriptional regulation of the ambient temperature response by H2A.Z-nucleosomes and HSF1 transcription factors in Arabidopsis. Mol Plant

Czechowski T, Stitt M, Altmann T, Udvardi MK, Scheible WR (2005) Genome-wide identification and testing of superior reference genes for transcript normalization in Arabidopsis. Plant Physiol 139: 5-17

Dai X, Bai Y, Zhao L, Dou X, Liu Y, Wang L, Li Y, Li W, Hui Y, Huang X, Wang Z, Qin Y (2017) H2A.Z Represses Gene Expression by Modulating Promoter Nucleosome Structure and Enhancer Histone Modifications in Arabidopsis. Mol Plant 10: 1274-1292

Dalvai M, Bellucci L, Fleury L, Lavigne AC, Moutahir F, Bystricky K (2012) H2A.Z-dependent crosstalk between enhancer and promoter regulates Cyclin D1 expression. Oncogene

Davie JR, Xu W, Delcuve GP (2016) Histone H3K4 trimethylation: dynamic interplay with pre-mRNA splicing. Biochem Cell Biol 94: 1-11

de Lucas M, Prat S (2014) PIFs get BRright: PHYTOCHROME INTERACTING FACTORs as integrators of light and hormonal signals. New Phytol 202: 1126-41

Deal R, Topp CN, McKinney EC, Meagher RB (2007) Repression of Flowering in Arabidopsis Requires Activation of FLOWERING LOCUS C Expression by the Histone Variant H2A.Z. The Plant Cell Online 19: 74-83

Deal RB, Kandasamy MK, McKinney EC, Meagher RB (2005) The nuclear actin-related protein ARP6 is a pleiotropic developmental regulator required for the maintenance of FLOWERING LOCUS C expression and repression of flowering in Arabidopsis. Plant Cell 17: 2633-46

Derkacheva M, Hennig L (2013) Variations on a theme: Polycomb group proteins in plants. J Exp Bot

Dhar S, Gursoy-Yuzugullu O, Parasuram R, Price BD (2017) The tale of a tail: histone H4 acetylation and the repair of DNA breaks. Philos Trans R Soc Lond B Biol Sci 372:

Dion MF, Altschuler SJ, Wu LF, Rando OJ (2005) Genomic characterization reveals a simple histone H4 acetylation code. Proc Natl Acad Sci U S A 102: 5501-6

Efroni I, Han SK, Kim HJ, Wu MF, Steiner E, Birnbaum KD, Hong JC, Eshed Y, Wagner D (2013) Regulation of leaf maturation by chromatin-mediated modulation of cytokinin responses. Dev Cell 24: 438-45

Eirin-Lopez JM, Gonzalez-Romero R, Dryhurst D, Ishibashi T, Ausio J (2009) The evolutionary differentiation of two histone H2A.Z variants in chordates (H2A.Z-1 and H2A.Z-2) is mediated by a stepwise mutation process that affects three amino acid residues. BMC Evol Biol 9: 31

Endoh M, Endo TA, Endoh T, Isono K, Sharif J, Ohara O, Toyoda T, Ito T, Eskeland R, Bickmore WA, Vidal M, Bernstein BE, Koseki H (2012) Histone H2A mono-ubiquitination is a crucial

step to mediate PRC1-dependent repression of developmental genes to maintain ES cell identity. PLoS Genet 8: e1002774

Engreitz JM, Ollikainen N, Guttman M (2016) Long non-coding RNAs: spatial amplifiers that control nuclear structure and gene expression. Nat Rev Mol Cell Biol 17: 756-770

Etherington GJ, Monaghan J, Zipfel C, MacLean D (2014) Mapping mutations in plant genomes with the user-friendly web application CandiSNP. Plant Methods 10: 41

Euskirchen GM, Auerbach RK, Davidov E, Gianoulis TA, Zhong G, Rozowsky J, Bhardwaj N, Gerstein MB, Snyder M (2011) Diverse roles and interactions of the SWI/SNF chromatin remodeling complex revealed using global approaches. PLoS Genet 7: e1002008

Faast R, Thonglairoam V, Schulz TC, Beall J, Wells JR, Taylor H, Matthaei K, Rathjen PD, Tremethick DJ, Lyons I (2001) Histone variant H2A.Z is required for early mammalian development. Curr Biol 11: 1183-7

Faircloth BC, Glenn TC (2014) Protocol: Preparation of an AMPure XP substitute (AKA Serapure).

Fan JY, Rangasamy D, Luger K, Tremethick DJ (2004) H2A.Z alters the nucleosome surface to promote HP1alpha-mediated chromatin fiber folding. Mol Cell 16: 655-61

Farrona S, Hurtado L, March-Diaz R, Schmitz RJ, Florencio FJ, Turck F, Amasino RM, Reyes JC (2011) Brahma is required for proper expression of the floral repressor FLC in Arabidopsis. PLoS One 6: e17997

Feng CM, Qiu Y, Van Buskirk EK, Yang EJ, Chen M (2014) Light-regulated gene repositioning in Arabidopsis. Nat Commun 5: 3027

Galvao VC, Collani S, Horrer D, Schmid M (2015) Gibberellic acid signaling is required for ambient temperature-mediated induction of flowering in Arabidopsis thaliana. Plant J 84: 949-62

Gendrel AV, Lippman Z, Martienssen R, Colot V (2005) Profiling histone modification patterns in plants using genomic tiling microarrays. Nat Methods 2: 213-8

Gevry N, Hardy S, Jacques PE, Laflamme L, Svotelis A, Robert F, Gaudreau L (2009) Histone H2A.Z is essential for estrogen receptor signaling. Genes Dev 23: 1522-33

Han SK, Sang Y, Rodrigues A, Biol F, Wu MF, Rodriguez PL, Wagner D (2012) The SWI2/SNF2 Chromatin Remodeling ATPase BRAHMA Represses Abscisic Acid Responses in the Absence of the Stress Stimulus in Arabidopsis. Plant Cell 24: 4892-906

Han SK, Wu MF, Cui S, Wagner D (2015) Roles and activities of chromatin remodeling ATPases in plants. Plant J 83: 62-77

Hargreaves DC, Crabtree GR (2011) ATP-dependent chromatin remodeling: genetics, genomics and mechanisms. Cell Res 21: 396-420

Hartwig B, James GV, Konrad K, Schneeberger K, Turck F (2012) Fast isogenic mapping-by-sequencing of ethyl methanesulfonate-induced mutant bulks. Plant Physiol 160: 591-600

He Y (2012) Chromatin regulation of flowering. Trends Plant Sci 17: 556-62

Heinz S, Benner C, Spann N, Bertolino E, Lin YC, Laslo P, Cheng JX, Murre C, Singh H, Glass CK (2010) Simple combinations of lineage-determining transcription factors prime cis-regulatory elements required for macrophage and B cell identities. Mol Cell 38: 576-89

Hiruma K, Onozawa-Komori M, Takahashi F, Asakura M, Bednarek P, Okuno T, Schulze-Lefert P, Takano Y (2010) Entry mode-dependent function of an indole glucosinolate pathway in Arabidopsis for nonhost resistance against anthracnose pathogens. Plant Cell 22: 2429-43

Hodges C, Kirkland JG, Crabtree GR (2016) The Many Roles of BAF (mSWI/SNF) and PBAF Complexes in Cancer. Cold Spring Harb Perspect Med 6:

Hu G, Cui K, Northrup D, Liu C, Wang C, Tang Q, Ge K, Levens D, Crane-Robinson C, Zhao K (2012) H2A.Z Facilitates Access of Active and Repressive Complexes to Chromatin in Embryonic Stem Cell Self-Renewal and Differentiation. Cell Stem Cell

Hu Y, Shen Y, Conde ESN, Zhou DX (2011) The role of histone methylation and H2A.Z occupancy during rapid activation of ethylene responsive genes. PLoS One 6: e28224

Hua S, Kallen CB, Dhar R, Baquero MT, Mason CE, Russell BA, Shah PK, Liu J, Khramtsov A, Tretiakova MS, Krausz TN, Olopade OI, Rimm DL, White KP (2008) Genomic analysis of

estrogen cascade reveals histone variant H2A.Z associated with breast cancer progression. Mol Syst Biol 4: 188

Huebert DJ, Kuan PF, Keles S, Gasch AP (2012) Dynamic changes in nucleosome occupancy are not predictive of gene expression dynamics but are linked to transcription and chromatin regulators. Mol Cell Biol 32: 1645-53

Hurtado L, Farrona S, Reyes JC (2006) The putative SWI/SNF complex subunit BRAHMA activates flower homeotic genes in Arabidopsis thaliana. Plant Mol Biol 62: 291-304

Ietswaart R, Wu Z, Dean C (2012) Flowering time control: another window to the connection between antisense RNA and chromatin. Trends Genet 28: 445-53

Imbalzano AN, Imbalzano KM, Nickerson JA (2013) BRG1, a SWI/SNF chromatin remodeling enzyme ATPase, is required for maintenance of nuclear shape and integrity. Commun Integr Biol 6: e25153

Jackson JD, Gorovsky MA (2000) Histone H2A.Z has a conserved function that is distinct from that of the major H2A sequence variants. Nucleic Acids Res 28: 3811-6

Jarillo JA, Pineiro M (2015) H2A.Z mediates different aspects of chromatin function and modulates flowering responses in Arabidopsis. Plant J 83: 96-109

Jegu T, Latrasse D, Delarue M, Hirt H, Domenichini S, Ariel F, Crespi M, Bergounioux C, Raynaud C, Benhamed M (2014) The BAF60 Subunit of the SWI/SNF Chromatin-Remodeling Complex Directly Controls the Formation of a Gene Loop at FLOWERING LOCUS C in Arabidopsis. Plant Cell

Jegu T, Veluchamy A, Ramirez-Prado JS, Rizzi-Paillet C, Perez M, Lhomme A, Latrasse D, Coleno E, Vicaire S, Legras S, Jost B, Rougee M, Barneche F, Bergounioux C, Crespi M, Mahfouz MM, Hirt H, Raynaud C, Benhamed M (2017) The Arabidopsis SWI/SNF protein BAF60 mediates seedling growth control by modulating DNA accessibility. Genome Biol 18: 114

Jiang W, Yang B, Weeks DP (2014) Efficient CRISPR/Cas9-mediated gene editing in Arabidopsis thaliana and inheritance of modified genes in the T2 and T3 generations. PLoS One 9: e99225

Jimenez-Useche I, Yuan C (2012) The effect of DNA CpG methylation on the dynamic conformation of a nucleosome. Biophys J 103: 2502-12

Jin C, Felsenfeld G (2007) Nucleosome stability mediated by histone variants H3.3 and H2A.Z. Genes Dev 21: 1519-29

John S, Sabo PJ, Johnson TA, Sung MH, Biddie SC, Lightman SL, Voss TC, Davis SR, Meltzer PS, Stamatoyannopoulos JA, Hager GL (2008) Interaction of the glucocorticoid receptor with the chromatin landscape. Mol Cell 29: 611-24

Jones AM, Chory J, Dangl JL, Estelle M, Jacobsen SE, Meyerowitz EM, Nordborg M, Weigel D (2008) The impact of Arabidopsis on human health: diversifying our portfolio. Cell 133: 939-43

Kadoch C, Hargreaves DC, Hodges C, Elias L, Ho L, Ranish J, Crabtree GR (2013) Proteomic and bioinformatic analysis of mammalian SWI/SNF complexes identifies extensive roles in human malignancy. Nat Genet 45: 592-601

Kim SI, Bresnick EH, Bultman SJ (2009) BRG1 directly regulates nucleosome structure and chromatin looping of the alpha globin locus to activate transcription. Nucleic Acids Res 37: 6019-27

Kitamura H, Matsumori H, Kalendova A, Hozak P, Goldberg IG, Nakao M, Saitoh N, Harata M (2015) The actin family protein ARP6 contributes to the structure and the function of the nucleolus. Biochem Biophys Res Commun 464: 554-60

Kleinmanns JA, Schatlowski N, Heckmann D, Schubert D (2017) BLISTER Regulates Polycomb-Target Genes, Represses Stress-Regulated Genes and Promotes Stress Responses in Arabidopsis thaliana. Front Plant Sci 8: 1530

Krietenstein N, Wal M, Watanabe S, Park B, Peterson CL, Pugh BF, Korber P (2016) Genomic Nucleosome Organization Reconstituted with Pure Proteins. Cell 167: 709-721 e12

Ku M, Jaffe JD, Koche RP, Rheinbay E, Endoh M, Koseki H, Carr SA, Bernstein BE (2012) H2A.Z landscapes and dual modifications in pluripotent and multipotent stem cells underlie complex genome regulatory functions. Genome Biol 13: R85

Kumar SV, Wigge PA (2010) H2A.Z-containing nucleosomes mediate the thermosensory response in Arabidopsis. Cell 140: 136-47

Kwok RS, Li YH, Lei AJ, Edery I, Chiu JC (2015) The Catalytic and Non-catalytic Functions of the Brahma Chromatin-Remodeling Protein Collaborate to Fine-Tune Circadian Transcription in Drosophila. PLoS Genet 11: e1005307

Lafos M, Kroll P, Hohenstatt ML, Thorpe FL, Clarenz O, Schubert D (2011) Dynamic regulation of H3K27 trimethylation during Arabidopsis differentiation. PLoS Genet 7: e1002040

Lai WKM, Pugh BF (2017) Understanding nucleosome dynamics and their links to gene expression and DNA replication. Nat Rev Mol Cell Biol 18: 548-562

Lamesch P, Berardini TZ, Li D, Swarbreck D, Wilks C, Sasidharan R, Muller R, Dreher K, Alexander DL, Garcia-Hernandez M, Karthikeyan AS, Lee CH, Nelson WD, Ploetz L, Singh S, Wensel A, Huala E (2012) The Arabidopsis Information Resource (TAIR): improved gene annotation and new tools. Nucleic Acids Res 40: D1202-10

Langmead B, Salzberg SL (2012) Fast gapped-read alignment with Bowtie 2. Nat Methods 9: 357-9

Lazaro A, Gomez-Zambrano A, Lopez-Gonzalez L, Pineiro M, Jarillo JA (2008) Mutations in the Arabidopsis SWC6 gene, encoding a component of the SWR1 chromatin remodelling complex, accelerate flowering time and alter leaf and flower development. J Exp Bot 59: 653-66

Lee K, Seo PJ (2017) Coordination of matrix attachment and ATP-dependent chromatin remodeling regulate auxin biosynthesis and Arabidopsis hypocotyl elongation. PLoS One 12: e0181804

Lee KM, Hayes JJ (1998) Linker DNA and H1-dependent reorganization of histone-DNA interactions within the nucleosome. Biochemistry 37: 8622-8

Lee N, Choi G (2017) Phytochrome-interacting factor from Arabidopsis to liverwort. Curr Opin Plant Biol 35: 54-60

Lessard J, Wu JI, Ranish JA, Wan M, Winslow MM, Staahl BT, Wu H, Aebersold R, Graef IA, Crabtree GR (2007) An essential switch in subunit composition of a chromatin remodeling complex during neural development. Neuron 55: 201-15

Li B, Pattenden SG, Lee D, Gutiérrez J, Chen J, Seidel C, Gerton J, Workman JL (2005a) Preferential occupancy of histone variant H2AZ at inactive promoters influences local histone modifications and chromatin remodeling. Proceedings of the National Academy of Sciences of the United States of America 102: 18385-18390

Li C, Chen C, Gao L, Yang S, Nguyen V, Shi X, Siminovitch K, Kohalmi SE, Huang S, Wu K, Chen X, Cui Y (2015a) The Arabidopsis SWI2/SNF2 chromatin Remodeler BRAHMA regulates polycomb function during vegetative development and directly activates the flowering repressor gene SVP. PLoS Genet 11: e1004944

Li C, Gu L, Gao L, Chen C, Wei CQ, Qiu Q, Chien CW, Wang S, Jiang L, Ai LF, Chen CY, Yang S, Nguyen V, Qi Y, Snyder MP, Burlingame AL, Kohalmi SE, Huang S, Cao X, Wang ZY, Wu K, Chen X, Cui Y (2016) Concerted genomic targeting of H3K27 demethylase REF6 and chromatin-remodeling ATPase BRM in Arabidopsis. Nat Genet 48: 687-93

Li G, Levitus M, Bustamante C, Widom J (2005b) Rapid spontaneous accessibility of nucleosomal DNA. Nat Struct Mol Biol 12: 46-53

Li H, Durbin R (2009) Fast and accurate short read alignment with Burrows-Wheeler transform. Bioinformatics 25: 1754-60

Li H, Handsaker B, Wysoker A, Fennell T, Ruan J, Homer N, Marth G, Abecasis G, Durbin R, Genome Project Data Processing S (2009) The Sequence Alignment/Map format and SAMtools. Bioinformatics 25: 2078-9

Li H (2011) A statistical framework for SNP calling, mutation discovery, association mapping and population genetical parameter estimation from sequencing data. Bioinformatics 27: 2987-93

Li M, Hada A, Sen P, Olufemi L, Hall MA, Smith BY, Forth S, McKnight JN, Patel A, Bowman GD, Bartholomew B, Wang MD (2015b) Dynamic regulation of transcription factors by nucleosome remodeling. Elife 4:

Li Z, Gadue P, Chen K, Jiao Y, Tuteja G, Schug J, Li W, Kaestner KH (2012) Foxa2 and H2A.Z mediate nucleosome depletion during embryonic stem cell differentiation. Cell 151: 1608-16

Light WH, Brickner DG, Brand VR, Brickner JH (2010) Interaction of a DNA zip code with the nuclear pore complex promotes H2A.Z incorporation and INO1 transcriptional memory. Mol Cell 40: 112-25

Lin R, Wang H (2004) Arabidopsis FHY3/FAR1 gene family and distinct roles of its members in light control of Arabidopsis development. Plant Physiol 136: 4010-22

Liu JC, Ferreira CG, Yusufzai T (2015) Human CHD2 is a chromatin assembly ATPase regulated by its chromo- and DNA-binding domains. J Biol Chem 290: 25-34

Liu X, Li B, GorovskyMa (1996) Essential and nonessential histone H2A variants in Tetrahymena thermophila. Mol Cell Biol 16: 4305-11

Livak KJ, Schmittgen TD (2001) Analysis of relative gene expression data using real-time quantitative PCR and the 2(-Delta Delta C(T)) Method. Methods 25: 402-8

Lu PY, Levesque N, Kobor MS (2009) NuA4 and SWR1-C: two chromatin-modifying complexes with overlapping functions and components. Biochem Cell Biol 87: 799-815

Luger K, Mader AW, Richmond RK, Sargent DF, Richmond TJ (1997) Crystal structure of the nucleosome core particle at 2.8 A resolution. Nature 389: 251-60

Luger K, Mader A, Sargent DF, Richmond TJ (2000) The atomic structure of the nucleosome core particle. J Biomol Struct Dyn 17 Suppl 1: 185-8

Ma KW, Flores C, Ma W (2011) Chromatin configuration as a battlefield in plant-bacteria interactions. Plant Physiol 157: 535-43

March-Diaz R, Garcia-Dominguez M, Florencio FJ, Reyes JC (2007) SEF, a new protein required for flowering repression in Arabidopsis, interacts with PIE1 and ARP6. Plant Physiol 143: 893-901

March-Diaz R, Garcia-Dominguez M, Lozano-Juste J, Leon J, Florencio FJ, Reyes JC (2008) Histone H2A.Z and homologues of components of the SWR1 complex are required to control immunity in Arabidopsis. Plant J 53: 475-87

March-Diaz R, Reyes JC (2009) The beauty of being a variant: H2A.Z and the SWR1 complex in plants. Mol Plant 2: 565-77

Marques M, Laflamme L, Gervais AL, Gaudreau L (2010) Reconciling the positive and negative roles of histone H2A.Z in gene transcription. Epigenetics 5: 267-72

Martin-Trillo M, Lazaro A, Poethig RS, Gomez-Mena C, Pineiro MA, Martinez-Zapater JM, Jarillo JA (2006) EARLY IN SHORT DAYS 1 (ESD1) encodes ACTIN-RELATED PROTEIN 6 (AtARP6), a putative component of chromatin remodelling complexes that positively regulates FLC accumulation in Arabidopsis. Development 133: 1241-52

Maruyama EO, Hori T, Tanabe H, Kitamura H, Matsuda R, Tone S, Hozak P, Habermann FA, von Hase J, Cremer C, Fukagawa T, Harata M (2012) The actin family member Arp6 and the histone variant H2A.Z are required for spatial positioning of chromatin in chicken cell nuclei. J Cell Sci 125: 3739-43

McCarthy DJ, Chen Y, Smyth GK (2012) Differential expression analysis of multifactor RNA-Seq experiments with respect to biological variation. Nucleic Acids Res 40: 4288-97

Medina-Rivera A, Defrance M, Sand O, Herrmann C, Castro-Mondragon JA, Delerce J, Jaeger S, Blanchet C, Vincens P, Caron C, Staines DM, Contreras-Moreira B, Artufel M, Charbonnier-Khamvongsa L, Hernandez C, Thieffry D, Thomas-Chollier M, van Helden J (2015) RSAT 2015: Regulatory Sequence Analysis Tools. Nucleic Acids Res 43: W50-6

Meneghini MD, Wu M, Madhani HD (2003) Conserved histone variant H2A.Z protects euchromatin from the ectopic spread of silent heterochromatin. Cell 112: 725-36

Merchant N, Lyons E, Goff S, Vaughn M, Ware D, Micklos D, Antin P (2016) The iPlant Collaborative: Cyberinfrastructure for Enabling Data to Discovery for the Life Sciences. PLoS Biol 14: e1002342

Michaels SD, Amasino RM (1999) FLOWERING LOCUS C Encodes a Novel MADS Domain Protein That Acts as a Repressor of Flowering. The Plant Cell Online 11: 949-956

Mizuguchi G, Shen X, Landry J, Wu WH, Sen S, Wu C (2004) ATP-driven exchange of histone H2AZ variant catalyzed by SWR1 chromatin remodeling complex. Science 303: 343-8

Molitor A, Latrasse D, Zytnicki M, Andrey P, Houba-Herin N, Hachet M, Battail C, Del Prete S, Alberti A, Quesneville H, Gaudin V (2016) The Arabidopsis hnRNP-Q Protein LIF2 and the PRC1 subunit LHP1 function in concert to regulate the transcription of stress-responsive genes. Plant Cell

Mondal T, Rasmussen M, Pandey GK, Isaksson A, Kanduri C (2010) Characterization of the RNA content of chromatin. Genome Res 20: 899-907

Mueller B, Mieczkowski J, Kundu S, Wang P, Sadreyev R, Tolstorukov MY, Kingston RE (2017) Widespread changes in nucleosome accessibility without changes in nucleosome occupancy during a rapid transcriptional induction. Genes Dev 31: 451-462

Mylne J, Greb T, Lister C, Dean C (2004) Epigenetic regulation in the control of flowering. Cold Spring Harb Symp Quant Biol 69: 457-64

Nagai S, Davis RE, Mattei PJ, Eagen KP, Kornberg RD (2017) Chromatin potentiates transcription. Proc Natl Acad Sci U S A 114: 1536-1541

Narlikar GJ, Sundaramoorthy R, Owen-Hughes T (2013) Mechanisms and functions of ATP-dependent chromatin-remodeling enzymes. Cell 154: 490-503

Nogales-Cadenas R, Carmona-Saez P, Vazquez M, Vicente C, Yang X, Tirado F, Carazo JM, Pascual-Montano A (2009) GeneCodis: interpreting gene lists through enrichment analysis and integration of diverse biological information. Nucleic Acids Res 37: W317-22

O'Malley RC, Huang SC, Song L, Lewsey MG, Bartlett A, Nery JR, Galli M, Gallavotti A, Ecker JR (2016) Cistrome and Epicistrome Features Shape the Regulatory DNA Landscape. Cell 166: 1598

Papamichos-Chronakis M, Watanabe S, Rando OJ, Peterson CL (2011) Global regulation of H2A.Z localization by the INO80 chromatin-remodeling enzyme is essential for genome integrity. Cell 144: 200-13

Park YJ, Dyer PN, Tremethick DJ, Luger K (2004) A new fluorescence resonance energy transfer approach demonstrates that the histone variant H2AZ stabilizes the histone octamer within the nucleosome. J Biol Chem 279: 24274-82

Pedmale UV, Huang SC, Zander M, Cole BJ, Hetzel J, Ljung K, Reis PAB, Sridevi P, Nito K, Nery JR, Ecker JR, Chory J (2016) Cryptochromes Interact Directly with PIFs to Control Plant Growth in Limiting Blue Light. Cell 164: 233-245

Probst AV, Mittelsten Scheid O (2015) Stress-induced structural changes in plant chromatin. Curr Opin Plant Biol 27: 8-16

Quinlan AR (2014) BEDTools: The Swiss-Army Tool for Genome Feature Analysis. Curr Protoc Bioinformatics 47: 11 12 1-34

Raisner RM, Hartley PD, Meneghini MD, Bao MZ, Liu CL, Schreiber SL, Rando OJ, Madhani HD (2005) Histone variant H2A. Z marks the 5′ ends of both active and inactive genes in euchromatin. Cell 123: 233

Ramirez F, Dundar F, Diehl S, Gruning BA, Manke T (2014) deepTools: a flexible platform for exploring deep-sequencing data. Nucleic Acids Res 42: W187-91

Rangasamy D (2010) Histone variant H2A.Z can serve as a new target for breast cancer therapy. Curr Med Chem 17: 3155-61

Ranjan A, Mizuguchi G, Fitzgerald PC, Wei D, Wang F, Huang Y, Luk E, Woodcock CL, Wu C (2013) Nucleosome-free Region Dominates Histone Acetylation in Targeting SWR1 to Promoters for H2A.Z Replacement. Cell 154: 1232-45

Ritter A, Inigo S, Fernandez-Calvo P, Heyndrickx KS, Dhondt S, Shi H, De Milde L, Vanden Bossche R, De Clercq R, Eeckhout D, Ron M, Somers DE, Inze D, Gevaert K, De Jaeger G, Vandepoele K, Pauwels L, Goossens A (2017) The transcriptional repressor complex FRS7-FRS12 regulates flowering time and growth in Arabidopsis. Nat Commun 8: 15235

Robinson MD, McCarthy DJ, Smyth GK (2010) edgeR: a Bioconductor package for differential expression analysis of digital gene expression data. Bioinformatics 26: 139-40

Rosa M, Von Harder M, Cigliano RA, Schlogelhofer P, Scheid OM (2013) The Arabidopsis SWR1 Chromatin-Remodeling Complex Is Important for DNA Repair, Somatic Recombination, and Meiosis. Plant Cell

Rudnizky S, Bavly A, Malik O, Pnueli L, Melamed P, Kaplan A (2016) H2A.Z controls the stability and mobility of nucleosomes to regulate expression of the LH genes. Nat Commun 7: 12958

Rymen B, Sugimoto K (2012) Tuning growth to the environmental demands. Curr Opin Plant Biol 15: 683-90

Sacharowski SP, Gratkowska DM, Sarnowska EA, Kondrak P, Jancewicz I, Porri A, Bucior E, Rolicka AT, Franzen R, Kowalczyk J, Pawlikowska K, Huettel B, Torti S, Schmelzer E, Coupland G, Jerzmanowski A, Koncz C, Sarnowski TJ (2015) SWP73 Subunits of Arabidopsis SWI/SNF Chromatin Remodeling Complexes Play Distinct Roles in Leaf and Flower Development. Plant Cell 27: 1889-906

Saez-Vasquez J, Gadal O (2010) Genome organization and function: a view from yeast and Arabidopsis. Mol Plant 3: 678-90

Salmon-Divon M, Dvinge H, Tammoja K, Bertone P (2010) PeakAnalyzer: genome-wide annotation of chromatin binding and modification loci. BMC Bioinformatics 11: 415

Santisteban MS, Kalashnikova T, Smith MM (2000) Histone H2A.Z regulats transcription and is partially redundant with nucleosome remodeling complexes. Cell 103: 411-22

Sarnowska E, Gratkowska DM, Sacharowski SP, Cwiek P, Tohge T, Fernie AR, Siedlecki JA, Koncz C, Sarnowski TJ (2016) The Role of SWI/SNF Chromatin Remodeling Complexes in Hormone Crosstalk. Trends Plant Sci 21: 594-608

Schatlowski N, Stahl Y, Hohenstatt ML, Goodrich J, Schubert D (2010) The CURLY LEAF interacting protein BLISTER controls expression of polycomb-group target genes and cellular differentiation of Arabidopsis thaliana. Plant Cell 22: 2291-305

Schnitzler GR, Cheung CL, Hafner JH, Saurin AJ, Kingston RE, Lieber CM (2001) Direct imaging of human SWI/SNF-remodeled mono- and polynucleosomes by atomic force microscopy employing carbon nanotube tips. Mol Cell Biol 21: 8504-11

Schotta G, Ebert A, Dorn R, Reuter G (2003) Position-effect variegation and the genetic dissection of chromatin regulation in Drosophila. Seminars in Cell & Developmental Biology 14: 67-75

Sequeira-Mendes J, Araguez I, Peiro R, Mendez-Giraldez R, Zhang X, Jacobsen SE, Bastolla U, Gutierrez C (2014) The Functional Topography of the Arabidopsis Genome Is Organized in a Reduced Number of Linear Motifs of Chromatin States. Plant Cell 26: 2351-2366

Seymour DK, Becker C (2017) The causes and consequences of DNA methylome variation in plants. Curr Opin Plant Biol 36: 56-63

Sheldon CC, Conn AB, Dennis ES, Peacock WJ (2002) Different regulatory regions are required for the vernalization-induced repression of FLOWERING LOCUS C and for the epigenetic maintenance of repression. Plant Cell 14: 2527-37

Shogren-Knaak M, Ishii H, Sun JM, Pazin MJ, Davie JR, Peterson CL (2006) Histone H4-K16 acetylation controls chromatin structure and protein interactions. Science 311: 844-7

Sijacic P, Bajic M, McKinney EC, Meagher RB, Deal RB (2017) Chromatin accessibility changes between Arabidopsis stem cells and mesophyll cells illuminate cell type-specific transcription factor networks. bioRxiv

Smith AP, Jain A, Deal RB, Nagarajan VK, Poling MD, Raghothama KG, Meagher RB (2010) Histone H2A.Z regulates the expression of several classes of phosphate starvation response genes but not as a transcriptional activator. Plant Physiol 152: 217-25

Srikanth A, Schmid M (2011) Regulation of flowering time: all roads lead to Rome. Cell Mol Life Sci 68: 2013-37

Sura W, Kabza M, Karlowski WM, Bieluszewski T, Kus-Slowinska M, Paweloszek L, Sadowski J, Ziolkowski PA (2017) Dual role of the histone variant H2A.Z in transcriptional regulation of stress-response genes. Plant Cell

Surface LE, Fields PA, Subramanian V, Behmer R, Udeshi N, Peach SE, Carr SA, Jaffe JD, Boyer LA (2016) H2A.Z.1 Monoubiquitylation Antagonizes BRD2 to Maintain Poised Chromatin in ESCs. Cell Rep

Suto RK, Clarkson MJ, Tremethick DJ, Luger K (2000) Crystal structure of a nucleosome core particle containing the variant histone H2A.Z. Nature Structural Biology 7: 1121

Swaminathan J, Baxter EM, Corces VG (2005) The role of histone H2Av variant replacement and histone H4 acetylation in the establishment of Drosophila heterochromatin. Genes Dev 19: 65-76

Tabas-Madrid D, Nogales-Cadenas R, Pascual-Montano A (2012) GeneCodis3: a non-redundant and modular enrichment analysis tool for functional genomics. Nucleic Acids Res 40: W478-83

Tessarz P, Kouzarides T (2014) Histone core modifications regulating nucleosome structure and dynamics. Nat Rev Mol Cell Biol 15: 703-8

Tian T, Liu Y, Yan H, You Q, Yi X, Du Z, Xu W, Su Z (2017) agriGO v2.0: a GO analysis toolkit for the agricultural community, 2017 update. Nucleic Acids Res

Todolli S, Perez PJ, Clauvelin N, Olson WK (2017) Contributions of Sequence to the Higher-Order Structures of DNA. Biophys J 112: 416-426

Tolstorukov MY, Sansam CG, Lu P, Koellhoffer EC, Helming KC, Alver BH, Tillman EJ, Evans JA, Wilson BG, Park PJ, Roberts CW (2013) Swi/Snf chromatin remodeling/tumor suppressor

complex establishes nucleosome occupancy at target promoters. Proc Natl Acad Sci U S A 110: 10165-70

Torigoe SE, Patel A, Khuong MT, Bowman GD, Kadonaga JT (2013) ATP-dependent chromatin assembly is functionally distinct from chromatin remodeling. Elife 2: e00863

Trapnell C, Roberts A, Goff L, Pertea G, Kim D, Kelley DR, Pimentel H, Salzberg SL, Rinn JL, Pachter L (2012) Differential gene and transcript expression analysis of RNA-seq experiments with TopHat and Cufflinks. Nat Protoc 7: 562-78

Turinetto V, Giachino C (2015) Multiple facets of histone variant H2AX: a DNA double-strand-break marker with several biological functions. Nucleic Acids Res 43: 2489-98

Urano K, Kurihara Y, Seki M, Shinozaki K (2010) 'Omics' analyses of regulatory networks in plant abiotic stress responses. Curr Opin Plant Biol 13: 132-8

Valdes-Mora F, Song JZ, Statham AL, Strbenac D, Robinson MD, Nair SS, Patterson KI, Tremethick DJ, Stirzaker C, Clark SJ (2012) Acetylation of H2A.Z is a key epigenetic modification associated with gene deregulation and epigenetic remodeling in cancer. Genome Res 22: 307-21

Valdes-Mora F, Gould CM, Colino-Sanguino Y, Qu W, Song JZ, Taylor KM, Buske FA, Statham AL, Nair SS, Armstrong NJ, Kench JG, Lee KML, Horvath LG, Qiu M, Ilinykh A, Yeo-Teh NS, Gallego-Ortega D, Stirzaker C, Clark SJ (2017) Acetylated histone variant H2A.Z is involved in the activation of neo-enhancers in prostate cancer. Nat Commun 8: 1346

van Zanten M, Tessadori F, McLoughlin F, Smith R, Millenaar FF, van Driel R, Voesenek LA, Peeters AJ, Fransz P (2010) Photoreceptors CRYTOCHROME2 and phytochrome B control chromatin compaction in Arabidopsis. Plant Physiol 154: 1686-96

Vardabasso C, Gaspar-Maia A, Hasson D, Punzeler S, Valle-Garcia D, Straub T, Keilhauer EC, Strub T, Dong J, Panda T, Chung CY, Yao JL, Singh R, Segura MF, Fontanals-Cirera B, Verma A, Mann M, Hernando E, Hake SB, Bernstein E (2015) Histone Variant H2A.Z.2 Mediates Proliferation and Drug Sensitivity of Malignant Melanoma. Mol Cell 59: 75-88

Vercruyssen L, Verkest A, Gonzalez N, Heyndrickx KS, Eeckhout D, Han SK, Jegu T, Archacki R, Van Leene J, Andriankaja M, De Bodt S, Abeel T, Coppens F, Dhondt S, De Milde L, Vermeersch M, Maleux K, Gevaert K, Jerzmanowski A, Benhamed M, Wagner D, Vandepoele K, De Jaeger G, Inze D (2014) ANGUSTIFOLIA3 Binds to SWI/SNF Chromatin Remodeling Complexes to Regulate Transcription during Arabidopsis Leaf Development. Plant Cell

Vergara Z, Gutierrez C (2017) Emerging roles of chromatin in the maintenance of genome organization and function in plants. Genome Biol 18: 96

Weber CM, Ramachandran S, Henikoff S (2014) Nucleosomes are context-specific, H2A.Z-modulated barriers to RNA polymerase. Mol Cell 53: 819-30

Weirauch MT, Yang A, Albu M, Cote AG, Montenegro-Montero A, Drewe P, Najafabadi HS, Lambert SA, Mann I, Cook K, Zheng H, Goity A, van Bakel H, Lozano JC, Galli M, Lewsey MG, Huang E, Mukherjee T, Chen X, Reece-Hoyes JS, Govindarajan S, Shaulsky G, Walhout AJM, Bouget FY, Ratsch G, Larrondo LF, Ecker JR, Hughes TR (2014) Determination and inference of eukaryotic transcription factor sequence specificity. Cell 158: 1431-1443

Whittle CM, McClinic KN, Ercan S, Zhang X, Green RD, Kelly WG, Lieb JD (2008) The genomic distribution and function of histone variant HTZ-1 during C. elegans embryogenesis. PLoS Genet 4: e1000187

Widom J (2001) Role of DNA sequence in nucleosome stability and dynamics. Q Rev Biophys 34: 269-324

Wigge PA (2013) Ambient temperature signalling in plants. Curr Opin Plant Biol 16: 661-6

Wu JI (2012) Diverse functions of ATP-dependent chromatin remodeling complexes in development and cancer. Acta Biochim Biophys Sin (Shanghai) 44: 54-69

Wu MF, Sang Y, Bezhani S, Yamaguchi N, Han SK, Li Z, Su Y, Slewinski TL, Wagner D (2012) SWI2/SNF2 chromatin remodeling ATPases overcome polycomb repression and control

floral organ identity with the LEAFY and SEPALLATA3 transcription factors. Proc Natl Acad Sci U S A 109: 3576-81

Wu MF, Yamaguchi N, Xiao J, Bargmann B, Estelle M, Sang Y, Wagner D (2015) Auxin-regulated chromatin switch directs acquisition of flower primordium founder fate. Elife 4: e09269

Wu Q, Lian JB, Stein JL, Stein GS, Nickerson JA, Imbalzano AN (2017) The BRG1 ATPase of human SWI/SNF chromatin remodeling enzymes as a driver of cancer. Epigenomics 9: 919-931

Wu SH (2014) Gene expression regulation in photomorphogenesis from the perspective of the central dogma. Annu Rev Plant Biol 65: 311-33

Xu XM, Moller SG (2011) The value of Arabidopsis research in understanding human disease states. Curr Opin Biotechnol 22: 300-7

Yang HD, Kim PJ, Eun JW, Shen Q, Kim HS, Shin WC, Ahn YM, Park WS, Lee JY, Nam SW (2016) Oncogenic potential of histone-variant H2A.Z.1 and its regulatory role in cell cycle and epithelial-mesenchymal transition in liver cancer. Oncotarget 7: 11412-23

Yang S, Li C, Zhao L, Gao S, Lu J, Zhao M, Chen CY, Liu X, Luo M, Cui Y, Yang C, Wu K (2015) The Arabidopsis SWI2/SNF2 Chromatin Remodeling ATPase BRAHMA Targets Directly to PINs and Is Required for Root Stem Cell Niche Maintenance. Plant Cell 27: 1670-80

Yoshida T, Shimada K, Oma Y, Kalck V, Akimura K, Taddei A, Iwahashi H, Kugou K, Ohta K, Gasser SM, Harata M (2010) Actin-related protein Arp6 influences H2A.Z-dependent and -independent gene expression and links ribosomal protein genes to nuclear pores. PLoS Genet 6: e1000910

Zhang D, Li Y, Zhang X, Zha P, Lin R (2016) The SWI2/SNF2 Chromatin-Remodeling ATPase BRAHMA Regulates Chlorophyll Biosynthesis in Arabidopsis. Mol Plant

Zhang D, Li Y, Zhang X, Zha P, Lin R (2017a) The SWI2/SNF2 Chromatin-Remodeling ATPase BRAHMA Regulates Chlorophyll Biosynthesis in Arabidopsis. Mol Plant 10: 155-167

Zhang T, Zhang W, Jiang J (2015) Genome-Wide Nucleosome Occupancy and Positioning and Their Impact on Gene Expression and Evolution in Plants. Plant Physiol 168: 1406-16

Zhang Y, Ku WL, Liu S, Cui K, Jin W, Tang Q, Lu W, Ni B, Zhao K (2017b) Genome-wide identification of histone H2A and histone variant H2A.Z-interacting proteins by bPPI-seq. Cell Res 27: 1258-1274

Zhao M, Yang S, Chen CY, Li C, Shan W, Lu W, Cui Y, Liu X, Wu K (2015) Arabidopsis BREVIPEDICELLUS interacts with the SWI2/SNF2 chromatin remodeling ATPase BRAHMA to regulate KNAT2 and KNAT6 expression in control of inflorescence architecture. PLoS Genet 11: e1005125

Zhao Y, Garcia BA (2015) Comprehensive Catalog of Currently Documented Histone Modifications. Cold Spring Harb Perspect Biol 7: a025064

Zhou CY, Johnson SL, Gamarra NI, Narlikar GJ (2016) Mechanisms of ATP-Dependent Chromatin Remodeling Motors. Annu Rev Biophys 45: 153-81

Zhu Y, Dong A, Shen WH (2013) Histone variants and chromatin assembly in plant abiotic stress responses. Biochim Biophys Acta 1819: 343-8

Zilberman D, Coleman-Derr D, Ballinger T, Henikoff S (2008) Histone H2A.Z and DNA methylation are mutually antagonistic chromatin marks. Nature 456: 125-9

Zink LM, Hake SB (2016) Histone variants: nuclear function and disease. Curr Opin Genet Dev 37: 82-89

Zofall M, Persinger J, Kassabov SR, Bartholomew B (2006) Chromatin remodeling by ISW2 and SWI/SNF requires DNA translocation inside the nucleosome. Nat Struct Mol Biol 13: 339-46

Zuryn S, Le Gras S, Jamet K, Jarriault S (2010) A Strategy for Direct Mapping and Identification of Mutations by Whole-Genome Sequencing. Genetics 186: 427-430

CHAPTER 3: A GENETIC SUPPRESSOR SCREEN TO IDENTIFY H2A.Z ANTAGONISTS

E. Shannon Torres, Katherine Duval, Stevin Bienfait, and Roger B. Deal

Abstract

Operating in diverse chromatin environments across the genome, histone variant H2A.Z appears to play context dependent roles in gene regulation based on other factors that it interacts with. Since mutations in other factors that act in opposition to H2A.Z might alleviate the requirement for H2A.Z for proper transcriptional activation, we performed a forward genetic suppressor screen to identify other factors that make H2A.Z necessary for proper transcriptional activation. The FLOWERING LOCUS C gene in Arabidopsis represses the transition from vegetative to reproductive development and requires H2A.Z incorporation by the SWR1 complex for proper transcriptional activation. In this study, we identified an EMS-generated mutant line that a) suppressed the early flowering phenotype of mutants defective in H2A.Z incorporation into chromatin, and b) concordantly alleviates the requirement of H2A.Z incorporation for proper *FLC* transcriptional activation. We used a sequencing-based method to map potentially causal mutations after backcrossing suppressor mutants to the parental *arp6* mutant line. We identified candidate missense mutations that may cause the suppressor phenotype: one candidate that is associated with a known repressor of *FLC* and 8 other genes that are currently uncharacterized. Experiments to try and complement the suppressor mutations with WT copies of the mutated genes have not been able to restore the suppressor phenotype back to *arp6*-like characteristics so far due to some ambiguity in the quantitative nature of the reporter phenotypes, and the fact that the candidate mutations are not null mutations. However, the candidate mutations identified in this screen still provide new directions to test for genetic interaction with ARP6. Future work to cross mutations in candidate genes to *arp6* mutants containing an *FLC* reporter construct to validate a causal mutation has potential for identifying H2A.Z-antagonists from the candidates identified in this screen. If we can identify the

causal mutation that is able to suppress the need for H2A.Z for transcriptional regulation, we will potentially learn about flowering time, *FLC* regulation, and why H2A.Z is needed for transcriptional activation at *FLC*.

Introduction

The complex environment of chromatin makes it difficult to parse out the function of any single chromatin protein *in vivo*. By probing individual relationships between interacting proteins, we can begin to deconstruct the chromatin context that define the roles of each factor involved in gene regulation. Genetic screens to identify mutants that relieve gene silencing have thus far been important for understanding the numerous factors involved in epigenetic gene silencing by discovering interactions between factors that we would not have been predictable otherwise (Schotta et al., 2003).

The highly conserved histone H2A variant H2A.Z appears to effect context specific regulation of gene transcription and chromatin organization across all eukaryotes (previous chapter, other references). When it is incorporated into chromatin by the SWR1 complex, H2A.Z can destabilize or stabilize nucleosomes as well as function in transcriptional activation and transcriptional repression (Mizuguchi et al., 2004; Deal et al., 2007; Marques et al., 2010). Some of these functions are correlated with specific factors associated with H2A.Z in chromatin (such as the H3.3 histone variant) or post-translational modifications of H2A.Z, including ubiquitination and acetylation (Jin and Felsenfeld 2007; Marques et al., 2010). However, much work is necessary to understand the seemingly opposing functions of H2A.Z and provide a mechanistic understanding of how this variant contributes to gene regulation and chromatin organization.

The Arabidopsis *Flowering Locus C* (*FLC*) gene acts as a developmental switch that represses the transition from vegetative to reproductive growth (Michaels and Amasino 1999). Proper *FLC* transcription requires H2A.Z incorporation into chromatin by the SWR1 complex (Deal et al., 2007). Mutants of SWR1 components are depleted of H2A.Z-containing nucleosomes, resulting in

decreased *FLC* transcription and therefore flower early (Deal et al., 2005; Choi 2007). Many other factors interact with the *FLC* locus to regulate *FLC* transcription and modulate development in response to environmental stimuli, including the SWI2/SNF2 complex (Ietswaart et al., 2012; Farrona et al., 2011). While H2A.Z acts to promote transcription at *FLC*, the BRM ATPase of the SWI2/SNF2 complex acts to repress *FLC* transcription (Farrona et al., 2011). Arabidopsis plants that lose the BRM ATPase, however are able to overcome the need for H2A.Z in proper transcriptional activation of *FLC* (Farrona et al., 2011).

Investigating the antagonistic interaction between BRM and H2A.Z provides one opportunity to understand what pressures make H2A.Z necessary for transcriptional activation in the context of other chromatin factors. Further work to uncover other H2A.Z antagonists would help us understand what additional properties of H2A.Z make it necessary for transcriptional activation and repression. Since factors such as histone deacetylases oppose the activating function of H2A.Z in other organisms (Meneghini et al., 2003), additional repressive factors may exist that make H2A.Z necessary for *FLC* expression in addition to BRM. For example, the structure or modifications of H2A.Z in nucleosomes may facilitate transcriptional activation by disrupting the interaction of histone H1 with H2A.Z-containing nucleosomes and therefore disrupting chromatin compaction (Lee and Hayes 1998). In addition to activating the transcription of *FLC* and other genes, H2A.Z is required to repress a subset of Arabidopsis genes (Smith et al., 2010; Deal et al., 2007). Comparing how mutants suppressing the function of H2A.Z at *FLC* influence the repression of other genes by H2A.Z will provide an opportunity to separate the positive and negative regulatory functions of H2A.Z in transcription.

In this work, we conducted a forward genetic suppressor screen in an attempt to identify additional factors that antagonize the transcriptional activating function of H2A.Z. Since mutants for components of the SWR1 complex, such as *arp6* mutants, are defective in incorporating H2A.Z into nucleosomes, they have an easily recognizable phenotype of early flowering due to a lack of proper *FLC* expression (Deal et al., 2007). Thus, *arp6* mutants were used for the genetic suppressor screen using flowering time and *FLC* transcript levels as readouts to search for H2A.Z antagonists (Deal et

al., 2007). We identified three EMS-mutagenized *arp6* mutant lines that restore flowering time and *FLC* transcripts to wild type-like levels, and one suppressor segregates as a single, recessive mutation after backcrosses. By mapping mutations that segregate with the suppressor phenotype in this suppressor line, we identified 9 candidate genes as potential H2A.Z antagonists. Further work is needed to validate whether these candidates genetically interact with ARP6 function and the transcriptionally activating role of H2A.Z. If we can identify the causal gene that antagonizes H2A.Z at the *FLC* locus, then we could potentially pinpoint specific properties of H2A.Z that are important for its role in transcriptional activation.

Results

eoa2 *mutants suppress physiological and molecular phenotypes caused by defective H2A.Z incorporation*

Mutations for components of the SWR1 complex that are defective for H2A.Z incorporation have an early flowering phenotype due to down-regulation of genes that regulate the transition from vegetative growth to reproductive growth (Deal et al., 2007). This includes the *FLC* gene that integrates stimuli from numerous pathways to modulate the time it takes a developing plant to bolt and produce flowers (Deal et al., 2007; Ietswaart et al., 2012). To identify factors that antagonize the role of H2A.Z in promoting gene transcription, we conducted a forward genetic suppressor screen using mutants for the ARP6 subunit of the SWR1 complex, that are depleted of H2A.Z-containing nucleosomes (Sura et al., 2017). Since H2A.Z incorporation into chromatin at the *FLC* locus is required for normal flowering time, we used flowering time and *FLC* transcript levels as our reporter phenotypes to conduct the screen (Deal et al., 2007; Farrona et al., 2011). We mutagenized *arp6* homozygous mutant seeds with ethyl methane sulfonate (EMS) to look for suppressors of the early flowering phenotype of *arp6* mutants, which we describe as the early flowering overcome in *arp6* (eoa) phenotype (Fig. 3.1). Mutations were brought to homozygosity in the M_2 generation and plants were screened to identify lines presenting the eoa phenotype (Fig. 3.1B). To measure developmental

time to flowering, we counted the number of rosette leaves that developed before the transition to bolting. In addition to the physiological delay in flowering time, we also measured changes in *FLC* transcript levels in the mutants by isolating RNA from *eoa2* mutants, WT plants, *arp6* mutants and performing RT-qPCR analyses. Therefore, the *eoa2* suppressor plants that overcame the early flowering phenotype of *arp6* mutants and showed increased *FLC* transcript levels contain mutations that make H2A.Z incorporation into chromatin no longer necessary for *FLC* transcriptional activation.

Three independent suppressor lines were initially identified because they contained plants that flowered significantly later than *arp6* and had elevated *FLC* transcript levels relative to *arp6* and/or WT. One line, which we called *eoa2,* is the primary focus of this chapter because it fit both of these criteria and proved most tractable for genetic crosses (Fig. 3.2A,B). The *eoa1* line had defects in reproductive organs (un-fused carpels and small, immature stamen), so we were not successful in backcrossing this line to *arp6* mutants. After backcrossing line *eoa3* to *arp6* mutants, we no longer observed suppression of the *arp6* flowering time phenotype in the F_2 generation, so work on this line was halted in favor of characterizing line *eoa2*. Two separate plants that suppressed the early flowering phenotype of *arp6* mutants from the screened generation of candidate *eoa2* mutants (M_3) were successfully backcrossed to the original *arp6* mutant line (Fig. 3.1C). Individuals from the F_2 generation consisting of self-pollinated progeny from this backcross that presented the suppressor phenotype were backcrossed to *arp6* mutants a second time. After this second backcross, we confirmed that these F_2 *eoa2* plants (BC2F2) still had the eoa phenotype which corresponded with an increase in *FLC* transcript levels even without proper H2A.Z incorporation (Fig. 3.1D and Fig. 3.2C-E). Plants in the BC2F2 population with the *eoa2* flowering-time phenotype segregated in a 3:1 ratio, suggesting that the phenotype is caused by one recessive mutation (Fig. 3.2F,G). While not every F_3 *eoa2* line maintains the delayed flowering time presented by their parent F_3 plant (esp. line 1), *eoa2* plants tend to show more WT-like flowering timing in the BC2F3 generation (Fig. 3.2H). The quantitative nature of counting leaf numbers to measure developmental timing means that some of the

eoa2 plants have more *arp6*-like flowering time due to the broad distribution of the phenotype in the population (Fig. 3.2H).

Mapping the eoa2 mutation identifies 9 candidate causal genes

Many approaches have been devised to accurately map EMS-generated point mutations (Zuryn et al., 2010; Austin et al., 2011; Hartwig et al., 2012; Allen et al., 2013). The method we selected to identify suppressor mutations uses EMS-generated single nucleotide polymorphisms (SNPs) as segregating alleles to map causal mutations rather than introducing variation by outcrossing to a different ecotype (Allen et al., 2013; Hartwig et al., 2012). EMS-generated mutations persisting in the pool of mutants provide a variable genetic background to identify a selected region of the genome that segregates with the mutant suppressor phenotype. This is useful since suppressor mutants may have phenotypic variation in different ecotypes that would complicate generating a mapping population.

To map the causal *eoa2* mutation in the BC2F2 plants, we used a genomic sequencing-based mapping approach (Allen et al., 2013). We collected leaf material from plants segregating with the *eoa2* phenotype and isolated genomic DNA from pools of 85 and 100 F_2 plants from two *eoa2* lines from independent backcrosses, and also from 50 plants from the *arp6* parental line used for backcrosses (Fig. 3.1E). After sequencing each sample so that we had at least 60x coverage of the genome, we mapped reads back to the genome and called mutations with high allele frequency as potential candidates for the causal mutation (Fig. 3.1F). By sequencing the genomes of a pool of *arp6* plants, we were also able to remove any strain specific polymorphisms from our analysis if they were already present in the *arp6* parental line (Fig 3.3A). We also only included mutations in our analysis that were shared between both segregating *eoa2* backcrossed lines (Fig. 3.3A). Using the Next-Generation Mapping (NGM) tool (Austin et al., 2014) to identify non-centromeric mutations with an allele frequency of > 0.85, we identified a 2MB region of interest on chromosome 3 with a high degree of homozygosity in the backcrossed suppressor mutants (Fig. 3.3B-C). To confirm these

mutations, we used a second software package called CandiSNP (Etherington et al., 2014) to call potential candidate SNPs. In the region of interest on chromosome 3, 9 genes collectively containing 11 missense mutations and annotated as functioning in the nucleus were identified as top candidates for causal suppressor mutations in *eoa2* plants by both algorithms (summarized in Table 3.1). No mutations to *FLC* were reported by either workflow. Most of the factors we identified as top candidates were not previously characterized or are only identified based on homology with specific protein families (Table 3.1). However, since the Polycomb Repressive Complex 2 (PRC2) is a known repressor of the *FLC* gene (Jiang, 2008), candidates encoding factors known to interact with PRC2 such as BLISTER (BLI, candidate 2) or enzymes with potential ubiquitination activity (candidates 4 and 8) that may interact with the related Polycomb Repressive Complex 1 were of particular interest (Schatlowski et al, 2010; Kleinmanns et al, 2017).

Complementation experiments are inconclusive

To identify whether any of these mutations were sufficient to cause the *eoa* phenotype, we performed complementation transformation experiments (Fig. 3.4A). We introduced wild-type copies of the mutated candidate genes into *eoa2* mutants presenting the *eoa2* suppressor phenotype to see if they could restore *arp6*-like flowering timing and *FLC* transcript levels in *eoa2* mutants (Fig. 3.4A). The genomic regions used for transformation included 2 kb upstream of the transcription start site and 1 kb downstream of the transcription termination site of the candidate gene. Amplicons ranged in size from 4.4-7.9 kb (Table 3.2). We successfully cloned genomic segments spanning 7 out of our 9 *eoa2* candidate genes into *E. coli* and then *Agrobacterium* to transform our complementation constructs into BC2F2 *eoa2* mutants (Fig. 3.4A). After a floral dip transformation, we selected for transformants and further genotyped them to confirm successful transformation with our complementation constructs (Fig. 3.4A). We then phenotyped the transformed T_1 individuals to see if they complemented the *eoa2* phenotype, restoring flowering time back to an *arp6*-like timeline and *FLC* transcripts back to *arp6*-like levels (Fig. 3.4A-C).

Due to the quantitative nature of our mutant phenotype, we also measured leaf numbers and *FLC* transcript levels in untransformed BC2F3 *eoa2* sibling plants along with confirmed *eoa2* transformants. This provided a way to verify that transformants showing *arp6*-like phenotypes are dependent on the presence of the complementation construct and not simply presenting *arp6*-like phenotypes. This could be the case if, for example, the plant transformed with the construct was not truly a homozygous *eoa2* mutant. Assessing untransformed siblings gave us a baseline measure of the penetrance of the *eoa2* phenotype for a particular T_0 transformed *eoa2* plant line, so we could judge whether our constructs were complementing the *eoa2* phenotype or if *arp6*-like phenotype would be expected for the line being analyzed. This is important because some untransformed BC2F3 *eoa2* lines present more *arp6*-like flowering time, even though they were the progeny of plants that presented the *eoa2* delayed flowering phenotype (Fig. 3.4B).

To assess whether the WT version of the mutated candidate genes could restore the physiological flowering time phenotype back to an *arp6*-like flowering time, we counted the number of rosette leaves each transformant had at the time of flowering. For each candidate, we were able to phenotype at least one T_1 plant from 3-5 individually transformed T_0 *eoa2* plants. Out of the 7 candidate genes that were transformed into *eoa2* mutants, none showed restoration back to *arp6*-like early flowering (Fig. 3.4). Since T_1 individuals were phenotyped, every plant represents an independent integration of the complementation construct into the genome that could result in variable outcomes for each plant. For the plants that showed more *arp6*-like flowering time (seen for 1T, 3T, 7T, and 9T in Figure 3.4), several untransformed siblings from the same T_0 parent line showed comparable leaf numbers at the time of flowering to these plants of interest (compare to 7S, 9S). This suggests that the earlier flowering for plants containing WT copies of candidate genes 7 and 9 is not necessarily due to the complementation construct. One plant each from *eoa2* lines transformed with candidates 1 and 3 had more *arp6*-like flowering time that was not present in untransformed *eoa2* sibling plants. Therefore, candidates 1 and 3 appear to be the most promising causal *eoa2* candidates based on flowering time phenotypes. Further characterization of the T_2

progeny of these plants is needed to determine if this restoration of early flowering time is heritable or not and whether the presence of the transgene is strictly required.

To evaluate the molecular effects of these complementation experiments on the *eoa2* mutants, we also used RT-qPCR to evaluate *FLC* transcript levels in WT plants, *arp6* mutants, *eoa2* untransformed siblings, and individuals from transformed lines. While many *eoa2* transformants containing the WT copies of the candidate genes did present a decrease in *FLC* transcript levels compared to corresponding *eoa2* plants, only candidates 6, 8, and 9 had a transformant with a decrease in *FLC* transcript levels below WT levels (Fig. 3.5). However, the untransformed sibling *eoa2* plants were compromised during RNA isolation. So, even though some of the *eoa2* lines transformed with candidate 8 appear to have a decrease in transcript levels, it is still possible that this line has low *FLC* transcript levels without the WT copy of the mutated candidate gene since we were not able to compare these observations to a sibling untransformed *eoa2* plant (Fig. 3.5). Although this might suggest that these three are promising candidates for future follow up experiments based on molecular phenotypes, none of these lines show restoration of early flowering time for phenotyped T_1 plants.

FLC shows tissue specific expression differences between *arp6* and WT

As we measured *FLC* transcription levels in our *eoa2* transformants, we observed a great deal of variability between WT and *arp6* mutants with some experiments showing that *FLC* transcript levels were higher in *arp6* mutants than WT plants. (Fig 3.5, esp. controls for candidates 6/8). We were confident in the transcriptionally promoting role of H2A.Z/SWR1 at the *FLC* locus, since our lab and others have repeatedly found that H2A.Z incorporation by the SWR1 complex is important for proper *FLC* transcriptional activation. Still, we wanted to test whether tissue type we were testing could explain some of the different transcript levels we were observing (Martin-Trillo et al., 2006; Lazaro et al., 2008; Deal et al., 2007). Most of the previous experiments used whole seedlings to measure *FLC* transcription levels. However, to preserve plants so we could associate transcript levels

with time to bolting for each phenotyped plant, we assessed *FLC* transcript levels in leaves of pre-flowering plants in our experiments. To test whether the variability in our observations could be due to differences in tissue make-up between samples, we measured *FLC* transcript levels between WT plants and *arp6* mutants in leaf, cotyledon, and the remaining green stem material (Fig. 3.6A). We found that although *FLC* transcripts were more abundant in cotyledons and stem material in WT plants than *arp6* mutants, *FLC* transcripts were found at higher levels in leaf tissue in *arp6* mutants compared to WT plants (Fig. 3.6B). These observations suggest that using whole seedlings would be a more robust way to evaluate the requirement for H2A.Z to promote *FLC* transcriptional activity.

ARP6 does not physically interact with BLISTER

Candidate 2, BLI, interacts with subunits of the Polycomb Repressive Complex 2, which is a known repressor of *FLC* transcription (Schatlowski et al., 2010). Although BLI is not required for the histone methylating function of Polycomb group proteins, it is also required to repress many Polycomb group targeted genes (Kleinmanns et al., 2017). By disrupting BLI structure in *eoa2* mutants, we may have inhibited the transcriptionally repressive function of the Polycomb repressive complex at *FLC*. Although the function of BLI has been tied to PRC2 function, transcriptional profiling of DE genes in *bli* and PRC2 mutants suggest that BLI also has PRC2 independent functions that are yet to be determined (Kleinmanns et al., 2017). In addition to testing whether WT *BLI* (candidate 2) candidate transformation experiments can complement our *eoa2* mutants, we decided to test whether BLI physically interacts with ARP6 to oppose its role in promoting transcription. Since *BLI* alleles have been previously characterized, we acquired two GFP-tagged BLI lines that complement two seperate *bli* null mutants (*bli-1* and *bli-11*) (Schatlowski et al., 2010; Kleinmanns et al., 2017). To test for physical interaction between ARP6 and BLI, we performed a co-immunoprecipitation experiment for GFP-BLI and ARP6 in WT and BLI-GFP lines. Using protein blots to test for ARP6 after a pull down for GFP-tagged BLI or reciprocally for GFP-tagged BLI after using antibodies to pull down ARP6, we saw no evidence of a direct physical interaction (Fig. 3.7A-

B). This suggests that if *BLI* contains the causal mutation, then the suppressor phenotype must be due to separate indirect functions of BLI and ARP6, rather than BLI interacting directly with ARP6 and the SWR1 complex to modulate *FLC* transcript levels.

Discussion

In this study, we identified a mutant line (*eoa2*) that suppressed the early flowering phenotype of *arp6* mutants and concordantly alleviates the requirement of H2A.Z incorporation for proper *FLC* transcriptional activation. We used a sequenced based mapping method and identified mutations in 9 candidate genes that might be causing the suppressor phenotype. To validate whether these identified mutations were causal, we transformed *eoa2* mutants with candidate constructs containing a WT copy of each candidate *eoa2* gene in an attempt to restore *arp6*-like phenotypes in the *eoa2* mutants. However, with the methods used here, we were ultimately not able to identify the causal mutation behind the *eoa2* phenotype using the resources and timeline allocated for this project. Here we discuss several challenges with the design of the screen and some alternatives to the methods we chose that might have impacted the outcome of the screen.

Challenges faced by the screen and mapping method

In our suppressor screen, we identified suppressors of the *arp6* phenotypes based on the molecular phenotype of *FLC* transcriptional changes in addition to delayed flowering time. However, the initial mutant that inspired the screen (*brm-1*) does not have delayed flowering even though *FLC* transcription is increased (Farrona et al., 2011). This is because other factors altered in brm-1 can by-pass *FLC* in the complicated process of flowering time regulation (Farrona et al., 2011). As an alternative method, we could have performed EMS mutagenesis on *arp6* mutants containing an *FLC* reporter construct, such as previously characterized *FLC:GUS* or *FLC:Luciferase* lines (Sheldon et al., 2002; Mylne et al., 2004). Using *FLC*-reporter constructs would have provided a more direct and thorough way to identify supressors based on *FLC* transcript levels rather than relying on flowering

time as an indirect measure of *FLC* transcript levels. It would have also been a more high-throughput, cost-effective and less labor intensive than measuring transcript levels by RT-qPCR.

The quantity and variety of factors that can be linked to a specific process (hypothesis-free) are two of the benefits of conducting a mutant screen. In our case, our screen was not saturated, meaning that we did not reach the full potential of factors that could be linked to overcoming arp6 mutant phenotypes. In the initial screen, +100 M_2 plants were identified in the green house as potential suppressor lines based on their time to flowering followed by more rigorous validation in a more controlled environment. During their time in the green house, many plants died due to temperature fluctuations that induced heat/drought stress. Thus, a portion of the mutants that could potentially result in changes in flowering time was removed from the screen due to environmental stressors.

After beginning our genetic screen, work was published showing that *arp6* mutants have problems with DNA damage repair and therefore have decreased recombination (Choi et al., 2013; Rosa et al., 2013). This means that by using the *arp6* mutants in our suppressor screen, there will be fewer opportunities for background EMS mutations to segregate away from the causal mutation. Consistently, after two backcrosses to the *arp6* parental line, we have a number of mutations with a high allele frequency to sort through in our suppressors than what other previous studies that have used sequencing based mapping techniques observed (Allen et al., 2013; Etherington et al., 2014). A greater load of SNPs could have also been present to begin with if our EMS-treatment was more damaging.

Traditional linkage-based genetic mapping methods in combination with sequencing could have helped us narrow down our candidates more accurately. There are several reasons why we chose not to perform traditional linkage-based mapping of the *eoa2* mutation. Bulk segregant analysis uses the segregation of alleles from two distinct ecotypes to identify the causal mutant with PCR or whole genome sequencing. Therefore our *arp6* mutation would need to be integrated into a second ecotype before backcrossing our eoa2 mutants to generate a mapping population. It is then more difficult to maintain the two mutations involved in the suppressor screen during genetic linkage crosses.

Therefore the linkage-based mapping method is more labor intensive and time consuming than mapping by sequencing alone. Also, if suppressor mutants are outcrossed into different ecotypes, background genetic differences can introduce unnecessary variability to phenotypes that are already difficult to score. Since other methods were able to map mutants without traditional mapping techniques, this suggested to us that it would be unnecessary and redundant to perform linkage-based mapping crosses in addition to mapping by sequencing (Zuryn et al., 2010; Austin et al., 2011; Hartwig et al., 2012; Allen et al., 2013). However, had we also conducted linkage crosses, we would have been able to more accurately narrow down which chromosome region carries the causal suppressor mutation. In addition, the frequencies of recombination may have alluded to the fact that there is decreased recombination in *arp6* mutants earlier.

Complementation method

We chose to try to complement our *eoa2* mutants by transforming them with a WT copy of the mutated candidate causal genes, but there are several alternative methods we could have used. Our candidate complementation constructs included a genomic region that included a candidate gene, and 2 kb upstream and 1 kb downstream of the gene. This focused our analysis on one gene with the surrounding regulatory region, which in some instances also included a neighboring gene. Complementing the *eoa2* mutants by transforming them with transformation-competent artificial chromosomes (TACs) that include larger genomic regions surrounding candidate genes or across regions of interest would have had a greater chance of getting the entire functional promoter region and any regulatory sequences required for the gene's transcription. Our mutants contain mutations in coding and non-coding regions, yet in order to make some prediction about their function our complementation approach focused on mutations in coding regions of genes. In the most general sense, complementing with large genomic regions, such as TACs would have been a way to complement mutations in non-coding sequences together with the surrounding genes. However, these TACs also include numerous genes and would have required additional validation steps to confirm

which of the many genes present on the construct were responsible for complementation. In contrast to the TAC method, by transforming the *eoa2* plants with a WT copy of candidate genes meant that we were specifically targeting the gene identified as containing a candidate causal mutation and minimizing effects from neighboring genes. Additionally, at the time we were choosing a complementation method, available TAC resources were sparse and were only available for a portion of our candidate genes and regions of interest.

Another way to test whether any of our candidates cause the *eoa2* phenotype is by crossing *arp6* to mutants for each of the candidate genes to look for suppression of the *arp6* flowering-time and *FLC* transcript level phenotypes. There are T-DNA insertion mutations for some of the candidate causal genes, which we could have used. However, only *BLI* (candidate 2) had alleles that had been previously characterized (Schatlowski et al., 2010). This meant that using a candidate genetic cross approach would have required extensive characterization and phenotyping of multiple mutant lines for each candidate gene before beginning genetic crosses to test for a suppressor phenotype. Alternatively, we could have tried to recreate the suppression phenotype with CRISPR/Cas9-generated insertion or deletion mutations to candidate genes in the *arp6* mutant background (Jiang et al., 2014). However, the CRISPR/Cas9 protocol was still being optimized for plants at the time we started this work.

By using T-DNA mutations, we would have been introducing truncated proteins or premature stop codons that would result in loss of all or part of the protein causing more drastic changes than the individual missense mutations observed in our candidates. Therefore, crossing candidate T-DNA mutants with *arp6* mutants would be evaluating more severe changes than what may be present in the *eoa2* mutants. By transforming *eoa2* mutants with WT candidate constructs, we were working to isolate alleles with missense mutations that could present phenotypes due to more specific changes in protein properties. These have the potential to provide a more detailed view of the candidate gene's function and how it interacts genetically with ARP6 and H2A.Z to regulate transcription. Also, if one of these missense mutations for our candidate genes was causal, we may be able to isolate

hypomorphic alleles for genes that would normally be lethal if we were evaluating completely null mutations. The CRISPR/Cas9 approach would have been amenable to introduce specific point mutations like the ones mapped in the original *eoa2* mutants.

Although we did not see convincing restoration of our *eoa2* mutants back to *arp6*-like phenotypes after transformation with our candidate constructs, there are several reasons this might be. We operated under the assumption that our mutation is a loss of function mutation. However, since the mutations result in non-synonymous amino acid changes instead of premature stop codons, the mutation could also be a gain of function mutation. It is also possible that our WT constructs were not properly expressed in our transformants. Since differentiating between expression of the WT allele that we introduced and the copy of the candidate gene with a missense mutation would be labor intensive, we opted instead to phenotype for flowering time and *FLC* transcript levels as a first pass to see if any candidates presented signs of restoring the phenotype back to *arp6*-like levels. Alternatively, one copy of the WT gene may not have been sufficient to restore the *arp6*-like phenotypes. We tested two lines of *eoa2* mutants transformed with candidate genes 2 and 3 into the T_2 generation, which would have presumably been homozygous for the inserted constructs. These were both lines that showed some indication of lower *FLC* transcription in the T_1 generation (not shown), but in the T_2 generation, they still had high levels of *FLC* transcription (Fig. 3.2). By further testing other lines, into the T_2 generation, we may still be able to restore *arp6*-like phenotypes to the candidate-transformed *eoa2* mutants. However, given the variability that is observed between, *FLC* levels in *arp6* and WT we may want to test whole plants rather than just leaves in future experiments.

Ultimately, several things made this mutant screen difficult and some could have been rectified had we used alternate methods. These include using an *FLC* reporter or using traditional genetic mapping method along side the sequencing-based mapping. Although we were not able to verify a causal mutation, this work allowed us to generate a mutant line that suppresses the need for H2A.Z function along with a pool of candidate causal mutations for future testing. Future work to test the function of the previously uncharacterized candidate genes that were perturbed in our mutant screen

has potential for providing novel insights to *Arabidopsis* genetics. By testing the hypothesis that BLI interacts genetically with ARP6 and H2A.Z, we could potentially also understand how the Polycomb Repressive Complex interacts with SWR1 function. The outcome of this work has important prospects to broaden our understanding of how H2A.Z contributes to transcriptional activation and provide insight into chromatin-based regulation of the *FLC* gene.

Materials and Methods

Plant material and growth conditions

Previously characterized *Arabidopsis thaliana* M_2 *arp6-1* T-DNA mutants (GARLIC_599_G03; Deal et al., 2005) that had been mutagenized a second time by ethyl methane sulfonate (EMS) and homozygosed were initially screened in the Biology Department green house (Emory University). Then, the progeny of lines that showed delayed flowering (M_3) were subsequently phenotyped in controlled environmental rooms. These plants and all those afterward were stratified at 4 °C in the dark for 2 days on soil, then germinated in controlled environmental rooms at 20 °C with long-day light conditions, unless otherwise specified. Counting rosette leaves after bolting was used as a developmental measure of time to flowering.

Assessing FLC *transcript levels*

Tissue was collected from pre-flowering plants, frozen in liquid nitrogen, and then ground in a 1.6 mL tube using a blue plastic pestle. For *FLC* transcript level evaluations for M_4 *eoa2* plants, RT-qPCR data was generated from pooled tissue of 4 whole seedlings (10 day post-stratification) grown on ½ MS plates. For evaluating *eoa2* plants after backcrosses, above-soil material from 3 F_3 *eoa2* plants were collected 12 (dps) and pooled for each of the two individually backcrossed *eoa2* lines. RNA was isolated from ground tissue using either the RNeasy Plant mini Kit (QIAgen) or the Spectrum ™ Plant Total RNA Kit (Sigma) and RNA was re-suspended in 30 μl of RNA-free H2O or elution buffer, respectively. RNA was quantified using a spectrophotometer, and DNA was removed

from 25 µl of each RNA sample using the Turbo DNA-free Kit (Ambion). For this reaction, samples were incubated with the DNase for 30 min at 37 °C. RNA was quantified again with the spectrophotometer after DNA was removed. Reverse transcriptase reactions were performed to generate cDNA from the isolated RNA using the SuperScript™ III First-strand Synthesis System (Invitrogen). Oligo-dT primers were used to specifically generate cDNA from mRNA in a 20 µl reaction. To asses relative *FLC* transcript levels, Real Time qPCR was performed on 1 µl of template cDNA using 2x Power SYBR Green PCR mix (Life Sciences) combined with primers targeting FLC (FLC9*,* Deal et al., 2007*)* and *PP2A*. Reactions were run on a StepOnePlus RealTime PCR system (AppliedBiosystems). Relative transcript abundance for *FLC* was determined using the $\Delta\Delta C_T$ method normalizing to WT samples and then to the endogenous reference gene *PP2A* transcript levels (Livak and Schmittgen 2001; Czechowski et al., 2005). Since there was optimization and changes between experiments, details regarding sample collection, genotyping, RNA isolation, and cDNA synthesis are summarized in table 3.3.

H2A.Z ChIP-qPCR

A 0.5 g pool of rosette leaf material was collected 10 hrs after dawn from mature rosette leaves (34 dps) from WT plants, arp6 mutants, and *eoa2* mutants. The *eoa2* plants are from the BC2F2 generation and present with *eoa2* phenotypes. We isolated cross-linked chromatin from purified nuclei as described in Gendrel et al., 2005. Chromatin was sonicated using a Bioruptor® (Diagenode) (40 min on high (45 sec on/ 15 sec off)). Each sample was diluted to 1.1 mL with ChIP dilution buffer (described in Gendrel et al., 2005), an aliquot of chromatin was moved to a separate tube (650 µl), and 50 µl was saved as an input reference sample. Using the chromatin aliquot, the H2A.Z-containing chromatin was immunoprecipitated using 1 µg of H2A.Z antibody purified to specifically recognize unmodified H2A.Z peptides (Deal et al., 2007). The chromatin solution was incubated with the H2A.Z antibody for 2 hr then for 1 more hour in combination with 60 µl of

DynabeadsTM Protein-A magnetic beads (Invitrogen). DNA collected from the immunoprecipitation and from the inputs was purified using 1.8x volume of SPRI beads (Beckman Coulter) then quantified with Quant-ITTM Picogreen® dsDNA Assay Kit (Invitrogen). Performed qPCR with the input and immunoprecipitated DNA using primers (400 nM) targeting the *FLC* promoter (FLC2) and the PP2A reference gene where we do not expect H2A.Z changes. We ran a 20 µl reaction on the StepOnePlus Real-Time PCR, using 2x Power SYBR Green PCR master mix (Applied Biosystems) and 5 µl of template DNA (diluted 1/100 for input and 1/8 for IP sample).

Mapping material and library preparation

A leaf section (~10 mg) from *eoa2* mutant individuals (85 from *eoa2* (line 1) and 100 from *eoa2* (line 2)) presenting the suppressor phenotype from the second F_2 generation were collected. Leaf sections were also collected and pooled from 50 *arp6* mutants. DNA was isolated from pools of *eoa2* line 1(3) and line 2(5) and *arp6* leaf tissue with a Phenol:chloroform extraction followed by ethanol precipitation. Precipitated DNA was re-suspended with 50 µl of 1xTE. DNA was quantified with the Quant-It Picogreen dsDNA Assay Kit (ThermoFisher) and run on a gel to confirm integrity of DNA. RNA was removed by an RNaseA digestion (0.5 µl into 50 µl of DNA solution) (Ambion) at 37 °C for 15 min. DNA was fragmented using sonication with the Bioruptor (Diagenode) on high for 10 rounds of 30 sec on 30 sec off (spinning samples down after 5 rounds) to generate 200-400 bp fragments. Fragments were purified with the MinElute PCR Purification kit (QIAgen) and eluted in 12 µl of molecular grade water. DNA Sequencing libraries were prepared from 1 µg each of pooled DNA from *eoa2* line 1 (3), *eoa2* line 2(5), and *arp6* (NEXTflex Rapid DNA-Seq Kit (BIOO Scientific) using the size-selected library prep option. For size selection, we used lower cut off for 300-400 bp 37.5 µl and upper cutoff volume of 35 µl. Amplified libraries were quantified using PicoGreen and evaluated on the Bioanalyzer (Emory Integrated Genomics Core). Sequenced at the Huntsman Cancer institute on the Illumina HiSeq2000, generating 125 bp paired-end reads.

We used 1 μg of sonicated DNA to prepare a sequencing library (NEXTflex Rapid DNA-seq (option 2), Bioo Scientific), and then sequenced on an Illumina HiSeq2000, generating 125 bp paired-end reads.

Data analysis for mutation mapping

We used two different mutation-mapping programs to call candidate SNPs: CandiSNP and Next-Generation EMS mutation mapping (NGM). Causal mutations were initially identified using the workflow that uses the NGM software (Austin et al., 2011), but instead of applying it to outcrossed lines, we followed a workflow to apply the software to our backcrossed mutant lines (Allen et al., 2013). Data analysis tools were executed within the iplant collaborative platform (currently CyVerse) (Merchant et al., 2016). Sequenced reads generated from *eoa2* line 1 mutants, *eoa2* line 2 mutants and *arp6* mutants were mapped against the *Arabidopsis thaliana* Ensembl19 reference genome using BWA mem software (version 0.7.4) with default settings. The aligned SAM file was converted to a position sorted BAM file and indexed using the samtools "SAM-to-sorted-BAM" iplant application (Li et al., 2009). SNPs were called using the samtools pileup program (v 0.1.16) and called against the TAIR10.23 genome (Li et al., 2009). SNPs that were called in the arp6 mutant genome were removed using a python script employing the grep command to identify lines that were unique to the eoa2 mutant genomes. The unique SNPs were converted to a format that can be used by the NGM program using a perl script provided by Austin et al., 2014. The resulting file was uploaded to the NGM portal (http://bar.utoronto.ca/ngm/) to generate genome plots and discordant chasity calculations for each SNP. Discordant chastity is a measure of the frequency of one non-reference base SNP calls relative to all other non-reference base observations. Using these calculations, NGM measures the ratio of natural variation compared to mutagenesis generated variation to target specific regions of the genome for analysis. To confirm mutations identified as significant by the NGM workflow, we repeated the mutant allele frequency calling using a second workflow using the CandiSNP program (Etherington et al., 2014).

For the second analysis, we used a subset of sequenced reads to minimize false positives that may be a result of over sequencing. By randomly generating a subset of mapped reads using the samtools view –s command, we analyzed at least 60.8 M reads for each sample, which resulted in approximately 60x fold coverage of the genome. Reads were then sorted and indexed with the SAMtools sort and index commands, respectively (Li and Durbin 2009; Li et al., 2009). We then generated .csv files of called SNPs using the pileup_to_SNPs.rb script provided by Etherington et al., 2014. Parameters used by the script to filter the output SNPs included a minimum depth of 50, minimum non-reference calls of 20 and PHRED score cutoff of 30. Using a ruby script provided by the corresponding author of Etherington et al., 2014 (get_unique_snps.rb), we removed SNPs from the eoa2 line 1 and line 2 genomes that were also called in the parental arp6 mutant genome. After using the Galaxy "Compare two datasets" tool (Afgan et al., 2016) to find the SNPs that are shared between eoa2 line 1 and line 2. The resulting tab delimited file was saved as a UTF-16 Unicode .txt file, then we used Microsoft Excel to save it as a .csv comma delimited file. We then uploaded the resulting file of SNPs shared by eoa2 lines 1 and 2 but not found in the arp6 parental line to the CandiSNP program (http://candisnp.tsl.ac.uk/) (Etherington et al., 2014). Data was analyzed by changing the allele frequency cutoff to >0.85 and using otherwise default parameters (which includes removing centromeric SNPs). The CandiSNP program generated allele frequencies, CAD scores, and annotated which genes were affected by the SNPs. Since chromosome 3 had a region of interest that was enriched for high allele frequency SNPs in both workflows, we further analyzed SNPs that were called as candidate causal mutations on chromosome 3 by both workflows. From this shared list of identified SNPs, 11 non-synonymous mutations in coding regions for 9 genes that were annotated with functions in the nucleus were identified as top candidate causal mutations (Table 3.1).

Cloning Candidate Suppressor Genes for Complementation Tests

PCR primers were designed for use with In-Fusion® HD Cloning Kit protocol (Clontech® Laboratories, Inc). Primers for the reaction were designed with a 20 bp regions targeting the

pCAMBIA1300 plasmid (http://www.cambia.org/daisy/cambia/585), and a second gene specific region targeting either 2 kb upstream of the TSS or 1 kb downstream of the TTS of the candidate gene being amplified. PCR amplicons range in size from 4.39 KB to 7.94 KB. Details regarding primer design are summarized in Table 3.3. Genomic regions spanning candidate *eoa2* genes (table x) were amplified from WT *Arabidopsis* DNA by performing PCR with Q5 High-Fidelity DNA Polymerase (NEB). We then used the In-Fusion® HD Cloning Kit protocol II (Clonetech® Laboratories, Inc.) to insert the PCR-amplified candidate genes into the linearized pCAMBIA1300 plasmid (using a 1:3 vector to insert ratio based on molar concentrations). We then transformed Stellar™ competent *E. coli* cells (Clontech) with the In-Fusion® reaction samples and used Sanger sequencing to confirm that cloning was successful. The verified vector was subsequently transformed into electrocompetent Agrobacterium cells (GV3101) that were used to transform the candidate genes into *eoa2* mutants by Floral Dip method (Clough and Bent 1998). The *eoa2* mutants used for transformations were $BC2F_3$ *eoa2* (line 2) mutants that suppressed the early flowering *arp6* phenotype based on the number of leaves for each plant at the time of bolting.

The T_1 transformants were sown on ½ Murashige and Skooge (MS) selection plates containing 35 μg/mL Hygromycin and 100 μg/mL Timentin. After 7 days on selection plates, the most successful seedlings were transferred to soil. After isolating DNA with either the Edwards Buffer Protocol or SPRI Bead genotyping protocol (details of which are summarized in Table X), plants were genotyped to confirm whether transformants contained the appropriate candidate construct. We used validation genotyping primers targeting the pCAMBIA1300 plasmid and a portion of the cloned candidate region (Table 3.4). Transformants were further phenotyped to determine whether they complemented the *eoa2* phenotype, returning to more *arp6*-like flowering time and *FLC* transcript levels.

Edwards buffer DNA isolation protocol

Grind sample in tube with liquid Nitrogen. Resuspend in 40 µl of Edwards buffer (200 mM Tris-HCl, pH 7.5; 250 mM NaCl; 25 mM EDTA, pH 8.0 (DNase); 0.5% SDS). Spin down for 4 min at 16,000x g. Move 350 µl of sup to new tube without disturbing pellet. Add an equal volume of isopropanol and mix will. Incubate for 5 min at room temperature, then spin down sample for 5 min at full speed (23,000 x g). Pour off supernatant, then wash with 500 µl of 70% ethanol. Invert, incubate for 2 min at RT, then spin again at full speed for 1 min. Repeat 70% ethanol rinse and spin, then after pouring off the super natant, air dry the DNA pellet for 10 min. Resuspend the DNA in 50 µl of dH2O and incubate at 4 °C. This material was used for PCR.

SPRI bead genotyping protocol

Collect small tissue sample into 50 µl of 1xPBS with 1% SDS (v/v). Use a tip to grind material until the solution is green, then remove any large tissue pieces, then spin down. Add 20 µl of plant solution to 36 ul of SPRI beads (1.8 x volume), mixing well. Incubate at RT for 5 min then place solution on a magnet and allow beads to collect. Remove supernatant and discard. Wash beads while on the magnet with 100 µl of 80% EtOH and incubate for 30 sec. Pull off EtOH and repeat for a second wash. After pulling off all supernatant, let the remaining beads dry on the magnet (about 5 min). Remove tubes from the magnet and re-suspend beads in 20 µl of elution buffer (TE or 10 mM Tris, pH 8) and let stand for 30 sec. After returning the beads to the magnet and allowing the beads to clear, move the supernatant containing the purified DNA to a new tube.

Co-IP to test for ARP6 and BLI interaction

Collect two inflorescence flower tissue samples each from WT (0.2 g and 0.6 g), *bli-1/bli-1* gBLI::BLI-GFP (2 x 0.151 g), *bli-11/bli-11* gBLI::BLI-GFP (2 x 0.36 g) plants (Schatlowski et al., 2010). Material was flash frozen in liquid nitrogen, pulverized with a mortar and pestle, and re-suspended in 2 volumes (mg/ml, i.e. 1 mL for 500 mg) of immunoprecipitation (IP) buffer (50 mM Tris, pH 7.5; 150 mM NaCl; 10 mM $MgCl_2$; 0.1% Nonidet P-40; 1mM β -mercaptoethnol; proteinase

inhibitor tablet, described in Deal et al., 2007). Samples were spun down at max speed (20,000 x g) for 5 min at 4 °C. The supernatant was then moved to a new tube and 20 µl aliquots from each sample were set-aside as input samples, mixed with 2 x Laemmli's Sample Buffer (125 mM Tris, pH 6.8; 4% SDS; 1% β -mercaptoethanol; 0.5% bromophenol blue; 20% glycerol), and frozen at -20 °C. The remaining supernatant was divided into separate tubes for IP experiments and the volume was adjusted to 400 µl with IP buffer if necessary. The WT samples were incubated for 1 hour at 4 °C with 1:100 dilution of α-ARP6 antibodies (4 µl, polyclonal), α-GFP antibodies (1 µl, abcam, ab290), and α-H2A.Z antibodies (4 µl, described in Deal et al., 2007) and BLI-GFP samples were incubated with the α-H2A.Z and α-GFP antibodies. Next, we incubated each sample for 1 hr at 4 °C with 20 µl of Protein-A magnetic beads (Invitrogen) that had been washed and re-suspended in IP buffer. After the incubations, tubes were placed on a magnet allowing the magnetic beads to adhere to the side of the tube. The supernatant was then discarded and 500 µl of IP buffer was added. The samples were removed from the magnet, incubated on a nutator for 15 min, and then returned to the magnet. These wash/incubation steps were repeated so that the samples were washed a total of three times in IP buffer. After the removing the supernatant for the final wash, we added 40 µl of 2 x Laemmli's Sample Buffer to each sample as a protein loading dye, then vortexed the samples, and froze them at -20 °C overnight. To prepare samples for protein blotting, IP and input samples were incubated at 100 °C for 5 min then spun down briefly. For protein blotting, one of the biological replicates for each genotype were run in two parallel Novex 4-12% Tris-Glycine gels (Invitrogen) along with ColorPlus™ Prestained Protein Marker (NEB), and then transferred to a nitrocellulose membrane. Membranes were blocked for 1.5 hrs in blocking solution consisting of PBSt (137 mM NaCl, 2.7 mM KCl, 10 mM Na_2HPO_4, 2 mM KH_2PO_4, with 0.05% TWEEN® 20) with 5% wt/v non-fat dry milk, blots were incubated overnight at 4 °C, rocking in blocking solution containing either primary α-GFP antibodies (Santa Cruz, SC-9996, at 1:400 dilution) or α–ARP6 antibodies (monoclonal C2, 1:100 dilution, Deal et al., 2005). After washing the membrane in PBSt, membranes were incubated at room

temperature for 1 hr with a 1:2000 dilution of blocking solution with secondary ECL Anti-Mouse Horseradish Peroxidase-conjugated secondary antibody (GE healthcare). After washing with PBSt, blots were incubated with ECL reagents for 3 min and proteins were visualized using Amersham Hyperfilm ™ ECL high performance chemiluminescence film (GE Healthcare). ARP6 and BLI-GFP were visualized as approximately 46 kD and 100 kD size bands, respectively. Blots were repeated with a third biological replicate as described, with the same results. Then a fourth biological replicate was performed, as a cross-linked ChIP experiment followed by blotting for the purified proteins (as described in Gendrel et al., 2005). 0.75g was used for WT and 0.5g was used for BLI-GFP lines. A 200 µl sample of chromatin was sonicated for 40 min (45 sec on/ 15 sec off) then diluted to 2 mL in ChIP dilution buffer and divided into two separate tubes for BLI-GFP samples or three separate tubes for WT samples.

Acknowledgements

This research was supported by funds from Emory University and funds awarded to E. Shannon Torres from the Ruth L Kirschstein Predoctoral Individual National Research Service Award through the National Institute of General Medicine of the National Institutes of Health under award number (F31GM113631-01A1). The content is solely the responsibility of the authors and does not necessarily represent the official views of the National Institutes of Health. I would like to thank Stevin Bienfait for excellent work generating the candidate complementation constructs, and Katie Duval for doing a really great job characterizing the transformants, conducting other related genetic experiments, and for all of her moral support. Dr. Paja Šijačić provided technical guidance for cloning and transformation experiments. Alex Kotlar provided computational assistance.

Figure 3.1

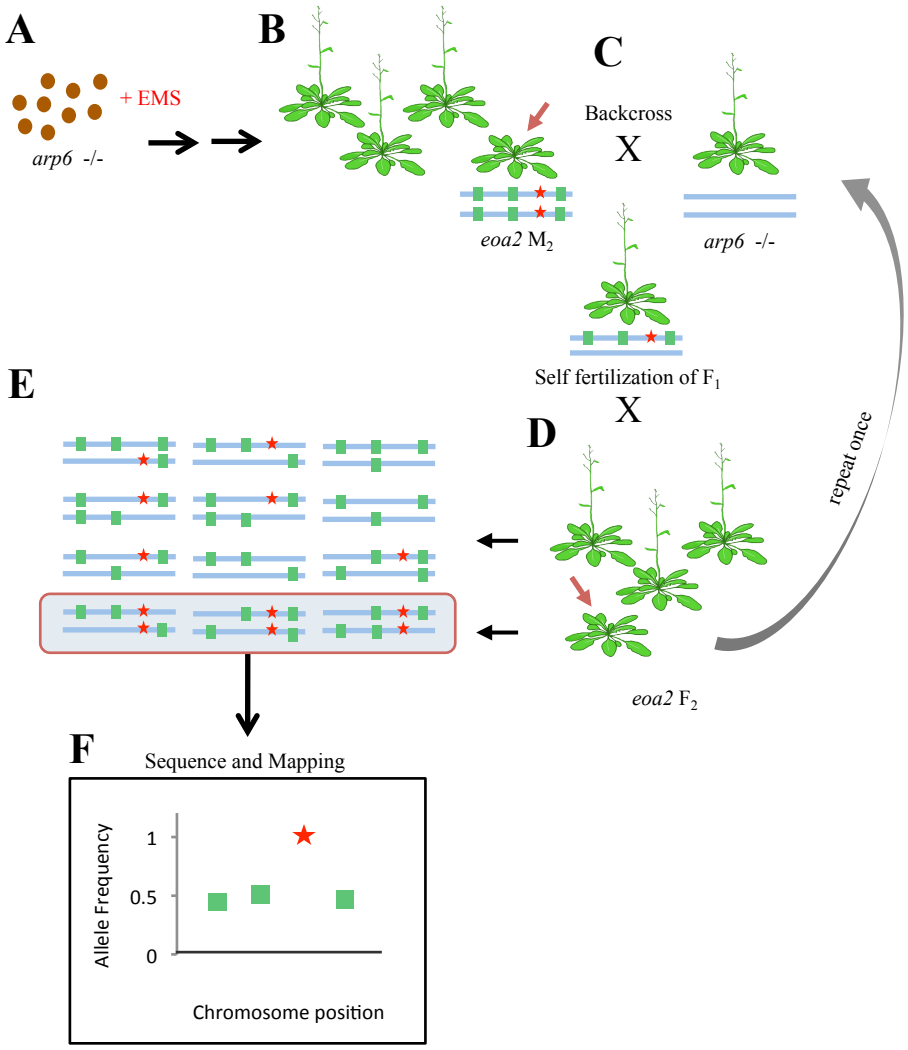

Figure 3.1. Forward genetic suppressor screen study design. (A) *arp6* mutant seeds were EMS mutagenized and these mutations were brought to homozygosity. (B) We screened this M_2 population for plants presenting an *arp6* suppressor phenotype that we describe as early flowering overcome in *arp6 (eoa)* (indicated by red arrow). (C) Plants showing the eoa phenotype in mutant line *eoa2* were backcrossed to the parental *arp6* mutant line followed by self fertilization of F_1 individuals and an additional round of back crossing. Below the plants involved in the genetic cross, the un-identified causal mutation is represented as a red star among other EMS mutations (green squares) on its

corresponding homologous chromosomes (blue lines). (D) F_2 plants were screened for those with the *eoa2* phenotype again and genomic DNA from a pool of these plants was isolated and sequenced. (E) Chromosomes from a representative pool of *eoa2* F_2 plants is shown demonstrating how if the mutation is recessive then the mutation and phenotype will segregate in a 3:1 ratio. Chromosome pairs within the red outline represent the plants segregating with the *eoa2* phenotype that are homozygous for the causal mutation but still have additional EMS-generated mutations present at different allele frequencies. Modified from Allen et al., (2012). (F) After sequencing and mapping mutations in the segregating population, we can identify the mutations with high allele frequency as potential candidates for the causal mutation.

Figure 3.2

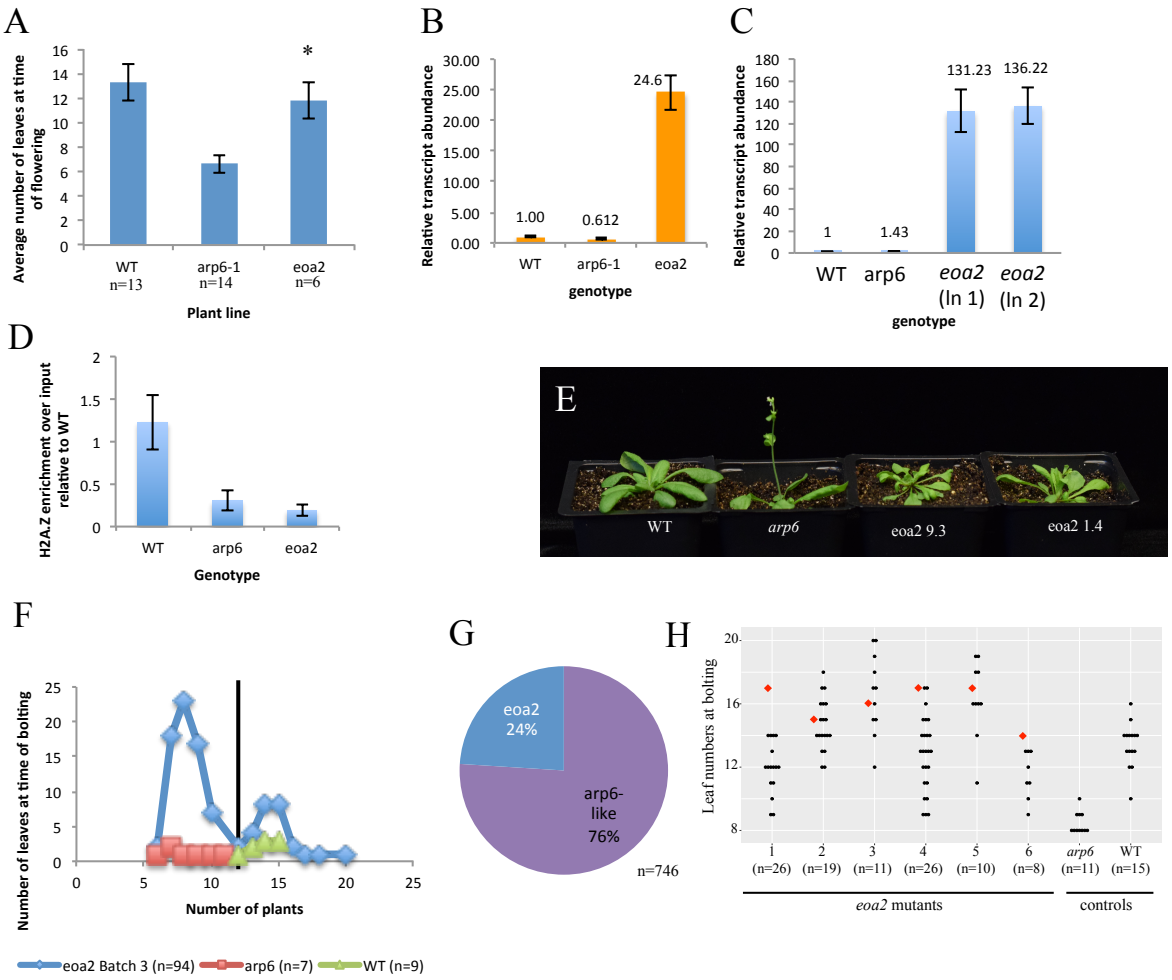

Figure 3.2. Identifying *eoa2* mutants and performing mapping backcrosses. (**A**) Histogram summarizing rosette leaf number counts from M_3 *eoa2* plants relative to WT and *arp6* plants at the time of bolting. * Designates significance by a p-value <0.05 by a Student's T-test. (**B**) Relative transcript abundance measuring *FLC* transcript levels in WT plants, *arp6* mutants, and an M_3 *eoa2* mutant using RT-qPCR. *FLC* levels were quantified relative to *ACT2* transcript levels using the $\Delta\Delta C_T$ method. (**C**) After two backcrosses into the parental *arp6* line, *FLC* levels were quantified relative to endogenous reference gene *PP2A* in two separate homozygosed *eoa2* mutant lines, using RT-qPCR and the $\Delta\Delta C_T$method. (**D**) Histogram comparing H2A.Z enrichment over input at the *FLC* first exon in *arp6* and *eoa2* plants relative to WT. (**E**) Picture showing plants at 22 days post stratification.

From left to right, WT plants, *arp6* mutants, and *eoa2* (line 1), and *eoa2* (line2) F_2 plants after two backcrosses ($BC2F_2$). (**F**) Line graph showing the distribution of the number of leaves presented by WT, *arp6*, and a representative *eoa2* F_3 population at the time of bolting. The vertical black line represents a cutoff between the homozygous *eoa2* plants presenting the suppressor phenotype and those that flower comparable to *arp6* plants. (**G**) Pie chart showing the proportion of plants in the total population of *eoa2* $BC2F_2$ plants phenotyped from both lines that suppressed the *arp6* early flowering phenotype. (**H**) Dot plot showing the distribution of the number of leaves at the time of bolding for *eoa2* $BC2F_3$ plants from 6 individual lines relative to *arp6* and WT plants. The red diamonds represent the number of leaves the parent $BC2F_2$ plant had at bolting.

Figure 3.3

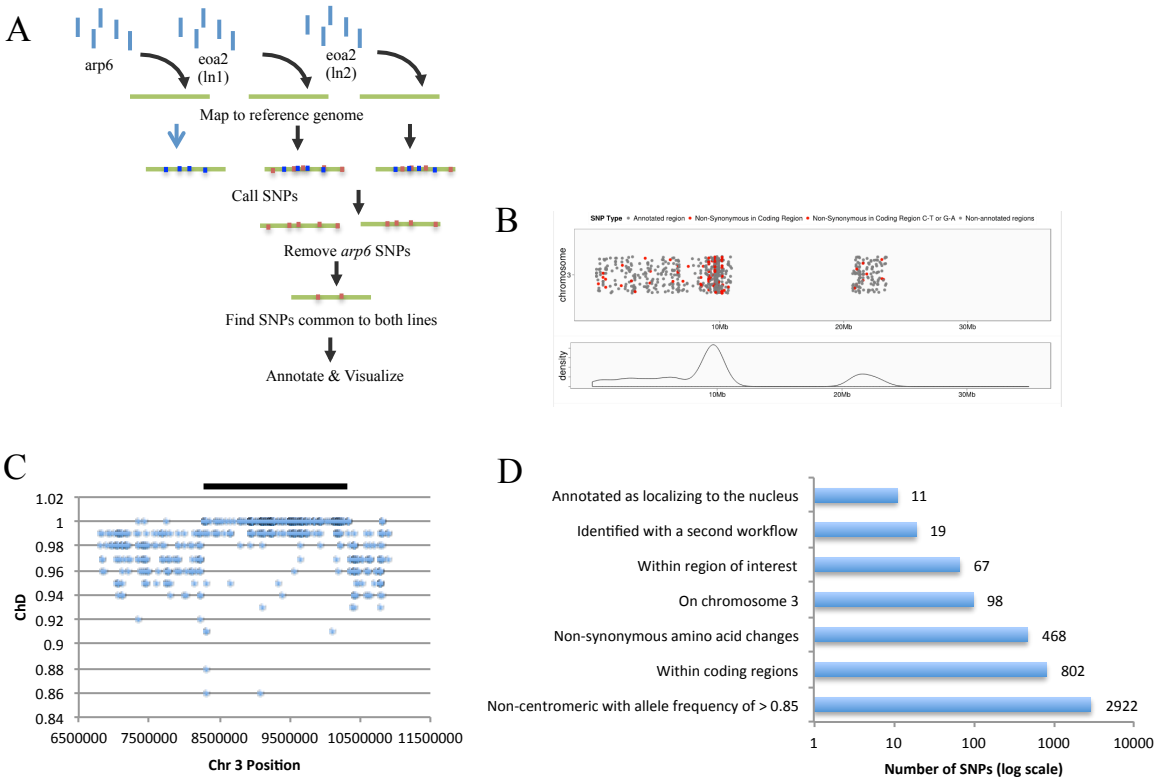

Figure 3.3. Identifying 9 candidate causal *eoa2* mutations. (**A**) Schematic summarizing the method used to map mutations by sequencing. Sequencing reads (blue lines) from *arp6* mutants and 2 separate backcrossed *eoa2* mutant lines were mapped to the Arabidopsis reference genome. Afterward, we identified single nucleotide polymorphisms (SNPs) that were different in the sequencing library compared to the reference genome. Any SNPs found in *arp6* mutants (blue dots) were removed from the analysis as well as any mutations that were not shared by the two *eoa2* mutant lines (orange dots). These SNPs were then annotated and visualized. (**B**) CandiSNP scatter plot (top) and density plot (bottom) showing SNP distribution across chromosome 3. The y axis for the scatter plot has no significance and dots are plotted at random as space permits, the x-axis corresponds to positions along chromosome 3. Red dots represent non-synonymous coding SNPs while grey dots represent all other SNPs. The y-axis for the density plot corresponds to the number of SNPs at each position across the genome, which is represented by the x-axis. (**C**) A scatter plot shows the

distribution of SNPs across a region of interest on chromosome 3 that is particularly dense with high allele frequency SNPs. The y-axis displays ChD which corresponds to allele frequency and the x-axis shows the corresponding position on chromosome 3. The 2.1 MB region of interest is demarcated by a dark bar at the top of the plot. (**D**) Bar graph showing how identified SNPs were narrowed down to our top candidate SNPs. Starting from the bottom and moving to the top, the y-axis describes the parameters we used to prioritize some candidates over less likely SNPs. The x-axis shows the number of SNPs (on a log scale) that were remaining after considering each parameter.

Figure 3.4

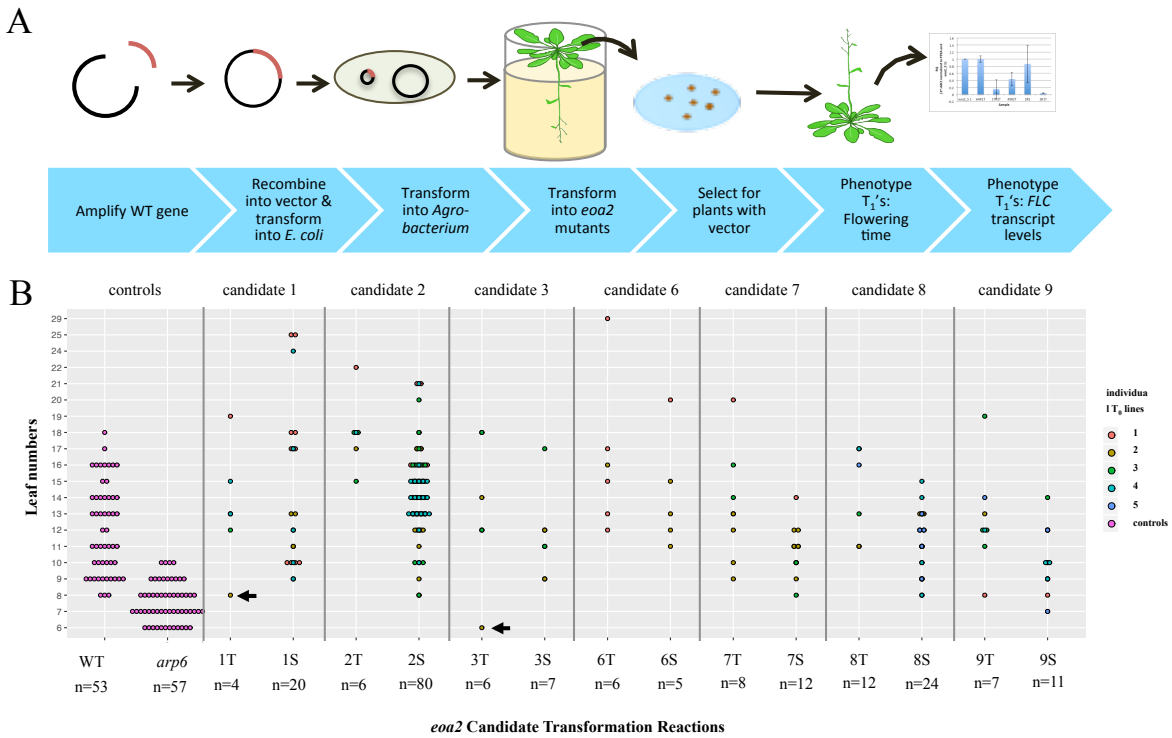

Figure 3.4. Phenotyping complementation transformations is inconclusive in identifying the causal *eoa2* mutation. (**A**) Diagram describing the workflow for generating and phenotyping the complementation transformants. (**B**) Dot plot displaying the number of rosette leaves individual plants had at the time of flowering for WT plants, *arp6* mutants, and either T_1 transformed individuals (T) or their untransformed siblings (S) from transformation reactions. Transformants include lines transformed with 7 different complementation constructs into *eoa2* mutants. The colors of the dots differentiate between up to 5 individual lines of either transformed (T) or untransformed siblings (S). Controls are represented by pink dots. Top candidates for complementation are indicated with arrows.

Figure 3.5

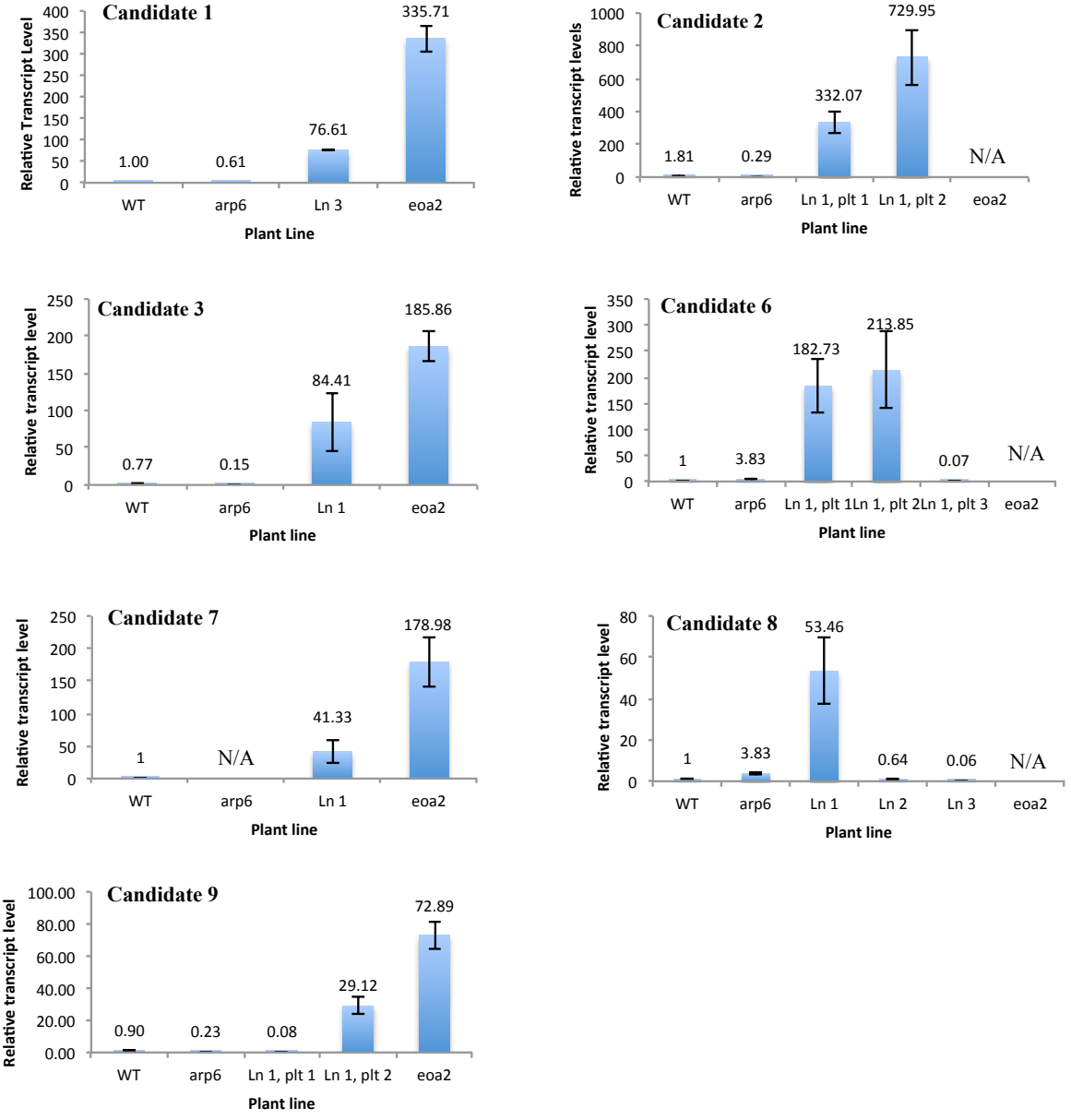

Figure 3.5. *FLC* levels were not rescued to *arp6*-like levels in *eoa2* complementation lines. Histograms show the relative transcript levels of *FLC* in WT relative to either *arp6* mutants, select *eoa2* lines transformed with the indicated candidate complementation construct, or an untransformed *eoa2* sibling. WT and *arp6* values for candidates 1, 2, 3, and 9 represent averages between two biological replicates while all other values represent individual plants. All transformed individuals are

T_1 except for candidates 2 and 3, which are based on T_2 individuals. Error bars show standard deviation for three technical replicates, or two biological replicates when applicable. N/A is indicated for plants that were missing from the analysis for technical reasons. Relative quantification of *FLC* was calculated relative to endogenous control *PP2A* using the $\Delta\Delta C_T$ method. (ln: line; plt: plant)

Figure 3.6

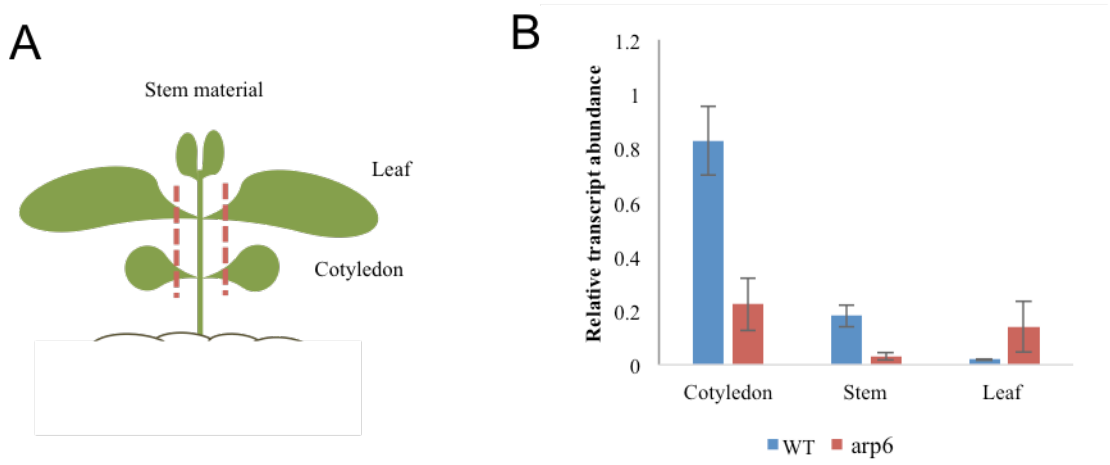

Figure 3.6. FLC shows tissue specific expression levels. (**A**) Diagram demonstrating the three seedling tissues that were tested for *FLC* transcript level differences. (**B**) Relative abundance of *FLC* transcript levels in cotyledon, stem and leaf tissue from WT plants and *arp6* mutants. *FLC* transcripts were quantified relative to *PP2A* transcript levels using the $\Delta\Delta C_T$ method.

Figure 3.7

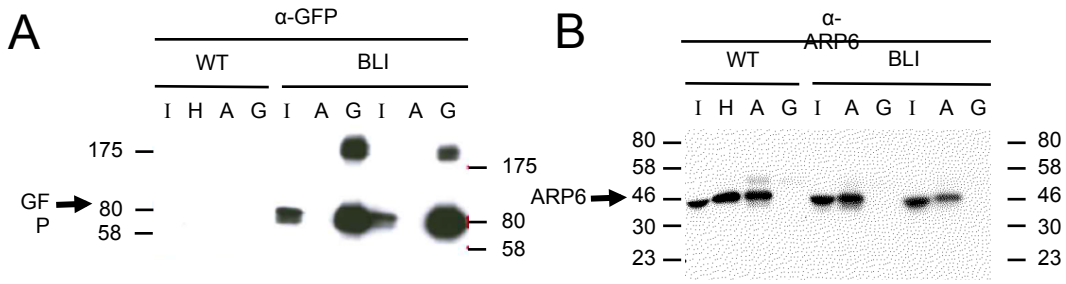

Figure 3.7. ARP6 and BLISTER do not physically interact. (**A**) Co-IP experiment visualized by a western blot with an anti-GFP antibody. Samples are indicated above the blot image as follows I – input material, H - H2A.Z IP, A – ARP6 IP, G – GFP IP. An arrow to the left indicates the GFP-sized band. (**B**) The same IP experiment blotted for anti-ARP6. An arrow to the left indicates ARP6-sized band.

Table 3.1. Top causal candidate *eoa2* mutations.

Cand. No.	Gene ID	Gene name	ΔAA	Cellular Localization	Function
1	AT3G23633	F-box associated ubiquitination effector family protein	Y/C	Unknown	Unknown
2	AT3G23980	BLI, BLISTER, KOLD SENSITIV 1, KOS1	E/K	Nucleus, golgi, cytosol	Regulates transcription, localizes with CURLY LEAF (CLF)
3	AT3G26010	Galactose oxidase/kelch repeat superfamily protein skp2-like	E/D; C/S	Nucleus	Unknown
4	AT3G26750	Ubiquitin-conjugating enzyme E2C-binding protein	L/V	Nucleus	Phosphatidylinositol biosynthetic process
5	AT3G26922	F-box/RNI-like superfamily protein	D/N	Nucleus	Unknown
6	AT3G27420	Unknown	T/S	Nucleus	Unknown
7	AT3G27500	Cysteine/Histidine-rich C1 domain family protein	R/L; F/Y	Nucleus	Signal transduction, oxidation-reduction process
8	AT3G27640	Transducin/WD40 repeat-like superfamily protein;	I/R	Nucleus	Nucleotide binding, Cul4- Ring E3 ubiquitin ligase
9	AT3G23610	DSPTP1, DUAL SPECIFICITY PROTEIN PHOSPHATASE 1	K/N	Nucleus, chloroplast, cytoplasm	Negative regulation of MAP kinase activity, De-phosphorylation

Table 3.1. Top causal candidate *eoa2* mutations. Candidate mutated genes from BC2F2 *eoa2* plants were identified by mapping-by-sequencing methods and top candidates were further selected based on criteria specified in Fig. 3.3. "Cand. No." signifies the designated candidate number we assigned to each gene. "Gene ID" shows the TAIR gene identifier, "Gene name" includes various names of the protein if characterized or other wise its associated protein family, "ΔAA" displays the non-synonymous one letter amino acid abbreviation to signify the amino acid changes caused by the identified SNP. The one to the left of the slash is the originally encoded amino acid and to the right is the new amino acid. " Cellular Localization" lists where the encoded protein is predicted to localize within the cell and "Function" lists any putative or confirmed functions associated with the factor.

Table 3.2 - Primers used for InFusion cloning of the candidate genes into the pCAMBIA Agrobacterium transformation vector

Rxn #	Gene ID/primer name	Primer sequence‡	bp	Tm	GC%	Q5 GS* Tm	Product size (bp)
9	At3g23610 Inf F	TCGAGCTCGGTACCCGGGAGAGTTTGTCCACACACAAA	38	118	55.3	62	4750
	At3g23610 Inf R2	CTCTAGAGGATCCCCGGGTTTGCCAATACACCTTTCCA	38	116	52.6		
1	At3g23633 Inf F	TCGAGCTCGGTACCCGGGTTTTAGGCCTTCGATTTTGG	38	118	55.3	61	4393
	At3g23633 Inf R	CTCTAGAGGATCCCCGGGGTGTAATCATTGGAGTTGGC	38	118	55.3		
2	At3g23980 Inf F	TCGAGCTCGGTACCCGGGTCCGTGCGGACAACAAAAT	37	118	59.5	63	7936
	At3g23980 InF R	CTCTAGAGGATCCCCGGGGCAACTGATTTGCATCCTTC	38	118	55.3		
3	At3g26010 Inf F	TCGAGCTCGGTACCCGGGCTGTGCATTTCTCTTTGTAAC	39	120	53.8	60	4765
	At3g26010 Inf R	CTCTAGAGGATCCCCGGGCACGATGTTCGTGCTTTGA	37	116	56.8		
4	At3g26750 Inf F	TCGAGCTCGGTACCCGGGAGGTGGAAGTGACGGTGA	36	118	63.9	64	5231
	At3g26750 Inf R	CTCTAGAGGATCCCCGGGGAGCATTACGTCGAGCTTC	37	118	59.5		
	At3g26750- 4 InF F2	TCGAGCTCGGTACCCGGGCATATCGATTTCGGCACAAT	38	118	55.3	61	5523
	At3g26750- 4 InF R2	CTCTAGAGGATCCCCGGGCGCTATGCTTGGTGGTGA	36	116	61.1		
5	At3g26922 Inf F	TCGAGCTCGGTACCCGGGGCTTTCGATGACAATGAAAC	38	118	55.3	60	4982
	At3g26922 Inf R	CTCTAGAGGATCCCCGGGACCCTCGATTCATTGTCAC	37	116	56.8		
	At3g26922- 5 InF F2	TCGAGCTCGGTACCCGGGCGTTTTGAAGGGGATTGAAA	38	118	55.3	61	4997
	At3g26922- 5 InF R2	CTCTAGAGGATCCCCGGGTTATAATCGCAGACGCATCG	38	118	55.3		
6	At3g27420 Inf F	TCGAGCTCGGTACCCGGGACGAGTTCACGAGCTGTTC	37	120	62.2	64	5401
	At3g27420 Inf R	CTCTAGAGGATCCCCGGGGCCAGGATAGACAAGCAAG	37	118	59.5		
7	At3g27500 Inf F	TCGAGCTCGGTACCCGGGTTTAACTACGATGGCCGGT	37	118	59.5	64	5600
	At3g27500 Inf R	CTCTAGAGGATCCCCGGGAACCCACGAGCAGAGTCC	36	118	63.9		
8	At3g27640 Inf F	TCGAGCTCGGTACCCGGGGGCTTCACGCCCCAATAA	36	118	63.9	63	6508
	At3g27640 Inf R	CTCTAGAGGATCCCCGGGACGTCCAAGAAACGAAGAAG	38	118	55.3		

‡The first 20 bases of the primer sequence consist of the InFusion cloning primer sequence followed by a gene specific portion
*Q5 GS Tm – Gene specific Tm calculated based on the Q5 polymerase parameters (https://tmcalculator.neb.com/#!/)

Table 3.3. Transformant qPCR methods and materials summary

Candidate	Plant	Date tissue was collected - age of plant (days post stratification)	No. of leaves at collection	Number of leaves at flowering	Genotyping		Primers	RNA isolation kit	RNA input amount * (ng)
					DNA isolation protocol	No. of PCR cycles			
1	26T1	7/6/16 – 14	4	8	SPRI beads	40	1.4 valid & pCAMBIAs	Specturm ™ Plant Total RNA Kit (Sigma)	416
2	49.4	2/8/16 – 17	?	10	Edwards buffer	30	2.3 valid & pCAMBIAs	RNeasy plant mini kit (QIAgen)	390
2	49.6	2/8/16 – 17	?	10	Edwards buffer	30	2.3 valid & pCAMBIAs	RNeasy plant mini kit (QIAgen)	390
3	80.1	4/4/16 – 10	4	18	Edwards buffer	30	3.3 valid & pCAMBIAs	RNeasy plant mini kit (QIAgen)	300
3	T2.2	?	?	?	?	?	3.3 valid & pCAMBIAs	Specturm ™ Plant Total RNA Kit (Sigma)	900
4	N/A	N/A	N/A	N/A	N/A	N/A	N/A	N/A	N/A
5	N/A	N/A	N/A	N/A	N/A	N/A	N/A	N/A	N/A
6	33.1	12/7/2015 - 21	8	14	Edwards buffer	35	pCAMBIAs & 6.1 valid	RNeasy plant mini kit (QIAgen)	**130
6	33.2	11/30/15 – 14	6	12	Edwards buffer	35	pCAMBIAs & 6.1 valid	RNeasy plant mini kit (QIAgen)	**130
6	33.3	12/12/15 – 26 (flowered on the 16th)	4 (tiny)	16	Edwards buffer	35	pCAMBIAs & 6.1 valid	RNeasy plant mini kit (QIAgen)	**130
7	271.4	4/4/16 – 10	4	9	Edwards buffer	30	pCAMBIAs & 7.4 valid	RNeasy plant mini kit (QIAgen)	300
8	219.1	12/12/2015-26	11 (tiny)	15	Edwards buffer	35	pCAMBIAs & 8.1 valid	RNeasy plant mini kit (QIAgen)	**130
8	36.1	11/30/2015 - 14	6	10	Edwards buffer	35	pCAMBIAs & 8.1 valid	RNeasy plant mini kit (QIAgen)	**130
8	183.1	12/7/2015-21	7 (small)	16	Edwards buffer	35	pCAMBIAs & 8.1 valid	RNeasy plant mini kit (QIAgen)	**130
9	6/7.1	7/15/16 – 23	4	12	SPRI beads	40	9.3 valid & pCAMBIAs	Specturm ™ Plant Total RNA Kit (Sigma)	540
9	6/7.2	7/11/16 – 19	6 (tiny)	11	SPRI beads	40	9.3 valid & pCAMBIAs	Specturm ™ Plant Total RNA Kit (Sigma)	540

*low amounts were collected so that we could have transcription data and leaf number data on the same plant. However, this means that the RNA input amounts were really low. The kit is supposed to work down to 1 pg of material.

** RNA amount was so low because some control samples were really low**.**

Table 3.4. Primers to confirm that Agrobacterium and Arabidopsis transformants have the correct insert. Used in combination with pCambia sense sequencing primer.

GeneID/primer name	Primer sequence	Primer length (bp)	Product length (bp)	Tm (°C)	GC%
At3g23633 confirm 1.4	TCCAACTTCATCAACCCACA	20	397	60	45
At3g23980 confirm 2.3	GCCCACCGTAAAAATCTTCAT	21	249		
At3g26010 confirm 3.3	CGTTACAAAGAGAAATGCACAGC	23	126	61	43
At3g27420 confirm 6.1	TTGAACAGCTCGTGAACTCG	20	125		
At3g27500 confirm 7.4	AAGATTGGCGTTCCAGCTTA	20	226	59	45
At3g27640 confirm 8.1	AAGAGGAAGGATCCGGTGAC	20	192	60	55
At3g23610 confirm 9.3	TGTCCACATTTTTGCACGAT	20	240	60	40

Literature Cited

Afgan E, Baker D, van den Beek M, Blankenberg D, Bouvier D, Cech M, Chilton J, Clements D, Coraor N, Eberhard C, Gruning B, Guerler A, Hillman-Jackson J, Von Kuster G, Rasche E, Soranzo N, Turaga N, Taylor J, Nekrutenko A, Goecks J (2016) The Galaxy platform for accessible, reproducible and collaborative biomedical analyses: 2016 update. Nucleic Acids Res 44: W3-W10

Allen RS, Nakasugi K, Doran RL, Millar AA, Waterhouse PM (2013) Facile mutant identification via a single parental backcross method and application of whole genome sequencing based mapping pipelines. Front Plant Sci 4: 362

Austin RS, Vidaurre D, Stamatiou G, Breit R, Provart NJ, Bonetta D, Zhang J, Fung P, Gong Y, Wang PW, McCourt P, Guttman DS (2011) Next-generation mapping of Arabidopsis genes. Plant J 67: 715-25

Austin RS, Chatfield SP, Desveaux D, Guttman DS (2014) Next-generation mapping of genetic mutations using bulk population sequencing. Methods Mol Biol 1062: 301-15

Choi K, Zhao X, Kelly KA, Venn O, Higgins JD, Yelina NE, Hardcastle TJ, Ziolkowski PA, Copenhaver GP, Franklin FC, McVean G, Henderson IR (2013) Arabidopsis meiotic crossover hot spots overlap with H2A.Z nucleosomes at gene promoters. Nat Genet 45: 1327-36

Clough SJ, Bent AF (1998) Floral dip: a simplified method for Agrobacterium-mediated transformation of Arabidopsis thaliana. Plant J 16: 735-43

Czechowski T, Stitt M, Altmann T, Udvardi MK, Scheible WR (2005) Genome-wide identification and testing of superior reference genes for transcript normalization in Arabidopsis. Plant Physiol 139: 5-17

Deal R, Topp CN, McKinney EC, Meagher RB (2007) Repression of Flowering in Arabidopsis Requires Activation of FLOWERING LOCUS C Expression by the Histone Variant H2A.Z. The Plant Cell Online 19: 74-83

Deal RB, Kandasamy MK, McKinney EC, Meagher RB (2005) The nuclear actin-related protein ARP6 is a pleiotropic developmental regulator required for the maintenance of FLOWERING LOCUS C expression and repression of flowering in Arabidopsis. Plant Cell 17: 2633-46

Etherington GJ, Monaghan J, Zipfel C, MacLean D (2014) Mapping mutations in plant genomes with the user-friendly web application CandiSNP. Plant Methods 10: 41

Farrona S, Hurtado L, March-Diaz R, Schmitz RJ, Florencio FJ, Turck F, Amasino RM, Reyes JC (2011) Brahma is required for proper expression of the floral repressor FLC in Arabidopsis. PLoS One 6: e17997

Gendrel AV, Lippman Z, Martienssen R, Colot V (2005) Profiling histone modification patterns in plants using genomic tiling microarrays. Nat Methods 2: 213-8

Hartwig B, James GV, Konrad K, Schneeberger K, Turck F (2012) Fast isogenic mapping-by-sequencing of ethyl methanesulfonate-induced mutant bulks. Plant Physiol 160: 591-600

Ietswaart R, Wu Z, Dean C (2012) Flowering time control: another window to the connection between antisense RNA and chromatin. Trends Genet 28: 445-53

Jiang W, Yang B, Weeks DP (2014) Efficient CRISPR/Cas9-mediated gene editing in Arabidopsis thaliana and inheritance of modified genes in the T2 and T3 generations. PLoS One 9: e99225

Jin C, Felsenfeld G (2007) Nucleosome stability mediated by histone variants H3.3 and H2A.Z. Genes Dev 21: 1519-29

Kleinmanns JA, Schatlowski N, Heckmann D, Schubert D (2017) BLISTER Regulates Polycomb-Target Genes, Represses Stress-Regulated Genes and Promotes Stress Responses in Arabidopsis thaliana. Front Plant Sci 8: 1530

Lazaro A, Gomez-Zambrano A, Lopez-Gonzalez L, Pineiro M, Jarillo JA (2008) Mutations in the Arabidopsis SWC6 gene, encoding a component of the SWR1 chromatin remodelling complex, accelerate flowering time and alter leaf and flower development. J Exp Bot 59: 653-66

Lee KM, Hayes JJ (1998) Linker DNA and H1-dependent reorganization of histone-DNA interactions within the nucleosome. Biochemistry 37: 8622-8

Li H, Durbin R (2009) Fast and accurate short read alignment with Burrows-Wheeler transform. Bioinformatics 25: 1754-60

Li H, Handsaker B, Wysoker A, Fennell T, Ruan J, Homer N, Marth G, Abecasis G, Durbin R, Genome Project Data Processing S (2009) The Sequence Alignment/Map format and SAMtools. Bioinformatics 25: 2078-9

Livak KJ, Schmittgen TD (2001) Analysis of relative gene expression data using real-time quantitative PCR and the 2(-Delta Delta C(T)) Method. Methods 25: 402-8

Marques M, Laflamme L, Gervais AL, Gaudreau L (2010) Reconciling the positive and negative roles of histone H2A.Z in gene transcription. Epigenetics 5: 267-72

Martin-Trillo M, Lazaro A, Poethig RS, Gomez-Mena C, Pineiro MA, Martinez-Zapater JM, Jarillo JA (2006) EARLY IN SHORT DAYS 1 (ESD1) encodes ACTIN-RELATED PROTEIN 6 (AtARP6), a putative component of chromatin remodelling complexes that positively regulates FLC accumulation in Arabidopsis. Development 133: 1241-52

Meneghini MD, Wu M, Madhani HD (2003) Conserved histone variant H2A.Z protects euchromatin from the ectopic spread of silent heterochromatin. Cell 112: 725-36

Merchant N, Lyons E, Goff S, Vaughn M, Ware D, Micklos D, Antin P (2016) The iPlant Collaborative: Cyberinfrastructure for Enabling Data to Discovery for the Life Sciences. PLoS Biol 14: e1002342

Michaels SD, Amasino RM (1999) FLOWERING LOCUS C Encodes a Novel MADS Domain Protein That Acts as a Repressor of Flowering. The Plant Cell Online 11: 949-956

Mizuguchi G, Shen X, Landry J, Wu WH, Sen S, Wu C (2004) ATP-driven exchange of histone H2AZ variant catalyzed by SWR1 chromatin remodeling complex. Science 303: 343-8

Mylne J, Greb T, Lister C, Dean C (2004) Epigenetic regulation in the control of flowering. Cold Spring Harb Symp Quant Biol 69: 457-64

Rosa M, Von Harder M, Cigliano RA, Schlogelhofer P, Scheid OM (2013) The Arabidopsis SWR1 Chromatin-Remodeling Complex Is Important for DNA Repair, Somatic Recombination, and Meiosis. Plant Cell

Schatlowski N, Stahl Y, Hohenstatt ML, Goodrich J, Schubert D (2010) The CURLY LEAF interacting protein BLISTER controls expression of polycomb-group target genes and cellular differentiation of Arabidopsis thaliana. Plant Cell 22: 2291-305

Schotta G, Ebert A, Dorn R, Reuter G (2003) Position-effect variegation and the genetic dissection of chromatin regulation in Drosophila. Seminars in Cell & Developmental Biology 14: 67-75

Sheldon CC, Conn AB, Dennis ES, Peacock WJ (2002) Different regulatory regions are required for the vernalization-induced repression of FLOWERING LOCUS C and for the epigenetic maintenance of repression. Plant Cell 14: 2527-37

Smith AP, Jain A, Deal RB, Nagarajan VK, Poling MD, Raghothama KG, Meagher RB (2010) Histone H2A.Z regulates the expression of several classes of phosphate starvation response genes but not as a transcriptional activator. Plant Physiol 152: 217-25

Sura W, Kabza M, Karlowski WM, Bieluszewski T, Kus-Slowinska M, Paweloszek L, Sadowski J, Ziolkowski PA (2017) Dual role of the histone variant H2A.Z in transcriptional regulation of stress-response genes. Plant Cell

Zuryn S, Le Gras S, Jamet K, Jarriault S (2010) A Strategy for Direct Mapping and Identification of Mutations by Whole-Genome Sequencing. Genetics 186: 427-430

CHAPTER 4: DISCUSSION – IMPLICATIONS AND FUTURE DIRECTIONS

The goal of my dissertation research was to understand mechanisms of how H2A.Z contributes to transcriptional regulation by understanding its interactions with other chromatin associating factors. Working toward this goal, I provided context for roles of H2A.Z in transcriptional regulation and nucleosome organization while generating numerous resources that will be helpful in future studies. I did this first by using molecular genomics tools to characterize the genetic interactions between H2A.Z and BRM (in the SWI2/SNF2 complex) and their roles in transcriptional regulation and nucleosomal organization (Chapter 2). I also conducted a mutant screen to identify factors that antagonize H2A.Z to promote transcription (Chapter 3). The sum of this work broadened our understanding of H2A.Z and factors that interact with H2A.Z to regulate transcription and chromatin organization. In this chapter, I discuss the implications of this work and several new hypotheses that followed.

Providing chromatin reference resources

Chromatin profiling studies are beginning to comprehensively document the chromatin environment surrounding different loci under different conditions, allowing us to define distinct chromatin states with specific functions (Sequeira-Mendes et al., 2014; Vergara and Gutierrez 2017). However, the chromatin states defined to date are still generalizations relative to the vast number of chromatin associating factors and histone modification combinations that exist across the genome (Han et al., 2015; Zhao and Garcia 2015; Vergara and Gutierrez 2017). The 34 genomic data sets (sequencing libraries) that were generated for this study will provide valuable reference resources as people continue to study H2A.Z, SWR1, BRM, SWI2/SNF2, or other factors that interact with them. By identifying genes that are direct targets of BRM and H2A.Z, I

provide an additional layer of information about regulatory factors acting at the targeted genes and regulating associated processes (Fig. 2.1-2.2).

Only 16% of the nucleosomes across the Arabidopsis genome are considered well-positioned, meaning that some loci are more suitable than others for evaluating changes in chromatin organization (Zhang et al., 2015). This work identified nucleosomes that have detectable changes in positioning or occupancy in either *brm-1* or *arp6-1* mutant backgrounds (Fig. 2.6, 2.9, 2.10). This provides a resource that describes the contributions of ARP6 and BRM that can also be integrated into future genomic studies that wish to incorporate the effects of ARP6 or BRM on nucleosome organization. These data sets will also help direct pilot studies that aim to measure nucleosome organization on a smaller, locus-specific scale in the future.

BRM and H2A.Z are not generally antagonistic to one another

These genomic data sets allowed us to test the hypothesis that H2A.Z normally antagonizes the transcriptionally repressive function of BRM based on a previously described genetic interaction between them at a specific locus (Farrona et al., 2011). My analysis demonstrated that H2A.Z and BRM are not generally antagonistic in transcriptional regulation or nucleosomal organization, but their roles break down into redundant, synergistic, and opposing-suppressive roles at different genes and in different nucleosomal contexts (Figure 2.1 and Fig. 2.6). For example, I found gene classes where both BRM and H2A.Z are needed individually as well as gene classes where BRM and H2A.Z incorporation function redundantly for gene activation or repression (Fig. 2.1). I also see gene classes where the role of either H2A.Z or BRM in chromatin antagonistically opposes the transcriptional promoting or repressing contribution of the other (Fig. 2.1).

Other studies have performed chromatin localization experiments and transcriptional profiling for either factor alone (Coleman-Derr and Zilberman 2012; Archacki et al., 2016; Sura et al., 2017). Yet we are the first to assess the overlap between components of the SWR1 and

SWI2/SNF2 chromatin remodeling complexes and their genetic interactions as evident through double mutant analyses. We are also the first to define the genomic effects of BRM depletion on nucleosome organization. For these analyses, I defined the direct effects of losing either H2A.Z-containing nucleosomes or BRM by describing chromatin changes that take place where either H2A.Z or BRM are localized in the genome (Fig. 2.6, Fig. 2.9). Then I assessed changes specifically at the transcription start sites of genes that are differentially expressed targets of BRM and H2A.Z (Fig. 2.11A). My approach determined the effects of either BRM or H2A.Z on nucleosome organization across the genome in a way that was a more direct and comprehensive measurement than approaches previously used to assess the genomic roles of H2A.Z in nucleosome organization (Sura et al., 2017). The genetic relationships and chromatin regulating roles of H2A.Z and BRM described by this work provide context for future studies that involve understanding how either factor interacts within the surrounding chromatin environment to contribute to transcriptional regulation.

Candidate eoa2 *mutations are potential H2A.Z antagonists*

To expand our knowledge about what factors make H2A.Z necessary for transcriptional activation, I conducted a forward genetic suppressor screen. Toward this goal, a mutant line (*eoa2)* was identified that suppressed the early flowering phenotype in *arp6* mutants. Additionally, I mapped mutations in this line that segregate with the suppressor phenotype after two backcrosses to the *arp6* parental line. Work to identify the mutated gene causing the *eoa2* suppressor phenotype in *arp6* mutant plants was ultimately inconclusive. However, The genes containing these potentially causal mutations now serve as a list of potential candidates that future studies can use to identify H2A.Z antagonists.

Potential for testing interactions with polycomb group proteins

Both the resources generated and the observations reported in this study will be useful for evaluating the interactions between BRM, H2A.Z and other chromatin factors. This work and that of many others has alluded to more context specific functions for both H2A.Z and BRM (Bönisch and Hake 2012; Han et al., 2015). In particular, I would be interested in assessing the roles that BRM and H2A.Z play in relation to the repressive Polycomb group (PcG) proteins. These include the proteins in the Polycomb repressive complex 1 (PRC1) and Polycomb repressive complex 2 (PRC2) which can modify histone tails and establish long-term transcriptional repression, especially for genes involved in stress response and development (Derkacheva and Hennig 2013; Molitor et al., 2016).

BRM is already known to antagonize the repressive function of PcG proteins (Wu et al., 2012; Li et al., 2015a; Li et al. 2016). Alternatively, H2A.Z and PcG proteins appear to have related functions in transcriptional repression (Molitor et al., 2016; Surface et al., 2016). In Arabidopsis, H2A.Z co-localizes with at least one PRC1 subunit and is needed for H3K27me3 by PRC2 at many genes (Carter et al., 2017; Molitor et al., 2016). Genomic data sets are publically available that define sites where loss of BRM influences tri-methylation of lysine 27 on histone H3 (H3K27me3), a mark that is applied by PRC2 (Li et al., 2015a). I would be interested in understanding whether BRM has more consistent roles relating to nucleosome organization and transcriptional regulation at loci that are targeted by PcG proteins and more specifically, at loci where H3K27me3 is perturbed in *brm* mutants. The data generated in this dissertation work could be used to test whether the presence or absence of H2A.Z at these sites contributes to any detectable differences in how BRM and PcG proteins interact. For example, loci that are repressed by the PRC2 complex and have H2A.Z containing nucleosomes at their transcription start sites may be more or less amenable to de-repression by BRM. By evaluating how BRM behaves in the presence of PcG proteins and H2A.Z, we may be able to define more specific roles for BRM in chromatin regulation and at the same time expand our understanding of PcG proteins and H2A.Z function. Since BRM is known to antagonize PcG protein function, further work to

understand their interaction has potential for understanding transcriptional memory of stress exposure and understanding plant plasticity during development in response to environmental stimuli (Brzezinka et al., 2016; Derkacheva and Hennig 2013).

Defense response mutations

In addition to providing context for how H2A.Z and the SWR1 complex interact with other chromatin associating factors, I also discovered some information that has implications for studying different subunits of the SWR1 complex. One study suggested that different SWR1 subunits have non-overlapping functions (Berriri et al., 2016). They showed that *arp6* mutants display increased disease resistance to bacterial infection while mutants for other SWR1 subunits (PIE1, SWC6) present more susceptibility to infection (Berriri et al., 2016). ARP6 and other SWR1 subunits also play important roles in maintaining genome integrity (Rosa et al., 2013). While evaluating nucleosome occupancy in *arp6* mutants, I identified many large deleted regions that have accumulated in the *arp6* mutant background (Fig. 2.7). Consequently, one explanation for why *arp6* mutants might present different phenotypes from the other SWR1-C subunits would be that background mutations arising in this line might make *arp6* mutants more resistant to infection.

I used GeneCodis to perform a Gene Ontology (GO) enrichment analysis (Carmona-Saez et al. 2007; Nogales-Cadenas et al., 2009; Tabas-Madrid et al., 2012; Tian et al., 2017) on genes that were annotated by PeakAnnotator software (Salmon-Divon et al., 2010) as overlapping with the deleted regions (1,654 genes) and are differentially expressed in *arp6* mutants but are not targeted by H2A.Z (1,189 genes). I specifically excluded H2A.Z targeted genes to focus the analysis on genes whose transcriptional change was more likely due to the deletion overlapping the gene than losing H2A.Z incorporation at that locus. The analysis revealed that this gene set (52 genes) is enriched for genes involved in defense response (6 genes), although they are mostly uncharacterized genes (Table 4.1). Still, additional genes affected by the deletions that are

targeted by H2A.Z or deletions in promoters and other regulatory regions near a gene involved in defense response could further impact the susceptibility of *arp6* mutants to infection. This further supports the hypothesis that the extra load of mutations in *arp6* mutants could potentially explain the increased resistance to infection observed for *arp6* mutants.

We could further test this hypothesis by generating new lines to knock down *ARP6* with RNAi or creating deletion mutations with CRISPR/Cas9 in WT plants. Then we could measure whether the line that was newly depleted of ARP6 function would present the same degree of resistance to bacterial infection as what is seen for mutants where the *arp6-1* mutation has persisted for generations. This would allow us to test whether secondary genomic disarray in SWR1-C mutants could explains some of the phenotypic variability between the mutants for different SWR1-C subunits (Berriri et al., 2016). If we do see such a difference between new mutations and continuously maintained mutant lines, then this would suggest a need for beginning mutant studies of SWR1 components and other chromatin regulating proteins from plants with a WT background. This would mean the chromatin field should consider shifting to using mutants that were backcrossed to WT plants, lines where the factor of interest is knocked down by RNAi, or by generating new CRISPER-mutated lines to avoid studying the cascade of effects that come from perturbing chromatin regulation.

Hypocotyl elongation phenotypes may indicate functional links to genetic interactions

In my work to uncover the chromatin context in which BRM and H2A.Z interact, I identified that both are enriched at genes regulated by light-responsive transcription factors PIF4, PIF5, and FRS9 (Fig. 2.13-2.15). This finding is consistent with my observation that both factors regulate genes involved in response to light stimuli (Fig. 2.2). Photomorphogenic phenotypes have been reported individually for mutants of ARP6 and BRM as well as PIF4, PIF5, and FRS9 transcription factors, which are enriched at H2A.Z and BRM regulated genes (Lin and Wang 2004; Pedmale et al., 2016; Lee and Seo 2017; Zhang et al., 2017a).

Many factors regulate hypocotyl elongation in response to variations in light wavelengths to allow plants to adjust their position and optimize their growth conditions (Cole et al., 2011). FRS9 promotes hypocotyl elongation selectively in response to red light, but not white or blue light (Fig. 4.1A-B; Lin and Wang 2004), while PIF4 and PIF5 promote hypocotyl elongation especially in response to low blue light conditions as part of the shade avoidance response (Fig. 4.1A-B; Pedmale et al., 2016). We also already know that BRM promotes hypocotyl elongation in response to all light types and especially far-red wavelengths (Fig. 4.1A-B; Zhang et al., 2017a). By contrast, ARP6 represses hypocotyl elongation in response to white light (Fig. 4.1A; Lee and Seo 2017).

Although, *arp6* mutants and *brm* mutants present opposite hypocotyl growth phenotypes relative to WT plants, we have not yet evaluated how hypocotyl elongation is impacted in *arp6;brm* double mutants in response to light. By measuring hypocotyl length of the *arp6;brm* double mutants in white light, we could test whether H2A.Z or BRM is epistatic or suppressive to the other in this process (Fig. 4.1A). This would allow us to determine whether they interact to contribute to hypocotyl elongation in response to light (Fig. 4.1C-D).

Growing seedlings elongate their hypocotyls in response to low blue light or high red light and other stimuli as a part of the shade-avoidance response to seek out better quality light sources (Ballare 1999). We currently do not know whether ARP6 regulates hypocotyl elongation in response to specific variations in light source, nor whether loss of ARP6 function would suppress the need for BRM to respond to particular light stimuli. By testing how either single *arp6* mutants or the *arp6;brm* double mutants respond specifically to red light waves compared to white light conditions, we could also further assess whether ARP6 regulates responses to specific light conditions and whether ARP6 functions epistatic to BRM or suppresses BRM phenotypes to regulate responses to different light sources (Fig. 4.1B). Additionally, FRS9 and PIF TFs show specific contributions to hypocotyl elongation in response to different light wavelengths (Fig. 4.1A-B; Lin and Wang 2004; Pedmale et al., 2016). If we observe light source-specific hypocotyl

elongation phenotypes similar to PIF4/PIF5 or FRS9, this could provide a functional link between the chromatin remodeling proteins and the related transcription factors.

BRM, H2A.Z, and PIF4 may regulate nuclear localization in response to light

Another recent study showed that several light-regulated loci are targeted to the nuclear periphery in response to light stimuli where they are transcriptionally activated (Feng et al., 2014). More specifically, at least one of these loci requires PIF4 for proper localization to the nuclear interior in the dark (Feng et al., 2014). Of the 6 loci that were identified, all of them are targeted by H2A.Z (4 genes), BRM (4 genes), PIF4 (4 genes), or a combination of the three (Table 4.2). Two of these were also transcriptionally down regulated in *brm* mutants. Other studies have suggested that the SWI2/SNF2 complex is important for large scale chromatin organization within the nucleus (Imbalzano et al., 2013; Jegu et al., 2014). Also, H2A.Z and SWR1 are involved in reactivation of loci that have been localized to the nuclear periphery in yeast, and in Arabidopsis they associate with nuclear matrix proteins (Light et al., 2010; Lee and Seo 2017). This leads us to hypothesize that the role of H2A.Z, BRM, and PIF4 at these genes may be necessary for proper targeting of the loci within the nucleus in response to different light conditions (Fig. 4.2). It would be interesting to test whether *brm* mutants or *arp6* mutants depleted of H2A.Z-containing nucleosomes disrupt light-dependent nuclear localization or transcriptional regulation of the genes defined by Feng et al., (2014) in different light conditions. Such an experiment has potential for linking the roles of H2A.Z/ARP6 and BRM within individual chromatin fibers to their functions in the greater nuclear environment.

The genes described in the previous study were targets of H2A.Z but were not DE in *arp6* mutants where H2A.Z was lost (Feng et al., 2014). One explanation for the role of H2A.Z at those targeted genes is that H2A.Z is important for localization of the locus within the nucleus to allow other factors to properly regulate transcription and nuclear organization of a gene under specific conditions (Fig. 4.2). My work to identify genes directly targeted by H2A.Z establishes a

foundational data set that can be used for future studies to explore the role of H2A.Z in plants to target genes to the nuclear periphery. Future work to test whether the H2A.Z target genes I defined are associated with the nuclear periphery under different environmental conditions would provide information about contextual changes that take place in the nucleus in response to different stimuli.

Similarly in this dissertation research, there were many BRM-targeted genes that were not DE in *brm* mutants. Other studies have suggested that the SWI2/SNF2 complex can disrupt gene loops along with regulating gene transcription (Jegu et al., 2014). Also, chromatin enriched for polycomb-repressed genes are enriched at the nuclear periphery, leading to the hypothesis that anchoring regions targeted by the PRC2 to the nuclear periphery contributes to distal chromatin interactions (Bi et al., 2017; Barneche and Baroux 2017). The role of BRM to destabilize nucleosomes at flanking regions where it binds may antagonize PcG function to result in loop disruption. Future studies that look at the role of BRM relative to gene looping and PcG protein function can use my nucleosome organization data to understand whether BRM dependent nucleosome organization corresponds with different gene loops or with repression and localization by the PcG proteins.

Implications for translational applications

The work accomplished in this dissertation research focused on the basic roles of H2A.Z/ARP6 and BRM within the nucleus. However, my findings have potential to inform translational work in medicine and agriculture as well. Both BRM and H2A.Z are important for regulating developmental and stress response genes and their associated processes (Fig 2.2; Archacki et al., 2016; Coleman-Derr and Zilberman 2012). I was able to contribute to our mechanistic understanding of factors that moderate transcription of stress response genes by evaluating their contributions to nucleosome organization and identifying other transcription factors that may interact to contribute to light-responses (Chapter 2). Flowering is a

developmental process that is responsive to the environmental conditions such as temperature and light (Srikanth and Schmid 2011). Therefore, any H2A.Z antagonists acting at *FLC* may also make the contribution of H2A.Z necessary for expression of other light or temperature responsive genes. We also observed the *eoa2* mutants that were generated exhibiting greater resistance to drought compared to WT or *arp6* plants. Therefore, work to identify the *eoa2* mutation responsible for the more drought resistant phenotype would be beneficial for understanding related processes with potential for cultivating more drought resistant crop plants. Although my work will not be immediately translated to agricultural applications, it contributes to our understanding of how important development and stress response processes are regulated at the chromatin level.

Even though plant and animal systems differ, Arabidopsis contains orthologs for ~70% of genes linked to human cancers (Jones et al., 2008; Xu and Moller 2011). H2A.Z and SWI2/SNF2 human orthologs are misregulated in many types of cancers and behave as oncogenes (Zink and Hake 2016; Hodges et al., 2016). There are mutations SWI2/SNF2 subunit homologs in ~20% of all human cancer types (Kadoch et al., 2013; Hodges et al., 2016). H2A.Z over-expression correlates with poor prognosis in breast, liver, and skin cancers, while low levels of H2A.Z expression promotes genome instability and has pathological repercussions (Hua et al., 2008; Rangasamy 2010; Vardabasso et al., 2015; Yang et al., 2016). Regulating the cellular levels of H2A.Z and BRM orthologs in human cancer cells has therefore been proposed as cancer therapeutic options (Wu et al., 2017; Rangasamy 2010). This research to understand transcriptional regulation and nucleosomal organization by H2A.Z and interacting proteins such as BRM in Arabidopsis provides context for future studies to understand mechanisms relating to agricultural advances in crop plants and treatments for human diseases.

Figure 4.1

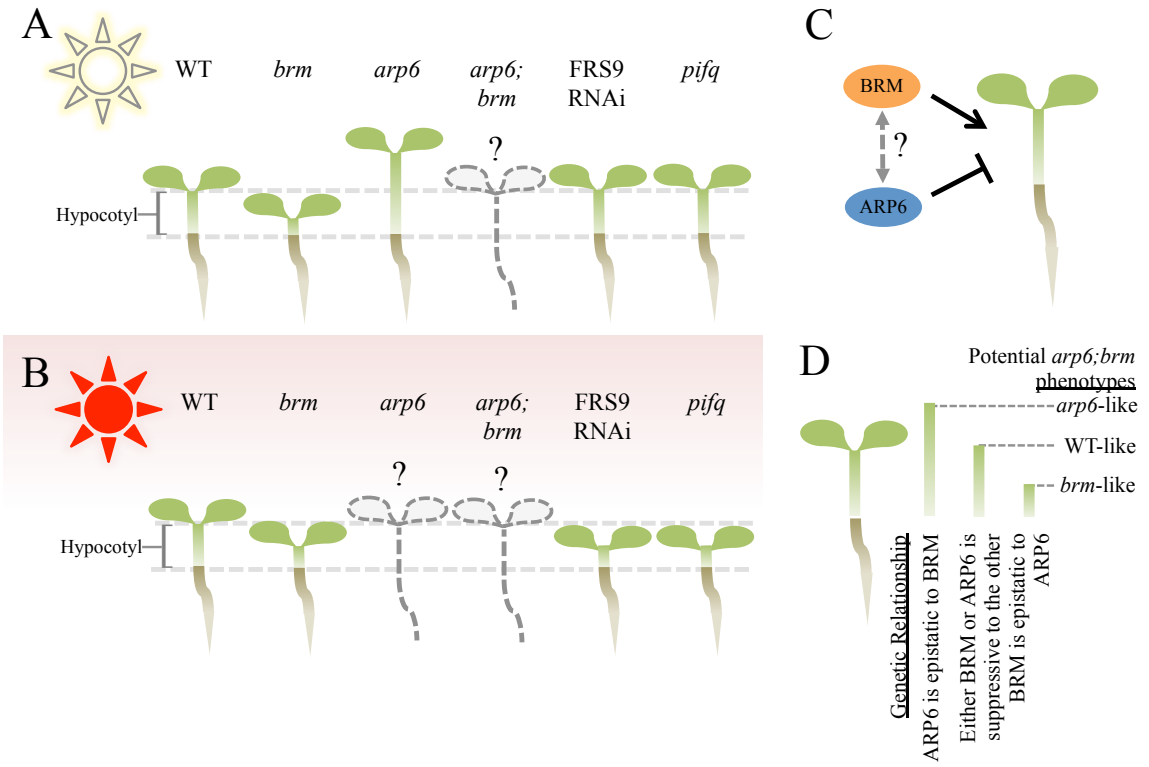

Fig. 4.1. Hypocotyl elongation phenotypes may indicate a physiological link between ARP6 and BRM function. (**A**) Diagram summarizing hypocotyl elongation phenotypes observed for *brm* mutants, *arp6* mutants, FRS9 RNAi lines, *pif1/3/4/5* quadruple mutants (*pifq*). Dark grey dotted lines represent *arp6;brm* double mutants since we do not know how hypocotyl elongation is effected in the double mutant. Light grey dashed lines represent the length of WT hypocotyls in normal white light conditions. (**B**) Diagram summarizing how red light affects hypocotyl elongation phenotypes for the same genetic backgrounds in A, with dark grey dotted lines representing the absence of information about *arp6* mutants or *arp6;brm* mutants. Light grey dashed lines represent the length of WT hypocotyls in normal white light conditions. (**C**) Schematic showing the current roles of ARP6 and BRM in hypocotyl elongation and the unknown genetic relationship between how ARP6 and BRM interact to regulate hypocotyl

elongation. (**D**) Green lines represent potential hypocotyl length phenotypes we may observe for *arp6;brm* double mutants. The corresponding genetic relationship between ARP6 and BRM mutants that would be indicated by these potential phenotypes is listed below.

Figure 4.2

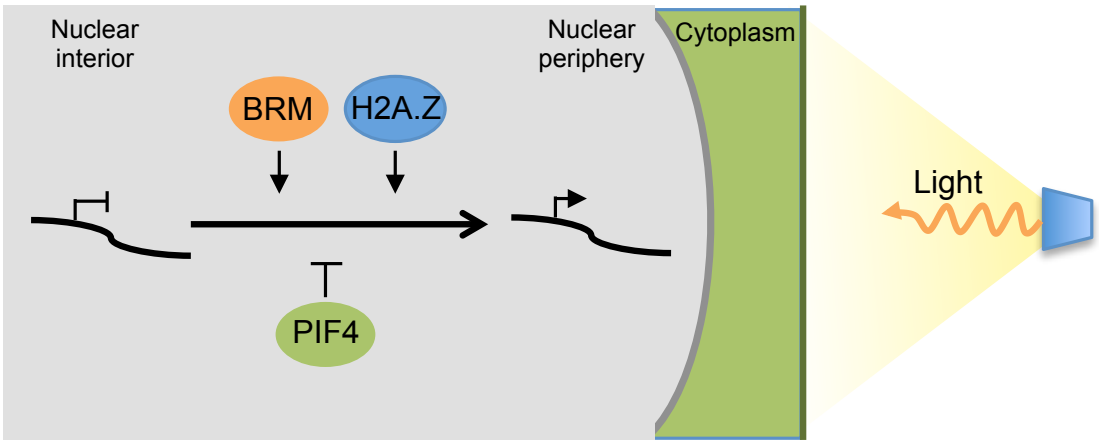

Figure 4.2. BRM and H2A.Z may contribute to nuclear localization of light-responsive genes together with PIF4 for their transcriptional activation. Feng et al. 2014 showed that PIF transcription factors oppose the movement of certain light responsive genes to the nuclear periphery during their transcriptional activation. In our data and other publically available data sets, we find that BRM, H2A.Z and PIF4 target the 6 genes that demonstrated this phenomenon. H2A.Z is involved in nuclear targeting of loci to the nuclear periphery in other organisms and at least one of the BRM targeted genes showed transcriptional down-regulated in our data. Future work to determine whether BRM and H2A.Z interact during nuclear localization of light-responsive genes could further our understanding of their roles in large-scale chromatin organization in the nucleus.

Table 4.1 – Disease resistance genes potentially impacted by deletions in *arp6* mutants.	
Gene ID	Protein name
AT1G15890	Disease resistance protein (CC-NBS-LRR class) family
AT5G47260	Probable disease resistance protein
AT5G43740	Disease resistance protein (CC-NBS-LRR class) family
AT2G15130	Plant basic secretory protein (BSP) family protein
AT5G36930	Disease resistance protein (TIR-NBS-LRR class) family
AT5G45510	Leucine-rich repeat (LRR) family protein

Table 4.1. Disease resistance genes potentially impacted by deletions in *arp6* mutants. Table summarizes the defense response genes that contain deletions in *arp6* mutants and are DE in *arp6* mutants even though they are not targeted by H2A.Z.

Table 4.2 - Genes with light responsive nuclear positioning are targeted by PIF4, H2A.Z, and BRM						
Gene	Gene ID	H2A.Z target	DE in *arp6*	BRM target	DE in *brm*	PIF4 target
CAB1*	At1g29930	X		X		X
CAB2*	At1g29920	X				
CAB3*	At1g29910	X				
GUN5	At5g13630	X		X	-	X
Plastocyanin 1	At1g76100	X		X		X
RBCS1A	At1G67090			X	-	X

Table 4.2. Genes with light responsive nuclear re-positioning are targeted by PIF4, H2A.Z, and BRM. Genes listed are those described by Feng, et al., (2014) as localizing to the nuclear interior in dark conditions until they are activated and repositioned to the nuclear periphery in light conditions. The table summarizes how the genes from my work that are either differentially expressed (DE) in *arp6* or *brm* mutants or that are targets of H2A.Z, BRM or PIF4 relate to their findings. X's and blank fields indicate that the described gene do and do not meet the criteria described in the column name above, respectively. "-" is used to indicate genes that are down-regulated in the tested mutant background. * indicates genes were dependent on PIF4 for nuclear localization to the interior in dark conditions (Feng et al., 2014).

Literature Cited

Abyzov A, Urban AE, Snyder M, Gerstein M (2011) CNVnator: an approach to discover, genotype, and characterize typical and atypical CNVs from family and population genome sequencing. Genome Res 21: 974-84

Afgan E, Baker D, van den Beek M, Blankenberg D, Bouvier D, Cech M, Chilton J, Clements D, Coraor N, Eberhard C, Gruning B, Guerler A, Hillman-Jackson J, Von Kuster G, Rasche E, Soranzo N, Turaga N, Taylor J, Nekrutenko A, Goecks J (2016) The Galaxy platform for accessible, reproducible and collaborative biomedical analyses: 2016 update. Nucleic Acids Res 44: W3-W10

Alazem M, Lin NS (2015) Roles of plant hormones in the regulation of host-virus interactions. Mol Plant Pathol 16: 529-40

Allan J, Fraser RM, Owen-Hughes T, Keszenman-Pereyra D (2012) Micrococcal nuclease does not substantially bias nucleosome mapping. J Mol Biol 417: 152-64

Allen RS, Nakasugi K, Doran RL, Millar AA, Waterhouse PM (2013) Facile mutant identification via a single parental backcross method and application of whole genome sequencing based mapping pipelines. Front Plant Sci 4: 362

Anders S, Pyl PT, Huber W (2015) HTSeq--a Python framework to work with high-throughput sequencing data. Bioinformatics 31: 166-9

Arabidopsis Genome I (2000) Analysis of the genome sequence of the flowering plant Arabidopsis thaliana. Nature 408: 796-815

Archacki R, Buszewicz D, Sarnowski TJ, Sarnowska E, Rolicka AT, Tohge T, Fernie AR, Jikumaru Y, Kotlinski M, Iwanicka-Nowicka R, Kalisiak K, Patryn J, Halibart-Puzio J, Kamiya Y, Davis SJ, Koblowska MK, Jerzmanowski A (2013) BRAHMA ATPase of the SWI/SNF Chromatin Remodeling Complex Acts as a Positive Regulator of Gibberellin-Mediated Responses in Arabidopsis. PLoS One 8: e58588

Archacki R, Yatusevich R, Buszewicz D, Krzyczmonik K, Patryn J, Iwanicka-Nowicka R, Biecek P, Wilczynski B, Koblowska M, Jerzmanowski A, Swiezewski S (2016) Arabidopsis SWI/SNF chromatin remodeling complex binds both promoters and terminators to regulate gene expression. Nucleic Acids Res

Austin RS, Vidaurre D, Stamatiou G, Breit R, Provart NJ, Bonetta D, Zhang J, Fung P, Gong Y, Wang PW, McCourt P, Guttman DS (2011) Next-generation mapping of Arabidopsis genes. Plant J 67: 715-25

Austin RS, Chatfield SP, Desveaux D, Guttman DS (2014) Next-generation mapping of genetic mutations using bulk population sequencing. Methods Mol Biol 1062: 301-15

Bailey TL, Boden M, Buske FA, Frith M, Grant CE, Clementi L, Ren J, Li WW, Noble WS (2009) MEME SUITE: tools for motif discovery and searching. Nucleic Acids Res 37: W202-8

Ballare CL (1999) Keeping up with the neighbours: phytochrome sensing and other signalling mechanisms. Trends Plant Sci 4: 97-102

Barah P, B NM, Jayavelu ND, Sowdhamini R, Shameer K, Bones AM (2016) Transcriptional regulatory networks in Arabidopsis thaliana during single and combined stresses. Nucleic Acids Res 44: 3147-64

Barneche F, Baroux C (2017) Unreeling the chromatin thread: a genomic perspective on organization around the periphery of the Arabidopsis nucleus. Genome Biol 18: 97

Bazett-Jones DP, Cote J, Landel CC, Peterson CL, Workman JL (1999) The SWI/SNF complex creates loop domains in DNA and polynucleosome arrays and can disrupt DNA-histone contacts within these domains. Mol Cell Biol 19: 1470-8

Becker JS, Nicetto D, Zaret KS (2016) H3K9me3-Dependent Heterochromatin: Barrier to Cell Fate Changes. Trends Genet 32: 29-41

Berger SL (2007) The complex language of chromatin regulation during transcription. Nature 447: 407-12

Berriri S, Gangappa SN, Kumar SV (2016) SWR1 Chromatin-Remodeling Complex Subunits and H2A.Z Have Non-overlapping Functions in Immunity and Gene Regulation in Arabidopsis. Mol Plant 9: 1051-65

Bevan M, Walsh S (2005) The Arabidopsis genome: a foundation for plant research. Genome Res 15: 1632-42

Bezhani S, Winter C, Hershman S, Wagner JD, Kennedy JF, Kwon CS, Pfluger J, Su Y, Wagner D (2007) Unique, shared, and redundant roles for the Arabidopsis SWI/SNF chromatin remodeling ATPases BRAHMA and SPLAYED. Plant Cell 19: 403-16

Bi X, Cheng YJ, Hu B, Ma X, Wu R, Wang JW, Liu C (2017) Nonrandom domain organization of the Arabidopsis genome at the nuclear periphery. Genome Res 27: 1162-1173

Bieluszewski T, Galganski L, Sura W, Bieluszewska A, Abram M, Ludwikow A, Ziolkowski PA, Sadowski J (2015) AtEAF1 is a potential platform protein for Arabidopsis NuA4 acetyltransferase complex. BMC Plant Biol 15: 75

Blower MD, Karpen GH (2001) The role of Drosophila CID in kinetochore formation, cell-cycle progression and heterochromatin interactions. Nat Cell Biol 3: 730-9

Bonisch C, Hake SB (2012) Histone H2A variants in nucleosomes and chromatin: more or less stable? Nucleic Acids Res 40: 10719-41

Bönisch C, Hake SB (2012) Histone H2A variants in nucleosomes and chromatin: more or less stable? Nucleic Acids Research 40: 10719-10741

Bourbousse C, Mestiri I, Zabulon G, Bourge M, Formiggini F, Koini MA, Brown SC, Fransz P, Bowler C, Barneche F (2015) Light signaling controls nuclear architecture reorganization during seedling establishment. Proc Natl Acad Sci U S A 112: E2836-44

Boyes DC, Zayed AM, Ascenzi R, McCaskill AJ, Hoffman NE, Davis KR, Gorlach J (2001) Growth stage-based phenotypic analysis of Arabidopsis: a model for high throughput functional genomics in plants. Plant Cell 13: 1499-510

Brzezinka K, Altmann S, Czesnick H, Nicolas P, Gorka M, Benke E, Kabelitz T, Jahne F, Graf A, Kappel C, Baurle I (2016) Arabidopsis FORGETTER1 mediates stress-induced chromatin memory through nucleosome remodeling. Elife 5:

Burton DR, Butler MJ, Hyde JE, Phillips D, Skidmore CJ, Walker IO (1978) The interaction of core histones with DNA: equilibrium binding studies. Nucleic Acids Res 5: 3643-63

Buszewicz D, Archacki R, Palusinski A, Kotlinski M, Fogtman A, Iwanicka-Nowicka R, Sosnowska K, Kucinski J, Pupel P, Oledzki J, Dadlez M, Misicka A, Jerzmanowski A, Koblowska MK (2016) HD2C histone deacetylase and a SWI/SNF chromatin remodeling complex interact and both are involved in mediating the heat stress response in Arabidopsis. Plant Cell Environ

Carmona-Saez P, Chagoyen M, Tirado F, Carazo JM, Pascual-Montano A (2007) GENECODIS: a web-based tool for finding significant concurrent annotations in gene lists. Genome Biol 8: R3

Carter B, Bishop B, Ho KK, Li H, Overway E, Dugard C, Huang R, Jia W, Zhang H, Carpita N, Pascuzzi P, Deal R, Ogas J (2017) The Chromatin Remodelers PKL and PIE1 Act in an Epigenetic Pathway that Determines H3K27me3 Homeostasis in Arabidopsis. In revision at Plant Cell.

Catala R, Medina J, Salinas J (2011) Integration of low temperature and light signaling during cold acclimation response in Arabidopsis. Proc Natl Acad Sci U S A 108: 16475-80

Chatterjee N, Sinha D, Lemma-Dechassa M, Tan S, Shogren-Knaak MA, Bartholomew B (2011) Histone H3 tail acetylation modulates ATP-dependent remodeling through multiple mechanisms. Nucleic Acids Res 39: 8378-91

Chen K, Xi Y, Pan X, Li Z, Kaestner K, Tyler J, Dent S, He X, Li W (2013) DANPOS: dynamic analysis of nucleosome position and occupancy by sequencing. Genome Res 23: 341-51

Choi K, Park C, Lee J, Oh M, Noh B, Lee I (2007) Arabidopsis homologs of components of the SWR1 complex regulate flowering and plant development. Development 134: 1931-41

Choi K, Zhao X, Kelly KA, Venn O, Higgins JD, Yelina NE, Hardcastle TJ, Ziolkowski PA, Copenhaver GP, Franklin FC, McVean G, Henderson IR (2013) Arabidopsis meiotic crossover hot spots overlap with H2A.Z nucleosomes at gene promoters. Nat Genet 45: 1327-36

Clapier CR, Iwasa J, Cairns BR, Peterson CL (2017) Mechanisms of action and regulation of ATP-dependent chromatin-remodelling complexes. Nat Rev Mol Cell Biol 18: 407-422

Clarkson MJ, Wells JR, Gibson F, Saint R, Tremethick DJ (1999) Regions of variant histone His2AvD required for Drosophila development. Nature 399: 694-7

Clough SJ, Bent AF (1998) Floral dip: a simplified method for Agrobacterium-mediated transformation of Arabidopsis thaliana. Plant J 16: 735-43

Cole B, Kay SA, Chory J (2011) Automated analysis of hypocotyl growth dynamics during shade avoidance in Arabidopsis. Plant J 65: 991-1000

Coleman-Derr D, Zilberman D (2012) Deposition of histone variant H2A.Z within gene bodies regulates responsive genes. PLoS Genet 8: e1002988

Cortijo S, Charoensawan V, Brestovitsky A, Buning R, Ravarani C, Rhodes D, van Noort J, Jaeger KE, Wigge PA (2017) Transcriptional regulation of the ambient temperature response by H2A.Z-nucleosomes and HSF1 transcription factors in Arabidopsis. Mol Plant

Czechowski T, Stitt M, Altmann T, Udvardi MK, Scheible WR (2005) Genome-wide identification and testing of superior reference genes for transcript normalization in Arabidopsis. Plant Physiol 139: 5-17

Dai X, Bai Y, Zhao L, Dou X, Liu Y, Wang L, Li Y, Li W, Hui Y, Huang X, Wang Z, Qin Y (2017) H2A.Z Represses Gene Expression by Modulating Promoter Nucleosome Structure and Enhancer Histone Modifications in Arabidopsis. Mol Plant 10: 1274-1292

Dalvai M, Bellucci L, Fleury L, Lavigne AC, Moutahir F, Bystricky K (2012) H2A.Z-dependent crosstalk between enhancer and promoter regulates Cyclin D1 expression. Oncogene

Davie JR, Xu W, Delcuve GP (2016) Histone H3K4 trimethylation: dynamic interplay with pre-mRNA splicing. Biochem Cell Biol 94: 1-11

de Lucas M, Prat S (2014) PIFs get BRright: PHYTOCHROME INTERACTING FACTORs as integrators of light and hormonal signals. New Phytol 202: 1126-41

Deal R, Topp CN, McKinney EC, Meagher RB (2007) Repression of Flowering in Arabidopsis Requires Activation of FLOWERING LOCUS C Expression by the Histone Variant H2A.Z. The Plant Cell Online 19: 74-83

Deal RB, Kandasamy MK, McKinney EC, Meagher RB (2005) The nuclear actin-related protein ARP6 is a pleiotropic developmental regulator required for the maintenance of FLOWERING LOCUS C expression and repression of flowering in Arabidopsis. Plant Cell 17: 2633-46

Derkacheva M, Hennig L (2013) Variations on a theme: Polycomb group proteins in plants. J Exp Bot

Dhar S, Gursoy-Yuzugullu O, Parasuram R, Price BD (2017) The tale of a tail: histone H4 acetylation and the repair of DNA breaks. Philos Trans R Soc Lond B Biol Sci 372:

Dion MF, Altschuler SJ, Wu LF, Rando OJ (2005) Genomic characterization reveals a simple histone H4 acetylation code. Proc Natl Acad Sci U S A 102: 5501-6

Efroni I, Han SK, Kim HJ, Wu MF, Steiner E, Birnbaum KD, Hong JC, Eshed Y, Wagner D (2013) Regulation of leaf maturation by chromatin-mediated modulation of cytokinin responses. Dev Cell 24: 438-45

Eirin-Lopez JM, Gonzalez-Romero R, Dryhurst D, Ishibashi T, Ausio J (2009) The evolutionary differentiation of two histone H2A.Z variants in chordates (H2A.Z-1 and H2A.Z-2) is mediated by a stepwise mutation process that affects three amino acid residues. BMC Evol Biol 9: 31

Endoh M, Endo TA, Endoh T, Isono K, Sharif J, Ohara O, Toyoda T, Ito T, Eskeland R, Bickmore WA, Vidal M, Bernstein BE, Koseki H (2012) Histone H2A mono-

ubiquitination is a crucial step to mediate PRC1-dependent repression of developmental genes to maintain ES cell identity. PLoS Genet 8: e1002774

Engreitz JM, Ollikainen N, Guttman M (2016) Long non-coding RNAs: spatial amplifiers that control nuclear structure and gene expression. Nat Rev Mol Cell Biol 17: 756-770

Etherington GJ, Monaghan J, Zipfel C, MacLean D (2014) Mapping mutations in plant genomes with the user-friendly web application CandiSNP. Plant Methods 10: 41

Euskirchen GM, Auerbach RK, Davidov E, Gianoulis TA, Zhong G, Rozowsky J, Bhardwaj N, Gerstein MB, Snyder M (2011) Diverse roles and interactions of the SWI/SNF chromatin remodeling complex revealed using global approaches. PLoS Genet 7: e1002008

Faast R, Thonglairoam V, Schulz TC, Beall J, Wells JR, Taylor H, Matthaei K, Rathjen PD, Tremethick DJ, Lyons I (2001) Histone variant H2A.Z is required for early mammalian development. Curr Biol 11: 1183-7

Faircloth BC, Glenn TC (2014) Protocol: Preparation of an AMPure XP substitute (AKA Serapure).

Fan JY, Rangasamy D, Luger K, Tremethick DJ (2004) H2A.Z alters the nucleosome surface to promote HP1alpha-mediated chromatin fiber folding. Mol Cell 16: 655-61

Farrona S, Hurtado L, March-Diaz R, Schmitz RJ, Florencio FJ, Turck F, Amasino RM, Reyes JC (2011) Brahma is required for proper expression of the floral repressor FLC in Arabidopsis. PLoS One 6: e17997

Feng CM, Qiu Y, Van Buskirk EK, Yang EJ, Chen M (2014) Light-regulated gene repositioning in Arabidopsis. Nat Commun 5: 3027

Galvao VC, Collani S, Horrer D, Schmid M (2015) Gibberellic acid signaling is required for ambient temperature-mediated induction of flowering in Arabidopsis thaliana. Plant J 84: 949-62

Gendrel AV, Lippman Z, Martienssen R, Colot V (2005) Profiling histone modification patterns in plants using genomic tiling microarrays. Nat Methods 2: 213-8

Gevry N, Hardy S, Jacques PE, Laflamme L, Svotelis A, Robert F, Gaudreau L (2009) Histone H2A.Z is essential for estrogen receptor signaling. Genes Dev 23: 1522-33

Han SK, Sang Y, Rodrigues A, Biol F, Wu MF, Rodriguez PL, Wagner D (2012) The SWI2/SNF2 Chromatin Remodeling ATPase BRAHMA Represses Abscisic Acid Responses in the Absence of the Stress Stimulus in Arabidopsis. Plant Cell 24: 4892-906

Han SK, Wu MF, Cui S, Wagner D (2015) Roles and activities of chromatin remodeling ATPases in plants. Plant J 83: 62-77

Hargreaves DC, Crabtree GR (2011) ATP-dependent chromatin remodeling: genetics, genomics and mechanisms. Cell Res 21: 396-420

Hartwig B, James GV, Konrad K, Schneeberger K, Turck F (2012) Fast isogenic mapping-by-sequencing of ethyl methanesulfonate-induced mutant bulks. Plant Physiol 160: 591-600

He Y (2012) Chromatin regulation of flowering. Trends Plant Sci 17: 556-62

Heinz S, Benner C, Spann N, Bertolino E, Lin YC, Laslo P, Cheng JX, Murre C, Singh H, Glass CK (2010) Simple combinations of lineage-determining transcription factors prime cis-regulatory elements required for macrophage and B cell identities. Mol Cell 38: 576-89

Hiruma K, Onozawa-Komori M, Takahashi F, Asakura M, Bednarek P, Okuno T, Schulze-Lefert P, Takano Y (2010) Entry mode-dependent function of an indole glucosinolate pathway in Arabidopsis for nonhost resistance against anthracnose pathogens. Plant Cell 22: 2429-43

Hodges C, Kirkland JG, Crabtree GR (2016) The Many Roles of BAF (mSWI/SNF) and PBAF Complexes in Cancer. Cold Spring Harb Perspect Med 6:

Hu G, Cui K, Northrup D, Liu C, Wang C, Tang Q, Ge K, Levens D, Crane-Robinson C, Zhao K (2012) H2A.Z Facilitates Access of Active and Repressive Complexes to Chromatin in Embryonic Stem Cell Self-Renewal and Differentiation. Cell Stem Cell

Hu Y, Shen Y, Conde ESN, Zhou DX (2011) The role of histone methylation and H2A.Z occupancy during rapid activation of ethylene responsive genes. PLoS One 6: e28224

Hua S, Kallen CB, Dhar R, Baquero MT, Mason CE, Russell BA, Shah PK, Liu J, Khramtsov A, Tretiakova MS, Krausz TN, Olopade OI, Rimm DL, White KP (2008) Genomic analysis of estrogen cascade reveals histone variant H2A.Z associated with breast cancer progression. Mol Syst Biol 4: 188

Huebert DJ, Kuan PF, Keles S, Gasch AP (2012) Dynamic changes in nucleosome occupancy are not predictive of gene expression dynamics but are linked to transcription and chromatin regulators. Mol Cell Biol 32: 1645-53

Hurtado L, Farrona S, Reyes JC (2006) The putative SWI/SNF complex subunit BRAHMA activates flower homeotic genes in Arabidopsis thaliana. Plant Mol Biol 62: 291-304

Ietswaart R, Wu Z, Dean C (2012) Flowering time control: another window to the connection between antisense RNA and chromatin. Trends Genet 28: 445-53

Imbalzano AN, Imbalzano KM, Nickerson JA (2013) BRG1, a SWI/SNF chromatin remodeling enzyme ATPase, is required for maintenance of nuclear shape and integrity. Commun Integr Biol 6: e25153

Jackson JD, Gorovsky MA (2000) Histone H2A.Z has a conserved function that is distinct from that of the major H2A sequence variants. Nucleic Acids Res 28: 3811-6

Jarillo JA, Pineiro M (2015) H2A.Z mediates different aspects of chromatin function and modulates flowering responses in Arabidopsis. Plant J 83: 96-109

Jegu T, Latrasse D, Delarue M, Hirt H, Domenichini S, Ariel F, Crespi M, Bergounioux C, Raynaud C, Benhamed M (2014) The BAF60 Subunit of the SWI/SNF Chromatin-Remodeling Complex Directly Controls the Formation of a Gene Loop at FLOWERING LOCUS C in Arabidopsis. Plant Cell

Jegu T, Veluchamy A, Ramirez-Prado JS, Rizzi-Paillet C, Perez M, Lhomme A, Latrasse D, Coleno E, Vicaire S, Legras S, Jost B, Rougee M, Barneche F, Bergounioux C, Crespi M, Mahfouz MM, Hirt H, Raynaud C, Benhamed M (2017) The Arabidopsis SWI/SNF

protein BAF60 mediates seedling growth control by modulating DNA accessibility. Genome Biol 18: 114

Jiang W, Yang B, Weeks DP (2014) Efficient CRISPR/Cas9-mediated gene editing in Arabidopsis thaliana and inheritance of modified genes in the T2 and T3 generations. PLoS One 9: e99225

Jimenez-Useche I, Yuan C (2012) The effect of DNA CpG methylation on the dynamic conformation of a nucleosome. Biophys J 103: 2502-12

Jin C, Felsenfeld G (2007) Nucleosome stability mediated by histone variants H3.3 and H2A.Z. Genes Dev 21: 1519-29

John S, Sabo PJ, Johnson TA, Sung MH, Biddie SC, Lightman SL, Voss TC, Davis SR, Meltzer PS, Stamatoyannopoulos JA, Hager GL (2008) Interaction of the glucocorticoid receptor with the chromatin landscape. Mol Cell 29: 611-24

Jones AM, Chory J, Dangl JL, Estelle M, Jacobsen SE, Meyerowitz EM, Nordborg M, Weigel D (2008) The impact of Arabidopsis on human health: diversifying our portfolio. Cell 133: 939-43

Kadoch C, Hargreaves DC, Hodges C, Elias L, Ho L, Ranish J, Crabtree GR (2013) Proteomic and bioinformatic analysis of mammalian SWI/SNF complexes identifies extensive roles in human malignancy. Nat Genet 45: 592-601

Kim SI, Bresnick EH, Bultman SJ (2009) BRG1 directly regulates nucleosome structure and chromatin looping of the alpha globin locus to activate transcription. Nucleic Acids Res 37: 6019-27

Kitamura H, Matsumori H, Kalendova A, Hozak P, Goldberg IG, Nakao M, Saitoh N, Harata M (2015) The actin family protein ARP6 contributes to the structure and the function of the nucleolus. Biochem Biophys Res Commun 464: 554-60

Kleinmanns JA, Schatlowski N, Heckmann D, Schubert D (2017) BLISTER Regulates Polycomb-Target Genes, Represses Stress-Regulated Genes and Promotes Stress Responses in Arabidopsis thaliana. Front Plant Sci 8: 1530

Krietenstein N, Wal M, Watanabe S, Park B, Peterson CL, Pugh BF, Korber P (2016) Genomic Nucleosome Organization Reconstituted with Pure Proteins. Cell 167: 709-721 e12

Ku M, Jaffe JD, Koche RP, Rheinbay E, Endoh M, Koseki H, Carr SA, Bernstein BE (2012) H2A.Z landscapes and dual modifications in pluripotent and multipotent stem cells underlie complex genome regulatory functions. Genome Biol 13: R85

Kumar SV, Wigge PA (2010) H2A.Z-containing nucleosomes mediate the thermosensory response in Arabidopsis. Cell 140: 136-47

Kwok RS, Li YH, Lei AJ, Edery I, Chiu JC (2015) The Catalytic and Non-catalytic Functions of the Brahma Chromatin-Remodeling Protein Collaborate to Fine-Tune Circadian Transcription in Drosophila. PLoS Genet 11: e1005307

Lafos M, Kroll P, Hohenstatt ML, Thorpe FL, Clarenz O, Schubert D (2011) Dynamic regulation of H3K27 trimethylation during Arabidopsis differentiation. PLoS Genet 7: e1002040

Lai WKM, Pugh BF (2017) Understanding nucleosome dynamics and their links to gene expression and DNA replication. Nat Rev Mol Cell Biol 18: 548-562

Lamesch P, Berardini TZ, Li D, Swarbreck D, Wilks C, Sasidharan R, Muller R, Dreher K, Alexander DL, Garcia-Hernandez M, Karthikeyan AS, Lee CH, Nelson WD, Ploetz L, Singh S, Wensel A, Huala E (2012) The Arabidopsis Information Resource (TAIR): improved gene annotation and new tools. Nucleic Acids Res 40: D1202-10

Langmead B, Salzberg SL (2012) Fast gapped-read alignment with Bowtie 2. Nat Methods 9: 357-9

Lazaro A, Gomez-Zambrano A, Lopez-Gonzalez L, Pineiro M, Jarillo JA (2008) Mutations in the Arabidopsis SWC6 gene, encoding a component of the SWR1 chromatin remodelling

complex, accelerate flowering time and alter leaf and flower development. J Exp Bot 59: 653-66

Lee K, Seo PJ (2017) Coordination of matrix attachment and ATP-dependent chromatin remodeling regulate auxin biosynthesis and Arabidopsis hypocotyl elongation. PLoS One 12: e0181804

Lee KM, Hayes JJ (1998) Linker DNA and H1-dependent reorganization of histone-DNA interactions within the nucleosome. Biochemistry 37: 8622-8

Lee N, Choi G (2017) Phytochrome-interacting factor from Arabidopsis to liverwort. Curr Opin Plant Biol 35: 54-60

Lessard J, Wu JI, Ranish JA, Wan M, Winslow MM, Staahl BT, Wu H, Aebersold R, Graef IA, Crabtree GR (2007) An essential switch in subunit composition of a chromatin remodeling complex during neural development. Neuron 55: 201-15

Li B, Pattenden SG, Lee D, Gutiérrez J, Chen J, Seidel C, Gerton J, Workman JL (2005a) Preferential occupancy of histone variant H2AZ at inactive promoters influences local histone modifications and chromatin remodeling. Proceedings of the National Academy of Sciences of the United States of America 102: 18385-18390

Li C, Chen C, Gao L, Yang S, Nguyen V, Shi X, Siminovitch K, Kohalmi SE, Huang S, Wu K, Chen X, Cui Y (2015a) The Arabidopsis SWI2/SNF2 chromatin Remodeler BRAHMA regulates polycomb function during vegetative development and directly activates the flowering repressor gene SVP. PLoS Genet 11: e1004944

Li C, Gu L, Gao L, Chen C, Wei CQ, Qiu Q, Chien CW, Wang S, Jiang L, Ai LF, Chen CY, Yang S, Nguyen V, Qi Y, Snyder MP, Burlingame AL, Kohalmi SE, Huang S, Cao X, Wang ZY, Wu K, Chen X, Cui Y (2016) Concerted genomic targeting of H3K27 demethylase REF6 and chromatin-remodeling ATPase BRM in Arabidopsis. Nat Genet 48: 687-93

Li G, Levitus M, Bustamante C, Widom J (2005b) Rapid spontaneous accessibility of nucleosomal DNA. Nat Struct Mol Biol 12: 46-53

Li H, Durbin R (2009) Fast and accurate short read alignment with Burrows-Wheeler transform. Bioinformatics 25: 1754-60

Li H, Handsaker B, Wysoker A, Fennell T, Ruan J, Homer N, Marth G, Abecasis G, Durbin R, Genome Project Data Processing S (2009) The Sequence Alignment/Map format and SAMtools. Bioinformatics 25: 2078-9

Li H (2011) A statistical framework for SNP calling, mutation discovery, association mapping and population genetical parameter estimation from sequencing data. Bioinformatics 27: 2987-93

Li M, Hada A, Sen P, Olufemi L, Hall MA, Smith BY, Forth S, McKnight JN, Patel A, Bowman GD, Bartholomew B, Wang MD (2015b) Dynamic regulation of transcription factors by nucleosome remodeling. Elife 4:

Li Z, Gadue P, Chen K, Jiao Y, Tuteja G, Schug J, Li W, Kaestner KH (2012) Foxa2 and H2A.Z mediate nucleosome depletion during embryonic stem cell differentiation. Cell 151: 1608-16

Light WH, Brickner DG, Brand VR, Brickner JH (2010) Interaction of a DNA zip code with the nuclear pore complex promotes H2A.Z incorporation and INO1 transcriptional memory. Mol Cell 40: 112-25

Lin R, Wang H (2004) Arabidopsis FHY3/FAR1 gene family and distinct roles of its members in light control of Arabidopsis development. Plant Physiol 136: 4010-22

Liu JC, Ferreira CG, Yusufzai T (2015) Human CHD2 is a chromatin assembly ATPase regulated by its chromo- and DNA-binding domains. J Biol Chem 290: 25-34

Liu X, Li B, GorovskyMa (1996) Essential and nonessential histone H2A variants in Tetrahymena thermophila. Mol Cell Biol 16: 4305-11

Livak KJ, Schmittgen TD (2001) Analysis of relative gene expression data using real-time quantitative PCR and the 2(-Delta Delta C(T)) Method. Methods 25: 402-8

Lu PY, Levesque N, Kobor MS (2009) NuA4 and SWR1-C: two chromatin-modifying complexes with overlapping functions and components. Biochem Cell Biol 87: 799-815

Luger K, Mader AW, Richmond RK, Sargent DF, Richmond TJ (1997) Crystal structure of the nucleosome core particle at 2.8 A resolution. Nature 389: 251-60

Luger K, Mader A, Sargent DF, Richmond TJ (2000) The atomic structure of the nucleosome core particle. J Biomol Struct Dyn 17 Suppl 1: 185-8

Ma KW, Flores C, Ma W (2011) Chromatin configuration as a battlefield in plant-bacteria interactions. Plant Physiol 157: 535-43

March-Diaz R, Garcia-Dominguez M, Florencio FJ, Reyes JC (2007) SEF, a new protein required for flowering repression in Arabidopsis, interacts with PIE1 and ARP6. Plant Physiol 143: 893-901

March-Diaz R, Garcia-Dominguez M, Lozano-Juste J, Leon J, Florencio FJ, Reyes JC (2008) Histone H2A.Z and homologues of components of the SWR1 complex are required to control immunity in Arabidopsis. Plant J 53: 475-87

March-Diaz R, Reyes JC (2009) The beauty of being a variant: H2A.Z and the SWR1 complex in plants. Mol Plant 2: 565-77

Marques M, Laflamme L, Gervais AL, Gaudreau L (2010) Reconciling the positive and negative roles of histone H2A.Z in gene transcription. Epigenetics 5: 267-72

Martin-Trillo M, Lazaro A, Poethig RS, Gomez-Mena C, Pineiro MA, Martinez-Zapater JM, Jarillo JA (2006) EARLY IN SHORT DAYS 1 (ESD1) encodes ACTIN-RELATED PROTEIN 6 (AtARP6), a putative component of chromatin remodelling complexes that positively regulates FLC accumulation in Arabidopsis. Development 133: 1241-52

Maruyama EO, Hori T, Tanabe H, Kitamura H, Matsuda R, Tone S, Hozak P, Habermann FA, von Hase J, Cremer C, Fukagawa T, Harata M (2012) The actin family member Arp6 and

the histone variant H2A.Z are required for spatial positioning of chromatin in chicken cell nuclei. J Cell Sci 125: 3739-43

McCarthy DJ, Chen Y, Smyth GK (2012) Differential expression analysis of multifactor RNA-Seq experiments with respect to biological variation. Nucleic Acids Res 40: 4288-97

Medina-Rivera A, Defrance M, Sand O, Herrmann C, Castro-Mondragon JA, Delerce J, Jaeger S, Blanchet C, Vincens P, Caron C, Staines DM, Contreras-Moreira B, Artufel M, Charbonnier-Khamvongsa L, Hernandez C, Thieffry D, Thomas-Chollier M, van Helden J (2015) RSAT 2015: Regulatory Sequence Analysis Tools. Nucleic Acids Res 43: W50-6

Meneghini MD, Wu M, Madhani HD (2003) Conserved histone variant H2A.Z protects euchromatin from the ectopic spread of silent heterochromatin. Cell 112: 725-36

Merchant N, Lyons E, Goff S, Vaughn M, Ware D, Micklos D, Antin P (2016) The iPlant Collaborative: Cyberinfrastructure for Enabling Data to Discovery for the Life Sciences. PLoS Biol 14: e1002342

Michaels SD, Amasino RM (1999) FLOWERING LOCUS C Encodes a Novel MADS Domain Protein That Acts as a Repressor of Flowering. The Plant Cell Online 11: 949-956

Mizuguchi G, Shen X, Landry J, Wu WH, Sen S, Wu C (2004) ATP-driven exchange of histone H2AZ variant catalyzed by SWR1 chromatin remodeling complex. Science 303: 343-8

Molitor A, Latrasse D, Zytnicki M, Andrey P, Houba-Herin N, Hachet M, Battail C, Del Prete S, Alberti A, Quesneville H, Gaudin V (2016) The Arabidopsis hnRNP-Q Protein LIF2 and the PRC1 subunit LHP1 function in concert to regulate the transcription of stress-responsive genes. Plant Cell

Mondal T, Rasmussen M, Pandey GK, Isaksson A, Kanduri C (2010) Characterization of the RNA content of chromatin. Genome Res 20: 899-907

Mueller B, Mieczkowski J, Kundu S, Wang P, Sadreyev R, Tolstorukov MY, Kingston RE (2017) Widespread changes in nucleosome accessibility without changes in nucleosome occupancy during a rapid transcriptional induction. Genes Dev 31: 451-462

Mylne J, Greb T, Lister C, Dean C (2004) Epigenetic regulation in the control of flowering. Cold Spring Harb Symp Quant Biol 69: 457-64

Nagai S, Davis RE, Mattei PJ, Eagen KP, Kornberg RD (2017) Chromatin potentiates transcription. Proc Natl Acad Sci U S A 114: 1536-1541

Narlikar GJ, Sundaramoorthy R, Owen-Hughes T (2013) Mechanisms and functions of ATP-dependent chromatin-remodeling enzymes. Cell 154: 490-503

Nogales-Cadenas R, Carmona-Saez P, Vazquez M, Vicente C, Yang X, Tirado F, Carazo JM, Pascual-Montano A (2009) GeneCodis: interpreting gene lists through enrichment analysis and integration of diverse biological information. Nucleic Acids Res 37: W317-22

O'Malley RC, Huang SC, Song L, Lewsey MG, Bartlett A, Nery JR, Galli M, Gallavotti A, Ecker JR (2016) Cistrome and Epicistrome Features Shape the Regulatory DNA Landscape. Cell 166: 1598

Papamichos-Chronakis M, Watanabe S, Rando OJ, Peterson CL (2011) Global regulation of H2A.Z localization by the INO80 chromatin-remodeling enzyme is essential for genome integrity. Cell 144: 200-13

Park YJ, Dyer PN, Tremethick DJ, Luger K (2004) A new fluorescence resonance energy transfer approach demonstrates that the histone variant H2AZ stabilizes the histone octamer within the nucleosome. J Biol Chem 279: 24274-82

Pedmale UV, Huang SC, Zander M, Cole BJ, Hetzel J, Ljung K, Reis PAB, Sridevi P, Nito K, Nery JR, Ecker JR, Chory J (2016) Cryptochromes Interact Directly with PIFs to Control Plant Growth in Limiting Blue Light. Cell 164: 233-245

Probst AV, Mittelsten Scheid O (2015) Stress-induced structural changes in plant chromatin. Curr Opin Plant Biol 27: 8-16

Quinlan AR (2014) BEDTools: The Swiss-Army Tool for Genome Feature Analysis. Curr Protoc Bioinformatics 47: 11 12 1-34

Raisner RM, Hartley PD, Meneghini MD, Bao MZ, Liu CL, Schreiber SL, Rando OJ, Madhani HD (2005) Histone variant H2A. Z marks the 5′ ends of both active and inactive genes in euchromatin. Cell 123: 233

Ramirez F, Dundar F, Diehl S, Gruning BA, Manke T (2014) deepTools: a flexible platform for exploring deep-sequencing data. Nucleic Acids Res 42: W187-91

Rangasamy D (2010) Histone variant H2A.Z can serve as a new target for breast cancer therapy. Curr Med Chem 17: 3155-61

Ranjan A, Mizuguchi G, Fitzgerald PC, Wei D, Wang F, Huang Y, Luk E, Woodcock CL, Wu C (2013) Nucleosome-free Region Dominates Histone Acetylation in Targeting SWR1 to Promoters for H2A.Z Replacement. Cell 154: 1232-45

Ritter A, Inigo S, Fernandez-Calvo P, Heyndrickx KS, Dhondt S, Shi H, De Milde L, Vanden Bossche R, De Clercq R, Eeckhout D, Ron M, Somers DE, Inze D, Gevaert K, De Jaeger G, Vandepoele K, Pauwels L, Goossens A (2017) The transcriptional repressor complex FRS7-FRS12 regulates flowering time and growth in Arabidopsis. Nat Commun 8: 15235

Robinson MD, McCarthy DJ, Smyth GK (2010) edgeR: a Bioconductor package for differential expression analysis of digital gene expression data. Bioinformatics 26: 139-40

Rosa M, Von Harder M, Cigliano RA, Schlogelhofer P, Scheid OM (2013) The Arabidopsis SWR1 Chromatin-Remodeling Complex Is Important for DNA Repair, Somatic Recombination, and Meiosis. Plant Cell

Rudnizky S, Bavly A, Malik O, Pnueli L, Melamed P, Kaplan A (2016) H2A.Z controls the stability and mobility of nucleosomes to regulate expression of the LH genes. Nat Commun 7: 12958

Rymen B, Sugimoto K (2012) Tuning growth to the environmental demands. Curr Opin Plant Biol 15: 683-90

Sacharowski SP, Gratkowska DM, Sarnowska EA, Kondrak P, Jancewicz I, Porri A, Bucior E, Rolicka AT, Franzen R, Kowalczyk J, Pawlikowska K, Huettel B, Torti S, Schmelzer E, Coupland G, Jerzmanowski A, Koncz C, Sarnowski TJ (2015) SWP73 Subunits of Arabidopsis SWI/SNF Chromatin Remodeling Complexes Play Distinct Roles in Leaf and Flower Development. Plant Cell 27: 1889-906

Saez-Vasquez J, Gadal O (2010) Genome organization and function: a view from yeast and Arabidopsis. Mol Plant 3: 678-90

Salmon-Divon M, Dvinge H, Tammoja K, Bertone P (2010) PeakAnalyzer: genome-wide annotation of chromatin binding and modification loci. BMC Bioinformatics 11: 415

Santisteban MS, Kalashnikova T, Smith MM (2000) Histone H2A.Z regulats transcription and is partially redundant with nucleosome remodeling complexes. Cell 103: 411-22

Sarnowska E, Gratkowska DM, Sacharowski SP, Cwiek P, Tohge T, Fernie AR, Siedlecki JA, Koncz C, Sarnowski TJ (2016) The Role of SWI/SNF Chromatin Remodeling Complexes in Hormone Crosstalk. Trends Plant Sci 21: 594-608

Schatlowski N, Stahl Y, Hohenstatt ML, Goodrich J, Schubert D (2010) The CURLY LEAF interacting protein BLISTER controls expression of polycomb-group target genes and cellular differentiation of Arabidopsis thaliana. Plant Cell 22: 2291-305

Schnitzler GR, Cheung CL, Hafner JH, Saurin AJ, Kingston RE, Lieber CM (2001) Direct imaging of human SWI/SNF-remodeled mono- and polynucleosomes by atomic force microscopy employing carbon nanotube tips. Mol Cell Biol 21: 8504-11

Schotta G, Ebert A, Dorn R, Reuter G (2003) Position-effect variegation and the genetic dissection of chromatin regulation in Drosophila. Seminars in Cell & Developmental Biology 14: 67-75

Sequeira-Mendes J, Araguez I, Peiro R, Mendez-Giraldez R, Zhang X, Jacobsen SE, Bastolla U, Gutierrez C (2014) The Functional Topography of the Arabidopsis Genome Is Organized in a Reduced Number of Linear Motifs of Chromatin States. Plant Cell 26: 2351-2366

Seymour DK, Becker C (2017) The causes and consequences of DNA methylome variation in plants. Curr Opin Plant Biol 36: 56-63

Sheldon CC, Conn AB, Dennis ES, Peacock WJ (2002) Different regulatory regions are required for the vernalization-induced repression of FLOWERING LOCUS C and for the epigenetic maintenance of repression. Plant Cell 14: 2527-37

Shogren-Knaak M, Ishii H, Sun JM, Pazin MJ, Davie JR, Peterson CL (2006) Histone H4-K16 acetylation controls chromatin structure and protein interactions. Science 311: 844-7

Sijacic P, Bajic M, McKinney EC, Meagher RB, Deal RB (2017) Chromatin accessibility changes between Arabidopsis stem cells and mesophyll cells illuminate cell type-specific transcription factor networks. bioRxiv

Smith AP, Jain A, Deal RB, Nagarajan VK, Poling MD, Raghothama KG, Meagher RB (2010) Histone H2A.Z regulates the expression of several classes of phosphate starvation response genes but not as a transcriptional activator. Plant Physiol 152: 217-25

Srikanth A, Schmid M (2011) Regulation of flowering time: all roads lead to Rome. Cell Mol Life Sci 68: 2013-37

Sura W, Kabza M, Karlowski WM, Bieluszewski T, Kus-Slowinska M, Paweloszek L, Sadowski J, Ziolkowski PA (2017) Dual role of the histone variant H2A.Z in transcriptional regulation of stress-response genes. Plant Cell

Surface LE, Fields PA, Subramanian V, Behmer R, Udeshi N, Peach SE, Carr SA, Jaffe JD, Boyer LA (2016) H2A.Z.1 Monoubiquitylation Antagonizes BRD2 to Maintain Poised Chromatin in ESCs. Cell Rep

Suto RK, Clarkson MJ, Tremethick DJ, Luger K (2000) Crystal structure of a nucleosome core particle containing the variant histone H2A.Z. Nature Structural Biology 7: 1121

Swaminathan J, Baxter EM, Corces VG (2005) The role of histone H2Av variant replacement and histone H4 acetylation in the establishment of Drosophila heterochromatin. Genes Dev 19: 65-76

Tabas-Madrid D, Nogales-Cadenas R, Pascual-Montano A (2012) GeneCodis3: a non-redundant and modular enrichment analysis tool for functional genomics. Nucleic Acids Res 40: W478-83

Tessarz P, Kouzarides T (2014) Histone core modifications regulating nucleosome structure and dynamics. Nat Rev Mol Cell Biol 15: 703-8

Tian T, Liu Y, Yan H, You Q, Yi X, Du Z, Xu W, Su Z (2017) agriGO v2.0: a GO analysis toolkit for the agricultural community, 2017 update. Nucleic Acids Res

Todolli S, Perez PJ, Clauvelin N, Olson WK (2017) Contributions of Sequence to the Higher-Order Structures of DNA. Biophys J 112: 416-426

Tolstorukov MY, Sansam CG, Lu P, Koellhoffer EC, Helming KC, Alver BH, Tillman EJ, Evans JA, Wilson BG, Park PJ, Roberts CW (2013) Swi/Snf chromatin remodeling/tumor suppressor complex establishes nucleosome occupancy at target promoters. Proc Natl Acad Sci U S A 110: 10165-70

Torigoe SE, Patel A, Khuong MT, Bowman GD, Kadonaga JT (2013) ATP-dependent chromatin assembly is functionally distinct from chromatin remodeling. Elife 2: e00863

Trapnell C, Roberts A, Goff L, Pertea G, Kim D, Kelley DR, Pimentel H, Salzberg SL, Rinn JL, Pachter L (2012) Differential gene and transcript expression analysis of RNA-seq experiments with TopHat and Cufflinks. Nat Protoc 7: 562-78

Turinetto V, Giachino C (2015) Multiple facets of histone variant H2AX: a DNA double-strand-break marker with several biological functions. Nucleic Acids Res 43: 2489-98

Urano K, Kurihara Y, Seki M, Shinozaki K (2010) 'Omics' analyses of regulatory networks in plant abiotic stress responses. Curr Opin Plant Biol 13: 132-8

Valdes-Mora F, Song JZ, Statham AL, Strbenac D, Robinson MD, Nair SS, Patterson KI, Tremethick DJ, Stirzaker C, Clark SJ (2012) Acetylation of H2A.Z is a key epigenetic modification associated with gene deregulation and epigenetic remodeling in cancer. Genome Res 22: 307-21

Valdes-Mora F, Gould CM, Colino-Sanguino Y, Qu W, Song JZ, Taylor KM, Buske FA, Statham AL, Nair SS, Armstrong NJ, Kench JG, Lee KML, Horvath LG, Qiu M, Ilinykh A, Yeo-Teh NS, Gallego-Ortega D, Stirzaker C, Clark SJ (2017) Acetylated histone variant H2A.Z is involved in the activation of neo-enhancers in prostate cancer. Nat Commun 8: 1346

van Zanten M, Tessadori F, McLoughlin F, Smith R, Millenaar FF, van Driel R, Voesenek LA, Peeters AJ, Fransz P (2010) Photoreceptors CRYTOCHROME2 and phytochrome B control chromatin compaction in Arabidopsis. Plant Physiol 154: 1686-96

Vardabasso C, Gaspar-Maia A, Hasson D, Punzeler S, Valle-Garcia D, Straub T, Keilhauer EC, Strub T, Dong J, Panda T, Chung CY, Yao JL, Singh R, Segura MF, Fontanals-Cirera B, Verma A, Mann M, Hernando E, Hake SB, Bernstein E (2015) Histone Variant H2A.Z.2 Mediates Proliferation and Drug Sensitivity of Malignant Melanoma. Mol Cell 59: 75-88

Vercruyssen L, Verkest A, Gonzalez N, Heyndrickx KS, Eeckhout D, Han SK, Jegu T, Archacki R, Van Leene J, Andriankaja M, De Bodt S, Abeel T, Coppens F, Dhondt S, De Milde L, Vermeersch M, Maleux K, Gevaert K, Jerzmanowski A, Benhamed M, Wagner D, Vandepoele K, De Jaeger G, Inze D (2014) ANGUSTIFOLIA3 Binds to SWI/SNF Chromatin Remodeling Complexes to Regulate Transcription during Arabidopsis Leaf Development. Plant Cell

Vergara Z, Gutierrez C (2017) Emerging roles of chromatin in the maintenance of genome organization and function in plants. Genome Biol 18: 96

Weber CM, Ramachandran S, Henikoff S (2014) Nucleosomes are context-specific, H2A.Z-modulated barriers to RNA polymerase. Mol Cell 53: 819-30

Weirauch MT, Yang A, Albu M, Cote AG, Montenegro-Montero A, Drewe P, Najafabadi HS, Lambert SA, Mann I, Cook K, Zheng H, Goity A, van Bakel H, Lozano JC, Galli M, Lewsey MG, Huang E, Mukherjee T, Chen X, Reece-Hoyes JS, Govindarajan S, Shaulsky G, Walhout AJM, Bouget FY, Ratsch G, Larrondo LF, Ecker JR, Hughes TR (2014) Determination and inference of eukaryotic transcription factor sequence specificity. Cell 158: 1431-1443

Whittle CM, McClinic KN, Ercan S, Zhang X, Green RD, Kelly WG, Lieb JD (2008) The genomic distribution and function of histone variant HTZ-1 during C. elegans embryogenesis. PLoS Genet 4: e1000187

Widom J (2001) Role of DNA sequence in nucleosome stability and dynamics. Q Rev Biophys 34: 269-324

Wigge PA (2013) Ambient temperature signalling in plants. Curr Opin Plant Biol 16: 661-6

Wu JI (2012) Diverse functions of ATP-dependent chromatin remodeling complexes in development and cancer. Acta Biochim Biophys Sin (Shanghai) 44: 54-69

Wu MF, Sang Y, Bezhani S, Yamaguchi N, Han SK, Li Z, Su Y, Slewinski TL, Wagner D (2012) SWI2/SNF2 chromatin remodeling ATPases overcome polycomb repression and control floral organ identity with the LEAFY and SEPALLATA3 transcription factors. Proc Natl Acad Sci U S A 109: 3576-81

Wu MF, Yamaguchi N, Xiao J, Bargmann B, Estelle M, Sang Y, Wagner D (2015) Auxin-regulated chromatin switch directs acquisition of flower primordium founder fate. Elife 4: e09269

Wu Q, Lian JB, Stein JL, Stein GS, Nickerson JA, Imbalzano AN (2017) The BRG1 ATPase of human SWI/SNF chromatin remodeling enzymes as a driver of cancer. Epigenomics 9: 919-931

Wu SH (2014) Gene expression regulation in photomorphogenesis from the perspective of the central dogma. Annu Rev Plant Biol 65: 311-33

Xu XM, Moller SG (2011) The value of Arabidopsis research in understanding human disease states. Curr Opin Biotechnol 22: 300-7

Yang HD, Kim PJ, Eun JW, Shen Q, Kim HS, Shin WC, Ahn YM, Park WS, Lee JY, Nam SW (2016) Oncogenic potential of histone-variant H2A.Z.1 and its regulatory role in cell cycle and epithelial-mesenchymal transition in liver cancer. Oncotarget 7: 11412-23

Yang S, Li C, Zhao L, Gao S, Lu J, Zhao M, Chen CY, Liu X, Luo M, Cui Y, Yang C, Wu K (2015) The Arabidopsis SWI2/SNF2 Chromatin Remodeling ATPase BRAHMA Targets Directly to PINs and Is Required for Root Stem Cell Niche Maintenance. Plant Cell 27: 1670-80

Yoshida T, Shimada K, Oma Y, Kalck V, Akimura K, Taddei A, Iwahashi H, Kugou K, Ohta K, Gasser SM, Harata M (2010) Actin-related protein Arp6 influences H2A.Z-dependent and -independent gene expression and links ribosomal protein genes to nuclear pores. PLoS Genet 6: e1000910

Zhang D, Li Y, Zhang X, Zha P, Lin R (2016) The SWI2/SNF2 Chromatin-Remodeling ATPase BRAHMA Regulates Chlorophyll Biosynthesis in Arabidopsis. Mol Plant

Zhang D, Li Y, Zhang X, Zha P, Lin R (2017a) The SWI2/SNF2 Chromatin-Remodeling ATPase BRAHMA Regulates Chlorophyll Biosynthesis in Arabidopsis. Mol Plant 10: 155-167

Zhang R, Erler J, Langowski J (2017b) Histone Acetylation Regulates Chromatin Accessibility: Role of H4K16 in Inter-nucleosome Interaction. Biophys J 112: 450-459

Zhang T, Zhang W, Jiang J (2015) Genome-Wide Nucleosome Occupancy and Positioning and Their Impact on Gene Expression and Evolution in Plants. Plant Physiol 168: 1406-16

Zhang Y, Ku WL, Liu S, Cui K, Jin W, Tang Q, Lu W, Ni B, Zhao K (2017c) Genome-wide identification of histone H2A and histone variant H2A.Z-interacting proteins by bPPI-seq. Cell Res 27: 1258-1274

Zhao M, Yang S, Chen CY, Li C, Shan W, Lu W, Cui Y, Liu X, Wu K (2015) Arabidopsis BREVIPEDICELLUS interacts with the SWI2/SNF2 chromatin remodeling ATPase

BRAHMA to regulate KNAT2 and KNAT6 expression in control of inflorescence architecture. PLoS Genet 11: e1005125

Zhao Y, Garcia BA (2015) Comprehensive Catalog of Currently Documented Histone Modifications. Cold Spring Harb Perspect Biol 7: a025064

Zhou CY, Johnson SL, Gamarra NI, Narlikar GJ (2016) Mechanisms of ATP-Dependent Chromatin Remodeling Motors. Annu Rev Biophys 45: 153-81

Zhu Y, Dong A, Shen WH (2013) Histone variants and chromatin assembly in plant abiotic stress responses. Biochim Biophys Acta 1819: 343-8

Zilberman D, Coleman-Derr D, Ballinger T, Henikoff S (2008) Histone H2A.Z and DNA methylation are mutually antagonistic chromatin marks. Nature 456: 125-9

Zink LM, Hake SB (2016) Histone variants: nuclear function and disease. Curr Opin Genet Dev 37: 82-89

Zofall M, Persinger J, Kassabov SR, Bartholomew B (2006) Chromatin remodeling by ISW2 and SWI/SNF requires DNA translocation inside the nucleosome. Nat Struct Mol Biol 13: 339-46

Zuryn S, Le Gras S, Jamet K, Jarriault S (2010) A Strategy for Direct Mapping and Identification of Mutations by Whole-Genome Sequencing. Genetics 186: 427-430